The Bengal Fan: architecture, morphology and depositional processes at different scales revealed from high-resolution seismic and hydroacoustic data

Dissertation

zur Erlangung des
Doktorgrades der Naturwissenschaften

im Fachbereich 5
der Universität Bremen

vorgelegt von
Tilmann Schwenk
Bremen
2003

Table of contents

Chapter 1: General introduction

1.1 Main objectives and aim of this study

Large submarine fans as Amazon, Bengal, Congo, Indus and Mississippi Fan are topics of research for a better understanding of their depositional processes as well as for their hydrocarbon potential and their potential to act as a recorder of long- and short-term climatic changes. Typically located on passive continental margins, these fans are classified as fine-grained, mud-rich systems with a sand content of less than 30%, fed by a canyon incised into a wide shelf acting as a point source. Sediment is derived from large river systems building major deltaic complexes and transporting huge amounts of suspended material. Due to river transport mechanism, erosive power and type of weathering, the load of the river is a result of climatic and tectonic conditions on land, and its provenance and variations can become well documented in marine deposits (Bouma, 2000; Bouma, 2001; Richards et al., 1998).

In general, mud-rich submarine fans can be subdivided into an upper, middle and lower fan. Large channel-levee systems develop at the canyon mouth on the upper fan, transform downslope on the middle fan into more sinuous systems, and finally terminate in depositional lobes on the lower fan (Bouma, 2000; Bouma, 2001; Richards et al., 1998). Frequent avulsions on the upper fan lead to vertical and lateral stacking of numerous channel-levee systems on the middle and lower fan as observed e.g. on Amazon, Indus and Bengal Fan (Curray et al., 2003; Damuth et al., 1988; Emmel and Curray, 1985; Kenyon et al., 1995; Kolla and Schwab, 1995; Pirmez and Flood, 1995). Transport of the sediment is made by mixed-load turbidity currents traveling through the channel-levee systems. Along this path, an effective sand separating process occurs by overspilling of fine-grained material onto the levees and deposits of coarse-grained material on the channel floor and within the terminating lobes, leading to a significant reservoir potential of both, also in so-called mud-rich, fine-grained fans (Bouma, 2001; Hiscott et al., 1997; Lopez, 2001; Richards et al., 1998).

However, even if general architecture, geometry and depositional processes of submarine fans are well known, accurate characterization of individual fans and their specific architectural elements is required to improve the depositional models for their development and finally to determine their reservoir architecture as well as to understand the sedimentary record of terrestrial and global climate changes (Bouma, 2001; Lopez, 2001; Richards et al., 1998; Stow and Mayall, 2000). To study these topics, the Bengal Fan is well suited as the largest submarine fan on Earth, which was formed as a direct result of the India-Asia collision and the resulting uplift of the Himalayas (Fig. 1.1). Therefore, this fan was the focus of three expeditions with the German research vessel R/V Sonne in 1994 and 1997 in co-operation between the Federal Institute for Geoscience and Natural Resources (BGR), Hannover and the University of Bremen (Fig. 1.1). During these cruises, the sediment echosounder, bathymetric swath-sounder and multi-frequency high-resolution seismic data were collected, which are presented in this study (Kudrass and Ship-

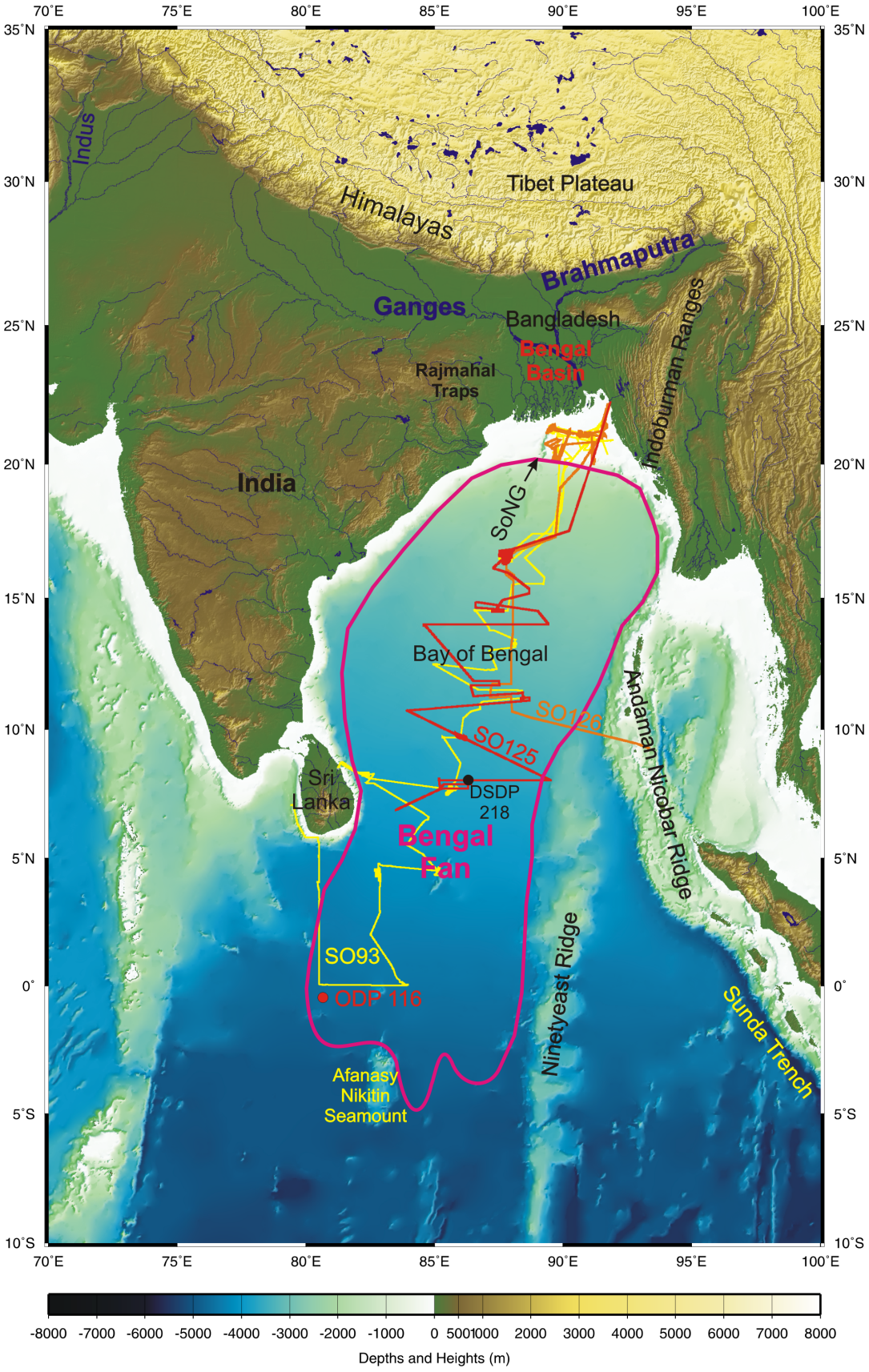

Figure 1.1: *Overview map showing the Bengal Fan, Bengal Basin and the Ganges-Brahmaputra rivers draining the Himalayas. Topography and bathymetry is from GEBCO 2003 Digital Atlas, BODC, © National Environmental Research Council. Boundaries of the fan are redrawn from Emmel and Curray (1985) and Stow et al. (1990). Also drawn in are the cruise tracks of SO93, SO125 and SO126 expeditions.*

board Scientific Party, 1994; Kudrass and Shipboard Scientific Party, 1998; Spieß et al., 1998).

The objective of this study is to document the architecture of the Bengal Fan at different scales by investigating individual channel-levee systems and large channel-levee complexes as well as the general stratigraphy and changes as a function of water depth and shelf distance. Based on the analysis of sedimentary patterns, evolutionary and depositional processes should be identified and characterized, and interpreted with respect to tectonic and/or climatic events. Finally, an important motivation for this study was the support of two IODP proposals for drilling in the Bengal Fan (France-Lanord et al., 2001; Spieß et al., 2002).

The text is organized as follows: In the first part of the preface Chapter 1, data acquisition and processing especially of the seismic data are described, and a detailed introduction to the Bengal Fan and to channel-levee systems is given. In the last part of the Chapter 1, short outlines of the three manuscripts are presented, which follow in Chapters 2, 3 and 4. The text is completed by a summary and an outlook on possible future research in the study area in Chapter 5.

1.2 Methods

Data presented in this study were collected with the German research vessel Sonne during the Cruises SO93 in 1994 and SO125 as well as SO126 in 1997, using the GeoB multichannel seismic system, the sediment echosounder Parasound and the multibeam swathsounder Hydrosweep (Kudrass and Shipboard Scientific Party, 1994; Kudrass and Shipboard Scientific Party, 1998; Spieß et al., 1998). During seismic profiling, all three systems were operated simultaneously. All presented multichannel seismic data and most of the sediment echosounding and bathymetric data were gathered during Cruise SO125. In total, more than 2100 km of seismic data and at least 1100 km of Parasound and Hydrosweep data were processed and analyzed for this study.

1.2.1 The GeoB multichannel seismic system

1.2.1.1 Data acquisition

During SO125 Cruise, the GeoB marine multichannel seismic system was used, which includes different seismic sources, a seismic streamer with programmable hydrophone arrays, a streamer control unit, a recording unit and a trigger unit (Spieß et al., 1998) (Fig. 1.2). Navigation data were provided by the ship's Global Positioning System (GPS).

As seismic sources, a GI Gun with reduced chamber volumes of both chambers of 2 x 0.4 L and a Sodera S15 watergun of 0.16 L volume were operated in an alternating mode. The main frequencies of the guns are 100-500 Hz and 200-1600 Hz, respectively. A time interval of 13 s between shots of different sources was chosen and the ship's speed was 4.9 knots, leading to a distance of 66 m between shots of the same source. Both sources were operated with an air pressure of 145 bar. Seismic signals were collected with an oil-filled streamer (Syntron Inc.) including a lead-in cable of 30 m length, a

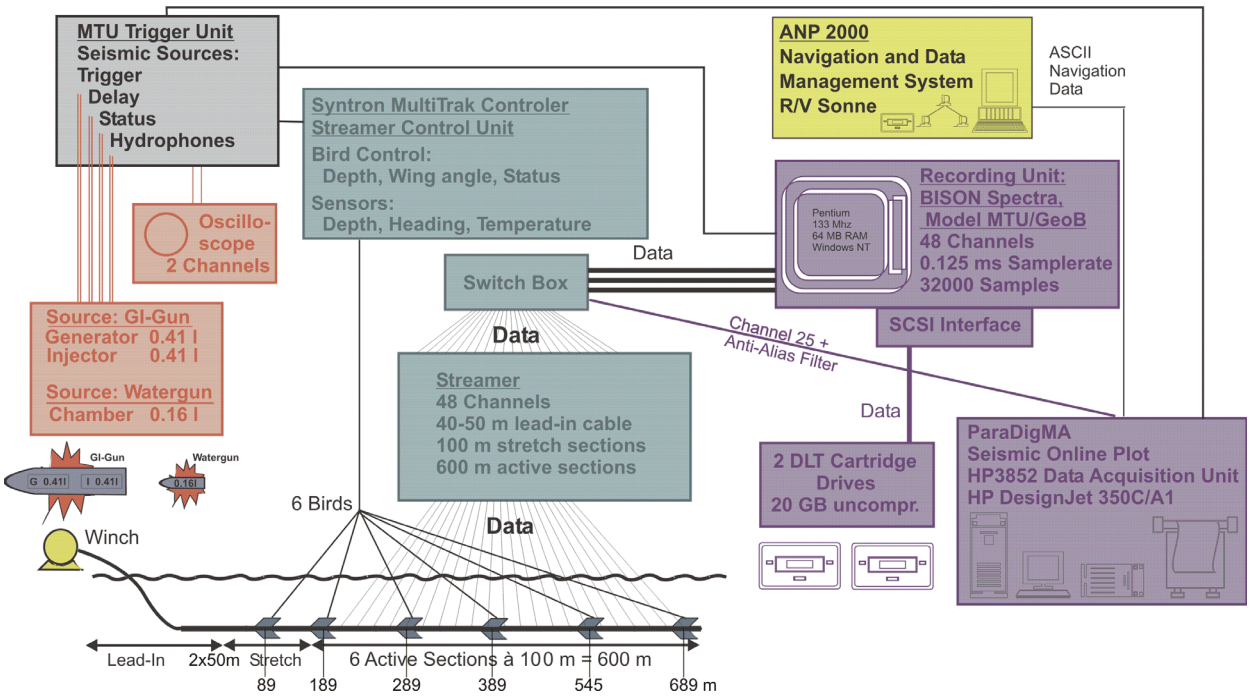

Figure 1.2: *Acquisition system of multichannel seismic data operated during RV Sonne cruise SO125. Adapted from Spieß et al. (1998).*

stretch section of 100 m length and six active sections of 100 m length each. The streamer is equipped with separately programmable hydrophone subgroups of different length to optimize resolution and bandwidth of the received signals and to avoid destructive interferences. In the Bay of Bengal, 48 groups with a length of 6.25 m and a spacing of 12.5 m were chosen. Attached to the streamer, six MultiTrak remote units (so-called birds) were used to keep the streamer at 2.5 m water depth by adjustable wings, remotely controlled with a PC-based control unit. Additionally, the birds provide depth and heading information, which are stored for each shot.

The data recording unit consists of a switch box and a 48 channel seismograph (Bison Inc.). The switch box connects the streamer with the seismograph and allows assigning the streamer hydrophone subgroups to individual recording channels. The seismograph was specially designed for the University of Bremen to operate at high shot and sampling rates for recording of very high resolution seismic data. After analog filtering (8-4000 Hz), pre-amplifying by a factor of 1000 (60dB) and demultiplexing, the data were stored in SEG-Y format on DLT cartridges (20GB) with a sampling rate of 0.125 ms and a recording length of 4000 ms. A recording delay was adjusted according to the water depth. During SO125 Cruise, an online plot of one streamer channel was generated by an additionally PC-based unit (ParaDigMA system) for quality control. All units, the seismic sources, the seismograph, the MultiTrak controller and the online plotter were controlled by a trigger unit based on a real-time controller interface card (SORCUS).

1.2.1.2 Data processing

Standard seismic processing as filtering, stacking and migration was carried out with the public domain software package Seismic Un*x (SU) (Stockwell, 1997). Due to the high frequency content of GI Gun and Watergun data, an improved CDP-sorting and static correction is needed which accounts for lateral and vertical movement of the streamer. For CDP-sorting and static correction of the GI Gun data, a custom geometry processing package (Zühlsdorff, 1999) was used. This flow utilized 1) shot number and time information, 2) navigation information, 3) depth information of the birds and 4) heading information of the birds. First, a time interpolation was carried out to resample all information to a same time interval. Based on the navigation and the heading data, reflection midpoints between source and receiver positions were calculated for each trace. Then CDP´s were defined as small circles (bins) with distinct sizes and distances located on the cruise track. Next, each reflection midpoint was assigned to the one CDP bin with the minimum distance to the center of the bin. As a result, for each shot and recording channel a CDP number is determined. After that, a static correction time was calculated for each trace using lateral linear interpolation of depth information of the birds for each receiver position. Finally, the static correction time and CDP numbers are written into the trace headers of each record, followed by the main processing including filtering, static correction, NMO correction within CDP gathers, CDP stack and migration.

For the watergun it turned out that the above described static correction method was not sufficiently accurate. This is caused by small depth variations of the streamer between the birds, which were not covered by the linear interpolation of depths. Since these variations are about half the wavelength of the watergun signal or more, destructive interference occurs by stacking CDP gathers. Therefore, a static correction method has been developed by Gutowski et al. (2002), which uses the accurate depth information of the Parasound sediment echosounder recorded simultaneously during seismic surveys at an accuracy on the order of 10 centimeters. The seismic data were sorted into CDP bins as described above, followed by a NMO correction. For both data sets, seismic and Parasound, an automatic first arrival detection was applied. Then the CDP bins were assigned to the nearest Parasound reflection points, and the difference between seismic and Parasound first arrival times were calculated for each channel. These time differences were used as static correction for all CDP gathers, automatically including both streamer and source statics. Finally, the main processing was done as described for the GI Gun.

Processing of the data presented in this study was carried out using a CDP distance of 10 m for the short profiles presented in Chapter 3 and 20 m for the long profiles presented in Chapter 4. These values lead to 7-9 fold coverage for the short profiles and 13-15 fold coverage for the long profiles, chosen as a compromise between high lateral resolution, improvement of signal/noise ratio and manageability of the large data files. Velocity analysis revealed that due to the combination of a relatively short streamer and water depths between 2500 m and 3750 m, a NMO correction with a constant velocity of

1500 m/s could be applied. Interpretation of the seismic data was carried out with the commercial software package Kingdom Suite 7.2 (Seismic Micro Technology, Inc.).

1.2.2 The digital sediment echosounder Parasound

The Parasound system is a hull-mounted sediment echosounder permanently installed on R/V Sonne. The system makes use of the parametric effect by emitting two high-amplitude, high frequency sound-waves, which generate a secondary sound-wave of the difference frequency. The secondary wave is concentrated in a small cone (of the high frequency wave) with an aperture of only 4° (3 dB points). Therefore, the Parasound system provides an excellent lateral resolution of only ~7% of the water depth. Difference frequencies between 2.5 and 5.5 kHz can be generated, the data presented in this study were collected using 4 kHz. Resulting from this frequency, the vertical resolution of the Parasound system is on the order of a few decimeters. Depending on the sediment type, signal penetration varies between 10 and 200 m (Grant and Schreiber, 1990). To ensure vertical sound transmission, the system is roll, pitch and heave compensated. The data were digitally recorded with the software ParaDigMA for further processing and display (Spieß, 1993). Sampling rate of the digitized data is 40 kHz. Processing of the data includes bandpass filtering from 2-6 kHz to remove acoustic and electronic noise and graphical filter methods to enhance display quality.

1.2.3 The swath sounding system Hydrosweep

As the Parasound system, the Hydrosweep swath sounder is a hull-mounted system permanently installed on R/V Sonne. Generating 59 pre-formed beams over an angle of 90°, the system provides depth information for a swath with a width of twice the water depth (Grant and Schreiber, 1990). Each beam is characterized by the same aperture of 2.3°, therefore the footprints of the distinct beams increase from the central to the outer beams. The footprints for water depths around 2500 m as bathymetric data presented in Chapter 2 varies between 90 m and 200 m from the center to outer parts of the swath. The operating frequency of the Hydrosweep system is 15.5 kHz. Depth errors of the outer beams due to refraction were avoided using a patented calibration process. The system generates a fore-aft looking swath at regular intervals. Depth values of this swath were compared to stored values of the central beam. By calculating a best fit of the central beam and the fore-aft profile, Hydrosweep estimates a mean sound velocity, which is used for computation of all depth values. This configuration ensures that residual depth errors are less than 0.5% of the water depth (Grant and Schreiber, 1990).

Processing of the Hydrosweep data was carried out with the public-domain software package MultiBeam, including correction of the navigation data and editing of the depth values (Caress and Chayes, 1996). For editing, MultiBeam provides automatic as well as interactive tools. Automatic tools were used to delete bad outer beams and abnormal depth values or slope gradients within one swath. Systematic errors associated to distinct beam numbers producing so-called rails, i.e. depth shifts parallel to the cruise track, were

eliminated or reduced by an additional tool developed from H. v. Lom, University of Bremen. Finally, a time-intensive interactive editing was carried out. All processing steps had to be carried out carefully, since bathymetric structures in the study area and artifacts are on similar scales. After processing, data were gridded and displayed with the public domain software package GMT (Wessel and Smith, 1998).

1.3 The Bengal Fan: Geometry and development as functions of tectonics and climate

The formation of the Bengal Fan started in the early Eocene as result of the uplift of the Himalayas and the Tibetan plateau due to the collision of India with Asia (Curray and Moore, 1971; Curray, 1994; Curray et al., 2003). The fan is recently mainly fed by the Ganges and Brahmaputra rivers, which drain the northern and southern slope of the Himalayas and have built up a large delta in the Bengal Basin (Fig. 1.1). Discharging more than 1 x 10^9 t/yr of sediment load, this river system is today ranked first among all rivers in the world (Milliman and Meade, 1983). The sediment discharge reaches the deep sea fan through a canyon deeply incised into the shelf, the „Swatch of No Ground“ (SoNG, see Fig. 1.1) (Kottke et al., 2003; Kudrass et al., 1998; Michels et al., 2003). Two distinct fans are recognized, separated by the Ninetyeast Ridge. The eastern fan is called the Nicobar fan and has been inactive since Mid-Pleistocene times due to the convergence of the Ninetyeast Ridge with the Sunda Trench (Fig. 1.3) (Curray et al., 2003). The following descriptions will therefore concentrate on the fan western of the Ninetyeast Ridge, the Bengal Fan in the strict sense.

1.3.1 Geometry and morphology

The Bengal Fan is bordered to the west and north by the continental slope of eastern India and the continental slope of Bangladesh (Fig. 1.1). The eastern margin is defined by the northern end of the Sunda Trench and the accretionary prism of the Sunda Subduction Zone (Curray et al., 2003). This prism spans from the Indoburman Ranges in Myanmar (former Burma) over the Andaman Nicobar Ridge to the Mentawai Islands southwest of Sumatra (Fig. 1.3). The apex of the fan is located at 20°N in 1400 m water depth and the distal boundary is mapped at ~7° S in water depths of almost 5000 m (Fig. 1.1) (Curray et al., 2003; Emmel and Curray, 1985). Krishna et al. (2001a) placed the southern boundary at 7°40´S based on long north-south seismic profiles. Moreover, sediments attributed to the Bengal Fan and/or Nicobar Fan were also drilled at DSDP Site 211 near 10°S (see Fig. 1.3) and Himalayan-derived silicate detritus was even found on a seamount in the Central Indian Ocean at 12°57´S (Banakar et al., 2003; Curray et al., 2003). However, the length of the fan reaches at least 2800 km, the width varies between 1430 km at 15°N and 830 km at 6°N (Fig. 1.1) and the maximum thickness of post-collision sediments is 16 km near the shelf break (Brune et al., 1992; Curray, 1994; Curray et al., 2003). Therefore, the Bengal Fan covers an area of approximately 2.8–3.0 x 10^6 km^2 and has a volume of 12.5

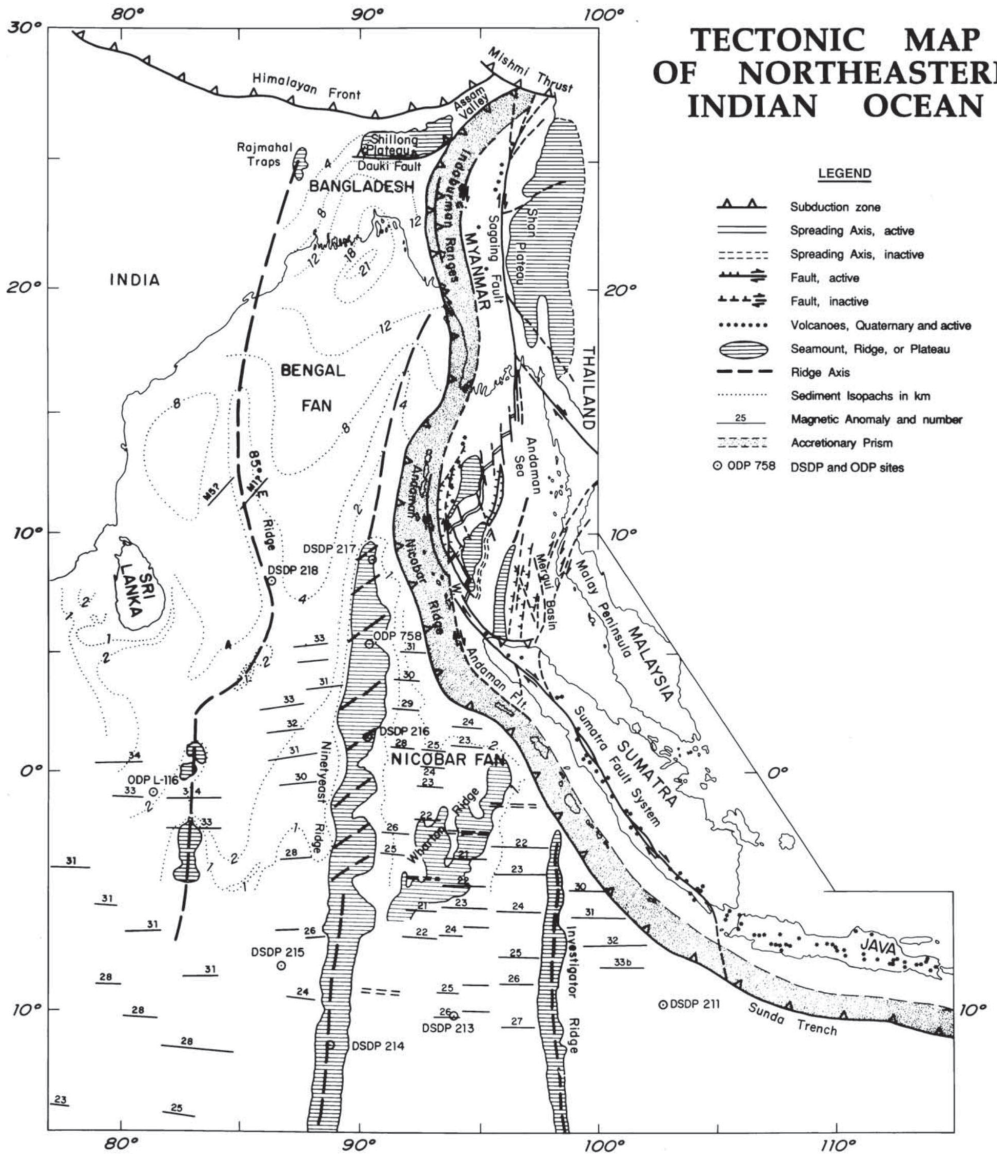

Figure 1.3: *Tectonic map of the Bay of Bengal and adjacent areas from Curray et al. (2003).*

x 10^6 km^3 of post-collision sediments, making it the largest sediment fan on Earth (Curray, 1994; Curray et al., 2003).

The surface of the Bengal Fan is characterized by numerous leveed turbiditic channels. Based on seismic and hydro-acoustic data collected between 1968 and 1986, Curray et al. (2003) mapped the most prominent surface channels (Fig. 1.4). As known from other submarine fans, only one active channel exists, connecting the lower fan to the supplying shelf canyon (Babonneau et al., 2002; Emmel and Curray, 1985; Pirmez and Flood, 1995). On the Bengal Fan, the active channel can be traced downfan to the equator over a distance of 2220 km (Curray et al., 2003). Frequent avulsions on the upper fan caused the formation of new channel-levee systems and abandonment of the former active channel. The number of channels decreases downfan due to reoccupation of older channels by the active channel, leading to a tributary pattern of channels (Fig. 1.4) in contrast to a distributary pattern observed on other fans, as for example for the Amazon Fan (Curray et al., 2003; Pirmez and Flood, 1995).

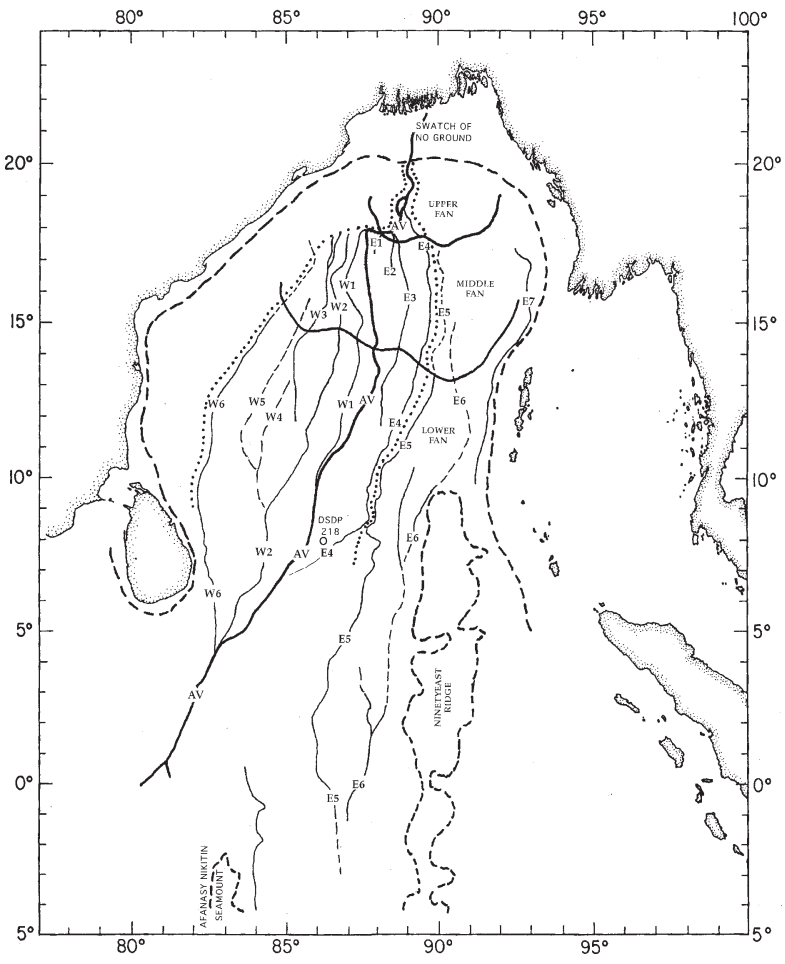

Figure 1.4: *Map of the surface channels on the Bengal Fan and its subdivisions. Thick line (AV) represents the active channel; dashed lines are less certain channels. Heavy dashed line marks the shelf edge and bathymetric heights. Dotted line borders the most recently active subfan. From Curray et al. (2003).*

The Bengal Fan has been divided into three subfans (Figure 1.4) (Curray et al., 2003; Emmel and Curray, 1985). The upper fan is characterized by an averaged channel gradient of ~2.39 m/km and a fan gradient of about 5.7 m/km. The talweg of the active channel has aggraded above the level of the fan beside the levees. In contrast, the active channel on the middle fan is characterized by a talweg cutting into the fan surface, and the channel gradient as well as the fan gradient average around 1.68 m/km. The boundary between upper and middle fan is defined by this transition of the active channel, from a depositional to an erosional system. Furthermore, a significant decrease of the channel cross-sectional area occurs at the boundary between upper and middle fan, which follows approximately the 2250 m water depth contour. At about 2900 m water depth, the boundary between the middle and the lower fan was placed based on a drop of the gradients to less than about 1 m/km. Curray et al. (2003) used these channel gradients to estimate velocities for large turbidity currents traveling through the active channel. They calculated a velocity of 10 m/s for the upper fan, 5.1 m/s for the middle fan and 4.0-4.4 m/s for the lower fan. As a result of these estimates, a large turbidity current would need 72 hours to reach the end of the active channel near the equator (Curray et al., 2003).

1.3.2 Initiation of fan deposition and Tertiary growth

The initial development of the crust underlying the Bengal Fan started with the breakup of Gondwanaland in the Early Cretaceous and the following separation of Greater India from Antarctica. From magnetic anomalies and plate tectonic reconstructions, this separation event was dated to 120 Ma (Curray and Moore, 1971; Gopala Rao et al., 1997; Lee and Lawver, 1995; Moore et al., 1974). Coincident with the separation, the Kerguelen hot spot created a large eruption of continental flood basalts on the Indian subcontinent, the Rajmahal traps (Figs. 1.1 and 1.3) (Gopala Rao et al., 1997). First drifting in NW-direction,

India changed at ~95±5 Ma the movement to a more northward direction (Gopala Rao et al., 1997). After this plate reorganization, the Indian plate was affected during its northward journey by two hot spots producing two volcanic ridges, the 85°E-Ridge and the Ninetyeast-Ridge (Krishna, 2003; Krishna et al., 2001b). The Ninetyeast Ridge was formed by the Kerguelen hot spot between 95±5 Ma and 38 Ma directly beneath the spreading center on the young oceanic crust (Gopala Rao et al., 1997; Krishna et al., 2001b). In contrast, the 85°E Ridge was created in intraplate position on old oceanic crust according to a new scenario published by Krishna (2003). Following this scenario, the formation started at 85 Ma in the northern Bay of Bengal at the ocean-continent boundary, and terminated at 60 Ma at the position of the Afanasy Nikitin Seamount located at 5°S (Fig. 1.5) (Krishna, 2003). However, other authors connected the 85°Ridge with the Rajmahal traps (see Fig. 1.3) and postulated that both are produced by the Crozet hot spot, now located near the Crozet Islands (Curray et al., 2003; Curray and Munasinghe, 1989; Subrahmanyam et al., 1999).

Further northward drifting of India closed the Tethian Ocean and caused finally the first collision with Asia in the Mid-Paleocene (~59 Ma) and the initial creation of the Bay of Bengal (Alam et al., 2003; Curray et al., 2003; Lee and Lawver, 1995). Prior to the collision, a thick continental rise prism of pre-Eocene pre-Bengal Fan sediments was deposited off the east coast of India (Curray et al., 2003). The first collision phase is a „soft collision“ between the northernmost part of the Indian Shield and the southern part of Tibet (Fig. 1.6). In the middle Eocene at ~44 Ma, the collision changed to a „hard“ continent-continent collision and the orogeny of the Himalayas began (Alam et al., 2003; Lee and Lawver, 1995). In the Bengal Basin, the influx of clastic sediments rapidly increased at this time (Alam et al., 2003). Consequently, the development of the Bengal Fan started probably in middle Eocene during ongoing collision at the northern end of the Bay of Bengal and continued by progradation until present. This onset of real post-collision Ben-

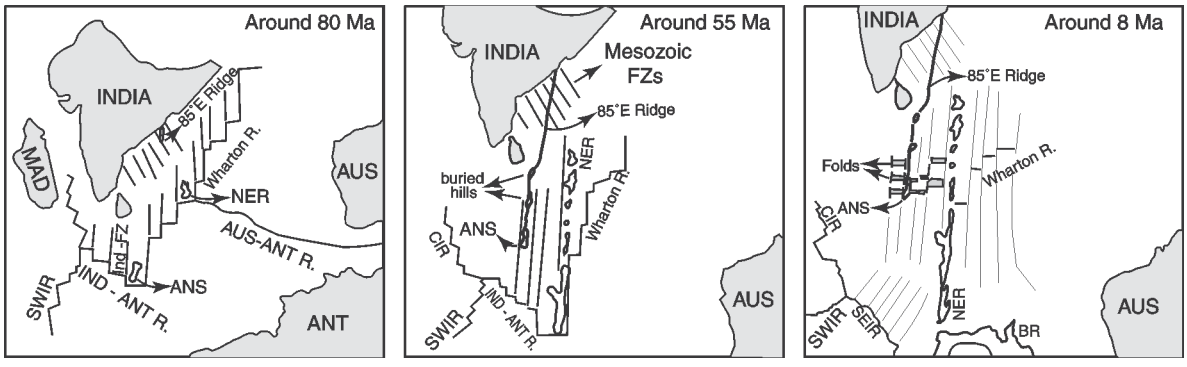

Figure 1.5: *Sketch displaying the development of the 85°E Ridge and the Ninetyeast Ridge during northward drifting of India. ANS=Afanasy Nikitin Seamount, NER=Ninetyeast Ridge, SWIR=Southwest Indian Ridge, SEIR=Southeast Indian Ridge and CIR=Central Indian Ridge. At 80 Ma (Left), constructing of the 85°E Ridge by a hotspot in the northern Bay of Bengal and formation of the ANS occurred simultaneously. The Kerguelen hotspot formed the NER. Around 55 Ma (Middle), the hotspot forming the 85°E Ridge reached the ANS and ceased, the Kerguelen hotspot was still forming the Ninetyeast Ridge. In the late Miocene (Right), a deformation event caused long-wavelength folds and the convergence of the ANS. From Krishna (2003).*

gal Fan deposition is marked by a strong unconformity traced through the whole fan (Curray, 1994; Curray et al., 2003; Curray and Moore, 1971; Moore et al., 1974). Drilling of this unconformity at the very distal fan (DSDP 211 and 215, see Fig. 1.3), at the Indoburman Ranges and at the Andaman Nicobar Islands revealed a hiatus, which spans from Paleocene to middle Eocene at the Indoburman Ranges, from Paleocene to late Eocene at the Andaman Nicobar Ranges, from Paleocene to late Miocene at DSDP 215 and from Paleocene to Pliocene at DSDP 211. Therefore this hiatus is thought to represent a phase of non-deposition, which separates the sediments into the pre-Eocene pre-collision fan and the post Paleocene post-collision fan. Due to the prograding character of the fan, the hiatus is longer with increasing distance from the apex of the fan (Curray, 1994; Curray et al., 2003). However, drilling on the Lower Fan at DSDP Site 218 and ODP Leg 116 did not reach the base (Cochran, 1990; Curray et al., 2003; Stow et al., 1990; von der Borch et al., 1974), therefore the real onset of development of the Bengal Fan itself is not confirmed by drilling yet.

By the early Miocene (22 Ma), a major collision between India and Tibet in the north and between India and Burma in the east occurred (Fig. 1.6). As a result, the Bengal Basin obtained the shape of a remnant ocean basin and rapid uplift of the eastern Himalayas and the Indoburman Ranges took place, causing significantly increased sedimentation in the Bengal Basin (Alam et al., 2003). Oldest sediments drilled in the Bengal Fan are dated to 17 Ma, found in Hole 718 of ODP Leg 116 (Stow et al., 1990). Since then, turbiditic sedimentation dominated at the location of ODP Leg 116, and provenance studies revealed that most of the material was derived from erosion of the Himalayas (Cochran, 1990; Derry and France-Lanord, 1996; Stow et al., 1990). Nd and Sr isotopic data show that the primary source has been the High Himalayan Crystalline throughout the deposition of ODP Leg 116 sediments (Derry and France-Lanord, 1996). In late Miocene (7.5-8 Ma), the sediments were affected by intraplate deformation of the Indian Ocean lithosphere leading to a strong unconformity visible in seismic data (Cochran, 1990; Curray et al., 2003; Curray and Moore, 1971; Gordon et al., 1998; Krishna et al., 2001a; Moore et al., 1974). This deformation is caused by concentration of compressional stress related to the continuing collision of India with Asia and has been inter-

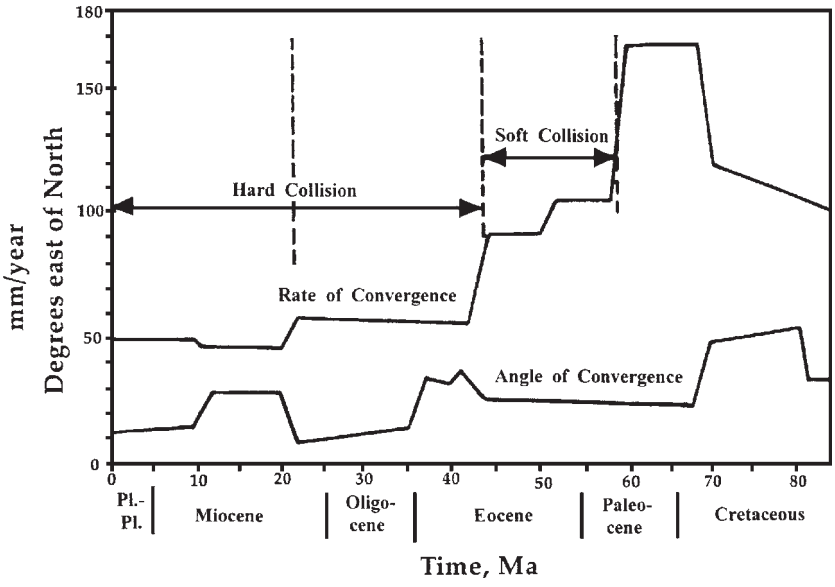

Figure 1.6: *Rate and angle of convergence between India and Asia. Abrupt changes indicate collision events. Modified from Alam et al. (2003) and Lee and Lawver (1995).*

preted as diffuse plate boundary due to splitting of the Indo-Australian Plate into the Indian, Australian, and Capricorn plates (Gordon et al., 1998; Krishna et al., 2001a).

Sedimentation of silty turbidites with high accumulation rates at ODP Leg 116 from early Miocene to latest Miocene suggest rapid erosion and thus continuing uplift of the Himalayas during this period (Cochran, 1990). In the latest Miocene around 7 Ma, a significant change of sedimentation occurred: lithology changed from silty to muddy, grain size and sedimentation rates decreased, smectite replaced illite as the dominant clay and $\delta^{13}C$ values of organic carbon increased (Cochran, 1990; Derry and France-Lanord, 1996; France-Lanord and Derry, 1994; Stow et al., 1990). Cochran (1990) interpreted the decrease of sedimentation rate and the lithological change as a result of mean sea-level rise occurring at that time, which shifted the depocenter landwards and cut off the sediment delivery from the shelf. From the change in clay mineralogy, Derry and France-Lanord (1996) concluded that at 7 Ma the erosional regime changed from physical erosion to chemical weathering suggesting that sediment residence time in the flood plain foreland increased and erosion rates in the Himalayas decreased. The change of $\delta^{13}C$ values of organic carbon reflects a change in vegetation from C3 to C4 plants indicating that floodplain weathering took place in soils stabilized by C4 grasses (Derry and France-Lanord, 1996; France-Lanord and Derry, 1994). Finally, the decreased erosion rates may be caused by a reduction in the tectonic uplift rate of the Himalayas around 7 Ma (Derry and France-Lanord, 1996). Synchronous to the changes in marine deposition, an intensification of the Asian monsoon has been observed, but the detailed relationship between both events is presently not completely understood (Derry and France-Lanord, 1996).

Parallel to environmental changes and deformation events in the Indian Ocean, major tectonic events were thought to have occurred in the Himalayas between 7 and 8 Ma, namely a rapid uplift of the Tibetan Plateau and the initiation of east-west extension. The initiation of slip along the largest dated normal fault within Tibet started at ~8 Ma, and a rejuvenation of the Main Central Thrust was also suggested for ~8 Ma (Harrison et al., 1992; Harrison et al., 1995; Harrison et al., 1998; Pan and Kidd, 1992). This change of deformation style is maybe the result of a rapid uplift of the Tibetan Plateau by at least 1000 m due to convective processes in the mantle lithosphere (Harrison et al., 1995; Molnar et al., 1993). However, the described changes in sediments from ODP Leg 116 at ~7 Ma, especially the decrease of sedimentation rate and grain size, do not seem to be an expected result of a rapid uplift scenario.

In the Mid-Pliocene, a new sedimentation phase began in the Bengal Basin with a rapidly increased sedimentation rate filling quickly large troughs. Finally, a fluvio-deltaic environment established, followed by the development of the present basin configuration in the late Pliocene (Alam et al., 2003). In the Bengal Fan, lithology of the ODP Leg 116 changed in the Pliocene for a short period back to coarser silty turbidites (Cochran, 1990; Stow et al., 1990). Concurrently, another deformation event of the Indian Ocean lithos-

phere occurred in the Pliocene at 4.0-5.0 Ma, maybe linked with the change of turbidites (Krishna et al., 2001a).

1.3.3 Pleistocene development

In the Mid-Pleistocene (~1 Ma), sedimentation reversed to similar characteristics as prior to 7 Ma, in particular, lithology changed from muddy to silty, sedimentation rate increased, grain-sizes increased and the dominant clay switched back from smectite to illite (Cochran, 1990; Derry and France-Lanord, 1996; Stow et al., 1990). These changes are attributed to a marked intensification of glaciations, both global and regional. The more intense glacial variations produced greater sea-level variations, which may have caused the complete exposure of the shelf during glacial maximums and therefore a direct delivery of the river sediment load to the fan (Cochran, 1990). Moreover, the intensification of glaciation in the Himalayan region led to decreasing weathering intensity and in addition, the following increase of physical erosion suggests an increase in the tectonic rate of uplift after the Mid-Pleistocene (Derry and France-Lanord, 1996). As in Mid-Pliocene, a deformation event within the Indian Ocean lithosphere occurred simultaneously with the change in sedimentation character (Krishna et al., 2001a).

Within the Upper Fan Pleistocene sediments, four distinct units (channel-levee complexes) can be distinguished by seismic stratigraphy (Curray et al., 2003). Tracing of the bases of complexes to DSDP Site 218 revealed an age of 1.9 Ma to 0.96 Ma for the oldest complex, followed by the second complex built up between 0.96 Ma and 0.465 Ma and the third complex developed between 0.465 Ma and 0.125 Ma. Consequently, the present complex started about 125,000 years ago according to Curray et al. (2003). The four complexes show lateral shifting due to shifting of the location of the supplying canyon, which is determined by the location of river mouths at sea-level lowstands. In contrast, during highstands and falling sea level rivers are free to select a new course (Curray et al., 2003). In contrast to the present channel-levee complex, the three older complexes had more than one canyon, but it is not clear, if the canyons were active simultaneously or sequentially. However, each canyon fed only one active channel-levee system at any given time (Curray et al., 2003). The existence of more than one canyon suggests that several rivers may have flowed separately into the Bay of Bengal during much of the Pleistocene (Curray et al., 2003).

1.3.4 Holocene build-up and processes

Substantial insights into the transport and depositional processes on the shelf and fan of the sediments delivered by the Ganges and Brahmaputra during the Holocene resulted from geological and geophysical investigations during SO 93 and SO 126 Cruises (Hübscher et al., 1998; Hübscher et al., 1997; Kottke et al., 2003; Kudrass et al., 1998; Michels et al., 1998; Michels et al., 2003; Weber et al., 1997; Weber et al., 2003; Wiedicke et al., 1999). Main results describe the activity of the fan during the Holocene sea-level rise and highstand including transport processes of sediments from the delta to the deep

sea across the flooded shelf. In particular, it has been shown that the outer levees bordering the active channel at 16°30´N mainly grew between 12,800 and 9,700 yr B.P., and a 7 m long core from the inner part of the channel-levee system at this location recovered only sediments deposited during the Holocene (Hübscher et al., 1997; Weber et al., 1997). Gravity cores from the Lower Fan in the vicinity of the active channel revealed also turbiditic activity during the Holocene (Weber et al., 1997; Weber et al., 2003). In contrast, Holocene sediments away from the active channel are of pelagic or hemipelagic origin (Weber et al., 2003). However, the Bengal Fan shows significant growth during the most recent sea-level rise and highstand at least along the active channel-levee system, which is in contrast to common sequence stratigraphic models (Hübscher et al., 1997; Weber et al., 1997; Weber et al., 2003).

The transport of the sediments from the delta to the deep-sea fan takes place through the Canyon “Swatch of No Ground” deeply incised into the shelf (Fig. 1.1). The head of the canyon is located 30 – 35 km off the coastline and 100 km west of the main delta of the Ganges and Brahmaputra Rivers, which join 150 km upstream of the shoreline (Kottke et al., 2003; Kudrass et al., 1998; Michels et al., 2003). Since the onset of sea-level rise and the development of the Ganges-Brahmaputra delta 10,000 - 11,000 yr BP, the canyon is not directly connected to the rivers (Goodbred Jr. and Kuehl, 2000a; Goodbred Jr. and Kuehl, 2000b). Two processes delivered the sediments from the river mouth to the canyon: During fair weather conditions, tidal currents transported plumes of suspended river load to the canyon, during stormy weather conditions, sediment was resuspended on the inner shelf and transported by storm-generated bottom currents towards the canyon. In both cases, currents lost most of the suspended particles in the deep water of the canyon and sediments were trapped in the canyon (Kudrass et al., 1998; Michels et al., 2003).

High sedimentation rates up to 50 cm/yr as found in the canyon head would result in a complete fill of the canyon during a few centuries. Therefore, an export of the sediments from the canyon to the deep sea must have occurred at regular time intervals, and the canyon consequently acted only as a temporary trap (Kudrass et al., 1998; Michels et al., 2003). Bathymetric data, sediment echosounder data and gravity cores indicate first, that continuous transport occurred within the canyon by gravity driven currents, and second, that episodic transport occurred by low-density turbiditic currents as well as slumps and slides (Kottke et al., 2003; Michels et al., 2003). These episodic transports were triggered by catastrophic events like earthquakes on decennial to centennial time scale and removed large amounts of sediments out of the canyon to the deep-sea Bengal Fan (Kottke et al., 2003; Michels et al., 2003). As a result of the described transport mechanism, 30-50% of the sediment river load was guided through the canyon to the fan (Goodbred Jr. and Kuehl, 2000a; Michels et al., 1998).

During Holocene, the sediment transport was strongly influenced by the development of the river delta in the Bengal Basin. Before 15,000 yrs BP, the river discharge was greatly reduced due the arid climate in south Asia, and therefore sediment transport to the fan

was also reduced in spite of the direct connection between Ganges-Brahmaputra rivers and the “Swatch of No Ground” (Goodbred Jr. and Kuehl, 2000a; Goodbred Jr. and Kuehl, 2000b). The following intensification of the southwest monsoon led to a more humid climate and an enormous river discharge in the early Holocene (11,000–7,000 yr BP) of at least 2.3 x higher than present (Goodbred Jr. and Kuehl, 2000a). Parallel to this strengthening of the humid climate, the levee growth of the active channel occurred mainly between 12,800 and 9,700 yr BP during sea-level rise (Weber et al., 1997). Continuing rapid sea-level rise extended the accommodation space in the Bengal Basin. The immense fluvial sediment discharge was sufficient to aggradate the delta and to maintain a relative shoreline stability until 7000 yr BP in contrast to many other deltas (Goodbred Jr. and Kuehl, 2000b). This may have finally led to the deceleration of levee growth on the fan after 9,700 yr BP as reported by Weber et al. (1997).

After 7000 yr BP, fluvial sediment load was reduced to values similar to present related to a decrease in strength of the southwest monsoon, and the sea-level rise decelerated. Since then, the delta was characterized by switching between transgression and progradation of both rivers independently. At last, Ganges and Brahmaputra joined around 3000 yr BP and a delta similar to the present system developed (Goodbred Jr. and Kuehl, 2000b). Transgression and progradation of the delta were both mainly controlled by fluvial input and local tectonics, i.e. subsidence of inland tectonic basins, which trapped sediments, and uplift of terraces, which affected river switching (Goodbred Jr. and Kuehl, 2000b). Generally, sedimentation in the Bengal Basin during Holocene was controlled by an interaction of not only regional tectonics and sea-level rise, but also by local tectonic events and local climatic changes, which both influenced sediment delivery and sediment storage (Allison et al., 2003; Goodbred Jr. and Kuehl, 2000a; Goodbred Jr. and Kuehl, 2000b; Goodbred Jr. et al., 2003; Heroy et al., 2003). These processes primarily affected the Bengal Basin, but thereby also an impact on the development of the Bengal Fan during the Holocene must be expected.

1.4 Development and architecture of channel-levee systems

Channel-levee systems have been found in the upper parts of large submarine fans, such as the Amazon Fan (Damuth et al., 1988; Flood et al., 1991; Pirmez and Flood, 1995), the Congo Fan (Babonneau et al., 2002; Droz et al., 1996), the Mississippi Fan (Twichell et al., 1991; Weimer, 1991), the Indus Fan (Kenyon et al., 1995; Kolla and Schwab, 1995) and last but not least the Bengal Fan (Emmel and Curray, 1985). Therefore, it can be stated that channel-levee systems are main architectural elements of such fans. Common to all these fans is the existence of a canyon incised into the shelf, acting as a point source for turbidity currents (Bouma, 2001; Richards et al., 1998).

1.4.1 Initial development

Self-channelization of turbidity currents after leaving the canyon is the initial step to build-up channel-levee systems. This process, based on the simultaneous deposition and

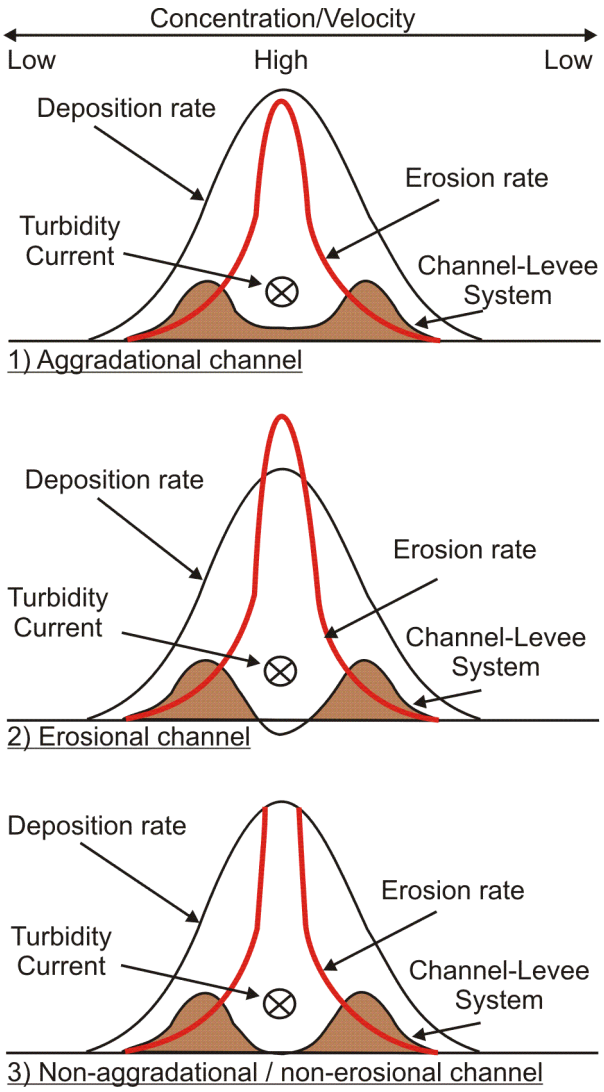

Figure 1.7: *Mechanics of channel-formation by different erosion and deposition rates perpendicular to the flow direction due to decreasing concentration and velocity from the center to each side of the flow. Modified from Imran et al. (1998).*

erosion by turbidity currents, was numerically modeled by Imran et al. (1998): When the turbidity currents depart the canyon, they also spread laterally across to the main flow direction, and thus the concentration and the velocity of the current decrease from the center of the flow to either side (Fig. 1.7). Since the deposition rate reveals a linear dependency on the concentration, but the erosion rate depends on the velocity to a power that is at least 2, erosion rate decreases more rapidly in the transverse direction than the deposition rate. As a result, the net deposition is minimized along the extended axis of the canyon in the center of the flow, and maximized towards both sides of the center of the flow (Fig. 1.7).

Depending on the ratio of deposition rate to erosion rate, the channel floor can incise into the preexisting seafloor, can be stable or can rise above the surrounding areas (Fig. 1.7). The model run also revealed that the main parameters controlling the self-channelization are the gradient of fan slope and the grain size. On lower fan slopes, smaller grain sizes favor channelization. As a further result of this model, a succession of turbidity currents, each with a relatively long body, is required for an effective construction of levees bordering the channel (Imran et al., 1998).

1.4.2 General morphology

After initial development, channels tend to meander as is observed from all submarine fans, which are not tectonically controlled (Clark et al., 1992). Compilation of channel sinuosities from several fans shows, that maximum sinuosity is reached at a distinct valley slope, and this threshold seems to be a characteristic parameter for each submarine fan (Clark et al., 1992). Generally it can be stated that channels seek for a smooth longitudinal profile to be in an equilibrium state with turbidity currents and their sediment load (Babonneau et al., 2002; Lopez, 2001; Pirmez and Flood, 1995). To reach this equilibrium slope, mainly two processes occur: changes of the channel sinuosity and incision or aggradation of the channel talweg. Concurrently, morphology and geometry of the channel depend on current parameters as velocity, density and frequency. These parameters of the

turbidity currents were in turn modified during their passage through the channel by deposition of suspended material, entrainment of ambient seawater or erosion of sediments. Obviously, changes in turbidity currents lead to changes of morphological parameters as slope or sinuosity, on the other hand, changes of these morphological parameters, for instance due to avulsions, affect the turbidity currents parameter. Therefore, an interaction between both parameter sets controls finally the appearance of submarine channels (Babonneau et al., 2002; Clark et al., 1992; Lopez, 2001; Peakall et al., 2000a; Pirmez and Flood, 1995).

1.4.3 Architecture and evolution of sinuous channels

Based on seismic data imaging the youngest channel on the Mississippi Fan (Kastens and Shor, 1985; Stelting et al., 1985), a three-stage model for the development of medium- to high-sinuosity, aggradational submarine channels has been developed by Peakall et al. (2000a; 2000b). Following this model (Fig. 1.8), the initial stage is characterized by lateral migration at bend apices with accumulation of channel talweg deposits, possibly accompanied by point-bar development. The second stage is an equilibrium phase with a stable planform geometry and nearly vertical aggradation. During this stage, the channel acts mainly as a bypass zone. The last stage is an abandonment phase with channel filling by mass-flow deposits or hemipelagic sediments (Fig. 1.8). From their analysis, Peakall et al. (2000a; 2000b) concluded first, that downstream movement of submarine channel bends does not occur and bend crossover points are locally stable, and second, that cut-off loops are not common in submarine channels. Both results distinguish submarine channels significantly from subaerial channels (Peakall et al., 2000a; Peakall et al., 2000b).

From studies of Quaternary and Tertiary West African fans with 3-D seismic, Kolla et al. (2001) present a variety of sinuous channel developments (Fig. 1.9). The identified channel behaviors are separated into elementary channel migrations and complex channel migrations, both producing sinuous loops. Generally, channels develop by channel aggradation and lateral migration with varying ratios. Following the terminology of Kolla et al. (2001), elementary migrations show generally the same behavior from the beginning to the end of loop creation, i.e., the same ratio between vertical and lateral movement. Complex migrations are characterized by more than one type of elementary channel behav-

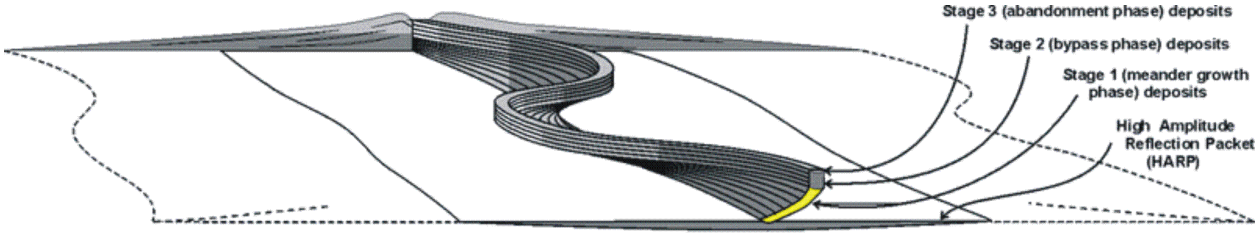

Figure 1.8: *Block model of bend evolution and sedimentary architecture based on data from Mississippi Fan. Three evolutionary stages are found for aggradational, sinuous submarine channels. From Peakall et al. (2000a).*

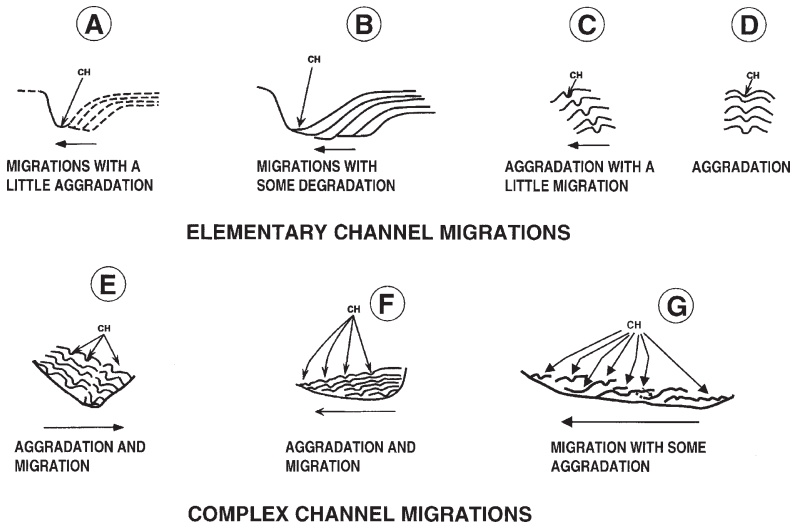

Figure 1.9: *Sketches of different channel behaviors at a sinuous loop in cross sections. Elementary channel migrations (A-D) show the same behavior from start to end of migration. Complex channel migrations (E-F) consist of more than one elementary channel behavior. Sketches base on 3-D seismic data from West African fans. From Kolla et al. (2001).*

iors, i.e., the ratio between vertical and lateral migration varies within a single sinuous loop (Fig. 1.9). Once reaching the maximum sinuosity, just aggradation may occur, or cut-offs may occur, or channel avulsion with following construction of a new channel segment may occur (Kolla et al., 2001).

Like Peakall et al. (2000a; 2000b), Kolla et al. (2001) pointed out the difference between submarine and subaerial channels, but emphasize on the different modes of sinuosity evolution: migration of submarine channels occurs complex and show different modes as described, but subaerial channel migration is characterized by only lateral movement. Even if at least one cut-off loop appears in their data, Kolla et al. (2001) stated that cut-off loops are not as common in submarine fans, which agrees with the model of Peakall et al. (2000a; 2000b) and results from the Indus and Mississippi fan (Kenyon et al., 1995; Weimer, 1991). However, some cut-off loops were identified at the youngest channel on the Amazon fan (Pirmez and Flood, 1995), and numerous cut-off loops have been observed at the Congo fan (Babonneau et al., 2002).

1.4.4 Avulsion processes and the resulting depositional pattern

Distributary patterns of channels found on several submarine fans as Amazon, Bengal, Congo, Mississippi or Danube fans suggest that avulsions are important processes on submarine fans and significantly control the distribution of sediments (Babonneau et al., 2002; Curray et al., 2003; Emmel and Curray, 1985; Kenyon et al., 1995; Popescu et al., 2001; Twichell et al., 1991). The best-studied example of such processes is the Amazon Fan, where seismic data were ground-truthed with coring of 17 sites during ODP Leg 155 (Flood et al., 1995). Results are summarized in a model from Lopez (2001), which bases mainly on studies of Flood et al. (1991), Pirmez and Flood (1995), and Hiscott et al. (1997) (Fig. 1.10).

Before avulsion, the channel floor aggrades by deposition of massive to graded sand sequences above the level of the surrounding areas between the channel-levee systems. These sands within the channel floor are recognized in seismic data as High Amplitudes Reflections (so-called HARS). As mentioned earlier, aggradation and sinuosity generate an equilibrium profile of the channel floor. Intense erosion by turbidity currents causes

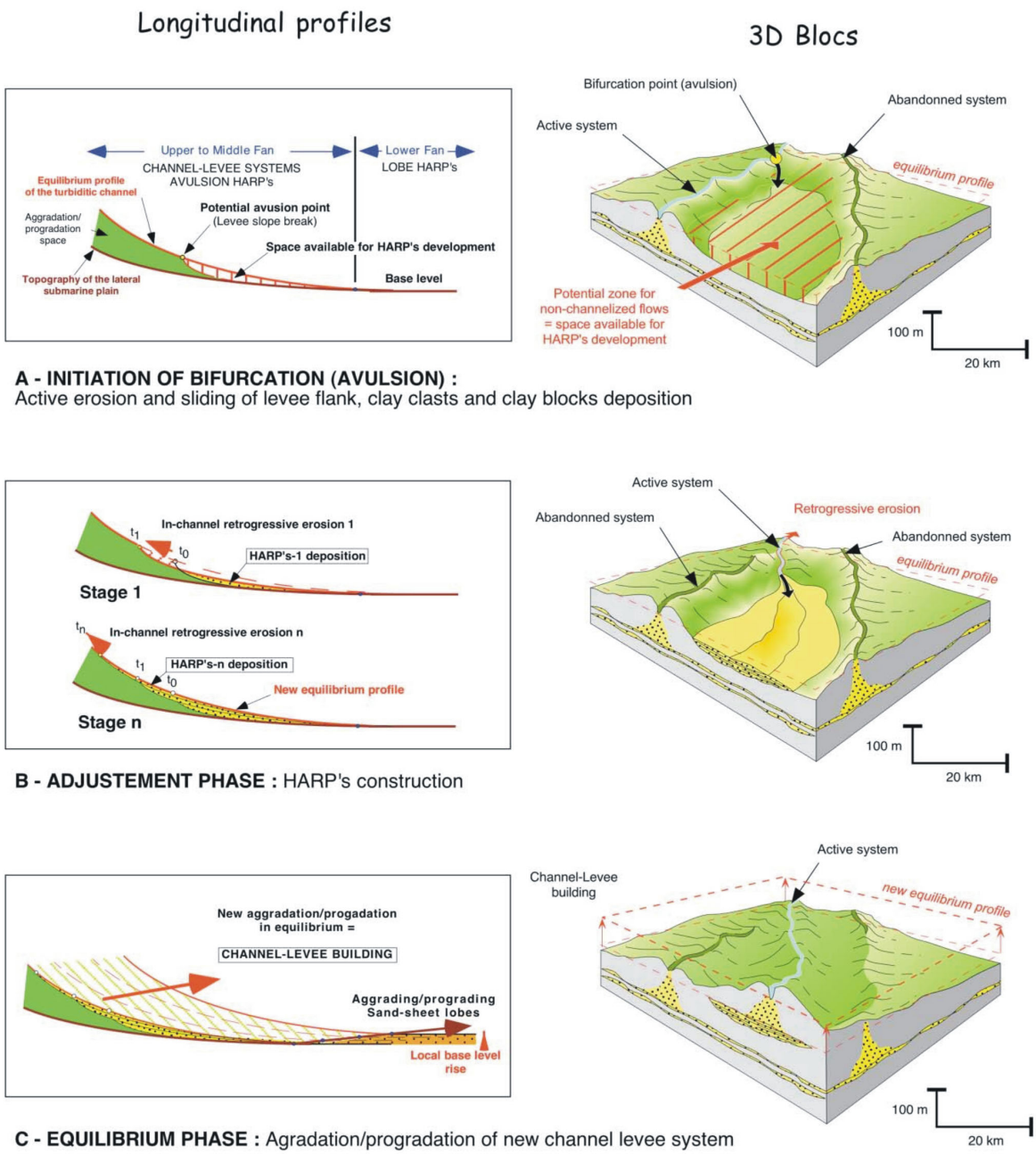

Figure 1.10: *Schematic channel profiles and block diagrams illustrating avulsion processes and resulting construction of HARPS and new channel-levee systems on quaternary Amazon Fan. From Lopez (2001).*

inner levee slope failures, sediment overflow and finally levee breaching (Fig. 1.10 A). The turbidity currents spread non-channelized into the intrachannel lows and form sheet-like bodies. The avulsion leads to a knickpoint in the channel profile and disrupts its equilibrium. In the following adjustment phase, the system reaches a new graded profile by intrachannel retrogressive erosion upslope of the knickpoint and rapid deposition downslope of the knickpoint (Fig 1.10 B). Since the eroded channel-floor is mainly built up by sand deposits, the sheet-like bodies downslope of the knickpoint consist mainly of sands. These sands appear in seismic profiles as High Amplitude Reflection Packets (so-called HARPS). After reaching a new equilibrium, levees start to grow downfan by progradation from the avulsion point and channelize the turbidity currents. Subsequently, sands are deposited

along the channel axis and fine-grained material is building the levees (Fig. 1.10 C). These autocyclic processes lead finally to the depositional pattern of individual channel-levee systems and HARPS found on the Quaternary Amazon Fan (Lopez, 2001). Similar processes are also confirmed for the late quaternary channel-levee systems on the Danube Fan (Popescu et al., 2001).

1.4.5 Structure and flow of turbidity currents

The nature of turbidity currents building up channel-levee systems is mainly derived from their deposits, since direct observations are certainly rare. Principally, two processes of overbanking of channelized flows are proposed in the literature: a small overspill focused at channel bends or saddles and a quasi-continuous overspill over long distances and time (Fig. 1. 11). The first process was introduced by Piper and Normark (1983) examining data from the Navy Fan, and named as “flow-stripping”. The “flow-stripping” process was explained by the non-ability of the upper part of a turbidity current to follow the channel at a sharp bend, therefore the current splits into two parts, and the upper part continues the flow in pre-bend direction (Piper and Normark, 1983) (Fig. 1.11, left). These processes deposit small units at the outer meander bends and have also been documented from other fans as Amazon Fan (Hiscott et al., 1997), Mississippi Fan (Twichell et al., 1991) or Monterey Fan (McHugh and Ryan, 2000) and additionally from the Northwest Atlantic Mid-Ocean Channel (NAMOC) (Klaucke and Hesse, 1996; Klaucke et al., 1998).

However, based on several observations and tank experiments, Peakall et al. (2000a; 2000b) concluded that a further process of overbanking is required, a “continuous overspill”. These observations include direct measurements in Lake Superior, tracing of individual turbidites over long distances at the NAMOC and on Navy Fan and the observed decrease of channel cross-section areas as well as grain-size distribution in levees on Amazon Fan (Hesse, 1995; Hiscott et al., 1997; Peakall et al., 2000a; Peakall et al., 2000b; Piper and Deptuck, 1997; Piper and Normark, 1983). Additionally, tank experiments show that flows with thicknesses of more than twice the channel depth follow a sinuous channel without flow-stripping (Peakall et al., 2000a). Thus, Peakall et al. (2000a; 2000b) developed a model, which predicts highly stratified turbidity currents with significant supra-levee thickness. These currents form broad overbank bodies of low-concentration fluid traveling along the entire channel length, which lead to the required continuous overspill onto the levees (Fig. 1.11, right).

On the Amazon Fan, complex patterns of echo-facies suggest complicated overspill processes (Hiscott et al., 1997). On the one hand, overspill is focused at outer bends of meanders and at saddles, on the other hand, turbidity currents produce semicontinuous overspill along the whole channel (Hiscott et al., 1997). Nevertheless, it was not possible to correlate individual turbidites between sites of ODP Leg 155, not even over 65 km as shortest distance between two sites (Hiscott et al., 1997). From upper to lower fan, the median grain-size of levees increased with decreasing levee heights, and generally, a fining upward is observed in all levee successions cored during ODP Leg 155 (Flood et

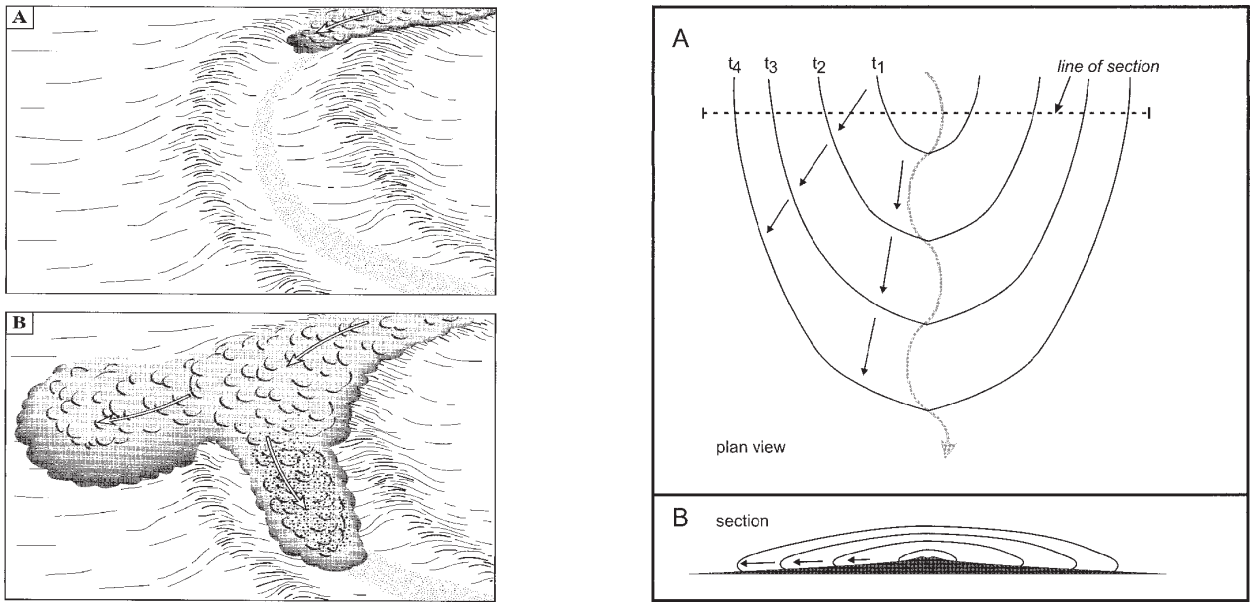

Figure 1.11: *Flow-stripping (left) vs. continuous overspill (right). Left: A flow is unable to follow the bend and splits into two parts. Right: Development of a large overbank fluid wedge with time (t1-t4) as planform view and cross-section view. Both figures are from Peakall et al. (2000a).*

al., 1995; Hiscott et al., 1997). Therefore, a single type of mixed-load turbidity current carrying coarse sand at the bottom and fine mud at the top are thought to have constructed the channel-levee systems on Amazon Fan (Hiscott et al., 1997). If levees are flat, coarser material can overspill as at the begin of levee development or as on the lower fan, where levees are generally flat. If levees on upper and middle fan reach a distinct height, only fine-grained material from the upper part of the currents is able to overspill (Hiscott et al., 1997).

1.4.6 Reservoir potential of channel-levee systems

As mentioned above, turbidity currents flowing through channel-levee systems on submarine fans carry both, sands and muds. During this travel, sands and muds were vertically separated within the flow and therefore deposited in different sedimentary and structural units. Whereas the muds mainly build the levees, the sands construct aggrading channel floors or travel through the full length of the channel to develop lobes at the channel mouth. If avulsion processes occur, sheet-like sand bodies, which appear as HARPS in seismic data, were deposited downstream of the avulsion points. Therefore, channel-fills, HARPS and depositional lobes at the end of the channels have likely potential as hydrocarbon reservoirs (Kolla et al., 2001; Lopez, 2001; Peakall et al., 2000a; Richards et al., 1998).

Based on this conclusion, oil companies increased during the last decade exploration of Cenozoic passive margin submarine fans, i.e. on the Brazilian margin, Gulf of Mexico or along the West-African continental slope (Kolla et al., 2001; Lopez, 2001; Stow and Mayall, 2000). Thereby, the exploration targets shifted from shelf areas to deep water systems in depths between 800 and 2000 m (Lopez, 2001). It is estimated that more than 1200 oil

and gas fields, including discoveries and producing fields, are known in deep water turbidites and related systems (Stow and Mayall, 2000).

On the tertiary Congo Fan, the fills of the highly sinuous channels have been the main exploration targets in the recent years (Kolla et al., 2001). As reported above, these channels are characterized by complex migrations of the sinuous loops, which control the reservoir architecture (see Fig. 1.9). The ratio of lateral migration vs. vertical aggradation determines the extent of lateral vs. vertical stacking of reservoir lithologies (Kolla et al., 2001). Another important factor is the amalgamation of the sand influencing the connectivity of reservoirs. Amalgamation in vertically stacked channel fills result in good vertical reservoir connectivity. Lateral reservoir connectivity also depends on how closely spaced the lateral migrations occurs. If the migrations are discrete and separated, the lateral reservoir continuity is poor. However, lateral migration of loops appears continuous if closely spaced discrete channels are below seismic resolution. Therefore, even channels, which look like continuous migrated in seismic data, may have poor connectivity (Kolla et al., 2001). This example demonstrates that the architecture of submarine channels is complex and therefore the revealing of their true reservoir potential and connectivity is difficult and demands seismic imaging with sufficient detail (Kolla et al., 2001). Therefore, high resolution 3-D seismic data with supplemental coring is required to study the development and architecture of sinuous submarine channels and finally to improve the predictive understanding of reservoirs in deep-sea turbidite systems (Kolla et al., 2001; Lopez, 2001; Stow and Mayall, 2000)

1.5 Outlines

In this section, short outlines for the three manuscripts presented in chapters 2, 3, and 4 are given.

• *Chapter 2: Frequent channel avulsions within the active channel-levee system of the middle Bengal Fan - an exceptional channel-levee development derived from Parasound and Hydrosweep data, T. Schwenk, V. Spieß, C. Hübscher, M. Breitzke. Published in Deep Sea Research II, 2003, Vol. 50, pp. 1023-1045.*

In this manuscript, the active channel-levee system of the middle Bengal Fan is studied by a combined analysis of Parasound echosounder and Hydrosweep swathsounder data. Morphological parameters of the channel are analyzed, and the structure of the levees is examined. The results are used to describe the mechanism and evolution of the built-up of the active channel-levee system mainly controlled by frequent avulsions within the system. The development of the system is then discussed and compared with other submarine fans as the Amazon or Congo fans as well as with theoretical models.

• *Chapter 3: The architecture and evolution of the Middle Bengal Fan in vicinity of the active channel-levee system imaged by high-resolution seismic data. T. Schwenk, V. Spieß, M. Breitzke, C. Hübscher. To be submitted to Marine and Petroleum Geology.*

High-resolution seismic data collected with a GI Gun and a Watergun are used to reveal the structure of the active channel-levee system and the buried channel-levee sys-

tems on the Middle Bengal Fan. Four seismic facies are defined and interpreted. Downfan changes of the individual channel-levee systems are analyzed, and differences between active and buried systems are discussed. Two evolutionary scenarios for the active and one buried system are developed and discussed with respect to results derived from other fans. Finally, the reservoir potentials of channel-levee systems in the study area are described.

• *Chapter 4: Architecture and stratigraphy of the Bengal Fan with respect to shelf distance revealed from high resolution seismic data. T. Schwenk and V. Spieß. To be submitted to Journal of Geophysical Research.*

High-resolution seismic data collected on four long east-west profiles located on the upper Middle fan, the upper Lower Fan and the central Lower Fan are analyzed. The architecture of surface and buried channel-levee systems and their downfan variations are revealed and compared with previous publications. The built-up of distinct channel-levee complexes on the upper Middle Fan is discussed and compared with coring results and existing descriptions of complexes. The seismic stratigraphy of the southern profiles is linked to results of DSDP Site 218 and of the ODP Leg 116 sites, located in the very distal fan. Finally, the seismic results are discussed with respect to deformation events in the central Indian Ocean and to tectonic and climatic events in the source area, i.e. the Himalayan.

Chapter 2: Frequent channel avulsions within the active channel-levee system of the middle Bengal Fan - an exceptional channel-levee development derived from Parasound and Hydrosweep data

Tilmann Schwenk, Volkhard Spieß, Christian Hübscher, Monika Breitzke

Manuscript published in Deep Sea Research II, 2003, Volume 50 (5), pp. 1023-1045

2.1 Abstract

The active channel-levee system of the middle Bengal Fan was studied by a combined analysis of Parasound echosounder and Hydrosweep swathsounder data. The channel is characterized by highly variable sinuosities. Compared to other mud-rich submarine fans, an exceptionally low channel slope is found. The system can be subdivided into inner and outer zones of significantly different depositional architecture.

The inner zone consists of the active channel and sharply separated vertical blocks, which are characterized by parallel, distinct reflectors and planforms of bends. These blocks are interpreted as abandoned channel segments (cut-off loops).

The outer zones represent undisturbed levees, which are constructed of parallel and wedge-shaped sedimentary units. The wedge-shaped units, varying significantly in thickness and lateral extent, are found at the outer convex arcs of active and abandoned channel loops caused by overspilling of channelized turbidity currents at sharp bends. The parallel units are the deposits of turbidity currents, which spread their sediments over wide areas as their size significantly exceeding the cross-section of the channel. The complex vertical and horizontal distribution of partially small sedimentary units suggests a more complicated deposition in time and space as hitherto reported from other submarine fans.

Within the inner zone, more than 20 cut-off loops were identified over a channel length of 90 km. In contrast to most other large mud-rich submarine fans, channel avulsions within the active channel-levee system is a frequent process during its evolution. In particular, a temporal succession of at least 4 cut-off loops was reconstructed in the southern study area, indicating channel avulsion on average every 750 years. Channel avulsion seems to be a repetitious process caused by erosion through turbidite currents in a highly sinuous channel.

Compared to other submarine fans, no morphological parameter shows a remarkable difference except the channel slope, which is significantly smaller than for example on Amazon, Congo and Mississippi fans. The interaction between this low channel slope and the flow parameter of the turbidity currents is most likely the reason for the instability of the active channel planform leading to an exceptionally large number of meander loop breaches and cut-off loops.

Keywords: Bay of Bengal, submarine fans, channel-levee systems, channel avulsions, turbidity currents, cut-off loops, Parasound sediment echosounder, Hydrosweep swath sounder.

2.2 Introduction

The Bengal Fan is beside the Amazon, Indus and Mississippi fans one of the large mud-rich submarine fans on Earth, which are typically located on passive continental margins. Studies of these submarine fans are motivated by their hydrocarbon potential and by their potential as recorders of long- and short-term climatic changes (Bouma, 2001; Richards et al., 1998). In general, the architecture and geometry of submarine fans are well known and depositional models for characterization and classification have been established (Bouma, 2000; Richards et al., 1998; Stow and Mayall, 2000). The factors controlling fan architecture are tectonics, climate, nature of sediment input and sea-level fluctuations (Bouma, 2000; Richards et al., 1998). Bouma (2000) used those factors and two end-members in terms of the sand/clay ratio (coarse-grained vs. fine-grained) to characterize fan systems. Another classification is based on the volume and grain size of sediment input and the nature of the supply system, leading to twelve models of submarine fan systems (Richards et al., 1998). All these models subdivide fine-grained or mud-rich submarine fans into an upper, middle and lower fan. The upper fan is dominated by a single, large channel-levee system connected to a large submarine canyon. Further downslope, the middle fan is characterized by sinuous leveed channels, which terminate in depositional lobes on the lower fan (Bouma, 2000; Bouma, 2001; Richards et al., 1998). However, these are models and as such describe general features, but do not accurately characterize individual fans (Richards et al., 1998). Especially the evolution of sinuosities and the reservoir architecture of recent deep-sea fans are particularly poorly understood due to the lack of 3-D or closely spaced, high-resolution 2-D seismic data (Kolla et al., 2001). Thus, for a significant improvement of models describing submarine fans, examination of the architectural elements and their three-dimensional geometry is required (Stow and Mayall, 2000).

The Bengal Fan was the focus of three expeditions in 1994 and 1997 with the German research vessel Sonne in co-operation between the University of Bremen and the Federal Institute for Geoscience and Natural Resources (BGR), Hannover (Fig. 2.1). To study the architecture and evolution of a channel-levee system in detail, echosounder and very high-resolution seismic data were collected on a closely spaced grid of 55x60 km area at 16°30´ N (Fig. 2.1) in 1997 during the SO 125 Cruise (Spieß et al., 1998). Results of the SO 93 Expedition in 1994 showed that in this area a channel-levee system with a complex structure has developed during the last 15,000 years (Hübscher et al., 1997; Weber et al., 1997). Additional data were collected during the SO 126 Expedition (Kudrass and Shipboard Scientific Party, 1998) in the same area.

In this paper, we present a combined analysis of narrow beam Parasound sediment echosounder and multibeam Hydrosweep swathsounder data to document the morphology and structure of the active channel-levee system and to reconstruct its evolutionary stages.

2.3 Background

2.3.1 Channel-levee systems

Channel-levee systems are known as the main architectural element of large submarine fans, such as the Amazon Fan (Damuth et al., 1988; Pirmez and Flood, 1995), the Mississippi Fan (Twichell et al., 1991; Weimer, 1991), the Indus Fan (Kenyon et al., 1995; Kolla and Schwab, 1995) and the Bengal Fan (Emmel and Curray, 1985). Channel-levee systems were formed by simultaneous erosion and deposition of suspended sediment during the passage of a succession of turbidity currents (Imran et al., 1998). The channels tend to meander, which is controlled mainly by the gradient of the valley floor, but also the frequency and type of sediment load of turbidity currents. Changes of these factors lead to channel meandering to adjust the channel gradient so that turbidity currents are in equilibrium with the sediment load (Flood et al., 1991; Pirmez and Flood, 1995; Weimer, 1991). From a comparison of valley slopes and sinuosities of several channel-levee systems, Clark et al. (1992) inferred that channel sinuosity increases with decreasing valley slope, but only to a certain maximum of sinuosity. If valley slopes decrease further, the channel-levee systems react with decreasing sinuosity. This threshold seems to be a unique parameter for each non-tectonically controlled fan (Clark et al., 1992). After the initial development of such a channel-levee system, the build-up of the system varies with the nature of the turbidity currents. Large turbidity currents with thicknesses much higher than the channel relief and extensions much broader than the channel width cause semicontinuous overspilling of sediments onto extensive areas. Small, mainly channelized turbidity currents overspill only at meander bends and saddles in levees and therefore produce sedimentation events on small areas (Hiscott et al., 1997; McHugh and Ryan, 2000; Peakall et al., 2000a; Piper and Normark, 1983). On several submarine fans, this overspill process produces sediment waves on the levees (Hübscher et al., 1997; Kenyon et al., 1995; McHugh and Ryan, 2000).

2.3.2 Bengal Fan

The development of the Bengal Fan, the largest submarine fan on Earth, started in the early Eocene after the collision of India with Asia and the resulting uplift of the Himalayas (Curray, 1994). The fan extends over a length of 3000 km from 20° N to 9° S, its width varies between 1430 km at 15°N and 830 km at 6°N (Emmel and Curray, 1985), covering the entire Bay of Bengal (Fig. 2.1). Therefore, the area of the Bengal Fan has been calculated to be $3x10^6 km^2$ (Emmel and Curray, 1985). From seismic refraction data a maximum thickness of 16 km was derived for post-collision sediments near the shelf edge (Brune et al., 1992). Thus the approximate volume of these sediments is $12.5x10^6$ km^3, the approximate mass is $2.88x10^{16}$ t (including Nicobar fan and part of the outer Ganges-Brahmaputra delta) (Curray, 1994). Like the Amazon and Mississippi fans, the Bengal Fan evolved by stacking and overlapping of channel-levee systems (Damuth et al., 1988; Emmel and Curray, 1985; Weimer, 1991). Only one system is active at any one time, all others are abandoned (Emmel and Curray, 1985). In contrast to common sequence-stratigraphic

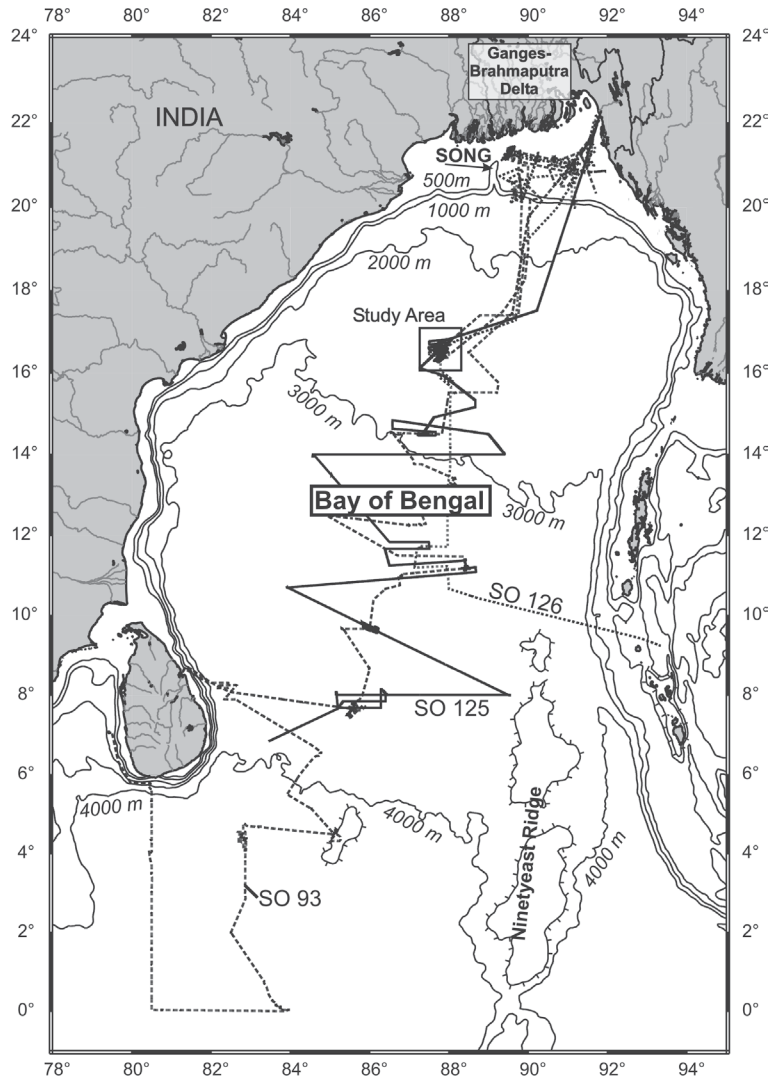

Figure 2.1: *Map of the Bay of Bengal with cruise tracks of SO 125 (solid line), SO126 (dotted line) and SO 93 (dashed line) expeditions and location of the study area. The canyon „Swatch of No Ground" (SoNG), deeply incised into the shelf, is clearly visible in the western part of the shelf. Bathymetry is satellite derived and shown by contour lines of 1000 m spacing (Smith and Sandwell, 1997).*

models, the Bengal Fan shows active growth during the most recent sea-level rise and the recent sea-level highstand (Weber et al., 1997).

The Bengal Fan is fed by the sediment load of the Ganges and Brahmaputra rivers, which drain the Himalayas (Fig. 2.1). The total sediment discharge today reaches 1-2x10^9 t/yr, ranking first among all rivers on Earth (Milliman and Meade, 1983). This enormous mass of sediment is distributed over the subaerial delta, the submarine delta and the deep-sea fan. Goodbred Jr. and Kuehl (2000a) calculated that during the last 7000 years roughly one third of the total load was deposited in each of these three domains. At present, 20 % of the total riverine sediment freight is deposited on the submarine delta, whereas 35 to 50 % is transferred to the deep sea fan (Michels et al., 1998). This transfer is channelled through the „Swatch of No Ground" (SoNG), a canyon deeply incised into the shelf (Fig. 2.1), which is connected to the active channel-levee system on the fan (Emmel and Curray, 1985; Kottke et al., 2003; Kudrass et al., 1998; Michels et al., 1998). The canyon acts as a temporary trap for sediment that has been resuspended by storms and tides on the delta (Kudrass et al., 1998; Michels et al., 1998). Inside the canyon, slides, slumps, episodic flow of low-density currents and quasi-continuous gravity-driven sediment flows remobi-

lize the sediment, which is then transported by turbidity currents to the fan (Kottke et al., 2003; Kudrass et al., 1998).

In the study area, approximately 500 km south of the „Swatch of No Ground“ at 16°30´N in 2600 m water depth (Fig. 2.1), the active channel-levee system is more than 40 km wide and the channel is 65 m deep (Hübscher et al., 1997). The sediments represent mostly fine-grained muddy turbidites (Weber et al., 1997). Most remarkable is the complex structure with a vertical segmentation between outer and several inner levees, previously interpreted as a constriction of a formerly 14 km wide channel in distinct phases (Hübscher et al., 1997). The outer levees mainly grew between 12,800 ^{14}C yr B.P. and 9700 ^{14}C yr B.P., whereas a 7m long core from the inner levees recovered only sediments deposited after termination 1b (9700 ^{14}C yr B.P.) (Weber et al., 1997).

2.4 Methods

In this paper, we present data collected with the sediment echosounder Parasound, recorded with the digital data acquisition system ParaDigMA (Spieß, 1993), and the multibeam swathsounder Hydrosweep DS (both designed and build by STN-Atlas Elektronik, Bremen, Germany). Both systems are permanently installed on the German research vessel Sonne.

2.4.1 The Hydrosweep DS System

Hydrosweep DS is a hull-mounted swath sonar system. It provides depth information for a swath with a width of twice the water depth by generating 59 pre-formed beams over an angle of 90°, operating at a frequency of 15.5 kHz. To avoid depth errors due to refraction of the outer beams, Hydrosweep uses a patented calibration process. At regular intervals the system generates a fore-aft looking swath and compares the values of these profiles with stored values of the central beam. Hydrosweep estimates a mean sound velocity by calculating a best fit between the depths of the central beam and the fore-aft profiles. This mean sound velocity is used for calculating all depth values. As a result of this configuration, the residual depth errors are smaller than 0.5% of water depth (Grant and Schreiber, 1990).

Processing and presentation of the bathymetric data were carried out with the public domain software packages MultiBeam and GMT (Caress and Chayes, 1996; Wessel and Smith, 1998). Processing includes correction of navigation data and automatic as well as interactive editing of bathymetric data. Interactive editing had to be carried out manually and carefully because of artifacts, which are on the same scale as the topographic features in the study area. For display, the data were gridded after editing.

2.4.2 The Parasound System

Parasound is a hull mounted, parametric narrow beam sediment echosounder. It is distinguished by a footprint diameter of only 7% of the water depth, providing an excellent lateral resolution. The system utilizes the parametric effect, which arises from nonlinear interaction between high frequency sound waves of finite amplitude. A difference frequency

between 2.5 and 5.5 kHz can be generated, which is focused to a cone with an opening angle of 4°. The vertical resolution of the Parasound System is on the order of a few decimeters, and signal penetration varies between 10 and 200 Meter depending on sediment type and attenuation (Grant and Schreiber, 1990). The received data were digitized (sampling rate: 40 kHz) and stored with the ParaDigMA software for further digital signal processing and display (Spieß, 1993). All presented depth figures were scaled from two-way traveltime to depth for a constant sound velocity of 1500 m/s.

2.5 Data

2.5.1 Bathymetry

Figure 2.2 shows the bathymetric data from the study area with contour lines on an artificially illuminated greyscale surface. The map also shows the track lines of the cruises SO 93, SO 125 and SO 126. Water depths range from 2480 m to 2680 m. Clearly visible is the active channel with a planform varying considerably from nearly straight to highly sinuous. The talweg width is ~500 m across the survey area. For the most part, the channel is strongly V-shaped as in line GeoB97-067 (Fig. 2.3). Channel width of these parts varies between 800m and 1 km. But on some locations point bars can be identified, where channel width increases up to 1.6 km. Talweg relief differs strongly between such locations, varying between 25 and 60 m. But generally, the relief of the channel decreases from 80 m to 60 m from north to south. Talweg depth reaches 2597 m at the northernmost line and increases to 2659 m ~50 km further south at the southernmost line. Accordingly, the general valley slope is 1.24 m/km, whereas the channel slope is 0.7 m/km. The active channel reveals a talweg length of 87 km over a direct distance 50 km, caused by a channel sinuosity varying between 1.05 and 3.5 with a mean value of 1.74. Sinuosity is greatest south of 16°30´ with an average value of 2 and a maximum of 3.5, north of 16°37´ the values are intermediate (around 1.5), and between 16°30´ and 16°37´ the sinuosity is close to 1.

Clearly visible in the bathymetry are depressions (up to 20 m deep) forming bends beside the active channel, but these are restricted to the northern part of the working area. Also the identified point bars at the inner side of the meander loops are visible only in the northern part of the working area (Fig. 2.2). These point bars reach widths up to 1 km perpendicular to the channel and length up to 2 km along the channel.

2.5.2 Architectural elements

Characteristic architectural elements found within the working area are presented in Figures 2.3 (Line GeoB97-067), 2.4 (Line GeoB97-PS10g), 2.5 (Line GeoB97-PS06g) and 2.6 (Line GeoB97-PS08g). Comparison between Lines GeoB97-067and GeoB97-PS10g reveals the changes in the internal structure of the channel-levee system from north to south. The lines indicate that the system can be divided into inner and outer zones:

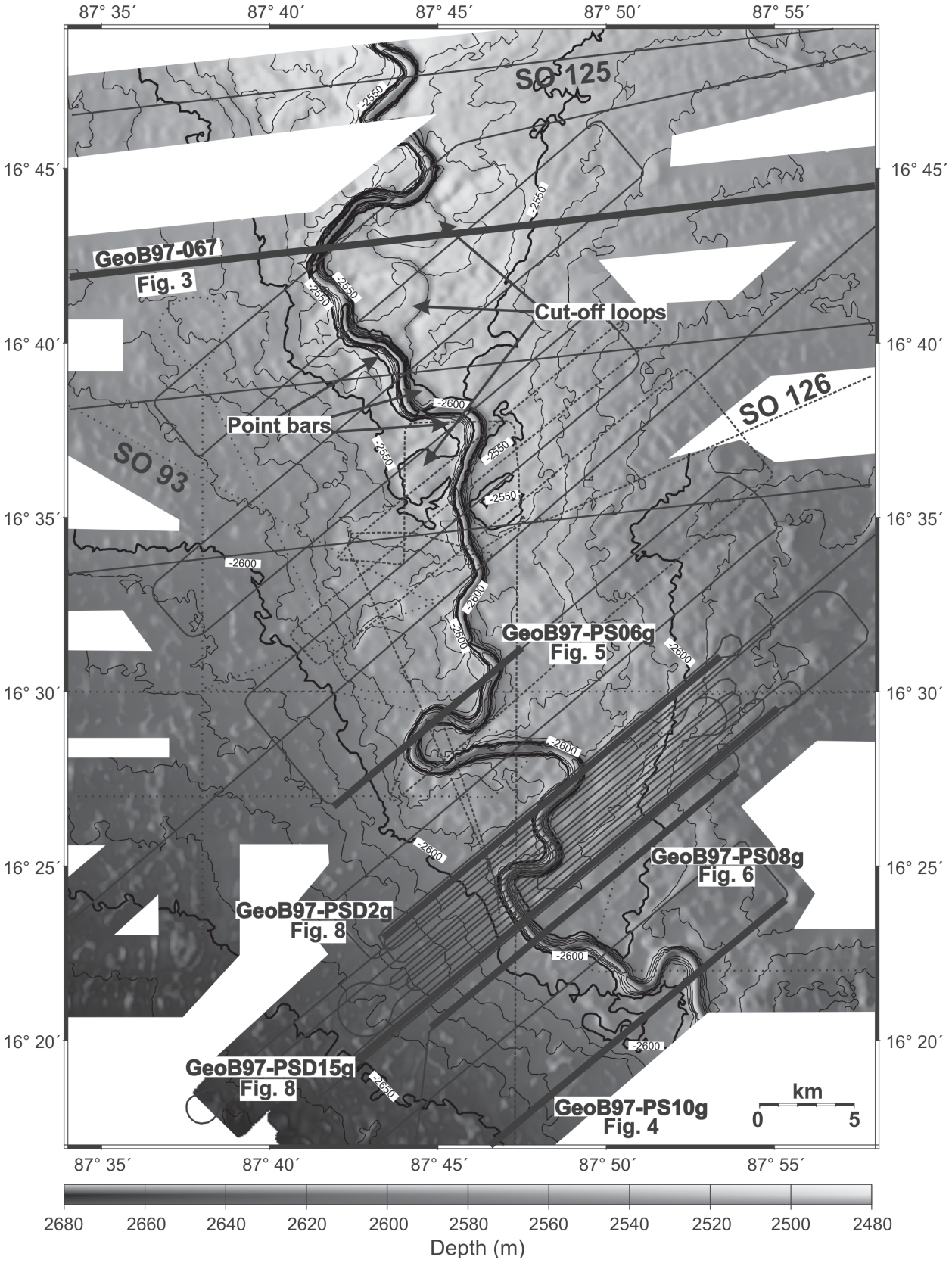

Figure 2.2: *Bathymetric map of the study area derived from Hydrosweep data of SO 125 and SO 93 cruise. Depth data are shown as artificially illuminated greyscale surface overlaid by contour lines of 10 m spacing. Thick black lines mark the Parasound lines presented in this paper. Thin black lines mark all Parasound lines available in the study area, solid line represents SO 125 cruise, dotted line represents SO 93 cruise and dashed line represents SO 126 cruise.*

2.5.2.1 Inner zone

The inner zone includes the active channel and several sharply separated vertical blocks, characterized by parallel, distinct reflectors of different amplitudes and spacing (Figs. 2.3-2.6). Most of these parallel reflectors are even, but some reflectors appear wavy or dipped. Also, thin transparent layers occur within these blocks. Widths of the vertical blocks range from 500 m to 3 km. Signal penetration in these vertical blocks reaches 90 m, but in most lines the base could not be resolved in the Parasound data. Therefore, their maximum vertical dimension may exceed 90 m. However, in the eastern part of Line GeoB97-PS08g the base of one block is visible (Block D in Fig. 2.6), and its relief is < 40 m.

Several of these blocks are associated with depressions in the sea floor, mainly in the northern part of the study area, where the relief of these depressions exceeds 10 m, e.g. in Line GeoB97-067 (Fig. 2.3). On the southern lines these depressions are rare and have a relief of only a few meters, as is visible west of the active channel on Line GeoB97-PS10g (Fig. 2.4) and east of the active channel in Line GeoB97-PS08g (Fig. 2.6). In general, vertical blocks in the southern part of the study area are not associated with depressions in the sea floor, and some blocks are completely covered by extensive horizontal layers (Figs. 2.4 and 2.6). For example, in the eastern part of Line GeoB97-PS10g different blocks are draped by the same sediment packages (Fig. 2.4). On Line GeoB97-PS08g, the maximum thickness of the sediment cover on top of the vertical block D reaches 40 m (Fig. 2.6).

Vertical transparent zones of different lateral extent are found between the layered vertical blocks. Below these transparent zones, an acoustic base could be not resolved in the Parasound data. The floor of the active channel is characterized by prolonged reflections with a high-amplitude surface reflector (Fig. 2.5). Signal penetration into the channel floor is less than 30 m.

To analyze the spatial distribution of the vertical blocks, all of them were plotted on a two-dimensional map. Based on similar attributes of the fill and proximity (in areas of closely spaced track lines), many of these blocks could be related and were connected for mapping. The resulting segments have the planforms of meander bends just as the bathymetric depressions associated with some of the vertical blocks (Figs. 2.7 and 2.2). Mapping of the outer limits of the inner zone reveals that the inner zone is restricted to a 15-20 km wide corridor (Fig. 2.7). The boundaries of this corridor are curvilinear and subparallel, due to the meander planform of the segments.

2.5.2.2 Outer zones

The outer zones are characterized by reflectors diverging towards the channel. The reflectors are distinct as well as prolonged and reveal a large variability in amplitudes. In addition, transparent layers occur, reaching thicknesses up to 5 m. The reflectors are truncated at the boundary with the inner zone (Figs. 2.3, 2.4 and 2.6). Signal penetration

varies between 50 and 90 m and generally decreases with distance from the active channel.

In all lines, an acoustic base is clearly visible as a strong reflector. In the eastern part of Line GeoB97-067, reflectors onlap onto the base. Sediment thickness above this base generally decreases from north to south (that is, from proximal to distal), but varies locally. On Line GeoB97-067 (Fig. 2.3), the thickness exceeds 70 m, on Line GeoB97-PS10g (Fig. 2.4) less than 50 m sediments were deposited above the base east of the inner zone. In the western part of Line GeoB97-PS10g, the acoustic base is interrupted by vertical blocks. West of these blocks, sediment thickness is ~ 45 m, but to the east sediment thickness reaches 70m (Fig. 2.4). Different from the general trend, sediment thickness in the more distal Line GeoB97-PS08g (~ 65 m, Fig. 2.6) exceeds that of the more proximal Line GeoB97-PS06g (~ 55 m, Fig. 2.5) (see also Fig. 2.2).

In the outer zones, acoustic units of different shape can be distinguished. In particular, we observe units with parallel or nearly parallel reflectors contrasting units with strongly divergent reflectors, building wedge-shaped sediment packages. These wedges can be found in Line GeoB97-PS10g (Fig. 2.4) and at the top of Line GeoB97-PS06g (Fig. 2.5), but not in Line GeoB97-067 (Fig. 2.3), where all reflectors are divergent and no wedge-shaped package within the outer zone is visible. A pronounced example for these stacked plate- and wedge-shaped patterns is the eastern part of Line GeoB97-PS08g (Fig. 2.6).

Stratigraphically, seven different acoustic units were identified. The lowermost unit is below the acoustic base and, in contrast to the other units, this unit dips down towards the inner zone and the reflectors of the uppermost layer are convergent towards the inner zone. Above the acoustic base, the Units I and IV are clearly wedge shaped. The wedge shape of Unit IV is more pronounced than that of Unit I, in which the reflectors become more parallel with distance from the inner zone. Laterally, Unit IV is less extensive than Unit I and therefore fully covered by Line GeoB97-PS08g. All other units reveal parallel reflectors and drape the underlying units (Fig. 2.6). Obviously, these stratigraphic units from the eastern levee could not be correlated to the western levee.

Another pattern in the outer zones is shown in two lines (Figure 2.8) selected from a detailed grid of 16 Parasound lines of 300 m spacing in the south of the working area (Figs. 2.2 and 2.9). In Lines GeoB97-PSD2g and GeoB97-PSD15g, which cross two different vertical blocks (A and C, see Figs. 2.8 and 2.9), the same sedimentary Unit III (Figure 2.8) can be identified within the eastern outer zone and can be correlated from a N-S orientated SO 126 Parasound line (see also Figs. 2.2 and 2.9). Unit III is acoustically transparent and appears also in Line GeoB97-PS08g (Fig. 2.6). Whereas in Line GeoB97-PSD2g Unit III covers the wedge-shaped Unit X, in Line GeoB97-PSD15g Unit III is found below the wedge-shaped Unit IV. But correlating of all stratigraphic units is only possible between Lines GeoB97-PSD15g and GeoB97-PS08g (spacing is 1 km), but not between Lines GeoB97-PSD2g and GeoB97-PSD15g, which have spacing of 4 km.

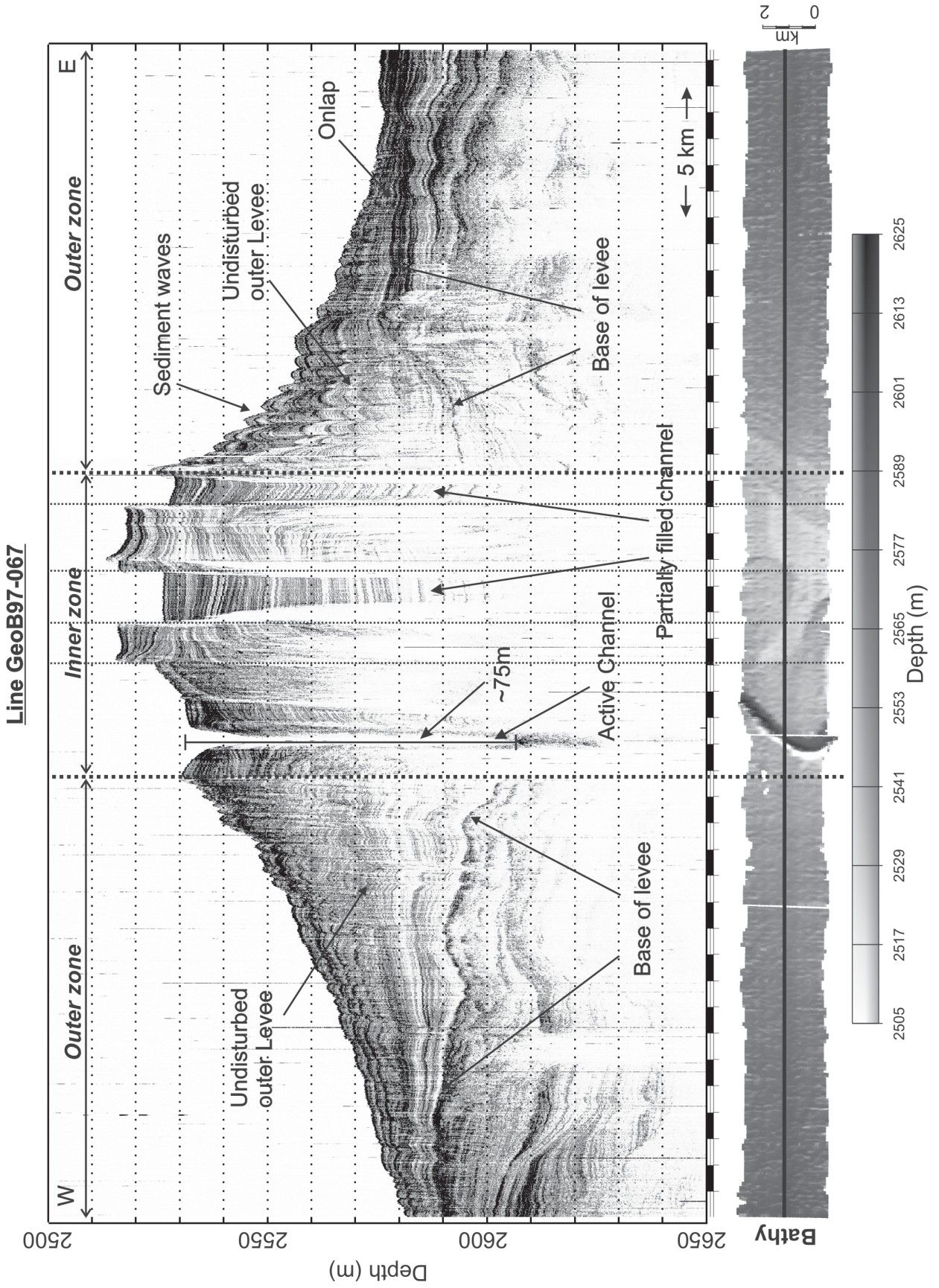

Figure 2.3: *Parasound and Hydrosweep data of Line GeoB97-067 in the northern part of the study area (see Fig. 2.2). Hydrosweep data are shown as grey shaded relief, the black line indicates the location of the Parasound line. Line GeoB97-067 has a length of 45 km and is E-W orientated, vertical exaggeration is 166. Thick dashed lines indicate boundaries between inner and outer zones, see text for discussion.*

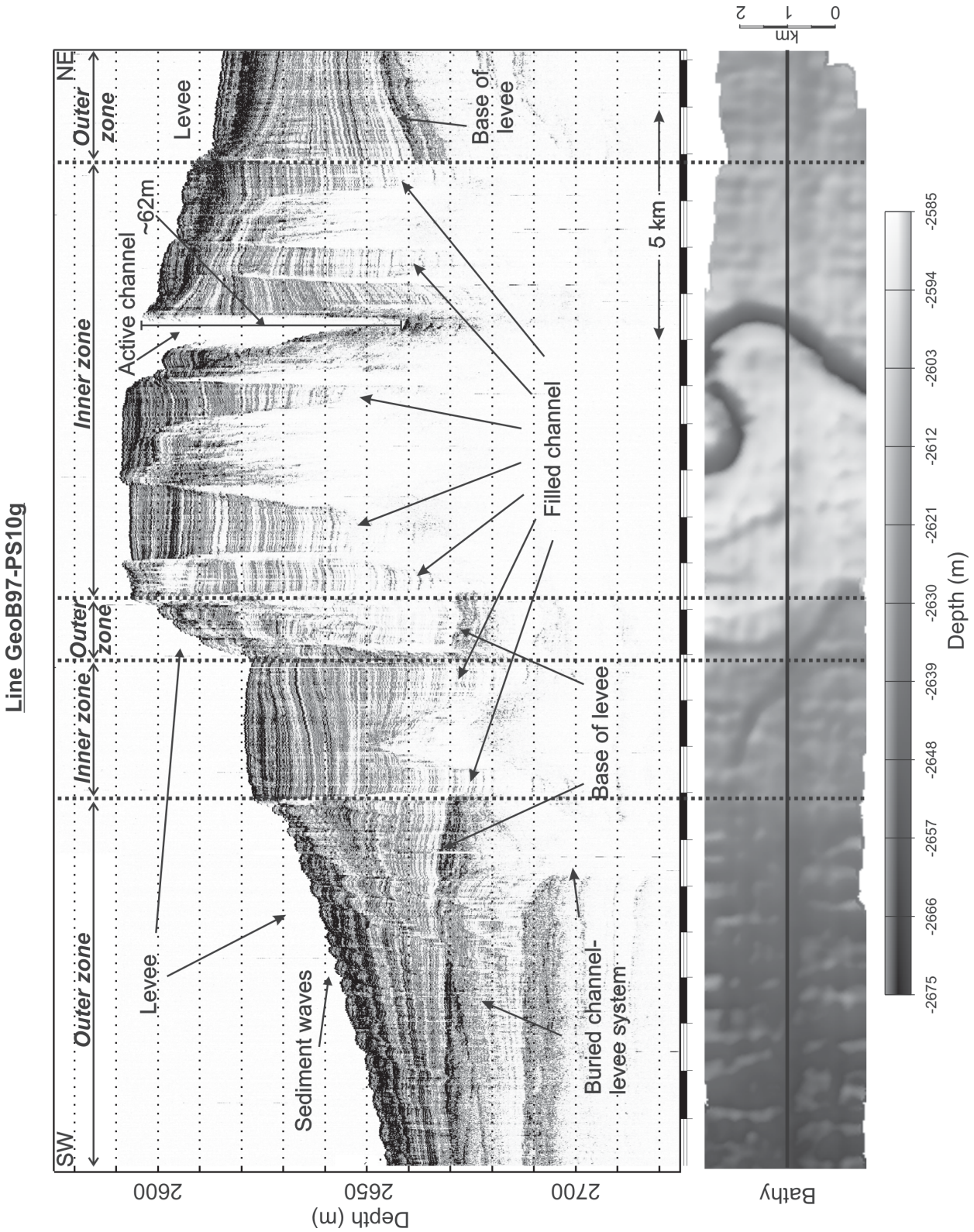

Figure 2.4: *Parasound and Hydrosweep data of Line GeoB97-PS10g, the southernmost line in the study area (see Fig. 2). Hydrosweep data are shown as grey shaded relief, the black line indicates the location of the Parasound line. Line GeoB97-PS10g has a length of ~24 km and is SW-NE orientated, vertical exaggeration is 81. Thick dashed lines indicate boundaries between inner and outer zones, the inner zone is crossed two times (refer to Figs. 2 and 7). See text for discussion.*

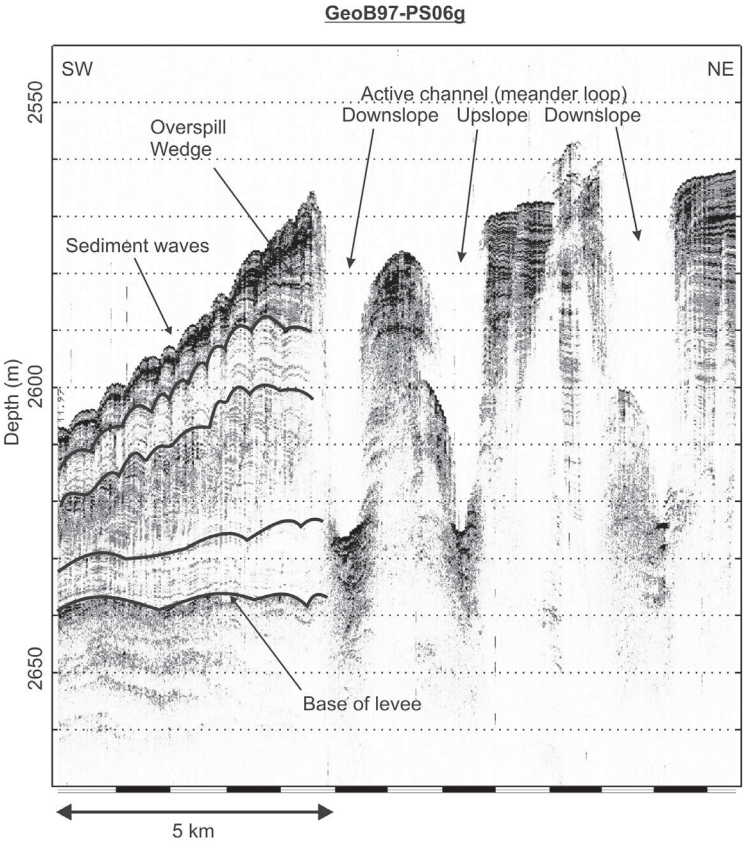

Figure 2.5: *Parasound section of Line GeoB97-PS06g crossing a meander loop three times. For location, refer to Fig. 2. The section has a length of 12,5 km and is SW-NE orientated, vertical exaggeration is 105. Main sedimentary units within the western levee are marked by bold lines.*

From these examples it is evident that the wedge-shaped units vary in vertical and horizontal dimensions as well as in shape. All wedge-shaped units abut against vertical blocks (Figs. 2.6 and 2.8) or the active channel (Fig. 2.5). The planform of Unit IV could be mapped, because of its small lateral extent and the close spacing of Parasound lines in this part of the study area. It turns out that the planform of Unit IV is tongue-shaped, and Unit IV abut against the vertical block C (Fig. 2.9). It should be noticed, that the along-channel extent (here NW-SE) of Unit IV does not exceed 5 km.

Sediment waves of different amplitudes and different apparent wavelengths exist in the study area, as in the eastern part of Line GeoB97-067 (Fig. 2.3), in the western part of Lines GeoB97-PS10g (Fig. 2.4) and GeoB97-PS06g (Fig. 2.5), and on both outer zones of Line GeoB97-PS08g (Fig. 2.6), Line GeoB97-PSD2g and Line GeoB97-PSD15g (Fig. 2.8). The sediment waves can be traced down to different sub-bottom depths on the lines.

2.6 Discussion

2.6.1 Abandoned channels

From our analyses of all lines in the study area we can conclude that some vertical blocks are associated with seafloor depressions forming meander bends, and a large number of vertical blocks could be connected to segments having the planform of a bend (Figs. 2.2, 2.3 and 2.7). Therefore, we interpret the vertical blocks as abandoned channel segments, i.e. sediment-filled cut-off loops or „oxbows“. Where vertical blocks are associated with sea-floor depressions, they may represent cut-off loops that have been only partially filled. Obviously, other cut-off loops were completely filled with sediment and in some cases also buried (Figs. 2.4 and 2.6).

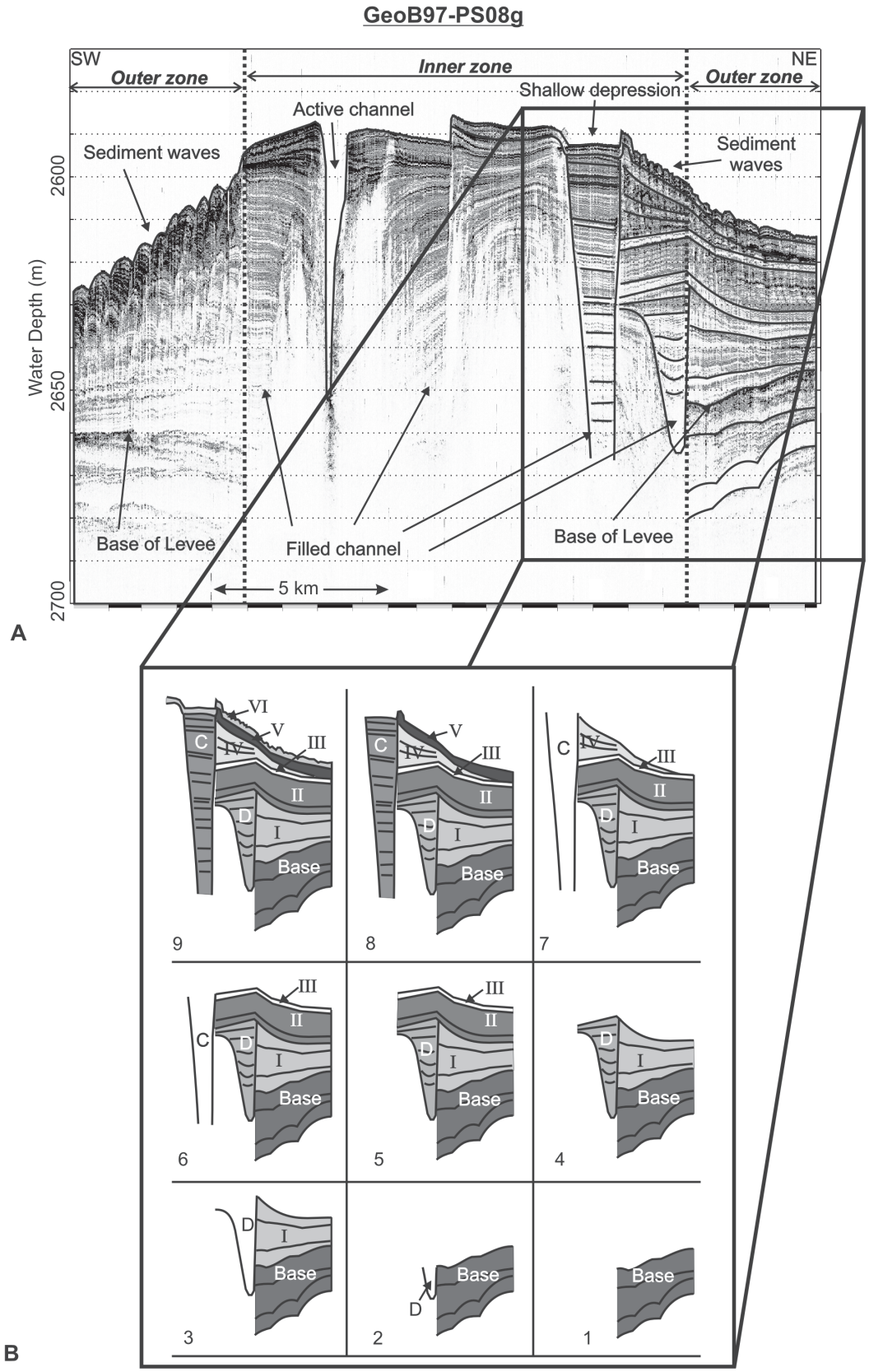

Figure 2.6: *Parasound data of Line GeoB97-PS08g. For location, refer to Fig. 2. The line has a length of 21 km and is SW-NE orientated, vertical exaggeration is 123. (A) Parasound line with line-drawing in the eastern part. Thick dashed lines indicate boundaries between inner and outer zones. (B) Sketch showing the development of the system in the eastern part of Line GeoB97-PS08g in 9 stages. In stage 9 (recent stage), 6 lateral and 2 vertical units are identified above the base of the levee. See text for detailed discussion.*

Because turbidity currents can more easily spill into cut-off loops than over the levees, cut-off loops act as efficient sediment traps. High amplitude reflectors also suggest this process for coarse-grained suspended load of the turbidity currents. Dipped and wavy reflectors probably image lateral velocity distribution within the part of the turbidity current stripped into the abandoned channel segment. Therefore apparent bedding of the reflectors depends on angle Parasound lines cross the cut-off loops.

Since the many cut-off loops do not represent channel segments that were simultaneously active, channel avulsion must have occurred frequently during the development of this channel-levee system. However, these avulsions were restricted to a 15-20 km wide corridor within the channel-levee system and did not lead to channel bifurcations (Fig. 2.7).

This interpretation of the inner zone is in contrast to Hübscher et al. (1997), who assumed these inner blocks to represent inner levees successively constricting a wide channel during distinct phases of channel development. However, this work was only based on a single line perpendicular to the channel, and therefore the complex pattern and planforms of the vertical blocks could not be identified. Additionally, this line did not cross one of the partially filled channels, so cut-off loops were not visible in the earlier bathymetric data (Hübscher et al., 1997, their Fig. 3).

In contrast to the inner zone consisting of the active channel and abandoned channel loops, we consider the outer zones to represent undisturbed levees, never destroyed by the active channel during the evolution of this channel-levee system.

2.6.2 Temporal succession of filled meander loops

Mapping of the cut-off loops provides information about relatively small individual architectural elements, which so far appear unrelated in space and time. To understand the evolution of the system, we can use the fact that the active channel may act as a distinct sediment source at meander bends in form of spill-over points. Accordingly, changes in depositional style and sedimentation rate will depend on channel geometry and distance to channel axis and bends.

In Parasound Line GeoB97-PS06g (Fig. 2.5), which crosses the western outer meander bend of the active channel, we can study sedimentation of the undisturbed outer levee, since the channel was never located farther west (Figs. 2.2 and 2.7). The uppermost, i.e. youngest unit on the western levee, is wedge shaped, whereas the deeper units reveal parallel layering (Fig. 2.5). As noticed in Chapter 2.5.2.2, several lines (e.g. Line GeoB97-PS08g, Fig. 2.6) document that closer to the active or filled channel the divergent wedges appear more pronounced, especially at outer meander bends. Apparently, the wedge-shaped units were built up in the immediate vicinity of active channel bends. Therefore, we can reconstruct from the sequence of these wedges in relation to spill-over points the temporal succession of active channel bends.

In the southern part of the study area we recognize that in Line GeoB97-PSD2G the Wedge X is covered by Unit III, which is covered again by Wedge IV in Line GeoB97-

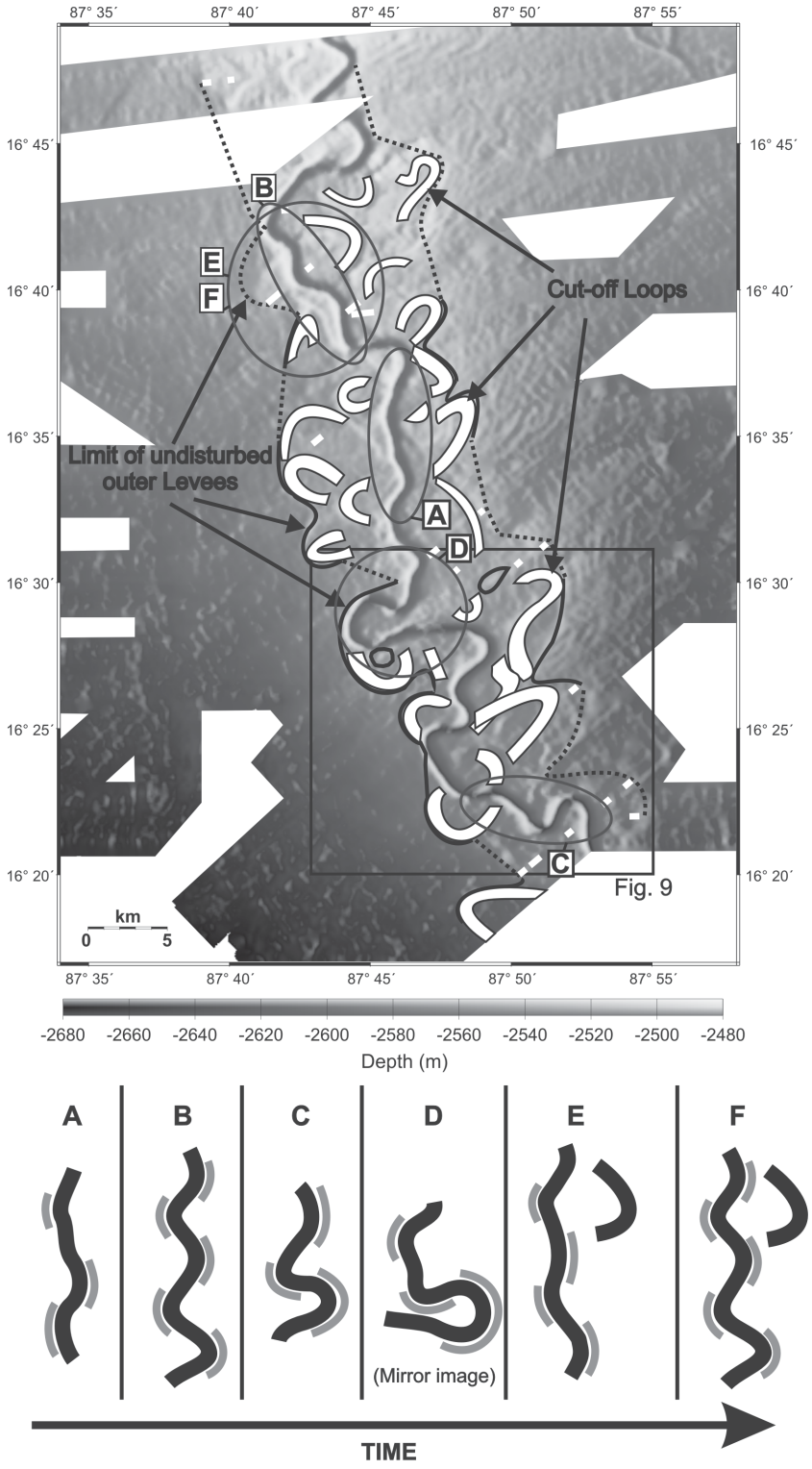

Figure 2.7: *Bathymetric map with redrawn channel segments. The bathymetry is shown as artificially illuminated greyscale surface. Black lines display the limits of the undisturbed outer levees, sections with dotted black lines are interpolated. White bends represent cut-off loops as interpreted from Parasound and Hydrosweep data. Small white squares illustrate filled channel segments interpreted from Parasound lines, which can not connected to bends. Below the map, a sketch of different channel planforms found in the study area is shown. These planforms represent snapshot-like the different evolutionary stages of the channel and illu-strate the general process of channel migrating caused by erosion (indicated by grey stripes) through turbidity currents at the cut-bars. This process must have occurred at various locations of the channel. See text for detailed discussion.*

PSD15G (Fig. 2.8). Accordingly, Unit X in GeoB97-PSD2G was deposited before Unit IV in Line GeoB97-PSD15G (Fig. 2.8). Because Unit X was deposited during the time when Channel A was active and Unit IV was deposited during the time when Channel C was active, we conclude that the filled Channel A in Line GeoB97-PSD2G was active at an earlier stage than the filled Channel C in Line GeoB97-PSD15G. Both channels (A and C) have been mapped in Figure 2.9. Between channels A and C another filled channel (B) is identified. We also conclude that Channel A must be bending to the west at its southern end due to the limit of the undisturbed outer levee (Figs. 2.8 and 2.9). Accordingly, Channel A must have been active before Channel B. In contrast, Channel C cuts through the filled Channel B, therefore representing a later stage (Fig. 2.9). In addition, Channel C could not have succeeded Channel B immediately, but instead one more position of the active channel must have existed when Channel B was refilled.

Finally, we can derive a temporal sequence from A through B to C for channel activity; at least four different channel positions must have existed during the evolution of this system in this specific area. Since the levees were built-up between 12,800 ^{14}C yr B.P. and 9700 ^{14}C yr B.P. (Weber et al., 1997) and Channel A as well as Channel C are associated with wedge shaped units within the levees, the sequence of the four channel passages must have happened within a time span of less than 3000 years. Accordingly, on average every 750 years channel avulsion occurred and the wedge shaped units represent sedimentation intervals of 750 years on average. If we assume that the cut-off loops were filled during the active stage of the succeeding channel passage, the channel fills also represent sedimentation of 750 years on average. This seems to be realistic, because Channel B was completely refilled before Channel C cut through it. Additionally, most of the identified cut-off loops were completely refilled or only one partially refilled cut-off loop exists for each line. Therefore, each filled cut-off loop provides an excellent high-resolution marine geological record.

2.6.3 Evolution of the channel-levee system

As a typical example for the evolution of the channel-levee system we discuss here the pattern of sedimentary units in Line GeoB97-PS08g as described in Chapter 2.5.2.2 (Fig. 2.6). In the eastern levee (see box in Figure 2.6) several distinct depositional phases can be identified. Two refilled channels (C, D) of different relief appear. Channel D has been completely filled and thereafter draped by 40 m of sediments. During its active stage, the relief of Channel D was 40 m. Channel C, which is also crossed by Line GeoB97-PSD15g (Fig. 2.8), is not completely filled and probably represents the last active channel prior to the currently active channel on this line. Channel C is characterized by a paleo-relief of > 70 m. Depositional units of different shape within the levee and above the filled Channel D suggest different sedimentation processes. Nine stages of the evolution of this channel-levee system have been reconstructed from the analysis of the depositional units (Fig. 2.6). Stage 9 corresponds to the line-drawing in Figure 2.6A and represents the most recent stage. In particular, following stages are identified in the Parasound data (Fig. 2.6B):

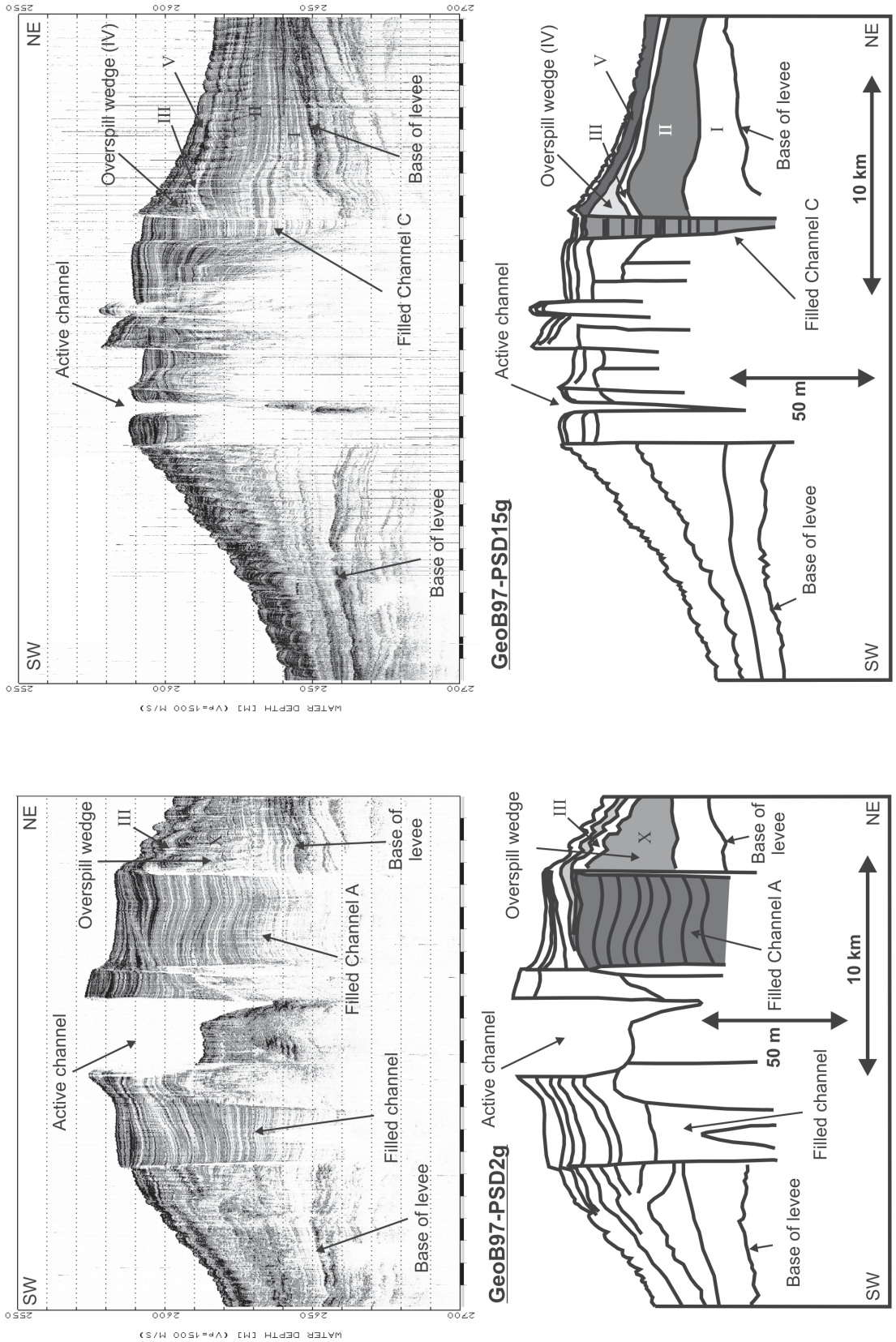

Figure 2.8: *Parasound data and line-drawings of Lines GeoB97-PSD2g (left) and GeoB97-PSD15g (right). Lines GeoB97-PSD2g and GEOB97-PSD15g are located in the south of the study area, where a detailed survey with 16 Parasound lines at 300 m spacing was carried out (see Figs. 2 and 9). Two different filled channels (A in GeoB97-PSD2g, C in GeoB97-PSD15g) with associated wedge shaped sedimentary units are crossed by the lines. From their relative stratigraphic position to Unit III (which occurs in both lines) we conclude, that Channel A was active before Channel C. See text for discussion.*

1. Below the base of the levee, a uniform sediment package exists with parallel to subparallel reflectors. The upper reflectors converge towards the inner zone. These sediments were deposited before the development of this channel-levee system began.
2. The active Channel D cuts a new passage through the sediment.
3. The wedge shaped sediment Unit I was built up as eastern levee during the activity of Channel D.
4. Channel D was abandoned after a channel avulsion and acted as an efficient sediment trap, which was filled much faster than deposition occurred on the eastern levee.
5. After the abandoned Channel D was completely filled, a sediment blanket draped uniformly the outer levee and the filled Channel D, preserving their uneven surface topography. The parallel reflectors suggest a greater distance to the active channel, which served as the main sediment source by spill-over. This stage can be divided into units II and III, where Unit III represents a transparent layer. Both units are also found in Line GeoB97-PSD15g (Fig. 2.8).
6. The active channel shifted to the east from an unknown previous position farther west. From comparison between lines, this channel has been identified as Channel C, which crosses Line GeoB97-PSD15g and has been mapped in Figure 2.9.
7. Another wedge shaped unit (IV, also found in GeoB97-PSD15g, see Fig. 2.8) was deposited on the eastern flank of the now active Channel C. The wedge shape of Unit IV is more pronounced than that of Unit I.
8. Again, the active channel moved to a new position and the now abandoned Channel C was filled. However, during this stage the abandoned Channel C did not act as efficiently as a sediment trap as Channel D did during Stage 4, probably due to a different amount of overspill. Therefore a sediment layer (Unit V) could be deposited at the same time on the outer levee.
9. When Channel C has been filled completely, sedimentation continued forming a uniform drape with sediment waves (Unit VI) along this part of the line.

In general, we can conclude that sedimentation on the levees apparently depends on two factors: 1) nature of the turbidity currents and 2) geometry of the channel. If the turbidity currents are completely constricted to the channel cross section, sedimentation occurs only near outer meander loops by overspilling due to the inability of an upper part of turbidity currents to follow a meandering channel. This is caused by the inertia of the current combined with the centrifugal force. As result of this process, wedge-shaped units formed such as Unit IV, with a tongue shaped base abut at the convex outer margin of the bends (Figs. 2.6, 2.8, and 2.9). These wedge-shaped units vary significantly in thickness and lateral extent**.** Several of the units appear relatively small, e.g. Unit IV, which suggests that the active stage of Channel C contributed only a small amount of sediment to the development of the levee at this location (Figs. 2.6 and 2.8). Other wedge-shaped units cover larger areas, and their divergent reflectors change into parallel reflectors with distance from the active channel, as e.g. in Unit I (Fig. 2.6). The differences in the extent and

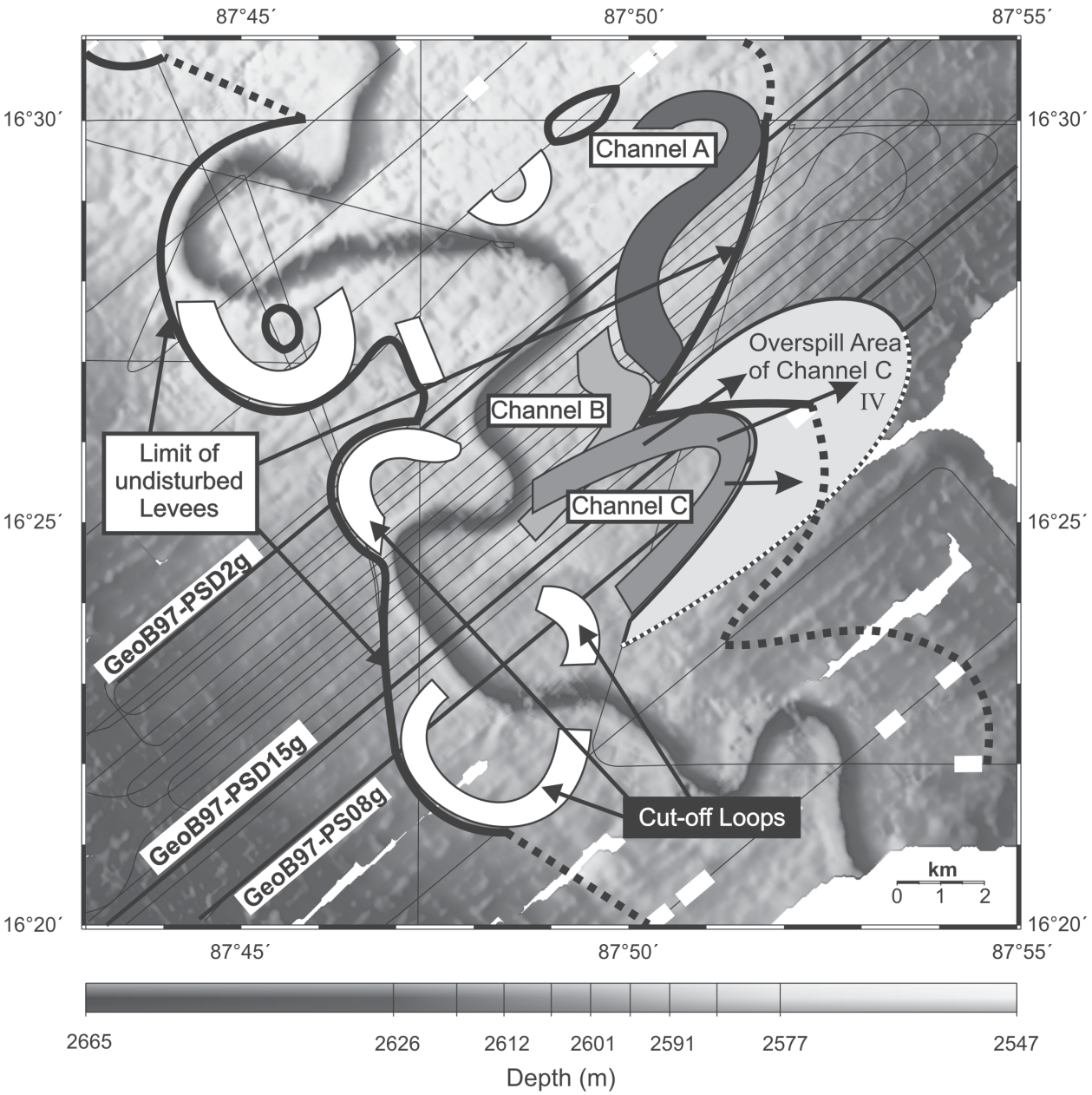

Figure 2.9: *Bathymetric map of the southern part of the study area (for location, refer to Fig. 7). The Lines GeoB97-PSD2g, GeoB97-PSD15g and GeoB97-PS08g are marked. The limits of undisturbed outer levees and the cut-off loops are drawn in as in Fig. 7. The grey marked channels were active in a temporal sequence of A (oldest) through B to C (youngest). Additionally, the base of Unit IV (the wedge shaped unit associated with Channel C) is displayed light grey demonstrating that Unit IV occupies a small portion of the total levee. Dotted part of border of Unit IV is interpolated. See also Figs. 5 and 8 as well as text for discussion.*

accentuation of the wedge shape units may be caused by differences in size, velocity and density of the turbidity currents.

In contrast, large sediment units bound by nearly parallel reflectors (as Units II, III and V, Fig. 2.6) indicate turbidity currents with thickness and extent significantly greater than the relief and width of the channel. During such turbidity flows sediment seems to be deposited over wide areas across the channel-levee system. These large turbidity currents must still have been guided by the channel, since sedimentation is restricted to a bend near the channel (Figs. 2.2 and 2.3).

Comparison with other submarine fans and channels show that depositional units abutting against outer meander bends are found on several fans. They were first described by Piper and Normark (1983) examining data from the Navy fan and explained by flow-stripping processes. These processes have also been documented from other fans as Mississippi Fan (Twichell et al., 1991) or Monterey Fan (McHugh and Ryan, 2000). Additionally, Hiscott et al. (1997) pointed out that on the Amazon Fan overspill is focused on the outer bends of meanders. From the NAMOC channel, fan shaped image patterns of high backscatter strength at sharp meander bends are reported and interpreted as wash-over fans, which form when deeper coarser portion of turbidity currents spill out of the channel due to centrifugal force (Klaucke and Hesse, 1996; Klaucke et al., 1998). However, all these examples vary significantly in terms of size of the channels, curvature of meander bends, size of the depositional units and estimated percentage of sediment volume stripped from the turbidity current. Therefore the processes may be similar, but the resulting deposits are unique for each channel-levee system.

The large units bounded by parallel reflectors suggest large overbank flows as required by the model of Peakall et al. (2000a). But it should be noticed, that we were not able to correlate depositional units neither over long distances along the channel nor across the channel (see Chapter 2.5.2.2). This is in contrast to the model of Peakall et al. (2000a), which is based on theoretical and experimental concepts as well as several observations of leveed channels, i.e. tracing of individual turbidites in the NAMOC system for up to 300 km from piston and gravity cores (Hesse, 1995). However, on Amazon fan individual turbidites found in cores of ODP Leg 155 could not be correlated between individual sites, not even between the closest sites (distance 65 km, Hiscott et al., 1997). Generally, Hiscott et al. (1997) concluded that complex distribution of echofacies suggests overspill processes complicated in detail for the Amazon Fan, which agree with our observations. But it should also kept in mind, that our study based on Parasound data characterized by significantly higher vertical and lateral resolution as conventional echosounding or seismic systems used in most studies from other fans.

All Parasound lines from the study area show sediment waves revealing a large variability in apparent wavelengths and amplitudes. Wavelengths appear different because wave fields seems to be orientated radial to the channel besides meander bends as observed on Monterey Fan (McHugh and Ryan, 2000). However, an asymmetry of the wavefields between western and eastern levee is not found. Additionally, no general asymmetry of the levees is observed suggesting that Coriolis-force is not a dominant factor during the evolution of the active channel-levee system in the study area.

Altogether the levees were built by either parallel or wedge-shaped sedimentary units. The locations of the latter are controlled by the geometry of the active channel during deposition. This spatial variability of deposition results in varying sediment units in the levees as mentioned in Chapter 2.5.2.2. As a further consequence, not only vertical stacking but also pronounced horizontal differences of sedimentation occur through time not

previously reported from other submarine fans. Accordingly, the exact regional reconstruction of the development in time and space of this complex channel-levee system would require an extensive spatial sampling program to acquire the necessary ground truth.

2.6.4 Mechanism of channel avulsion

We conclude that the system developed by successive cutting of the active channel into deposits of the central channel-levee system and rapidly refilling of the abandoned channel loops. To illustrate the channel avulsion process, planforms of different sinuosity representing different stages of the active channel were identified and redrawn in Figure 2.7 together with areas where levees are affected by erosion. The sequence of evolutionary stages can be attributed to a repetitious process: The planform of the channel changes from nearly straight to increasingly sinuous until a breach occurs, resulting again in a straightened channel segment (Fig. 2.7). In particular, a nearly straight channel segment (A) turns into a slightly sinuous channel segment (B) by the outward migration of loops due to erosion. Further outerbank erosion increases the curvature of the loops (C). The straight part of the channel moves downslope, compressing the distance between the upstream entrance and downstream exit of the meander loop (D). Finally, turbidity currents are able to cut the meander gap and create a new, straight channel segment, thereby leaving a cut-off loop (E). Then the process repeats itself and again, the straight channel segment changes into a slightly sinuous channel segment (F) as during the transition from A to B and simultaneously the cut-off loop will be refilled.

This process seems to repeat itself frequently at different locations in the study area, therefore the various evolutionary stages are represented today by different segments of the channel. Stages A and B are identified in the northern part of the study area. The point bars on the inner side of the meander loops in Stage B (see also Figure 2.2) indicate the outward migration of the loops on their outer sides (cut bars) due to erosion. The advanced stages C and D are found in the southern part of the study area. The transition from Stage D to Stage E must have occurred most recently in the northern part of the study area, where the cut-off loops are only partially refilled (see also Figure 2.2). Stage E probably represents the channel planform in the north before the now present points bars (Stage B) had developed, the sinuosity of Stage E is obviously similar to Stage A. Finally, Stage F is identical to Stage B in the northern study area. Consequently, further development of the system will lead to the breaching of narrow meander gaps as for example in the loop of Stage D (Fig. 2.7).

2.6.5 Why does frequent channel avulsion occur?

The most remarkable feature of this channel-levee system is the large number of more than 20 refilled cut-off loops over a channel length of 90 km. At the most submarine fans such high number of cut-off loops has hitherto not been identified. Kolla et al. (2001) show 3D-seismic data from the subsurface tertiary Congo Fan suggesting discrete channel migration or channel shifts. If channel shifting occurred to the inner (convex) side of a

meander loop, cut-off loops may have formed. Average amplitude displays of the 3-D seismic data show a highly sinuous channel with at least one cut-off loop over a channel length of 15 km (Kolla et al., 2001). From the recent Congo Fan Babonneau et al. (2002) reported numerous cut-off loops from one segment of the active channel but does not give an exact number. In contrast, no cut-off loops have been reported from the youngest channel-levee systems on the Indus Fan (Kenyon et al., 1995) and the Mississippi Fan (Weimer, 1991). On the Amazon Fan, nine cut-off loops were identified on the middle fan over a channel length of 280 km (Pirmez and Flood, 1995). However, a few more cut-off loops may be present, but could not be detected because they were buried or within older segments (Pirmez and Flood, 1995).

Peakall et al. (2000a) pointed out the general observation that the small number of cut-off loops is characteristic for submarine channels in contrast to subaerial rivers and Kolla et al. (2001) summarized that cut-off loops in deep water channels are uncommon. Based on data from the Mississippi Fan (Kastens and Shor, 1985), Peakall et al. (2000a) propose a model where bend growth including point bar deposition occurs only during the initial stage. After the channel has reached a planform equilibrium, the planform geometry remains stable and the channel acts as a bypass zone (Peakall et al., 2000a).

In contrast, we not only identified more than 20 cut-off loops from the combined Parasound and Hydrosweep analyses, but also found a large number of filled channels in our Parasound lines (Fig. 2.7). However, it was not possible to connect these channel segments to loops (Fig. 2.7). This may either be due to an insufficient density of survey lines or due to destruction of filled channel segments by subsequent channel avulsions (e.g. Channel B in Fig. 2.9). The channel avulsions probably limited the lifetimes and downcurrent extensions of several filled channel segments, especially near pronounced meander loops.

These frequent changes in position of the channel reveal a significant instability of the channel-levee system on the middle Bengal Fan. In principle, a channel attempts to maintain a constant or gradually decreasing slope (an equilibrium profile) through changes in sinuosity or through entrenchment/aggradation of the channel talweg (Pirmez and Flood, 1995). These changes are apparently in response to changes of the valley slope the channel system is built on. On the other hand, channel morphology depends on the flow parameters of turbidity currents travelling through it, i.e. flow velocity, density and frequency (Clark et al., 1992; Babonneau et al., 2002; Pirmez and Flood, 1995). Turbidity currents are controlled by the influx from the delivering rivers and are modified on their passage in the channel due to deposition of the transported material, entrainment of the ambient seawater or remobilization of sediment by erosion. Obviously, all these processes interact in a complex manner and influence the morphology of submarine channels (Hiscott et al., 1997; Peakall et al., 2000a; Pirmez and Flood, 1995).

The reason for the instability of the channel-levee system on the middle Bengal Fan is yet unknown. From our data we cannot conclude with certainty, whether the channel has

changed its geometry and morphology through time, especially, if older channels had a larger or smaller sinuosity. Assuming the channel did change its geometrical and morphological parameters, we would suppose the changes were caused by external factors, especially changes in sediment supply, because the valley slope remained constant in the study area. In other words, the channel requires changes in sinuosity due to changed flow parameters of the turbidity currents. However, since the planform of the now active channel in the south of the study area is similar to the identified cut-off loops we believe that there have been no principal changes in sinuosity during the life span of the present channel. This idea is supported by the fact that the width and relief of the refilled channel segments correspond to the width and relief of the active channel. Therefore we suggest that the nature of the turbidity currents did not change during the evolution of the active channel-levee system and that the channel instability is not caused by such changes.

By comparing the channel parameters with other submarine fans we notice that the valley slope as well as the channel slope are smaller than, for example, on the Amazon, Mississippi and Congo fans, whereas the sinuosities of the Indus, Amazon and Congo fans channels are similar to the sinuosity in our working area (Babonneau et al., 2002; Clark et al., 1992; Kenyon et al., 1995; Pirmez and Flood, 1995). In general, it is quite conceivable that because of the small valley slope the downslope-directed component of gravity-force is so small that the channel gains a higher degree of freedom to meander than a channel on a steeper fan. However, as explained in Chapter 2.6.4, only a highly sinuous channel produces cut-off loops because erosion of the planform is enhanced, leading to a repetitious process of loop growth and levee breaching. Also on Amazon and Congo fans cut-off loops were reported from channel segments with highest sinuosity (Babonneau et al., 2002; Pirmez and Flood, 1995). Maximum channel sinuosity is reached individual for each fan by a certain valley slope, which is influenced by the flow parameter of the turbidity currents (Clark et al., 1992). On both, Congo and Amazon fans, channels become highly sinuous when the channel slope decreases below 0.5 %, which is probably the threshold of channel slope for maximum sinuosity on both fans (Clark et al., 1992; Babonneau et al., 2002; Pirmez and Flood, 1995). This similarity may suggests similar flow parameters of turbidity currents on Amazon and Congo fans, but differences to flow parameter of turbidity currents in our study area on the middle Bengal Fan where high sinuosity occurs by channel slope of 0.07%.

Another factor controlling sinuosities of submarine channels is the maturity (relative age) of channel segments as suggested by Babonneau et al. (2002). Maturity is first controlled by the time that location of a channel segment is fixed, which depends mainly if channel talweg incises down to depths below the regional seafloor or aggradate. Deep incision inhibits channel bifurcation by avulsion, whereas aggradation leads to instability of a channel-levee system and finally to channel bifurcation by avulsion. Again, incision vs. aggradation depends on flow parameter of turbidity currents flowing through the channel-levee system. Since channel floor of the active channel on the Congo Fan is deeply in-

cised, Babonneau et al. (2002) suggest for the Congo Fan that avulsions associated with bifurcations are probably much less frequent than on Amazon Fan, where channel floor shows aggradation. But this difference may only explain why the channel of the Congo Fan is longer than the channel on Amazon Fan, even sinuosities are similar on both fans (Babonneau et al., 2002).

In particularly, highest sinuosity on Congo Fan is found upslope of most bifurcation points (relatively old segment), whereas on Amazon Fan the highest sinuosity is found downslope of most bifurcation points in a relatively young segment of the channel (Babonneau et al., 2002; Lopez, 2001; Pirmez and Flood, 1995). These observations may suggest that valley slopes have larger influence on sinuosity than age of channel segments. However, channel segment with highest sinuosity on Amazon Fan was active between 21,000 and 9,000 yr B.P. and the channel-levee system on the middle Bengal Fan is active since 12,800 ^{14}C yr B.P. (Pirmez and Flood, 1995; Weber et al., 1997). So both systems are characterized by a similar life span, although the active channel of the middle Bengal Fan shows no aggradation in contrast to the Amazon Fan.

Obviously, maturity depends also directly on frequency of turbidity currents. On Amazon Fan, frequency of turbidity currents was 0.15-0.3/yr during the built up of the youngest channel-levee complex during the last glacial maximum (Piper and Deptuck, 1997). On Congo Fan, present day activity is documented by submarine cable breaks and frequency of turbidity currents is estimated to 0.6/yr (Babonneau et al., 2002). Accordingly, frequencies of turbidity currents on Amazon Fan and Congo Fan are similar during their evolution. Unfortunately, no frequency of turbidity currents are reported from the Bengal Fan for the time the levees mainly built up (12,800 ^{14}C yr B.P. and 9700 ^{14}C yr B.P.). At present, in the Canyon „Swatch of No Ground“ mass movement events that are probably able to initiate turbidity currents reaching the deep-sea fan are indicated on centennial scale (Michels et al., 2003).

In summary, no simple and general relationships seem to exist between the different morphological parameters, maturity and flow parameter of turbidity currents applicable for each submarine fan and each channel-levee system. More probably, morphological parameters of submarine channels are controlled by a complex interaction between valley slopes and flow parameters of the turbidity currents individual for each submarine fan. Therefore we believe that the combination of the exceptionally low valley and channel slopes and (so far) unknown flow parameters of the turbidity currents in our study area leads to the planform instability of the active channel-levee system.

2.7 Conclusions

- The channel-levee system on the middle Bengal Fan is characterized by a large variability from low to high channel sinuosities and exceptionally low channel slope compared to other large mud-rich submarine fans.
- The system can be divided into inner and outer zones with significantly different depositional architecture.
- The inner zone consists of the active channel and sharply separated vertical blocks characterized by parallel, distinct reflectors. Since several of these blocks are associated with seafloor depressions forming bends and many of them can be connected to segments having the planform of a bend, we interpret them as cut-off loops.
- The outer zones represent undisturbed levees. Sedimentation on levees is extremely variable in time and space, leading to a complex vertical and lateral pattern of different shaped sedimentary units not previously described from other channel-levee systems. This pattern depends on the nature of the turbidity currents as well as geometry and morphology of the active channel during the deposition.
- Within the channel-levee system, more than 20 cut-off loops were identified. In contrast to most other submarine fans, channel avulsions within the active channel-levee system are a frequent process during the evolution of the middle Bengal Fan. In the southern study area, a temporal succession of at least 4 cut-off loops was identified, suggesting that channel avulsions had occurred on average every 750 years.
- Channel avulsion is a repetitious process of loop growth and levee breaching caused by erosion through turbidity currents.
- In general, the morphological parameters of submarine channels seem to be controlled by a complex interaction between valley slopes and flow parameters of the turbidity currents individual for each submarine fan. We believe that the combination of the low channel slope and the flow parameters of the turbidity currents cause the instability of the active channel planform, which finally leads to the exceptionally large number of cut-off loops in the study area.

2.8 Acknowledgements

This manuscript was greatly improved by the detailed constructive reviews of R. Hesse and U. v. Rad. We thank the captains and crews as well as all Parasound/Hydrosweep watch-keepers of R/V Sonne cruises 93, 125 and 126 for their support. This work was funded by DFG, Grant SP296/14, Graduiertenkolleg „Stoff-flüsse in marinen Geosystemen“, and BMBF, Grant 03G0125A.

Chapter 3: The architecture and evolution of the Middle Bengal Fan in vicinity of the active channel-levee system imaged by high-resolution seismic data

T. Schwenk, V. Spieß, M. Breitzke, C. Hübscher

To be submitted to Marine and Petroleum Geology

3.1 Abstract

High-resolution seismic data from the Middle Bengal Fan were analyzed to study the architecture of the fan in the vicinity of the active channel-levee system and to evaluate channel behaviors. The upper 600 m of the fan in the study area reveal a pattern of different sized channel-levee systems and High Amplitude Reflection Packets (HARPS) of varying thicknesses, which are interpreted as sandy deposits. No mass-flow deposits or hemipelagic drapes are found. Within the channel-levee systems, units of Chaotic High Amplitude Reflectors (CHARS), which represent aggraded and migrated channel axes, as well as abandoned channel fill deposits appear. All channels are characterized by erosional incision into underlying deposits, one buried channel-levee system terminates on the Middle Fan.

Within the active channel-levee system, numerous cut-off loops are found. The active channel segments as well as the cut-off loops show a broad spectrum of complex behaviors with different ratios of vertical aggradation and lateral migration not only along the channel, but also during the evolution of one channel loop. Floors of all cut off loops and the active channel have not aggradad above the surrounding seafloor. This morphological characteristic may lead to a long lifetime of the active channel-levee system resulting in the large number of cut-off loops.

In contrast, a detailed studied buried system shows no cut-off loops and is characterized by a more simple behavior, namely by a first phase of lateral migration followed by a second phase of simultaneous vertical aggradation and lateral migration until the abandonment of the system. The aggradation elevated the channel floor of this system above the level of the pre-existing surrounding seafloor. These architectural differences between the buried and the active system indicate that different loaded turbidity currents have built up both systems. The aggraded and migrated channel floors likely have reservoir potential, but a high-resolution 3-D seismic survey is necessary for final proof.

3.2 Introduction

Large submarine fans as the Bengal, Amazon, Mississippi and Congo Fans are major and in some regions dominating geologic features for building and shaping continental margins. It is therefore important to improve our understanding of their sedimentary architecture and of the depositional and transport processes acting within these turbiditic systems. One essential goal is to understand their potential for hydrocarbon reservoirs as well as for recording long-term and short-term climatic and oceanographic changes during Earth's history.

Generally, climate, tectonics, sea-level fluctuations as well as sediment type and volume are the four major factors controlling the development of submarine fans from erosion through transport to deposition (Bouma, 2001). Interaction occurs between these factors, as for example sea-level fluctuations are dependent on climate and tectonics. Climate controls the erosion in the sediment source area through temperature and precipitation, which in turn can cause variations in run off and fluvial transport capacity for sediments. Sea-level fluctuations have a major impact on sediment transport by controlling the extent of shelf areas, i.e., the distance between coast and shelf edge, which will have an effect on the sediment distribution processes particularly within fine-grained submarine fans. Therefore, changes in the sedimentary record of these fans may well reflect long and short-term climatic changes (Bouma, 2001).

Furthermore, deep-water passive margin Cenozoic submarine fans are recently the target of active exploration and drilling by oil companies due to their high reservoir potential (Lopez, 2001). Stow and Mayall (2000) estimate that 1200 – 1300 oil and gas fields are known from deep-water clastic systems and predict that these systems will be topics of oil and gas exploration for at least the next 25 years. Possible reservoirs in submarine fans are sands in abandoned channel-fills, sand-rich aggrading channels and laterally extensive sand sheets within lobes (Lopez, 2001; Richards et al., 1998). These potential reservoirs are the result of an effective sand separation from originally mixed load turbidity currents during their travel through long meandering channels (Hiscott et al., 1997; Lopez, 2001). Therefore, the stacking and character of architectural elements such as channel-levee systems or lobes have a major impact on the reservoir potential of submarine fans, leading to numerous research projects aiming for a better predictive understanding of reservoirs in deep offshore turbidite and related oilfields (Lopez, 2001; Richards and Bowman, 1998; Stow and Mayall, 2000).

In the last decade, several publications presented new data from submarine fans improving the understanding of architecture and growth processes of passive margin deep sea fans. From the Congo (Zaire) Fan, echo-sounding data, seismic data and piston cores were collected during the ZAIANGO-Project carried out by IRFREMER and TotalFinaElf to develop more accurate reservoir models for this system (Babonneau et al., 2002). Kolla et al. (2001) presented a study about the subsurface tertiary Congo Fan discussing the evolution of its channels sinuosities and the implications for reservoir architecture using 3-

D seismic data. Probably the best studied large, mud-rich submarine fan is the Amazon Fan, which was not only investigated with swath-sounding sonar, side-scan sonar, gravity cores and reflection seismics, but also deep penetrated at 17 sites during Ocean Drilling Program (OPD) Leg 155 in 1994 allowing a systematic calibration of seismic facies with the drilled sediment facies (Flood et al., 1995; Lopez, 2001). The key results of this leg are a better understanding of facies architecture, depositional processes and sequence stratigraphy of the Amazon fan. Especially the identification of sand-rich aggrading channels and sand sheets downfan of avulsion points resulted in an advanced prediction of reservoir potential of deep-sea turbidite systems (Lopez, 2001).

In this paper, we present very high-resolution seismic data imaging the upper 600m of the Middle Bengal Fan in the vicinity of the active channel-levee system. After a short introduction of the Bengal Fan and the previous work in the study area, we describe and discuss the seismic facies found in the study area. Next we give a detailed description of the vertical stacking of architectural elements and their downfan changes. We then compare the evolution and behavior of the active channel-levee system and a pronounced buried system and discuss the general build-up of the fan in the study area in comparison to other large submarine fans. Finally, the possible reservoir potential of channel-levee systems found in the study area will be discussed.

3.3 Geological setting

3.3.1 The Bengal Fan

The uplift of the Himalayas due to the collision between India and Asia started the development of the Bengal Fan in the early Eocene (Curray, 1994). Today, the Bengal Fan covers the entire Bay of Bengal from 20°N to 9°S over a length of 3000km with varying widths between 1430 km (at 15°N) and 830 km (at 6°N), yielding the largest submarine fan on Earth (Fig. 3.1) (Emmel and Curray, 1985). The area of the Bengal Fan is $3x10^6km^2$, the volume of the post collision sediments has been calculated to be $12.5x10^6km^3$ based on seismic refraction data revealing a maximum thickness of post collision sediments of 16 km at the shelf edge (Brune et al., 1992; Curray, 1994; Emmel and Curray, 1985). Based on the slope gradients of the active channel and the fan surface, Emmel and Curray (1985) subdivided the fan into three divisions (Fig. 3.1). In addition, size, morphology and structure of the upper-fan channels differ from those of the channels on Middle Fan and Lower Fan (Emmel and Curray, 1985).

In contrast to most other submarine fans (e.g. Amazon, Indus and Mississippi fans), the Bengal Fan is presently active, which is so far only known from the Congo Fan (Babonneau et al., 2002; Weber et al., 1997). The Bengal Fan is fed by the sediment load of the Ganges and Brahmaputra rivers dewatering the Himalayas (Fig. 3.1). Discharging a sediment load of $1\text{-}2x10^9t/yr$, the Ganges/Brahmaputra system delivers today more sediment than any other river system on Earth (Milliman and Meade, 1983). Approximately 35-50% of this enormous sediment freight reaches the deep sea fan at present; for the last

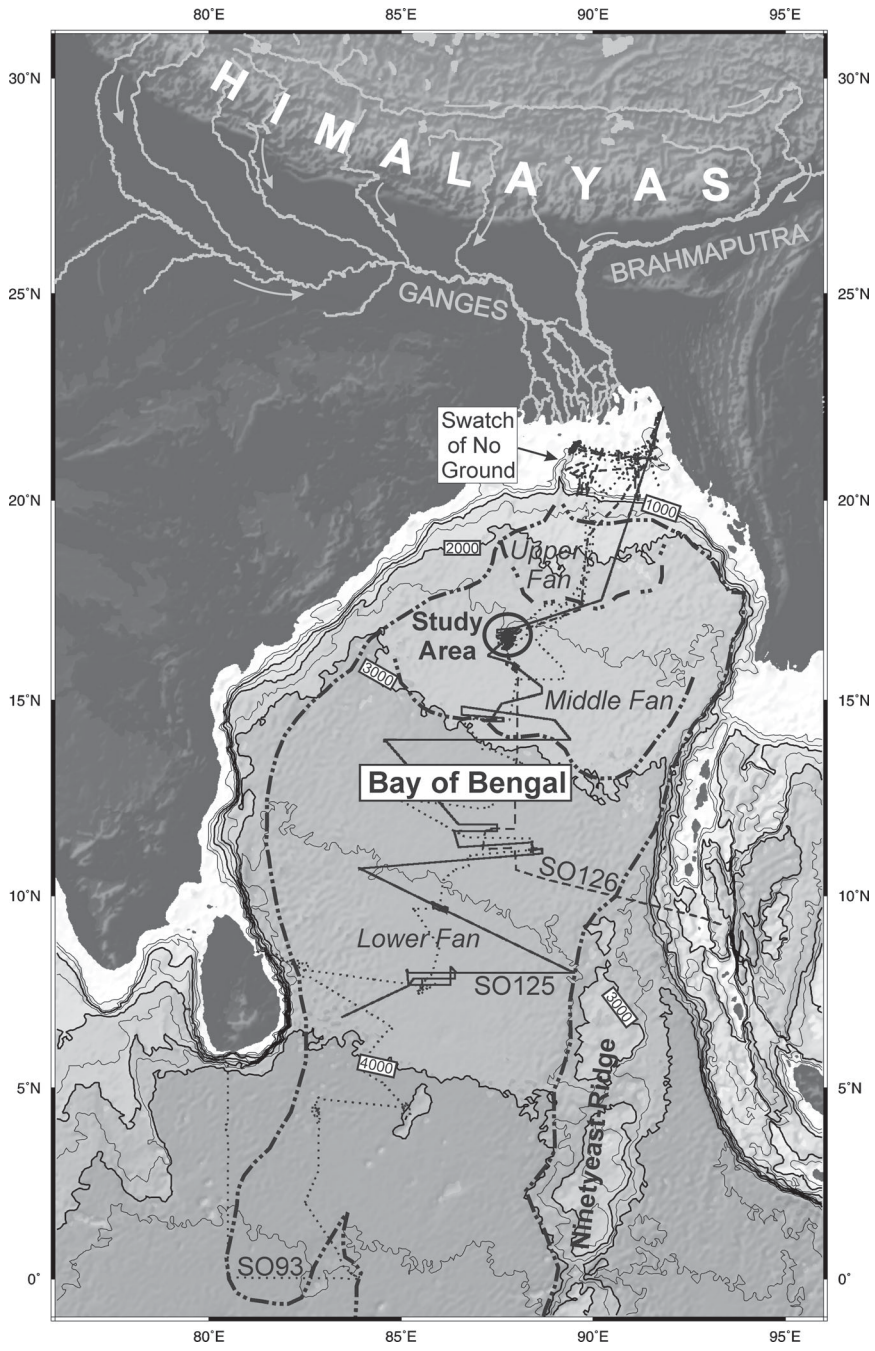

Figure 3.1: *Map showing the Bay of Bengal and the location of Ganges and Brahmaputra rivers dewatering the Himalayas. Boundary and subdivisions of the Bengal Fan (dashed-dotted lines) are redrawn from Emmel and Curray (1985). The tracks of SO 93 cruise (dotted line), SO 125 cruise (solid line) and SO 126 cruise (dashed line) are indicated as well as the study area (circle). Topography and bathymetry are satellite derived (Smith and Sandwell, 1997) and clearly displays the Shelf-Canyon „Swatch of No Ground“.*

7000 years this portion is estimated to be one third of the total riverine load (Goodbred Jr. and Kuehl, 2000a; Michels et al., 1998).

The transfer of the sediment from the delta to the fan is guided through a canyon deeply incised into the shelf, the „Swatch of No Ground“ (Fig. 3.1), which acts as a temporary trap for sediment that has been resuspended by storms and tides on the shelf (Emmel and Curray, 1985; Kudrass et al., 1998; Michels et al., 1998). The sediments inside the canyon were remobilized by gravity driven mass flows (maybe triggered by earthquakes) and then transported to the deep sea by turbidity currents (Kottke et al., 2003; Kudrass et al., 1998; Michels et al., 2003).

Generally, turbidity currents initially form channel-levee systems by erosion and deposition leading to a self-channelization and thereafter overspilling processes continue levee building (Hiscott et al., 1997; Imran et al., 1998; McHugh and Ryan, 2000; Peakall et al.,

2000a; Peakall et al., 2000b; Piper and Deptuck, 1997; Schwenk et al., 2003). Only one channel-levee system is active at any given time at most submarine fans including the Bengal Fan, but avulsion processes cause abandonment of channel segments and formation of new channel-levee systems (Babonneau et al., 2002; Emmel and Curray, 1985; Pirmez and Flood, 1995). Therefore, submarine fans grow vertically, laterally and downfan by stacking and overlapping of channel-levee systems. Consequently, channel-levee systems are the main architectural elements of the Bengal Fan similar to other large submarine fans like Amazon, Congo, Indus and Mississippi fans (Babonneau et al., 2002; Damuth et al., 1988; Emmel and Curray, 1985; Kolla and Schwab, 1995; Weimer, 1991).

3.3.2 Previous work in the study area

The study area, located approx. 400 km south of the shelf break around 16°30´N and 87°45'E in ~2600m water depth (Fig. 3.1), was the focus of three expeditions (SO 93, SO 125 and SO 126) with the German research vessel RV Sonne in 1994 and 1997 (Kudrass and Shipboard Scientific Party, 1994; Kudrass and Shipboard Scientific Party, 1998; Spieß et al., 1998). The active channel-levee system in this area is more than 40 km wide, the levee thickness varies between 50 and 70 meters, and the channel relief reaches 70 meters (Hübscher et al., 1997; Schwenk et al., 2003). The active channel is characterized by variable sinuosities between 1.05 and 3.5 (see Fig. 3.2) and a very low slope gradient of 0.7m/km (Schwenk et al., 2003).

The Parasound sediment echosounding data of SO 93 Cruise revealed a complex structure of the active channel-levee system with a strong vertical segmentation, previously interpreted as a narrowing of the channel in distinct phases (Hübscher et al., 1997). The gravity cores of SO93 cruise revealed mostly fine-grained muddy turbidites and dating of these sediments demonstrated that the levees of this system were mainly built up between 12,800 ^{14}C yr. B.P. and 9700 ^{14}C yr B.P. (Weber et al., 1997). Based on a single Parasound profile perpendicular to the channel from the SO93 Cruise, a closely spaced grid of Parasound and Hydrosweep data was collected during SO125 Cruise in 1997 covering an area of 55x60 km to provide spatial information about structures and processes (Spieß et al., 1998).

A combined analysis of both data sets showed that the vertical segmentation is the result of frequent levee avulsions within the channel-levee system leading to numerous abandoned channel segments, which are completely or partly refilled (Schwenk et al., 2003). More than 20 so-called cut-off loops were identified over a channel length of 90 km, which is in contrast to most other large mud-rich submarine fans (Kolla et al., 2001; Peakall et al., 2000a; Peakall et al., 2000b). Additionally, the combined analysis of Parasound and Hydrosweep data indicated a complex vertical and horizontal distribution of sedimentary units within the levees suggesting a pronounced variation of deposition in time and space (Schwenk et al., 2003). This depositional pattern is caused by different overspill events of different sized turbidity currents: turbidity currents with a smaller or similar size as the channel cross-section area may only or predominantly overspill at meander bends pro-

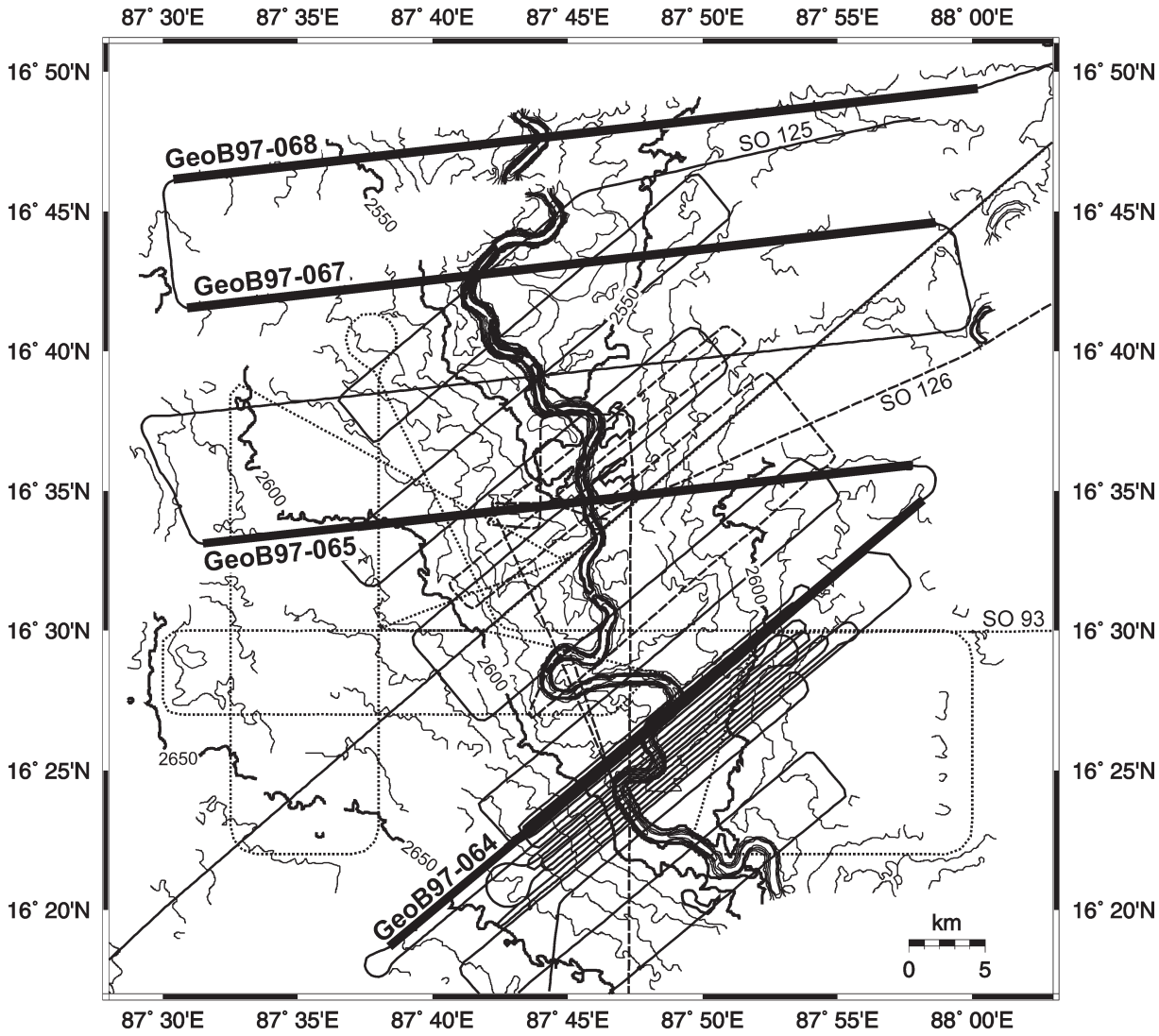

Figure 3.2: *Bathymetric contour map of the study area based on Hydrosweep data of SO 93 and SO 125 cruises. Contour spacing is 10 m. Thick solid lines indicate the location of the seismic profiles of SO 125 cruise shown in this paper. Tracks of Sonne cruises in the study area are marked by thin solid lines (SO 125), thin dotted lines (SO 93) and thin dashed lines (SO 126).*

ducing small depositional units, whereas turbidity currents significantly exceeding the cross-section of the channel deposit their suspended load over large areas (Schwenk et al., 2003).

3.4 Methods

3.4.1 Data acquisition

In the study area, seismic data were collected during SO 125 Cruise, whereas hydro-acoustic data were collected during SO 93 Cruise, SO 125 Cruise and SO 126 Cruise (Kudrass and Shipboard Scientific Party, 1994; Kudrass and Shipboard Scientific Party, 1998; Spieß et al., 1998). The seismic data were collected on four E-W profiles and two SE-NW profiles (Fig. 3.2) using two seismic sources in an alternating mode: A GI Gun with reduced chamber volumes of 2 x 0.4 L (100-500 Hz) and a Sodera S15 watergun of 0.16 L volume (200-1600 Hz). Seismic signals were collected by means of a 600-m long Syntron streamer equipped with separately programmable hydrophone subgroups of different

lengths. 48 groups with a length of 6.25 m and a group-spacing of 12.5 m were chosen for this study. Six remotely controlled bird units kept the streamer in approx. 2.5 m water depth and recorded the depth as well as the position of the streamer relative to the ships course by magnetic compasses. The seismic data were stored in SEGY format using a Bison seismograph with a sample rate of 0.125 ms, a recording length of 4 s and a water depth dependent delay. During seismic acquisition, the average ship speed was ~5.0 kn.

In addition to the seismic data, a dense spaced grid of hydroacoustic data was available from the study area collected with the hull-mounted sediment echosounder Parasound and the hull-mounted bathymetric swath sounder Hydrosweep (Fig. 3.2). The Hydrosweep system, operating at a frequency of 15.5 kHz, provides depth information for a swath width of twice the water depth by generating 59 pre-formed beams over an angle of 90° (Grant and Schreiber, 1990). Results of the combined analysis of the hydroacoustic data are summarized by Schwenk et al. (2003).

3.4.2 Data processing

As first step of seismic processing, binning was carried out with the GeoApp software package (Zühlsdorff, 1999). Reflection midpoints were calculated based on GPS navigation of the ship and the heading data of the bird units and sorted into bins. To image the complex structures of the study area with a high lateral resolution, a bin midpoint distance of 10 m was chosen leading to a 7-9 fold CDP coverage. Static corrections for the GI Gun data were based on the depth information of the birds and interpolation between them. Due to the short wavelength of the Watergun Data, static corrections for these data were based on precise depth information of the Parasound system as described in detail by Gutowski et al. (2002). A constant velocity of 1500 m/s was used for NMO correction. Finally, the data were stacked and migrated using a time-wavenumber domain migration. Processing was carried out with the public domain processing package Seismic Un*x (SU) (Stockwell, 1997). For displaying and interpretation purposes the commercial software package Kingdom Suite 7.0 (Seismic Micro Technology, Inc.) was used . The Hydrosweep data were taken from Schwenk et al. (2003).

3.5 Data

3.5.1 Seismic facies in the study area

Four main seismic facies types were identified in the study area (Fig. 3.3). In the following paragraphs, we describe and interpret these facies. The interpretation is based on results from drilling and seismic calibration in the Amazon Fan (Flood and Piper, 1997; Flood et al., 1995; Hiscott et al., 1997; Lopez, 2001; Pirmez and Flood, 1995):

1.) Seismic Facies 1 (Fig. 3.3) is characterized by dipping, low-amplitude reflectors diverging towards the center of the channel-levee systems and often downlapping onto a strong acoustic base reflector. Partly the reflectors appear wavy. This facies is identified in the levees of all channel-levee systems in the study area building relative transparent

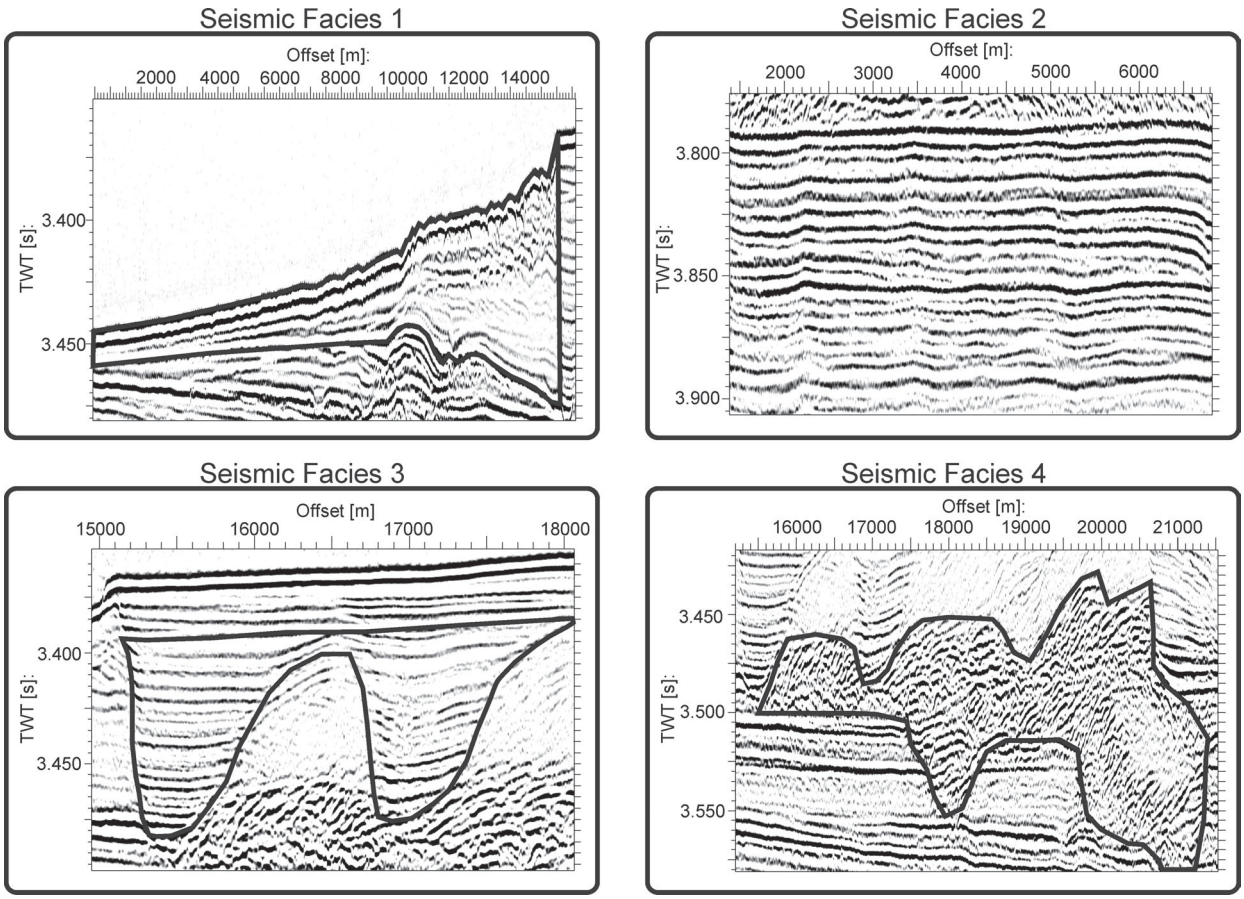

Figure 3.3: *Main seismic facies identified in the study area. Examples are taken from Profile GeoB97-068 (see Fig. 3.4). For easier identification, Facies 1, 3 and 4 are encircled by a bold black line. Notice the different scales for each figure as indicated by offset in meters and TWT in seconds. For detailed description and discussion, see text.*

wedge-shaped units. Thickness to width ratio of these units varies significantly from system to system.

We interpret this facies as fine-grained sediments deposited from overspilling of turbidity currents traveling through the adjacent channel. This interpretation is in agreement with results from the Amazon Fan, where drilling in similar seismic facies reveals fining upward deposition of inter-bedded and inter-laminated very fine sand, silt and mud turbidites (Hiscott et al., 1997; Lopez, 2001). Fining upward deposition is due to the stratification within mixed-load turbidity currents carrying coarse-grained material at the base and fine-grained material on the top of the flow (Hiscott et al., 1997; Lopez, 2001; Peakall et al., 2000a; Peakall et al., 2000b). Consequently, continuing building up of levees lead to a fining of the overspilled material deposited on top of the levees.

2.) Seismic Facies 2 (Fig. 3.3) consists of widespread packets of mostly parallel, high-amplitude reflectors. These HARPS (High Amplitude Reflection Packets) are intercalated between the channel-levee systems, and some of these packets extend from west to east across the entire study area. Especially in the shallower parts of the profiles, the reflectors of Seismic Facies 2 are onlapping on Seismic Facies 1. Many reflectors of Seismic Facies 2 can be traced over long distances, but several reflectors are also discontinuous or disrupted. Reflectors are incoherent or hummocky in some parts.

According to the HARPS found on Amazon fan, which correspond to thick beds of fine- or medium grained massive to graded sand, we interpret the HARPS in our study area as thick deposits of equivalent sediments (Hiscott et al., 1997; Lopez, 2001). On upper and middle Amazon Fan, these packets are the result of levee avulsions followed by unchannelized turbidity currents flowing in intrachannel lows. On the lower Amazon Fan, HARPS-like reflectors packets represent sandy lobes at the down-fan end of terminating channel-levee systems (Lopez, 2001).

3.) Seismic Facies 3 (Fig. 3.3) is characterized by parallel, distinct reflectors of medium amplitude. Seismic Facies 3 appears as vertical V-shaped blocks with sharp lateral edges. This seismic facies is found in the center of the active and of most buried channel-levee systems, but also within Seismic Facies 2, here with relatively high-amplitudes. In the active and some buried channel-levee systems, these vertical blocks are often associated with depressions in the seafloor or in overlying sediments.

By comparison with the results of the combined analysis of Hydrosweep and Parasound data of the study area (Schwenk et al., 2003), Seismic Facies 3 is interpreted as fill deposits of abandoned channel-levee systems or abandoned channel segments (cut-off loops). Whereas cut-off loops act as efficient sediment traps for overspilling turbidity currents from active channel segments (Schwenk et al., 2003), abandoned channel-levee systems were probably filled by overspilling turbidity currents of the succeeding active channel-levee system. If placed within the HARPS, Seismic Facies 3 represents filled unleveed channels as also found on Amazon Fan (Hiscott et al., 1997; Lopez, 2001).

4.) Seismic Facies 4 consists of chaotic, high amplitude reflectors (CHARS). The reflectors appear discontinuous, sometimes dipping and are found at the base of all channel-levee systems. Vertical and lateral extent as well as shape varies significantly between the different systems: The CHARS are either vertically stacked, or build dipping blocks, or form horizontally extended blocks. In the active system, Seismic Facies 4 is found beside and below the active and filled channels, in most buried systems, Seismic Facies 4 is also associated with filled channels. In all systems, this facies is deeply incised into the sediments beneath, i.e., in Seismic Facies 2 (HARPS) or 1 (levee deposits).

By comparison to the seismic facies on Amazon Fan, the CHARS in our study seem to correspond to the so-termed HARS (high amplitude reflectors) found there. These HARS are vertically stacked sets of high amplitude reflections marking the channel-axes and representing massive to graded sands on channel floors (Lopez, 2001). Constriction of sand deposition to the channel is again the result of stratification of mixed-load turbidity currents: The lower parts of turbidity currents, which are carrying the coarser material, are not able to overspill the levees (Hiscott et al., 1997; Lopez, 2001). On Amazon Fan, the deposition of sandy material leads to aggradation of all channel-levee systems above the level of the adjacent areas (Lopez, 2001; Pirmez and Flood, 1995). In contrast, on Middle Bengal Fan the CHARS appear with different shapes. If the CHARS are vertically stacked, we interpret them as aggradational channel fill as on Amazon Fan. If the CHARS are more

laterally spread and located beside the channels, we interpret them as point bars resulting from lateral channel migration due to erosion of the levees by turbidity currents. If the CHARS are building dipping blocks, they must be deposited by simultaneous lateral migration and aggradation of the channel axes. This simultaneous lateral migration and aggradation of submarine channels and their resulting depositional pattern are also observed on Tertiary Congo Fan (Kolla et al., 2001).

3.5.2 Vertical stacking of architectural elements

To describe in detail the vertical pattern of the architectural elements, we present GI-Gun data of three seismic profiles from the study area imaging the upper ~600 m of the fan: the northernmost Profile GeoB97-068, the central Profile GeoB97-065 and southernmost Profile GeoB97-064 (see Fig. 3.2). Time to depth conversion is calculated with a sound velocity of 1500m/s for the imaged upper sediment column.

3.5.2.1 Profile GeoB97-068

The east-west orientated Profile GeoB97-068 (Fig. 3.4) has a length of ~53 km. The active channel-levee system (A) is located in the center of the profile. East of the active channel-levee system, two small, partly filled channels are incised into the fan surface. The appearing width of the active system does not exceed 40 km, and maximum levee height reaches 90 m. The western levee is shaped by small-scale sediment waves. Four filled channels could be identified beneath the active channel. Sideways the filled channels, seismically transparent zones are found. Beside and below these filled channels, a broad zone of CHARS appears. These CHARS are deeply incised into underlying sediments, which consist of levee deposits as well as HARPS. Measured from the base of the levees, incisions of the CHARS reach values up to ~90 m, leading to a maximum thickness of the whole channel-levee system of 190 m. West of the floor of the active channel, a narrow zone of CHARS is found, which is only incised 20 m into underlying sediments.

The active system is settled onto eastward thinning HARPS, which are deposited on top of a buried system (E) west of the active system and in the low between System E and a buried system (B) east of the active system. Within the western part of these HARPS unleveed filled channels could be identified.

In the central part of System B, a complex pattern of three filled channels, partly cutting into each other, perched on a small unit of CHARS. Both, the channels and the CHARS, are incised into the underlying HARPS by 30 m. In the western part of System B, distinct, stacked levee deposits are attached to each channel. Further eastwards, the levee deposits onlap onto System E. Total thickness of System B from base of CHARS to top of levees is 105 m. The eastern levee sediments of System B onlap onto another levee deposit bordered by a filled channel with associated CHARS (C). Again, channel and CHARS are cutting into HARPS. As a curiosity, east of these channel-deposits and CHARS a levee is missing in System C, and HARPS interrupted by filled channels are located there instead. The total thickness of System C is just below 80 m.

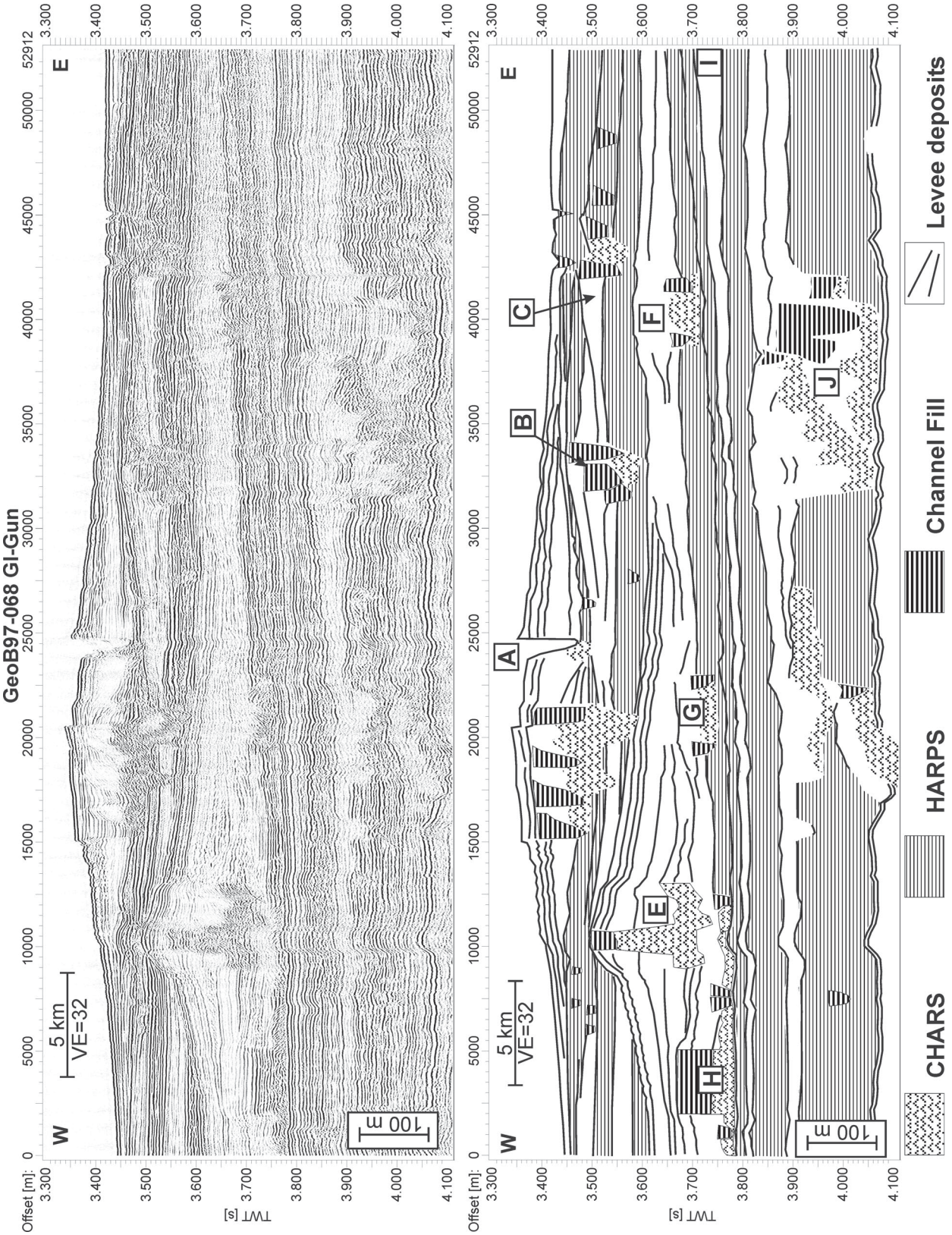

Figure 3.4: *Seismic section and line-drawing of Profile GeoB97-068 showing the architecture of the Bengal Fan imaged by GI-Gun data at the northern boundary of the study area (see Fig. 3.2 for location). The profile runs from west to east reaching a length of ~53 km, the section shows the uppermost ~600 m. Line-drawing reflects the four main seismic facies as defined in Fig. 3.3.*

Beneath systems B and C, HARPS with an average thickness of 50 m are deposited, terminating to the west as onlap onto a large buried channel-levee system (E). Above the western levee of this system, which shows sediment waves on top, a sequence of onlapping HARPS and levees can be identified. The central part of System E reveals a wide zone of CHARS. In contrast to the active channel-levee system, only one filled channel is found. This channel settles on top of CHARS, which build a vertical block with a broad base. The width of the filled channel is equal to the width of the vertical block of CHARS. Incision of CHARS into underlying deposits does not exceed 40 m and is therefore much smaller than in the active system. Levee height beside the filled channel remains below 130 m and the total thickness of System E reaches 180 m as maximum.

The System E is again build upon a low between the two smaller systems H and G. Both systems consist of some channel deposits and small CHAR zones, and both systems are 20 m incised into the underlying HARPS. Thickness of System H is ~85 m, whereas thickness of System G is less than 65 m. Levee deposits of Channel-Levee System E seems to onlap to the east onto a smaller system (F) located beneath. In the center of System F, two filled channel deposits enclose a small zone of CHARS. Channel fills cannot be traced upwards to the top of the levees, but depressions in the overlying HARPS indicate previously existing channels, which were not completely filled when the HARPS were deposited. Incision of CHARS and filled channels into underlying HARPS amounts to 30 m, the levee height beside the filled channels reaches 60 m and the maximum thickness of System F is close to 100 m.

Channel-levee systems F, G and H cut into the same HARPS spreading over the whole profile with nearly constant thickness of 60 m. Below these HARPS, a deposit (I), which is characterized by low amplitude reflectors like levee deposits, extends over the whole profile thinning from 40 m in the East to 15 m in the West. Deposit I is completely underlain by HARPS with varying thickness between 30 and 45 m.

At the base of the presented profile, a different depositional pattern appears. A 120 m thick unit of HARPS is deeply incised at more than one location, either by CHARS, or by channel deposits, or by transparent units. The base of these HARPS is marked by a pronounced reflector. In the center of the profile, a zone of transparent facies and CHARS cuts ~45 m deep into the HARPS. Further to the East, a complex pattern of filled channels and CHARS (J) is incised 120 m into the HARPS down to their base. There the CHARS build a basal unit overlain by a dipping block with a small channel deposit on top. To the west of System J, levee thickness decreases from 55 m to 20 m. To the east, levee thickness remains constant along the profile. The maximum thickness of System J reaches 175 m. The base of the HARPS is interrupted in the center of the profile by a dipping block of CHARS with an associated filled channel. Additionally, smaller filled channels are found within these lowermost HARPS.

3.5.2.2 Profile GeoB97-065

Profile GeoB97-065 (Fig. 3.5) is located 25 km southward of Profile GeoB97-068 and covers a length of 46 km on an east-west transect.

The active channel-levee system reveals four filled channels and a broad zone of CHARS is distributed within all of the inner section between the levees. Two deep incisions of CHARS into the underlying sediments could be identified: a vertical block in the eastern part of the system, and a dipping block in the western part of the system, both attached to a filled channel. Obviously, the active channel cuts through a filled channel. Maximum levee height is more than 60 m, and the incision depth of CHARS exceeds 80 m. The total thickness of the active channel-levee system is ~160 m. The width of the system has been determined to 36 km. Sediment waves occur on both levees.

Beneath the eastern levee of the active system, a smaller buried system (B) is located beneath thin HARPS. Three filled channels with associated CHARS are found to incise by 20 m into underlying HARPS. Different levee deposits are visible, their total height reaches 40 m. Maximum thickness of System B has been measured to be 60 m. Levee heights remain constant to the east and an eastward boundary could not be identified.

Beneath the western levee of the active system, widespread HARPS interrupted by unleveed channels are observed. These HARPS onlap onto a channel-levee system (D) in the westernmost part of the profile. Within System D, two filled channels are visible on top of a gently dipping zone of CHARS, which are cutting 45 m into underlying HARPS. The height of the eastern levee reaches 50 m, leading to a maximum thickness of at least 95 m for System D.

System D and its basal HARPS both onlap onto the large System E, which is characterized by two channel fill deposits perching on top of a CHAR zone. The CHARS build two units (one broad and vertical, one narrow and dipping), which have a joint base deeply incised into HARPS. Both vertical blocks reach up to the same level. The incision depth of the CHARS is 55 m and the levee height adjacent to the filled channels reaches nearly 95 m. A maximum thickness of 170 m is measured for Channel-Levee System E between both channel fills. As in the active system, sediment waves developed on both levees.

Located in the same depth towards the east, the western part of a smaller channel-levee system (F) is found, but it appears separated from System E. Within System F, a small zone of CHARS is visible, but no channel-fill deposits appear, although the depression at the top may suggest the existence of a partially filled channel. CHARS are incised only 10 m into HARPS below. The western levee height of System F exceeds 50m, and a total thickness of 60 m is derived for System F. Beneath Systems E and F, HARPS extend over the whole profile with varying thickness, decreasing eastward from 80 m to 25 m. An unconformity splits the HARPS into a thinner uniform part at the base and an onlapping thicker part.

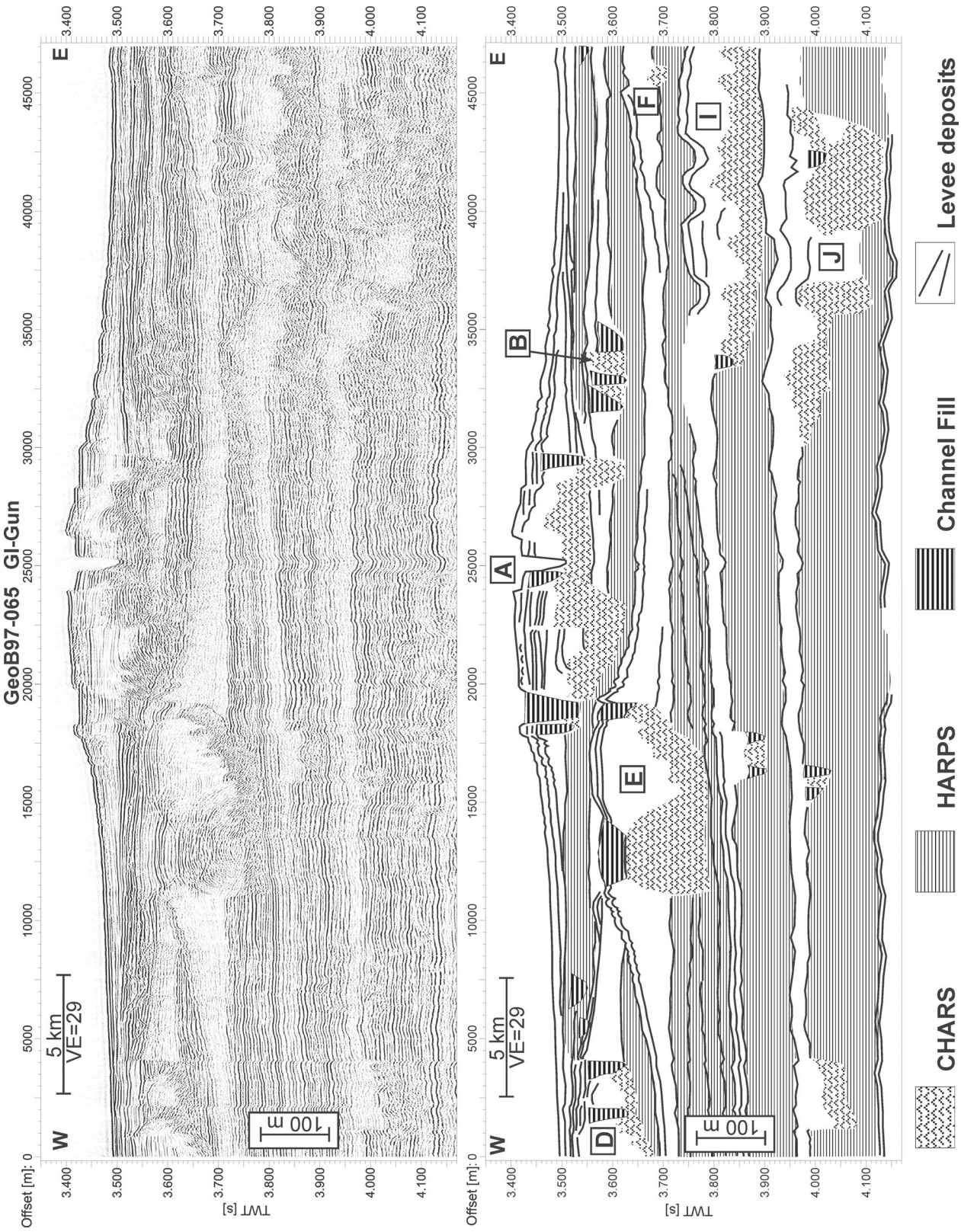

Figure 3.5: *Seismic section and line-drawing of Profile GeoB97-065 showing the architecture of the Bengal Fan imaged by GI-Gun data in the center of the study area (see Fig. 3.2 for location). The profile runs from west to east reaching a length of ~46 km, the section shows the uppermost ~600 m. Line-drawing reflects the four main seismic facies as defined in Fig. 3.3.*

At greater depth, a channel-levee system (I) with a wide zone of CHARS is identified in the east. This zone shows some peaks, but no associated channel-fill deposits, although the overlying HARPS also reveal some deep depressions over these peaks. Measured from the base of the western levee with a height of 45 m, the incision of System I into the HARPS cuts as deep as 75 m, adding to a total thickness of 120 m for System I. West of System I near the base of the levee, two filled channels with a CHAR zone appear, but there are no wedge shaped levee deposits adjacent to this complex. Its incision into the HARPS reaches 45 m. The underlying HARPS show a constant thickness of 80 m across the profile towards System I.

In the lowermost portion of the seismic profile, a channel-levee system with a complex structure (J) is identified. This system reveals a pattern of CHAR zones, transparent zones and filled channels, all deeply cutting into a thick layer of HARPS. The incisions reach 120 m and cut into the HARPS down to their base. The maximum thickness of Channel-Levee System J is 165 m. Westwards, 40 m high levee deposits decrease gently in thickness. Between System J and the western end of the profile, two more cuts into the lowermost HARPS occur. One cut is a narrow zone of a filled channel as well as CHARS reaching a depth of 45m. The other cut near the western margin of the profile is represented by CHARS incising down to 70 m. The pronounced base reflector of the HARPS is interrupted in the center and at the eastern edge of the profile.

3.5.2.3 Profile GeoB97-064

Profile GeoB97-064 (Fig. 3.6) is the southernmost profile in the study area. In contrast to profiles GeoB97-068 and GeoB97-065, Profile GeoB97-064 is a southwest-northeast traverse of ~45 km length, crossing the active channel 17 km south of Profile GeoB97-065 (Fig. 3.2)

The active channel-levee system is characterized by three filled channels and a widespread zone of CHARS, which is deeply incised at two locations by more than 70 m. CHARS attached at the westernmost as well as the easternmost filled channel appear as smoothly dipping thin zones. Levee height near the filled channels reaches 65 m, and the total maximum thickness of the active system amounts to 150 m. Sediment waves could be identified on both levees. Beneath the whole active system, HARPS with a maximum thickness of 100 m are found, interrupted by some filled channels and intercalated by two separated thin levee deposits in the Northeast (B). Both levee deposits are characterized by a less pronounced wedge shape, thicknesses below 20 m, the absence of a channel in the center as well as the occurrence of basal CHARS.

The thick layer of HARPS underlying the active system onlaps onto two buried channel-levee systems in the southwestern and northeastern part of the profile (E and F). Inside the HARPS, an unconformity can be traced from System E to the base of the lower levee of System B. Within the large System E, a wide CHARS zone with three distinct local heights could be identified. Each of these heights shows a filled channel deposit on its top and all three interfaces between CHARS and filled channels occur at the same

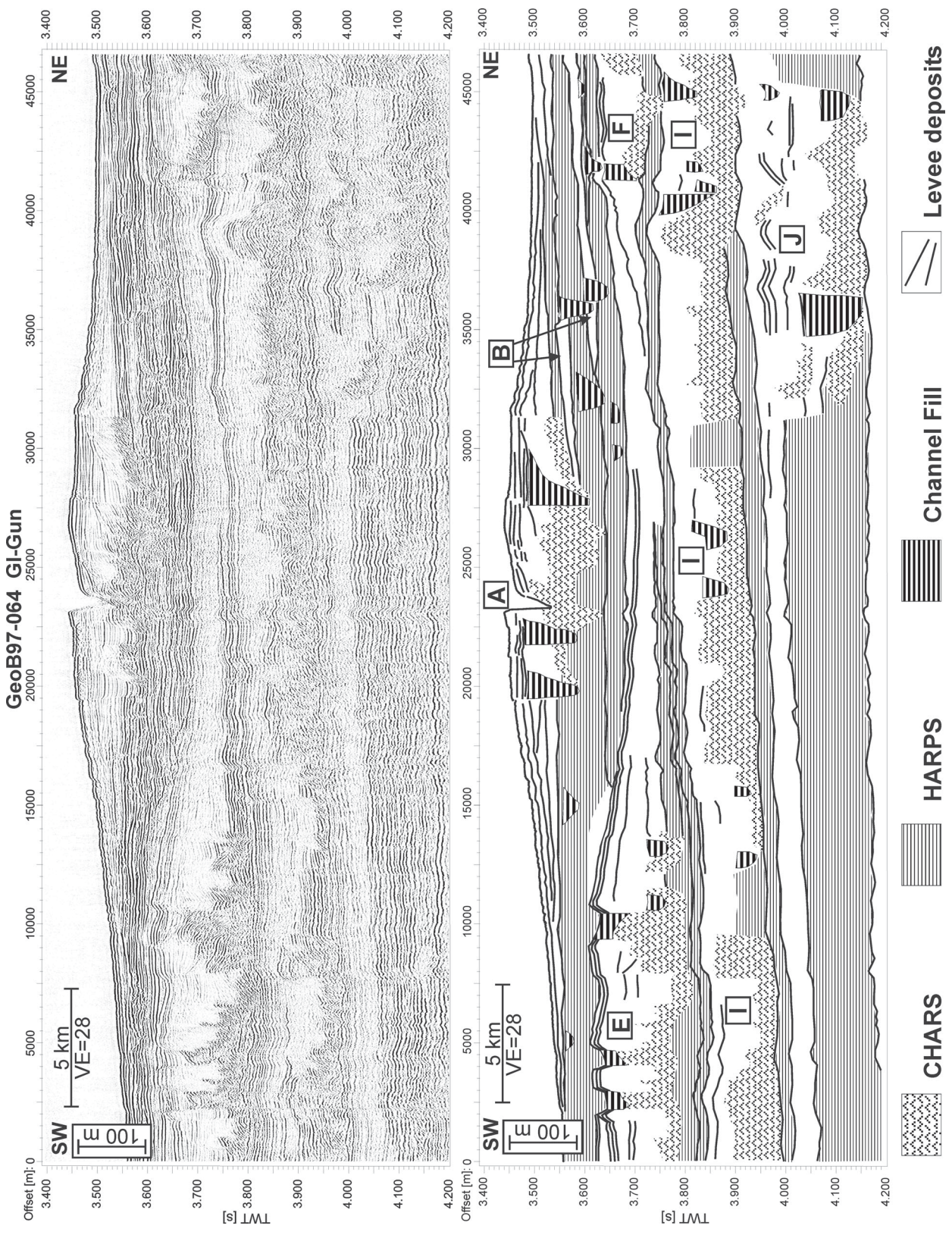

Figure 3.6: *Seismic section and line-drawing of Profile GeoB97-064 showing the architecture of the Bengal Fan imaged by GI-Gun data in the southern part of the study area (see Fig. 3.2 for location). In contrast to Profiles GeoB97-068 and GeoB97-065, Profile GeoB97-064 runs from south-west to north-east reaching a length of ~46 km, the section shows the uppermost ~600 m. Line-drawing reflects the four main seismic facies as defined in Fig. 3.3.*

depth level. The CHARS cut as deep as 40 m into HARPS. The maximum levee height is 110 m, and the maximum thickness of System E is close to 150 m. At the base of the eastern levee of System E, two small filled channels with surrounding CHARS were identified, also incised into the underlying HARPS.

Northeast of System E at the same depth level, a smaller system (F) settles on the same HARPS. Only the western levee of this system is imaged by the profile, a direct contact to the eastern levee of System E could not be identified. Visible on the profile is one filled channel with a thin, widespread zone of CHARS, which cut through the underlying HARPS into a deeper levee deposit. Incision depth of 35 m and levee height of 65 m are adding to nearly 100 m as total thickness of System F. The thickness of the HARPS underlying systems E and F increases from north-east to south-west, namely from 20 m at the western edge of System F to 50 m at the eastern edge of System E. An unconformity separates the HARPS into two units, one onlapping onto the other.

Below these HARPS, a complex channel-levee system occurs (I): broad zones of CHARS and associated channel fill deposits topped by levee deposits are spread over the entire profile, interrupted at two locations by narrow vertical blocks of HARPS revealing a maximum height of 75 m. Over most of the profile, thin HARPS of 20 m thickness underlie the System I, but in the easternmost 6 km of this profile, CHAR deposits of System I replace these HARPS. The thickness of System I varies between 130 and 95 m.

At the base of the presented profile, a channel-levee system (J) is centered in the northeast. Its western levee could be traced to the southwestern end of the profile and shows a nearly constant height of ~35 m. In the northeast, a complex structure of CHARS, filled channels, pronounced reflectors and transparent zones is observed. This structure cuts into HARPS by nearly 125 m, partly also through the base of the HARPS. Total thickness of System J is greatest near the northeastern boundary of the profile with 195 m. The HARPS underlying the western levee of System J are characterized by a thickness gently decreasing from 125 m in the northeast to 100 m in the southwest.

3.5.2.4 Downfan changes of architecture in the study area

To illustrate the downfan changes of the fan architecture and the structure of specific channel-levee systems in the study area, we present the line-drawings of profiles GeoB97-068, GeoB97-065 and GeoB97-064 in Figure 3.7. The description will concentrate on that channel-levee systems, which can be identified on all seismic profiles.

The active channel-levee system (A) generally shows a gently decrease of maximum thickness from 190 m to 150 m from north to south, but no principal changes in architecture within the study area was observed. On all profiles, several filled channels occur besides the active channel, and the base of the system is characterized by wide zones of CHARS. In addition, the CHARS are deeply incised into underlying sediments on all profiles. Changes are observed in shape of the CHARS zone, especially, if the CHARS occur as a more horizontal layer or as a more vertical or dipping block. But these changes occur from profile to profile and do not reveal a general north-south trend. An interesting obser-

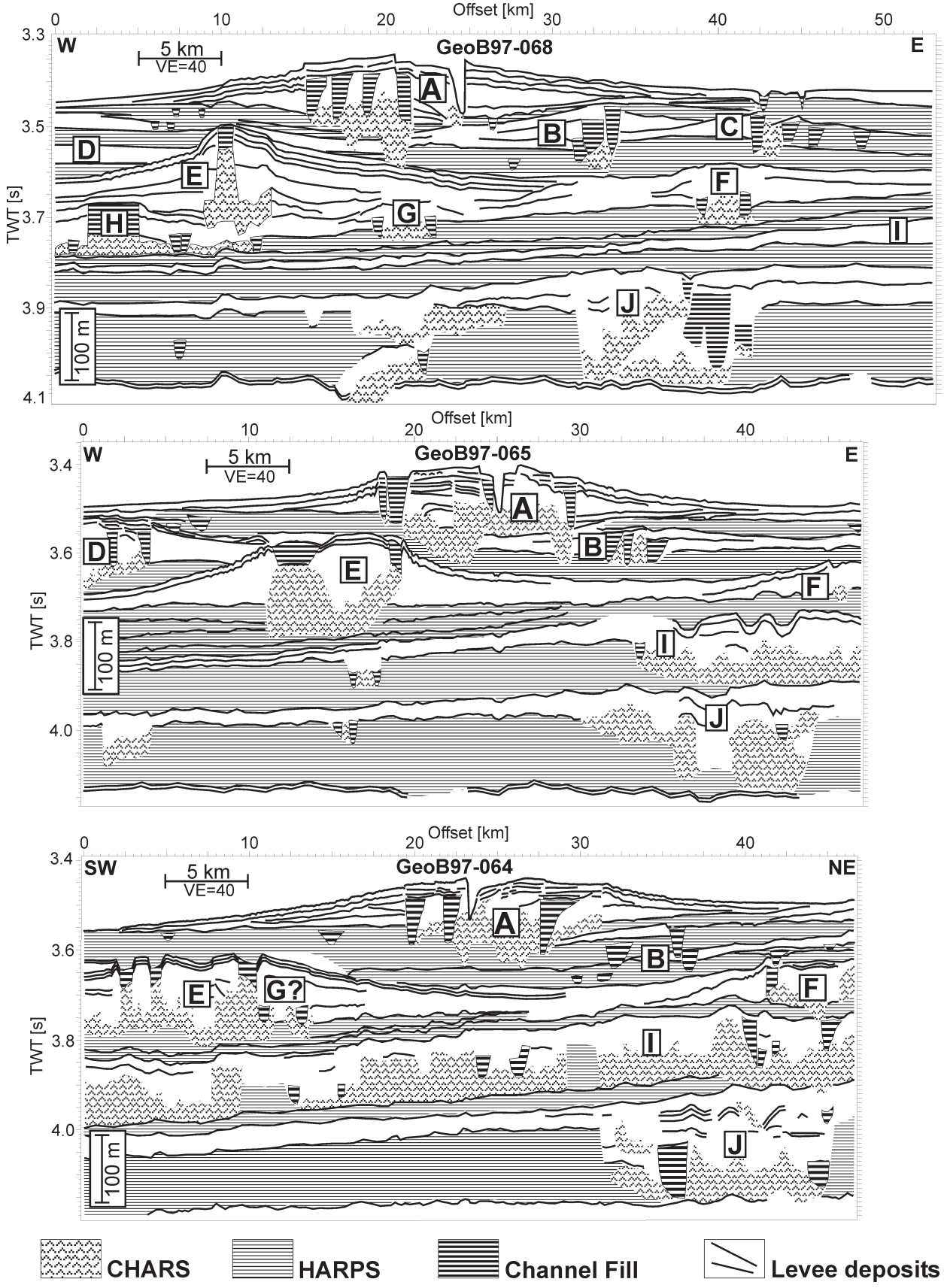

Figure 3.7: *Line-drawings of Profiles GeoB97-068, GeoB97-065 and GeoB97-064 illustrating the downfan changes of the fan architecture in the study area. The vertical and horizontal scales for all line-drawings are identical to simplify comparison between the profiles. Legend is the same as in Figs. 3.4, 3.5 and 3.6.*

vation is the fact that only on Profile GeoB97-068 a small isolated zone of CHARS occurs, which is attached to the active channel. On the other lines, the CHARS cover completely the center of the system between the levees, only interrupted by filled channels.

In contrast to the active system, System B shows significant variations between the northern- and the southernmost profile. On Profile GeoB97-068, System B is built of three filled channels cutting into each other with distinct, stacked levee deposits reaching a total thickness of 105 m. In the center of the study area (Profile GeoB97-065), three channels are located side by side in same depth, whereas levee deposits could not be clearly distinguished. System thickness is decreased to 60 m. On Profile GeoB97-064, two levee deposits appear, each 20 m thick and vertically separated by HARPS. Additionally, besides the leveed channels also unleveed channels occur. Obviously, the lower unit of both levee deposits on Profile GeoB97-064 is connected to the eastern levee of System B on Profile GeoB97-065, since the base of both levees appear at a depth of 3.59 s TWT at the eastern ends of profiles GeoB97-065 and GeoB97-064, where they come close (see Fig. 3.2). Furthermore, not only the maximum thickness of System B decreases, but also its lateral extent. Concurrently, the HARPS beneath the center of the active system change from a thin layer with a thickness of less than 40 m to a thick layer of up to 100 m thickness.

The next deeper system, which can be correlated between all profiles, is the large System E in the western part of the study area. As the active system, maximum thickness of System E decreases gently, i.e. from 180 m to 150 m from north to south. The principal structure of System E remains similar in the study area: in the center of the system a broad zone of CHARS appears, characterized by a wide horizontal base, on which vertical blocks reside. The number of these vertical blocks varies between one and three from profile to profile, but on all profiles, channel-fill deposits are found on top of the blocks. On each profile, the boundaries between the CHARS and channel-fill deposits are at the same depth level. With respect to the underlying sediments, System E is located in the low between two smaller systems (G and H) on Profile GeoB97-068, whereas on the southern profiles System E is deeply incised into HARPS. On the profiles south of GeoB97-068, no smaller systems could be identified beside or beneath System E, except for Profile GeoB97-064, where beneath the eastern levee of System E two small filled channels appear.

System F, which is located east of System E, is not fully imaged on all profiles in the study area, and therefore we cannot compare all its dimensions. However, it is noticeable that no filled channel deposits between the levee deposits are found on the northern profiles, although depressions in the overlying HARPS suggest the former existence of such channels. In contrast, on Profile GeoB97-064 channel-fill deposits are clearly visible. The HARPS beneath systems E and F can be correlated within the whole working area. Whereas the thickness of these HARPS remains nearly constant from west to east on Profile GeoB97-68, its thickness significantly decreases from west to east on profiles

GeoB97-065 and GeoB97-064. This is the result of a different north-south decrease of the thickness of these HARPS: beneath the western levee of System F, thickness decreases from 60 to 20 m from Profile GeoB97-068 to Profile GeoB97-064, but beneath the eastern levee of System E, thickness decreases only from 60 to 50 m from Profile GeoB97-068 to Profile GeoB97-064.

Variations of System I from north to south in the study area cannot be described, since none of the profiles covers the system completely. Nevertheless, it is found that the HARPS basing System I show increasing thickness from north to south, i.e. from 30-45 m on Profile GeoB97-68 to 95 m on Profile GeoB97-064. The underlying System J shows a complex pattern of CHARS and channel-fill deposits on all profiles and is therefore difficult to compare. However, the incision depth of CHARS into the underlying HARPS amounts to approx. 120 m on all profiles, whereas the western levee thickness of System J decreases gently from 55 m to 35 m from north to south.

West of System J, blocks of CHARS or filled channels, which cut into the HARPS adjacent to System J, are found on profiles GeoB97-068 and GeoB97-065, but in different dimensions and shapes. On Profile GeoB97-064, the HARPS west of System J remain undisturbed. The thickness of these HARPS does not change significantly from profile to profile and varies around 120 m. The base of the HARPS is interrupted at different locations on all profiles.

3.5.3 The active channel-levee system imaged by very high-resolution Watergun data

To describe the architectural elements of the active channel-levee system in more detail, we present very high-resolution Watergun data, which were collected simultaneously with GI Gun data along Profile GeoB97-067 (Fig. 3.8).

On this profile, the active channel-levee system is characterized by two partially filled channels adjacent to the active channel enclosed by levees reaching nearly 65 m height. Sediment waves appear on both levees, and these waves are more uniform on the eastern levee. The western levee is settled on HARPS, whereas the eastern levee is found on top of levee deposits again. The active as well as the filled channels are associated with wide zones of CHARS. Especially the CHAR block, which is connected to the easternmost filled channel, is deeply incised through levee deposits into the underlying HARPS. The incision depth is 95 m measured from the base of the active levee.

A close up of the Watergun data (Fig. 3.8) demonstrates that the CHARS block consists of numerous interrupted dipping reflectors stacked at an angle from the base of the CHARS upwards and sideways to the base of the filled channel. Continuous reflectors of weak amplitude appear above the CHAR zone. These reflectors change continuously and gradually from horizontal orientation to maximum dip angles of ~4° near the CHARS and the filled channel.

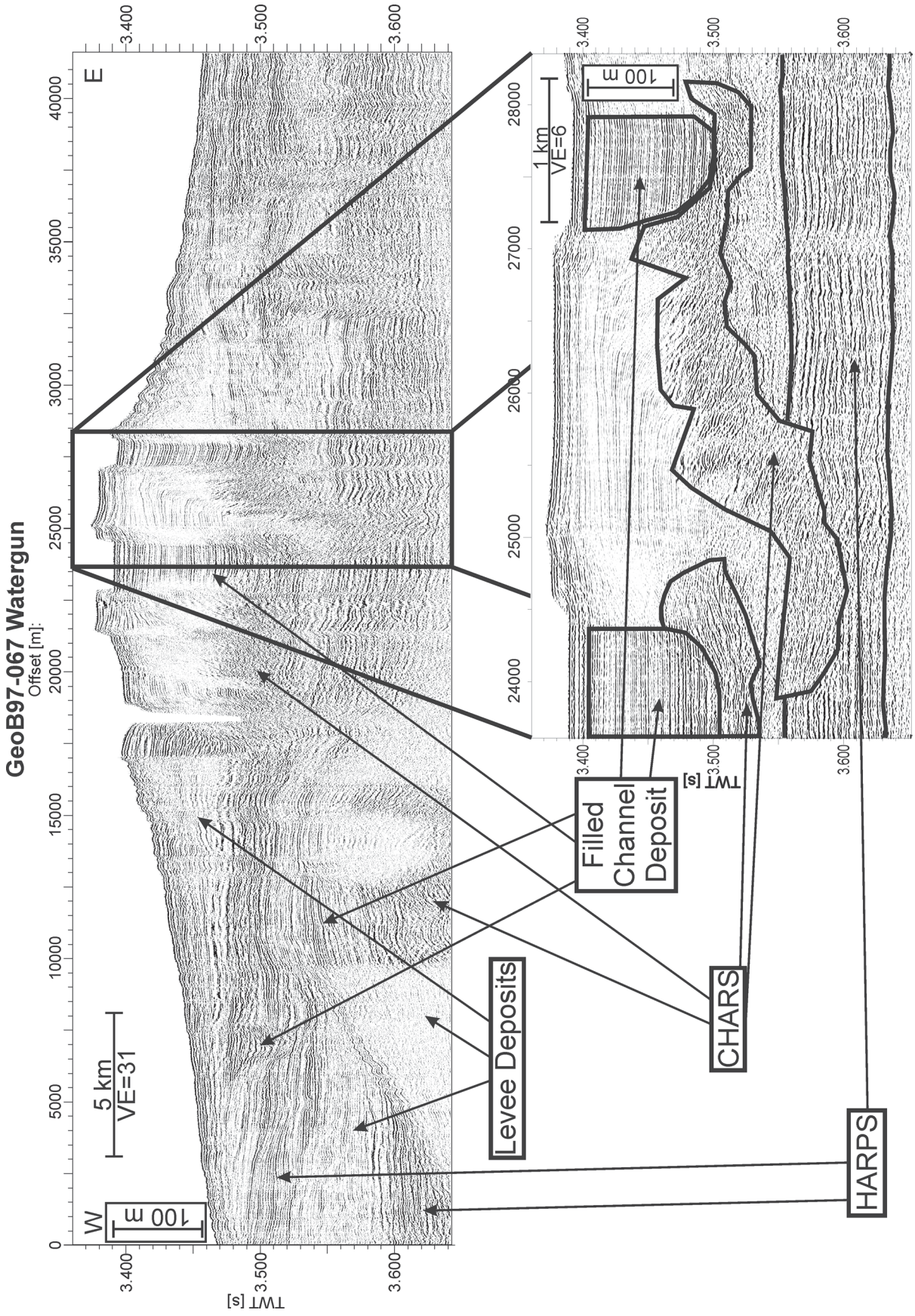

Figure 3.8: *Very high-resolution Watergun data of Profile GeoB97-067 imaging the active channel-levee system (see Fig. 3.2 for location). Close-up shows in detail the interpreted distribution of CHARS, HARPS and filled channel deposits in the eastern center of the system.*

3.6. Discussion

3.6.1. The evolution of the active channel-levee system

As described above, the active channel-levee system reveals a complex pattern of CHARS, filled channels and levee deposits. To illustrate the processes responsible for the individual architectural elements and the overall development of the complete active system to the present stage in space and time, we present a scenario based on the analysis of all seismic profiles shown in this study (Fig. 3.9).

At the start of the evolution of the active channel-levee system, turbidity currents erode a deep valley in HARPS, which fill a low between two older channel-levee systems (Stage 1, Fig. 3.9). Levees are built up by overspilling, and lateral migration and vertical aggradation of the channel occur simultaneously due to erosion and deposition of turbidity currents. This behavior first leads to the development of point bars and cut bars as levee walls and second to an apparently dipping zone of CHARS following the movement of the channel axis (Stages 2 to 5, Fig. 3.9). Later, the channel shows only lateral migration and no more vertical aggradation (Stage 6 and 7), resulting in a more horizontal distribution of the CHARS and a gradual build-up of the levees. Such a behavior of a channel is particularly observed at the easternmost filled channel on Profile GeoB97-067 (Fig. 3.8) and the westernmost filled channel on Profile GeoB97-065 (Fig. 3.5). The outward migration of the channel increases its sinuosity until a channel avulsion through the levee occurs as described in detail by Schwenk et al. (2003) (Stage 8).

The new channel segment tends to migrate outwards forming a cut bar as levee wall. Overspilling of turbidity currents leads to a rapid fill of the abandoned channel segment and deposition of sediments onto the levee behind the cut bar (Stage 9). Beside the lower part of the channel, a horizontal zone of CHARS starts to develop, whereas beside the upper part of the channel a seismically transparent zone occurs. Such transparent zones above lateral CHAR zones are found for instance beside and between the filled channels on Profile GeoB97-068 (Fig. 3.4). These zones are either the result of steep layers within the point bar scattering the sound energy or of thin, fine grained turbidites appearing very homogenous and therefore transparent for the used seismic signals. Further outward migrating of the channel increases the width of the transparent and CHARS zones, and after complete filling of the abandoned channel, deposition of sediments is more evenly distributed over both levees (Stage 10). The pure lateral migration may change to lateral migration with vertical degradation, if erosion by turbidity currents cuts deeper into the channel floor (Stage 11). As a result, apparently downward dipped CHAR zones develop as found east of the easternmost filled channel segment on Profile GeoB97-064 (Fig. 3.6).

Another channel avulsion may occur (Stage 12), now through higher levees than for the previous avulsion, and overspill from the new channel may not be able to completely fill the abandoned channel segment, but to create thin deposits on both levees, as found

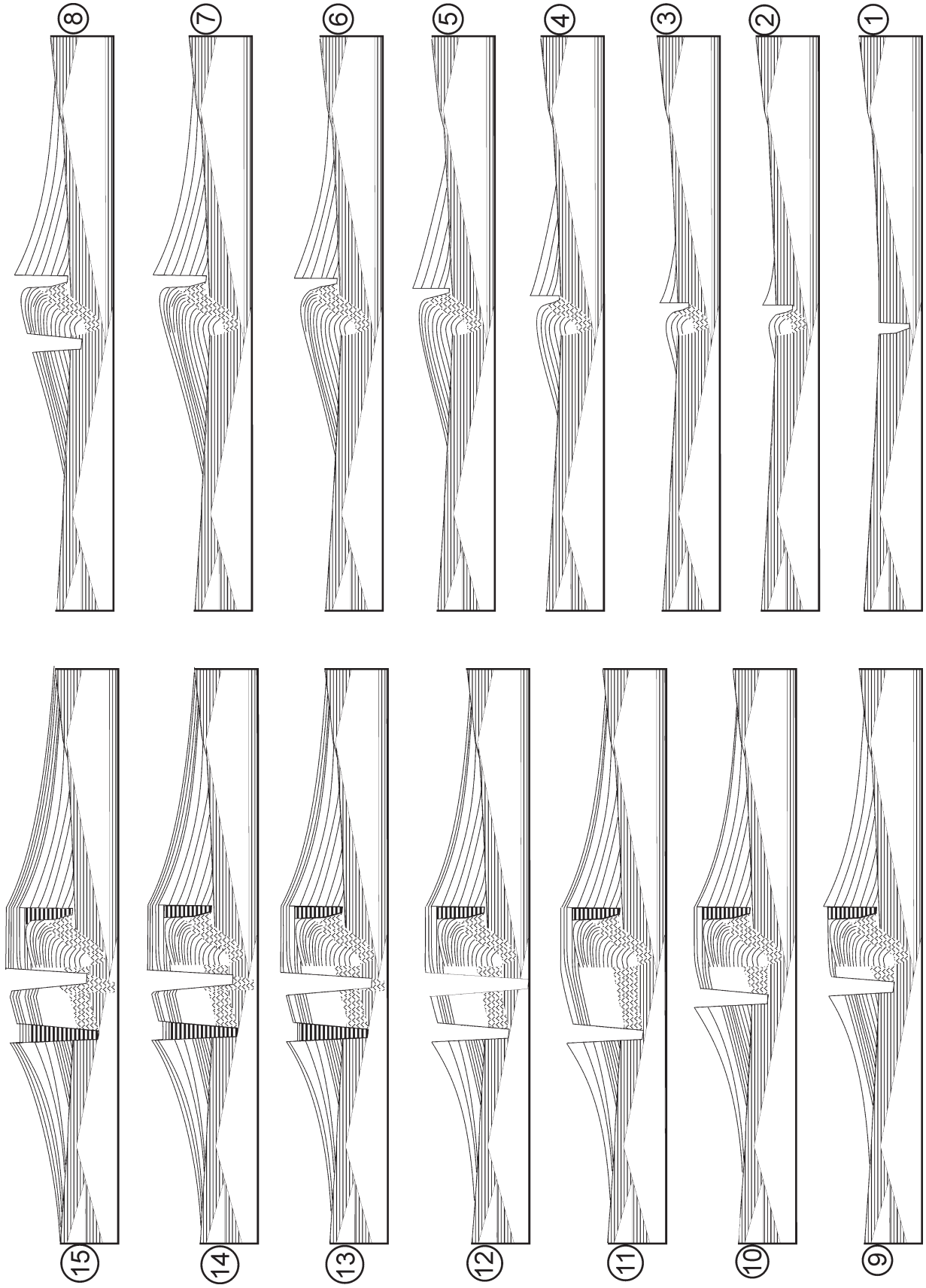

Figure 3.9: *Schematic sketch illustrating the principal development of the active channel-levee system based on all seismic profiles presented in this study. Shown are the different behaviors of the active channel and the resulting depositional patterns of the seismic facies found in the study area. Legend of seismic facies is the same as in Figs. 4, 5 and 6. For detailed discussion see text.*

on Profile GeoB97-067 (Fig. 3.8). This channel segment is characterized by mainly vertical aggradation with only a minor lateral migration (Stage 13 to 15). Consequently, sedimentation on both levees is nearly similar and neither a point bar nor a cut bar develops. Channels with a mainly vertical aggradation and less lateral migration are found on Profile GeoB97-068 and GeoB97-067 (Figs. 3.4 and 3.8). Stage 15 represents the principal present architectural style of the active channel-levee system in the study area, although some profiles show an even more complex architecture. In particular, more than the two illustrated filled channels are found on most profiles. However, the sketch exemplifies the development of the main architectural elements found on all profiles, especially the variability of CHAR zones, which appear as laterally extended units, dipping blocks or vertical blocks as well as combinations of these shapes.

For interpretation of such systems, their threedimensionality should always be kept in mind, leading to different appearances of a meandering channel and associated depositional units on seismic profiles. These differences occur as a function of the location of the profile relative to the channel geometry and to the direction of channel migration itself. After Peakall et al. (2000a, b), sinuous submarine channels are characterized by cross-fan lateral migration through bend growing only, but no downfan migration of meander bends takes place. Once reaching a planform equilibrium, the channel planform remains stable and only vertical aggradation occurs (Peakall et al., 2000a; Peakall et al., 2000b). A profile crossing such a channel at its bend apex will reveal a dipping CHAR block beneath the channel, but a profile crossing the same channel at a turn-over point will reveal a vertical block of CHARS. However, Kolla et al. (2001) stated that downstream migration of submarine channel bends may occur as it is common in subaerial channels. Obviously, this process would further complicate the depositional process and would produce finally broad sheet-like bodies of CHARS wider than individual channels, similar to deposits found at subaerial rivers (Peakall et al., 2000a; Peakall et al., 2000b).

Generally, the channel segments found in the active system in our study area showing a broad spectrum of behaviors. Their only common feature is the incision into the sediments underlying the system and aggradation only below the level of the seafloor beside the levees. But the incision depths of the channel segments vary significantly as documented on Profile GeoB97-068 by the large incision depth of several CHAR zones at abandonment segments in contrast to the shallow incision depth of the active channel segment. These deep incisions distinguish the active channel-levee system of the Middle Bengal Fan from the channel-levee systems on Amazon Fan where the HARS below the channels are perched on top of the HARPS due to vertical aggradation (Lopez, 2001; Pirmez and Flood, 1995). After the initial development, some channel segments reveal vertical aggradation together with lateral migration. The ratio between vertical and lateral migration depends on location of the profile as described above. In our data of the Bengal Fan, however, we also found pure lateral migration, vertical degradation and channels changing their migration from vertical and lateral to only lateral and vice versa. These

behaviors agree with the channel behaviors described by Kolla et al. (2001), but differ from channel descriptions of Amazon Fan (Lopez, 2001; Pirmez and Flood, 1995) and the process model for submarine channels developed by Peakall et al. (2000a, b). In contrast, Kolla et al. (2001) define two classes of channel migrations: elementary migrations showing the same behavior from the begin to the end of the development of a sinuous loop, and complex migrations showing combinations of elementary migrations during the development of a sinuous loop. As shown above, the active channel-levee system of the Middle Bengal Fan shows both, elementary and complex migrations, but it is still unclear, if downfan migration of channel loops occurs. The broad zones of CHARS found on some profiles may suggest downfan migration of channel loops, but it is also possible that succeeding cross-fan migrations could produce such depositions. However, only high-resolution 3-D seismic would help to answer this question.

We can summarize that the active channel-levee system of the Middle Bengal Fan is characterized by deep incisions into underlying sediments, frequent channel avulsions within the system and a broad spectrum of channel behaviors. Channel aggradation above the level of the surrounding seafloor never occurred, which may prevent abandonment of the system and therefore causes such a long lifetime that contributes to the large number of cut-off loops. Thus, the active channel in our study area differs significantly from channels on the Amazon Fan (Lopez, 2001; Pirmez and Flood, 1995) and the process channel model of Peakall et al. (2000a, b) which are based on data from Mississippi Fan, but shows a similar behavior as submarine channels of Tertiary Congo Fan described by Kolla et al. (2001). The broad spectrum of channel behaviors including the different incision depths suggest that turbidity currents, which have built the active channel-levee system, differ significantly in one or more parameters such as size, velocity or density.

3.6.2. The evolution of System E

Even if the dimensions of the buried System E are similar to the active system, its architectural style differs significantly from the active system suggesting a different system development. As mentioned above, System E is characterized by a CHAR zone consisting of a wide base with, depending on the profile, one to three vertical blocks that are topped by filled channel deposits. If more than one CHAR with a filled channel on top is found as on profiles GeoB97-065 and GeoB97-064 (Figs. 3.5 and 3.6), the surfaces between CHARS and filled channel deposits are at the same depth level. Therefore, we conclude that the vertical blocks and the attached filled channel deposits represent a single channel, which is cut by the profile at a meander loop. The vertical blocks of CHARS are interpreted as deposits resulting from a vertical aggradation of the channel, the filled channel deposits are interpreted to be the result of overspilling from an adjacent system after the System E was abandoned.

To illustrate the development of System E, we present a simplified model based on Profile GeoB97-065 (Fig. 3.10). The planform of the channel is shown together with the cross-section demonstrating the relationship between the appearance of a channel-levee

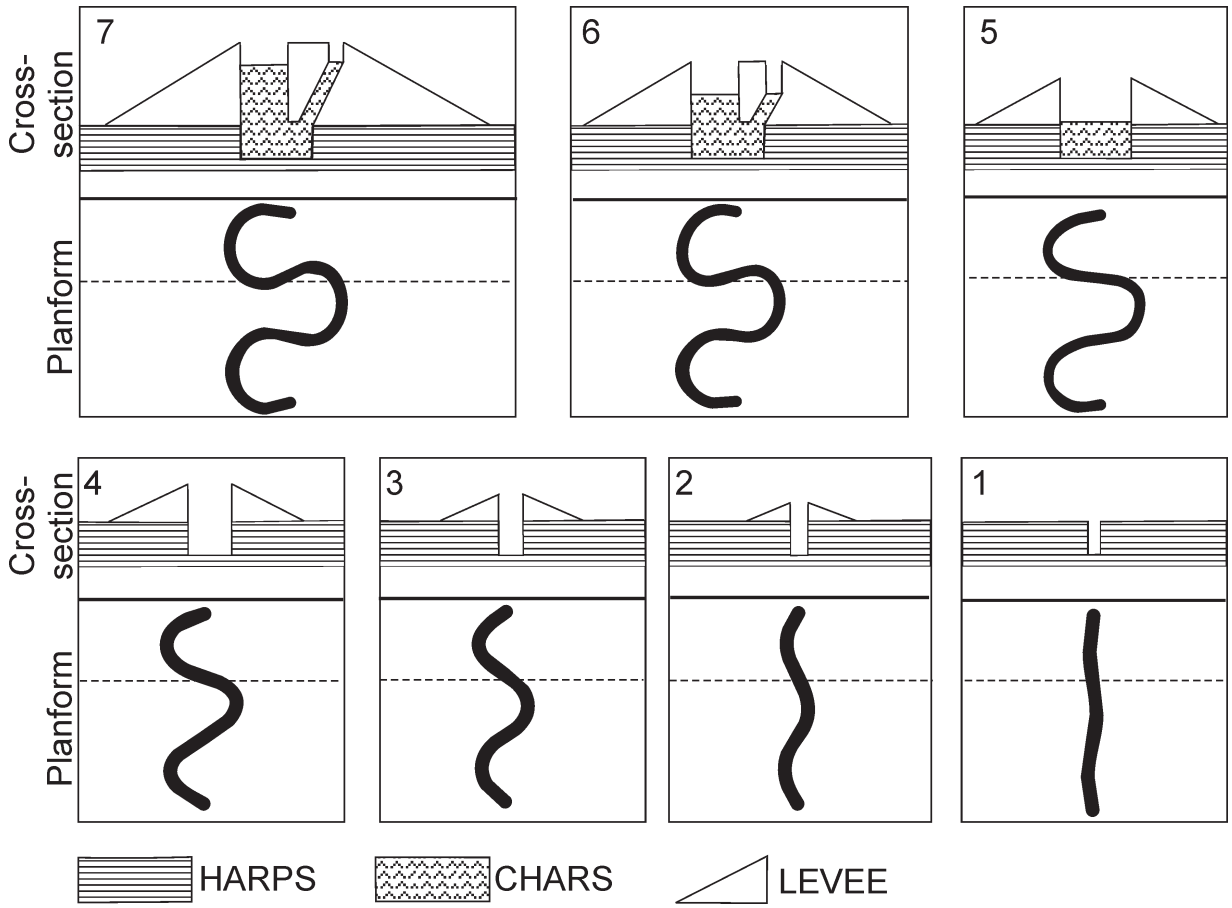

Figure 3.10: *Simplified model illustrating the development of Channel-Levee System E in Profile GeoB97-065. Drawn are the cross-section (atop) and the planform of the channel (below) from an initial stage (1) to the last active stage before the channel-levee system was abandoned (7). Dashed line on planform indicates location of the cross-section above. Legend of cross-section is the same as in figures before.*

system in a cross-section and its location with respect to a meander loop. The initial stage is thought as a nearly straight channel segment, eroding into the underlying HARPS. Accompanied by the build-up of levees, the channel starts meandering and its sinuosity increases gradually (Stages 2-4). The position of the profile leads to an increasing apparent channel width on the cross section. Obviously, no further erosion or aggradation occurs during these stages, since the base of the channel remains horizontal as indicated by the horizontal base of the CHARS in the present stage, but aggradation in stages 2-4 would lead to a V-shaped CHARS block. Only when the channel reaches a distinct sinuosity, vertical aggradation of the channel floor starts (Stage 5). On the cross section, channel width reaches its maximum, since the profile follows more or less the channel axis at this stage. Due to further meandering two channels may appear in the cross-section (Stage 6). The simultaneous meandering and vertical aggradation of the channel leads to a dipping block of CHARS beneath the right channel segment and a vertical block of CHARS beneath the left channel segment in the cross-section. The continuation of this process ends in Stage 7, which is similar to the last stage of System E before abandonment on Profile GeoB97-065.

This process model of System E demonstrates a more simple evolution compared to the active system. The initial stages of both systems seem to be similar during the erosional phase, but further development differs strongly. The most striking difference of System E to the active system is the absence of cut-off loops. The other remarkable difference is the behavior of the channel, when it first shows lateral migration due to bend growing and later additional vertical aggradation, which is particularly not observed in the active system. An interesting observation is that aggradation only starts when the channel planform reaches a distinct sinuosity. This may have been caused by changes in the nature of the turbidity currents, but it is also possible that this is a result of increasing sinuosity: increasing sinuosity leads to decreasing channel floor slope, which in turn reduces flow velocities and finally supports an increasing deposition of coarser sediments at the channel floor (Pirmez and Flood, 1995). Generally, the behavior of the channel is complex in terms of Kolla et al. (2001). Like the active system, System E does also not follow the process model of Peakall et al. (2000a, b), since their model predicts first lateral migration and vertical aggradation followed by a stage of vertical aggradation only. In System E, lateral migration due to bend growing took place until the last stage. Therefore, the absence of the cut-off loops may be indicate such a limited lifetime of the system, that further bend growing, which would have probably caused channel avulsions, not occurred. This limited lifetime may be the result of aggradation of the channel-floor above the seafloor in contrast to the active channel-levee system, since such aggradation of the channel-floor facilitates the turbidity currents to breach the levees (Babonneau et al., 2002; Lopez, 2001; Pirmez and Flood, 1995). The different behaviors of System E and the active system, especially the different level of aggradation, may suggest that different loaded turbidity currents build up these different systems.

3.6.3 Termination of System B and origin of HARPS

By comparing the profiles from north to south, it is obvious that only System B shows remarkable changes within the study area (Fig. 3.7). Thickness as well as lateral extent of System B strongly decrease from North to South. The architecture changes from a system of three filled channels, cutting into each other and each with an associated western levee, to two small channels with small levees intercalated by HARPS. Also unleveed channels take place within the HARPS beside and beneath the leveed channels on the southernmost profile. The significant decrease of the levee thickness, the presence of unleveed channels and the HARPS intercalating the levees indicate that System B terminates in the southern study area. Therefore, the HARPS intercalating the levees in the south are interpreted as a depositional lobe of one of the channels found in the north. Generally, the downfan characteristic of System B reveals that termination of channel-levee systems with associated depositional lobes may also occur on middle fans and not only on lower fans as described in general models of fine-grained submarine fans (Bouma, 2001; Richards et al., 1998).

On the other hand it is obviously from the discussion above, that HARPS may represent both, terminal lobes and avulsion lobes, which both appear similar in seismic data as described by Lopez et al. (2001) from the Amazon Fan (see also Chapter 3.1). Discontinuous reflectors and unconformities within the HARPS indicate different depositional processes. For instance, the thick HARPS beneath and beside the active channel-levee system on Profile GeoB97-064 (Fig. 3.6) may have been built up by different depositional events: the unconformity between the base of the levee of System B and the levee of System E may indicate that the lower part of these HARPS are the same deposit as the HARPS beneath System B on the northern profiles. Thus, this part of the HARPS may be the result of an avulsion process previous to the build-up of System B (Fig. 3.7). A depositional lobe of the terminating channel of System B may have further contributed to the HARPS below the active System on Profile GeoB97-064 followed by HARPS deposition due to the avulsion event before the active system developed. Altogether, this depositional scenario would explain the decreasing thickness of the HARPS beneath the active system from north to south within the study area. However, for the exact mapping and distinction of avulsion lobes and terminal lobes, more seismic profiles parallel to the channels would be needed (see also Lopez, (2001)).

3.6.4 Development of the Middle Bengal Fan in the vicinity of the active channel

In the following, we discuss in general the vertical development of depositional units found on all seismic profiles in the study area. The profiles reveal a pattern of channel-levee systems and HARPS, both showing a broad spectrum of sizes and geometries. In the study area it is common to all channel-levee systems that they are deeply incised into the underlying sediments suggesting that turbidity currents traveling through all systems reveal erosive power. This is in contrast to the channels on Amazon Fan, which are characterized by aggradation (Lopez, 2001; Pirmez and Flood, 1995), but in accordance to channels on Congo Fan which also are characterized by deep incisions (Babonneau et al., 2002). Even if the reason for deep incisions of some fan channels is not completely understood, the deep channel incisions on Congo Fan may be the result of the continuous activity of turbidity currents also during the last sea-level rise and highstand (Babonneau et al., 2002), which is also the case on Bengal Fan (Weber et al., 1997).

The deepest parts of all profile sections show the most complex depositional pattern (Fig. 3.7). On all profiles, erosion in the lowermost HARPS is clearly identifiable, but only System J is characterized by increasing western levee deposits towards the filled channel and CHARS, and only System J is traceable through all profiles. However, the wedge shape of the western levee of System J is much less pronounced than the shapes of shallower systems. Three hypotheses could explain the flatness of levees of System J: 1) Levees were eroded by turbidites building the HARPS. This hypothesis could be proven by truncated reflectors at top of the levees, but on none of the profiles truncated reflectors could be observed. Instead, most of the levee deposits contain weak reflectors or acoustic transparent zones, therefore truncated reflectors are difficult or impossible to detect in

these seismic data. 2) Levees were compressed by the weight of the overlying sediments. Since levees were built by fine-grained overspilling sediments of the upper dilute part of turbidity currents (Babonneau et al., 2002; Hiscott et al., 1997; Peakall et al., 2000a; Peakall et al., 2000b), they contain a much higher water content than HARPS or CHARS. Therefore, it might be considered that differential loading and compaction may cause preferential dewatering of levees and associated deformation. This would lead to vertical fluid flow, which may cause zones of incoherent and disturbed reflectors within the HARPS. 3) The character of turbidity currents flowing through System J was different from currents building the younger systems. Differences in composition of suspended sediments or velocity and size of the currents may lead to a less wedge shaped geometry of levees compared to the overlying, younger systems.

After activity of System J, HARPS with increasing thickness from north to south have been deposited, followed by System I, which can be identified on all profiles (Fig. 3.7). In contrast to the other discussed systems, System I changes strongly its location relative to the profiles. On the northernmost profile, only the western levee of System I appears, but on the southern profiles, its center is found further to the east. On the northeast – southwest orientated Profile GeoB97-064 (Fig. 3.6), only the center of the system with CHARS and filled channels is seen, but no levees. Therefore it is suggested that System I mainly runs from Northeast to Southwest through the study area.

Once System I had become inactive, HARPS were deposited on its top with decreasing thickness from north to south and additionally from east to west (Fig. 3.7). The unconformity found within these HARPS shows that at first deposition occurred also above the center of System I, followed by deposition only in the topographic low west of System I guiding the turbidity currents. On top of these HARPS, the systems E, F, G and H settle, and from Profile GeoB97-068 (Fig. 3.4, a succession of G, F and E is found, but the relationship in time between G and H can not resolved due to erosional disturbance of their levees by System E. System G is not identifiable on Profile GeoB97-065 (Fig. 3.5), but the filled channel found on Profile GeoB97-064 (Fig. 3.6) beneath the eastern levee of System E may belong to System G suggesting that System G was destroyed by System E in the around Profile GeoB97-065.

A remarkable feature of System F is that channel fills do not differ acoustically from levee deposits on the northern profiles, therefore the fillings are believed to be fine-grained sediments with similar acoustical characteristics as levee deposits. This may be the result of filling by fine-grained sediments of overspilling turbidity currents of the succeeding System E.

After activity of System E, non-channelized turbiditic deposition into the lows west and east of System E occurred as indicated by HARPS onlapping both, the western and eastern levee. Sedimentation of these HARPS is again followed by the build-up of channel-levee systems B and D on both sides of System E, but no obvious relationship between Systems D and B is detectable from the seismic profiles. Within the study area,

System B was the last active system previous to the recent active channel-levee system, interrupted by deposition of HARPS.

In summary, the upper ~600 m of the Middle Bengal Fan in the vicinity of the active channel-levee system are built up by a succession of channel-levee systems and HARPS, which are mainly the result of unchannelized turbiditic flows. In contrast to other submarine fans as Amazon Fan (e.g. Lopez, (2001), we could not identify large mass-flow deposits in seismic data from our study area, neither at the surface nor intercalated between channel-levee systems. On Amazon Fan, the mass flow deposits are the result of slope failures triggered by two processes: (1) Destabilization due to gas hydrate sublimation during rapid drops of sea-level and (2) rapid prodeltaic deposition during Glacial-Interglacial transitions due to deglaciation of the Andes causing overloading and sliding of slope deposits (Lopez, 2001; Maslin and Mikkelsen, 1997). The absence of mass-flow deposits in our study area may be caused by different reasons. First, the large distance to the upper slope: mass flow deposits on Amazon Fan have a downslope extent of maximal 200 km, our study area is located ~400 km south of the shelf break. Second, slope failures may have not occurred at the slopes in the Bay of Bengal. However, maximum slope gradients on Bengal Fan are steeper (36m/km) than on Amazon Fan (16m/km) (e.g., Pirmez and Flood, 1995; Curray et al., 2003). Thus, overloading at the Bengal slope must have inhibited by another process. For the Holocene it is known, that the outer shelf is sediment starved and that transport of delivered sediment through the Canyon „Swatch of No Ground“ into the active channel-levee system is highly efficient (Goodbred Jr. and Kuehl, 2000a; Kudrass et al., 1998; Michels et al., 1998). It is reasonable, that a similar efficient process during former sea-level rises and highstands prohibited slope failures as well. However, only high-resolution seismic data located closer to the upper slope could answer the question if mass-flow deposits occur.

3.6.5 Reservoir potential of channel-levee systems in the study area

Large submarine fans like the Bengal Fan contain possible reservoirs even if fine-grained sediments are dominating. This potential is caused by the sorting mechanism within mixed-loaded turbidity currents during their passage through long sinuous channels. Fine-grained material concentrates at the top of the flow and contributes to the levee building by overspilling, whereas the coarse-grained material is transported at the bottom of the flow. These sands were either deposited on the channel floor or in intrachannel lows after avulsion events, both sealed by muddy levee deposits, or finally in terminating lobes at the mouth of channels. Therefore, the aggraded channel floors and the sand sheets below avulsion points and at the end of channels are likely to be good reservoirs (Hiscott et al., 1997; Kolla et al., 2001; Lopez, 2001; Peakall et al., 2000a; Peakall et al., 2000b; Richards et al., 1998).

Analyzing the data in our study area suggests that the CHARS building the channel axes may have reservoir potential. However, reservoir potential of aggrading and migrating channels depend strongly from the connectivity and amalgamation of sand deposits.

The connectivity is controlled by the characteristic of channel migrations, i.e., if migrations occurred continuously or in discrete steps (Kolla et al., 2001). Channel migrations on the Middle Bengal Fan seem to have occurred continuously as imaged in our data. The more simple behavior of Channel E is likely to produce large sand bodies with sufficient connectivity. The complex behaviors of the active channel-levee system resulted in a broad area with complex pattern of CHARS, and connections between these individual channel floor deposits of the cut-off loops is difficult to establish. Additionally, due to the lack of downfan profiles the extensions and connectivity of the CHARS zones in along-channel direction is not known. Consequently, high-resolution 3-D seismic is definitely required for prediction of reservoir quality of channel-levee systems like the active channel-levee system in our study area.

3.7 Conclusions

- Based on high-resolution seismic data, four seismic facies were identified in the study area on the Middle Bengal Fan in vicinity of the active channel-levee system. Facies 1 is characterized by dipping low amplitude reflectors within levee structures and interpreted as fine-grained sediments deposited by overspilled material from turbidity currents. Facies 2 consists of wide high-amplitude reflector packets (HARPS) and are thought to represent thick beds of sands deposited as result of channel avulsions followed by unchannelized flows in intra channel lows. Facies 3 appears as V-shaped blocks of parallel, horizontal and distinct reflectors with medium amplitudes. This facies is interpreted as channels filled after abandonment. Facies 4 consists of chaotic, high amplitude reflectors (CHARS), which are discontinuous and mostly dipped. They are found below all channel floors and are interpreted as sands building vertically aggraded and laterally migrated channel axes.
- The upper 600 m of the Middle Bengal Fan are built up by a pattern of different sized channel-levee systems and HARPS. All channels are characterized by deeply incised CHARS into underlying sediments. Mass flow deposits and thick hemipelagic drapes are not observed in the study area.
- The active channel-levee system is characterized by channel avulsions within the system leading to numerous cut-off loops. The analysis of the seismic profiles reveals that the active channel shows a broad spectrum of different and complex behaviors with different ratios between vertical aggradation and horizontal migration. The different behaviors occurred not only along the system in the study area, but also within one channel segment during its evolution. However, neither the active channel nor one cut-off loop has aggraded above the level of the surrounding seafloor. This morphology causes probably a long lifetime of the system and contributes in that way to the large number of cut-off loops.
- In contrast to the active system, one buried channel-levee system (System E) with similar dimensions reveals no cut-off loops and shows a more simple behavior: In a first phase, only lateral migration occurred, followed by a second phase of simulta-

neously vertical aggradation and lateral migration until abandonment of the system. At the end of the evolution of System E, the channel floor was perched above the seafloor beside the levees, which favored channel avulsion and system abandonment and may have caused the absence of cut-off loops. The differences to the active system suggest significant differences between turbidity currents building both systems.

- Aggrading and migrating channel floors within the Middle Bengal Fan are likely to be good reservoirs, but their true potentials can only be predicted by means of high-resolution 3-D seismic.
- The thickness of one buried system (System B) decreases significantly downfan in the study accompanied by parallel thickening of the underlying HARPS, suggesting that this system terminates on the Middle Fan and that HARPS also represent terminal lobes at the end such terminating systems.

3.8 Acknowledgements

We thank the captains and crews as well as all seismic watch-keepers of R/V Sonne cruise 125 for their support. Martin Gutowski provided the static correction method for the Watergun data and carried out this processing step for the presented data. Lars Zühlsdorff provided the software GeoApp for geometry setting. This manuscript was improved by helpful comments of S. Krastel. This work was funded by DFG, Grant SP296/14, and BMBF, Grant 03G0125A.

Chapter 4: Architecture and stratigraphy of the Bengal Fan with respect to shelf distance revealed from high-resolution seismic data

T. Schwenk & V. Spieß

To be submitted to Journal of Geophysical Research

4.1 Abstract

High-resolution seismic data collected on four profiles located at the Lower Bengal Fan (8°N, 11°N, 14°N) and upper Middle Bengal Fan (17°N) were analyzed. Numerous channel-levee systems were identified, all characterized by erosional incision into underlying sediments. Significantly downfan decrease of average levee thickness and slightly downfan increase of average incision depth suggest that mix-load turbidity currents changes during their downfan travel into more coarse-grained currents by loosing the fine-grained fraction at the Upper Fan and Middle Fan.

On the upper Middle Fan, four channel-levee system complexes exist separated by regional unconformities, which are partly caused by switching of the feeding canyon or generating of non-channelized turbidity currents. The absence of hemipelagic drapes as well as mass-flow deposits and the dating of two surface channels (Weber et al., 1997; Weber et al., 2003) indicate activity of the Bengal Fan even during sea-level rises and highstands. The sequence of surface channels and the position of the active channel at 11° N we identified seem to require some reinterpretations of results published by Curray et al. (2003).

In all three profiles from the Lower Fan, regional unconformities were found. At 8°N, unconformities have Pliocene and Pleistocene age and were interpreted to be the equivalents of unconformities found in the central Indian Ocean, which are related to deformation events of the oceanic crust and to changes of sediment character (Krishna et al., 2001a). Faults terminating within Pleistocene sediments suggest tectonic activity at least within the Pleistocene at 8°N. The unconformities identified at 11°N and 14°N may result from tectonic events or sediment changes too. Beside these unconformities, variations of sedimentation rates in time and space determined at 8°N and the onset of channel-levee systems simultaneously to lithological changes at ODP Leg 116 indicate that tectonic events at the Bengal Fan and changes of sediment supply and transport occurred partly concurrently. Since sediment supply mainly depends on tectonics in the source area of the Ganges-Brahmaputra Rivers, it is reasonable that a link exists between tectonics of the Himalayas and deformation events of the Indian Ocean lithosphere.

4.2 Introduction

The Bengal Fan is fed by the sediment load of the Ganges and Brahmaputra, which drain the Himalayas, and is therefore well suited to analyze the link between tectonics and climate on the continent and the marine sedimentary record. As the largest submarine fan on Earth, the Bengal Fan is also quite suitable to study processes of deposition from turbidity currents and the resulting architecture in detail due to the spatial separation of important elements of a fan system.

The first scientific approach to the fan was made in the early 50^{ies} of the last century, and the name Bengal Fan was established in the early 70^{ies} (Dietz, 1953; Curray and Moore, 1971; Curray et al., 2003). Two major steps in research of the Bengal Fan were the drilling of DSDP Site 218 in 1972 at 8°N in the Lower Fan and ODP Leg 116 Sites in 1987 near the equator in the distal fan, allowing to assign ages to the seismic stratigraphy established in the 70^{ies} (Cochran, 1990; Curray and Moore, 1971; Moore et al., 1974; Stow et al., 1990; von der Borch et al., 1974). Many data from the Bengal Fan were collected by the Scripps Institution of Oceanography between 1968 and 1986, including sediment echo sounder data, seismic reflection and refraction data, gravity data and magnetic data, all summarized in the comprehensive publication of Curray et al. (2003). Furthermore, an additional seismic stratigraphy was proposed for the Bengal Fan as well as more magnetic and gravity data were analyzed by several Indian researchers to reveal the crustal structure, tectonics and sedimentation. (Gopala Rao et al., 1994; Gopala Rao et al., 1997; Krishna, 2003; Krishna et al., 2001b; Subrahmanyam et al., 1999; Subrahmanyam et al., 2001).

In 1994 and 1997, three expeditions with the German research vessel R/V Sonne (SO 93, SO 125 and SO 126) were carried out in the Bay of Bengal (Kudrass and Shipboard Scientific Party, 1994; Kudrass and Shipboard Scientific Party, 1998; Spieß et al., 1998). These expeditions led to several publications based on digital echosounding and swath-sounding data as well as gravity cores and dealing, for example, with stratigraphy and dating of the active channel-levee system (Hübscher et al., 1997; Weber et al., 1997), details of sedimentation processes in the “Swatch of No Ground” Canyon (Kottke et al., 2003; Michels et al., 2003), the analysis of physical sediment properties and their response to climate forcing (Weber et al., 2003), and the morphology, structure and development of the channel-levee system in the upper Middle Fan (Schwenk et al., 2003).

However, beside these studies contributing significantly to understanding the Bengal Fan, there is lack of published high-resolution multichannel seismic data. This kind of data was collected during the SO 125 Cruise (Spieß et al., 1998), and we present here four up to 500 km long seismic profiles from west to east at latitudes 8°N, 11°N, 14°N and 17°N. The purpose of this study is to document the architecture and stratigraphy of the Bengal Fan with respect to the distance from the shelf and main sediment source, to link the stratigraphy to DSDP and ODP drill holes, and finally, to relate the results to global or regional tectonic and climatic events.

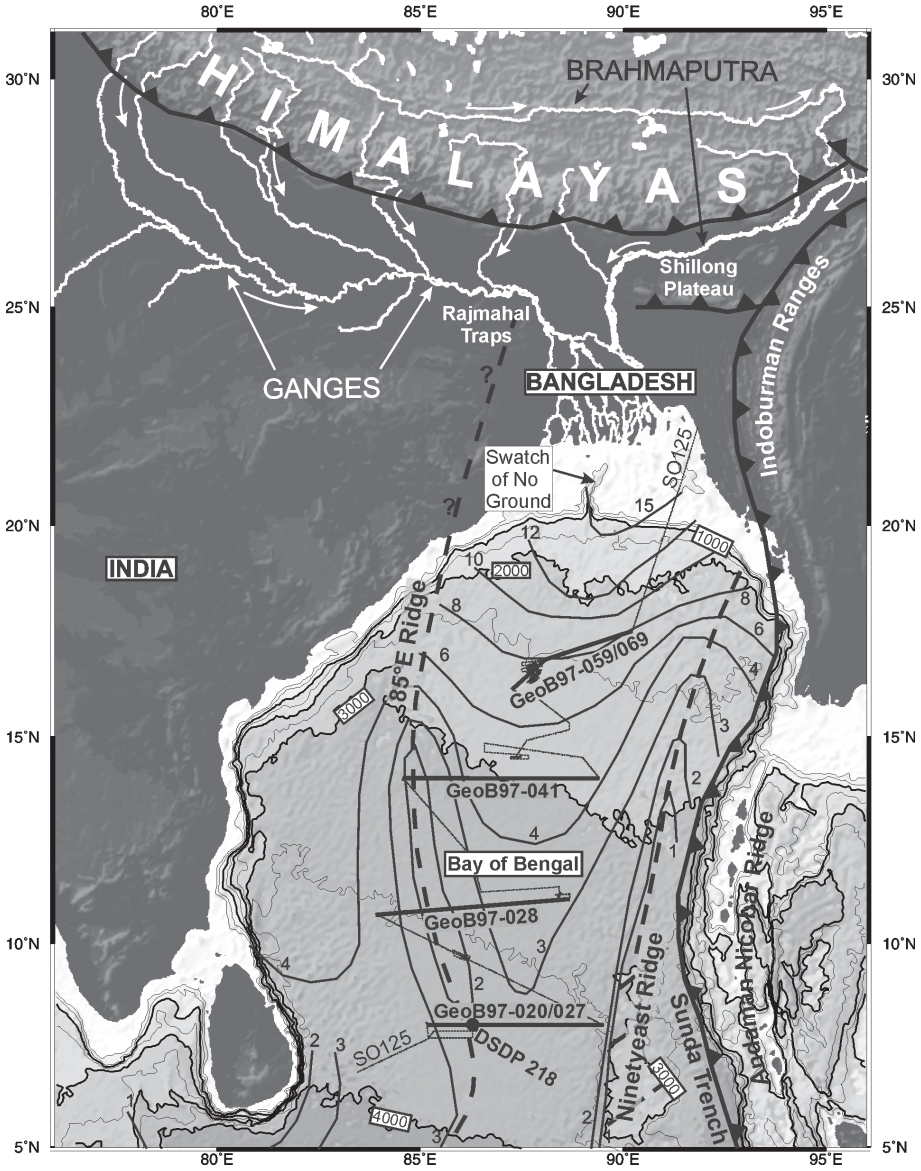

Figure 4.1: *Tectonic map of the Bay of Bengal and the drainage area of the Ganges and Brahmaputra Rivers. Thick dashed line indicate axes of the 85°E Ridge and Ninetyeast Ridge, thin lines show post-collision sediments isopachs in km. Tectonic features and isopachs are redrawn from Curray et al. (2003). Thin dotted line represents cruise track of SO 125 and thick lines are profiles presented in this study. Underlying bathymetry is satellite derived and given in 1000 m contours and gray scales (Smith and Sandwell, 1997).*

4.3 The Bengal Fan

4.3.1 Geometry and morphology

The Bengal Fan completely covers the Bay of Bengal and is insofar bordered to the north by the continental slope of Bangladesh, to the west by the continental slope of eastern India and to the east by the northern end of the Sunda trench and the accretionary prism of the Sunda Subduction Zone spanning from the Indoburman Ranges to the Andaman Nicobar Ridges (Fig. 4.1). From seismic studies, the southern boundary of the Bengal Fan is located at 7°40´S (Krishna et al., 2001a), but Bengal Fan sediments were also drilled at DSDP Site 211 near 10°S (Curray et al., 2003) and Himalayan-derived silicate detritus was even found on a seamount in the central Indian Ocean at 12°57´S (Banakar et al., 2003). However, the length of at least 2800 km, the maximum width of 1430 km, the area of $3x10^6 km^2$ and the volume of $12.5x10^6 km^3$ make the Bengal Fan to the largest submarine fan in the world (Curray, 1994; Curray et al., 2003; Emmel and Curray, 1985). In contrast to most other large submarine fans, the Bengal Fan was con-

tinuously active in the Holocene during sea-level rise and highstand (Weber et al., 1997; Weber et al., 2003).

The Bengal Fan is fed by the sediment load of the Ganges and Brahmaputra, which drain the Himalayas at its northern and southern slope, respectively (Fig. 4.1), and deliver their freight to the Bengal Delta, Bengal Shelf and the deep sea fan. Today, the transport of the sediments is guided through a single deeply incised shelf canyon called „Swatch of No Ground“ (SoNG): shelf sediments are resuspended by storms and tides, then temporarily trapped in the SoNG and finally released episodically to the deep sea by turbidity currents (Kottke et al., 2003; Kudrass et al., 1998; Michels et al., 1998; Michels et al., 2003). These turbidity currents build channel-levee systems, and, as known from other fans, only one active channel-levee system is connected to the canyon at any given time (Babonneau et al., 2002; Curray et al., 2003; Emmel and Curray, 1985; Pirmez and Flood, 1995). In contrast to most other large submarine fans, the recently active channel at the Middle Fan is characterized by numerous cut-off loops (Schwenk et al., 2003). On the Upper Fan, frequent avulsions caused abandonment of channels and formation of new channel-levee systems. Figure 4.2 shows the locations of the presently active channel-

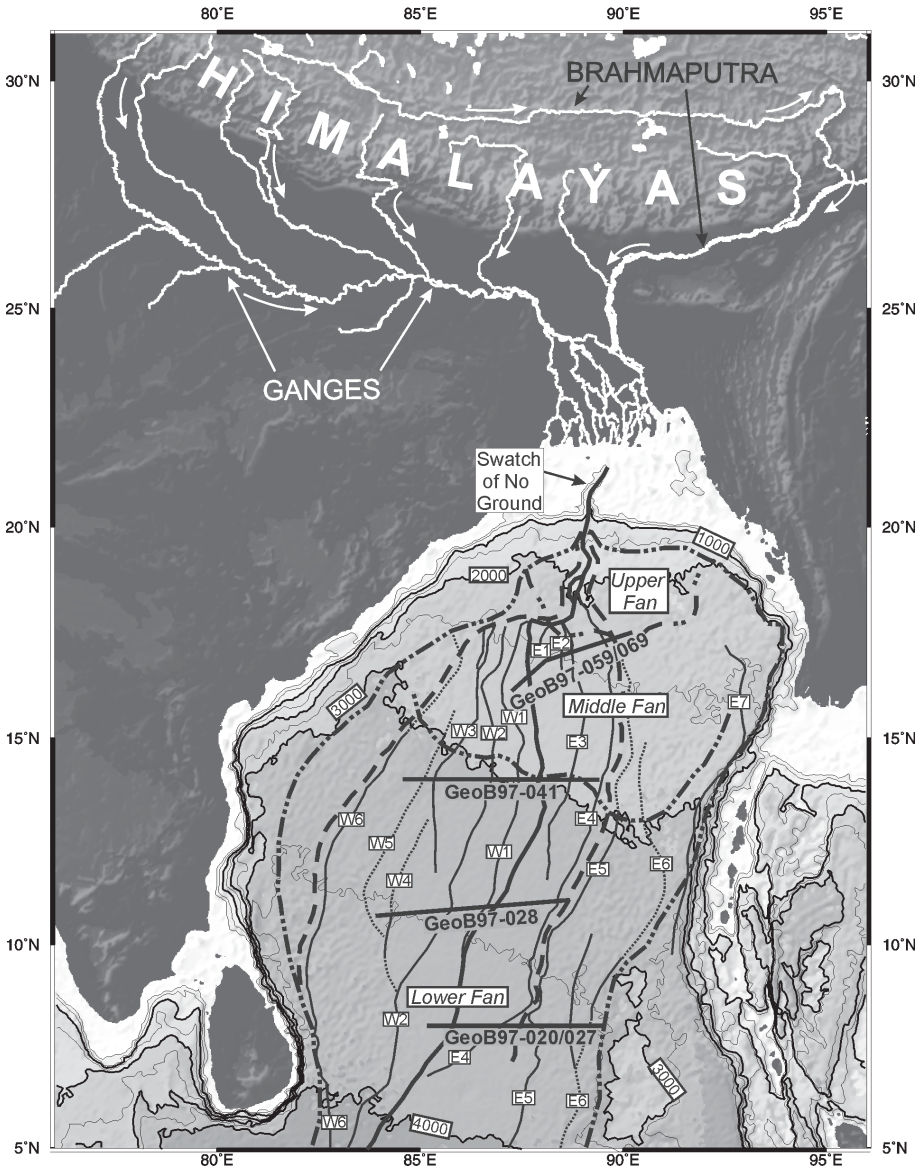

Figure 4.2: *Map showing the border and subdivisions of the Bengal Fan (dashed-dotted lines), the outline of the most recently active subfan (dashed line), the active channel (thick line) and abandoned channels (thin lines, thin dotted lines are less certain channels), all redrawn from Curray et al. (2003). Also drawn in are locations of seismic profiles presented in this study. Satellite derived bathymetry is represented by gray scales and 1000 m contour lines (Smith and Sandwell, 1997).*

levee system and abandoned systems on the seafloor as mapped by Curray et al. (2003). In contrast to the recent geologic situation, Curray et al. (2003) suggested that during late Tertiary and Quaternary more than one active canyon, fed by different rivers, has existed, but each canyon had only one active channel-levee system at any given time.

Based on the slope gradients of the fan surface and of the active channel as well as on the size, morphology and structure of the channel-levee systems, the Bengal Fan has been subdivided into Upper Fan, Middle Fan and Lower Fan (Curray et al., 2003; Emmel and Curray, 1985). The division boundaries are located near 2250 m and 2900 m water depth (Curray et al., 2003) (Fig. 4.2).

4.3.2 Tectonics

The oceanic crust underlying the present Bay of Bengal was generated by seafloor spreading in the early Cretaceous after the breakup of Gondwanaland and separation of Greater India from Antarctica 120 Ma ago (Curray and Moore, 1971; Gopala Rao et al., 1997; Moore et al., 1974). Greater India drifted in a NW direction and the resulting collision with Asia initially created the Bay of Bengal (Alam et al., 2003; Curray et al., 2003; Gopala Rao et al., 1997; Lee and Lawver, 1995). This collision started with a „soft collision“ in the Mid-Paleocene at about 59 Ma between the northernmost part of the Indian shield and South Tibet. In the early Eocene (44 Ma), the collision changed from a „soft“ to a „hard“ continent-continent collision associated with the begin of the Himalayan orogeny (Alam et al., 2003; Lee and Lawver, 1995). Consequently, deposition in the Bengal Fan may have started in the early Eocene at its northern end, and the fan was successively built up by progradation since that time (Curray, 1994; Curray et al., 2003). The thickness of the post-Paleocene deposited fan sediments reaches today ~16 km at the shelf edge south of Bangladesh (Brune et al., 1992; Curray, 1994; Curray et al., 2003) (Fig. 4.1).

Two major tectonic features separate the Bengal Fan into two basins (Fig. 4.1), the 85°E Ridge and the Ninetyeast-Ridge. Both are the products of hot spots but differ in the hot spot location: whereas the 85°E Ridge was formed in an intraplate position on old oceanic crust, the Ninetyeast Ridge was built on a young oceanic crust directly beneath a spreading center (Gopala Rao et al., 1997; Krishna, 2003; Krishna et al., 2001b). The formation of the 85°E Ridge started at 85 Ma in the northern Bay of Bengal on 35 my old crust and terminated at 60 Ma at the location of the ANS Seamount (5°S) (Krishna, 2003). The Ninetyeast-Ridge was formed by the Kerguelen Hot Spot between 95±5 Ma and 38 Ma (Gopala Rao et al., 1997; Krishna et al., 2001b). It is still under discussion, whether the 85°E Ridge is connected to the volcanic Rajmahal Traps in northeast India, or if the 85°E Ridge ends at the continent-ocean boundary in the northern Bay of Bengal and the Rajmahal Traps are formed by the Kerguelen Hotspot simultaneously to the separation of India from Antarctica at 118 Ma (Curray et al., 2003; Curray and Munasinghe, 1989; Gopala Rao et al., 1997; Krishna, 2003; Krishna et al., 2001b; Subrahmanyam et al., 1999).

The sediments of the Lower Bengal Fan were also influenced by intraplate deformation of the Indian Ocean lithosphere (Cochran, 1990; Curray et al., 2003; Curray and

Moore, 1971; Gordon et al., 1998; Krishna et al., 2001a; Moore et al., 1974). This deformation is caused by concentration of compressional stress related to the continuing collision of India with Asia and has been interpreted as diffuse plate boundary due to splitting of the Indo-Australian Plate into the Indian, Australian, and Capricorn plates (Gordon et al., 1998; Krishna et al., 2001a). Beneath the Bengal Fan, this diffuse plate boundary is limited to areas south of 10°N (Gopala Rao et al., 1997; Gordon et al., 1998; Krishna et al., 2001a). Whereas Gordon et al. (1998) suggested that the deformation started at 18 Ma, Krishna et al. (2001a) concluded from seismic data that the deformation occurred in distinct events in Miocene (8.0 - 7.5 Ma), in Pliocene (5.0 – 4.0 Ma) and in Pleistocene (0.8 Ma), with exception of areas east of 84°E and north of the equator, where the deformation occurs quasi-continuous since the Pliocene. The deformation events are restricted to distinct areas with some overlap, the Miocene deformation is located most southwards, the Pliocene deformation most northwards (Krishna et al., 2001a). Recently, the stop of subduction of the Indian Plate under the Himalayas has lead to intraplate deformation of the northern Indian plate and makes also the northern Bay of Bengal seismically active (Biswas and Majumdar, 1997).

4.3.3 Stratigraphy

The first seismic stratigraphic studies carried out in the Lower Bengal Fan revealed two major unconformities in the sediments named „Upper Unconformity“ and „Lower Unconformity“ (Curray and Moore, 1971). These unconformities were first dated by drilling at DSDP Sites 217 and 218 in 1972. For the Upper Unconformity, an age of latest Miocene was found, whereas drilling of the Lower Unconformity encountered a hiatus in the early Eocene (Curray et al., 2003; Moore et al., 1974). The latest Miocene unconformity coincides with the time of onset of intraplate deformation (Curray et al., 2003; Curray and Munasinghe, 1989). The hiatus represented by the Lower Unconformity is also found farther south in DSDP Sites 215 and 211 in the very distal fan, but comprises a much longer time period, namely from Paleocene to early Pliocene. Therefore, the hiatus is interpreted by Curray et al. (2003) as a period of non-deposition, which lasts longer farther away from the head of the fan due to the progradation of the fan. Consequently, the Lower Unconformity represents the begin of fan deposition and separates the sediments in the „real“ post-Paleocene Bengal Fan and the pre-Eocene pre-Bengal Fan deposition (Curray et al., 2003).

Seismic sections in the vicinity from ODP Leg 216 near the equator show two unconformities labeled as „A“ and „B“ (Cochran, 1990; Stow et al., 1990). The lower unconformity (“A”) separates the sediments in a pre-deformation and a syn-deformation sequence and is dated to has a late Miocene age between 7.5 and 8.0 Ma (Cochran, 1990). Accordingly, “Unconformity A” is thought to be the result of the onset of intraplate deformation in the late Miocene and corresponds to the „Upper Unconformity“, found 1000 km north near DSDP Site 218 (Cochran, 1990; Curray et al., 2003). In contrast to “Unconformity A”, “Unconformity B” is related to a change in sedimentation. Dating of “Unconformity B”

reveals an age of 0.8 Ma, and at this time, the lithology of ODP Leg 216 changes towards coarser turbidites and a significant increase in deposition rates is observed as well. So "Unconformity B" is interpreted to be the result of a major sedimentation pulse caused by intensification of glaciations around 0.8 Ma leading to greater sea-level variations and finally larger areas of exposed shelf regions (Cochran, 1990).

In the central Indian Ocean between 7°N and 11°S, Krishna et al. (2001a) analyzed the seismic stratigraphy of three north-south profiles (located at 81.5°E, 83.7°E and 87°E) and identified three regional unconformities. These unconformities were dated at ODP Leg 116 to have late Pleistocene age (0.8 Ma), earliest Pliocene age (5.0 – 4.0 Ma) and late Miocene age (8.0 -7.5 Ma). The Miocene unconformity is found between 1°S and 7°S; the Pliocene unconformity has developed farther northward between 7°N and 1.5°S, whereas the Pleistocene unconformity is concentrated around the equator (Krishna et al., 2001a). All unconformities were related to deformation events in the area of the diffuse plate boundary splitting the Indian Ocean lithosphere (Krishna et al., 2001a). The oldest and youngest unconformities correspond to the unconformities „A" and „B" of Cochran (1990) (Krishna et al., 2001a). Based on the regional extent of the unconformities, Krishna et al. (2001a) suggested that the „Upper Unconformity" at DSDP 218 (Curray and Moore, 1971; Moore et al., 1974) is the equivalent of their earliest Pliocene unconformity. This is in contrast to the interpretation of Cochran (1990) that the „Upper Unconformity" at DSDP Site 218 corresponds to "Unconformity A" at ODP Leg 116. Only the Pliocene and Pleistocene unconformities are also related to changes in sedimentation.

For the upper Lower Bengal Fan Gopala Rao et al. (1997) introduced a stratigraphic sequence of eight units (named H1 to H8 from shallow to deep) based on three long east-west multichannel seismic lines around 14°N. Only four sequence boundaries appear as major unconformities. Ages of these unconformities were interpreted by comparison with the stratigraphic results from ODP Leg 116 (Gopala Rao et al., 1997). As a result, these unconformities were dated as early Eocene, late Oligocene, late Miocene and late Pleistocene, and were correlated to the collision of India with Asia with the begin of fan deposition, lowered sea-levels in Oligocene, onset of intraplate deformation and lowered sea-level in Pleistocene, respectively (Gopala Rao et al., 1997).

To summarize the stratigraphic units identified by different authors cited above, it can be stated that four unconformities are found in sediments of the Bengal Fan dated to have an early Eocene age, a late Miocene age, an early Pliocene age and a late Pleistocene age. Confusingly, not all authors identified all unconformities, the „Upper Unconformity" around DSDP Site 218 was interpreted once as latest Miocene and once as earliest Pliocene and the unconformities were either associated with tectonic events or climatic changes.

4.3.4 Quaternary sequence of channel-levee complexes

On the Upper Bengal Fan, four distinct channel-levee complexes were identified by Curray et al. (2003) and named as Subfans A, B, C and D from oldest to youngest. Tracing of the subfan bases to DSDP Site 218 revealed an age of 1.8 Ma (Pliocene-Pleistocene

boundary) for the base of Subfan A and an age of 0.96 Ma for the base of Subfan B. The end of deposition of Subfan B is assumed at 0.465 Ma. Subfan C does not extend towards DSDP Site 218, but is thought to was active between 0.465 Ma and 0.125 Ma, because Subfan D as the presently active subfan is interpreted to be active from Wisconsin times (0.125 Ma) to present (Curray et al., 2003). From the distribution of the subfans, Curray et al. (2003) concluded that major shifting of canyons occurred during the Pleistocene and that subfans A, B and C were fed by more than one canyon, either simultaneously or in a sequence.

Within the recent Subfan D, eight channel-levee systems were identified, the active channel, four systems east of the active channel, named E1 to E4 and three channels west of the active channel, named W3 to W1 (Curray et al., 2003) (see Fig. 4.2). From the distribution of channels, first a westward shifting of the active channel was interpreted, followed by an eastward shifting. Particularly, E4 was the first active channel in the early period of Subfan D, followed by E3, E2, E1, W3, W2, W1 and the active channel (Curray et al., 2003). Dating of gravity cores from the active channel-levee system at 16°30´S demonstrates that its levees were mainly build up between 12,800 and 9,700 yr BP, therefore the last shift from W1 to the active channel must have occurred at 12,800 yr BP (Curray et al., 2003; Hübscher et al., 1997; Weber et al., 1997). Only one other of the abandoned surface channels could so far be dated exactly, revealing that this channel was inactive since 300,000 yr BP (Weber et al., 2003). Comparing the location (~88°25´E/ 11°11´N) and morphology, it is more than probable that this abandoned channel described by Weber et al. (2003) is identical to Channel E4 from Curray et al. (2003). Thus, an inconsistency exists between the dating of Weber (2003) and the description of Curray (2003) assigning Channel E4 to Subfan D, which following their opinion is active only since 125,000 yr BP.

4.4 Methods

Seismic data presented in this study were collected during R/V Sonne Cruise SO 125, using a GI Gun with chamber volumes of 2 x 0.4 l (main frequency: 100 – 500 Hz) and a streamer with 48 channels distributed in an active section of 600 m length (Spieß et al., 1998). For CDP-stacking, geometry setting was carried out using a binning algorithm sorting the reflection midpoints to binning midpoints based on GPS navigation and heading information of six birds attached on the streamer. A spacing of 20 m of the bin midpoints was chosen, leading to an average 13-fold CDP coverage. The data processing including static correction using the depth information of the birds, NMO-correction, stacking and migration and was carried out with the free software package Seismic Un*x (Stockwell, 1997). Due to the combination of a short streamer and large water depths in the study areas, a constant velocity of 1500 m/s was used for NMO-correction and migration. Interpretation was made with the commercial software package Kingdom Suite 7.2 (Seismic Micro Inc.).

4.5 Data

In the following chapter, we describe the architecture of the Bengal Fan imaged by high-resolution GI Gun data. Due to the penetration of the GI Gun signal, we concentrate on the upper 2 s TWT. The main architectural elements of all profiles are channel-levee systems. The levees are characterized by wedge-shaped structures, which often appear transparent and which are constructed of low to medium amplitude reflectors diverging towards the channel and onlapping onto the base of the levees. The channels are characterized by high amplitude reflectors. If these reflectors are chaotic, they are interpreted as aggrading channel floors, if these reflectors are parallel layered, they represent channel fills, which were deposited after channel segments or the system itself were abandoned (see Chapter 3). In strong meandering channel-levee systems, transparent vertical blocks with dipping reflectors on its base are observed adjacent to the channels. These blocks are thought to be point bars (see also Chapter 3). To describe the architecture of the profiles, we compare following vertical dimensions of the channel-levee systems: The maximum levee thickness measured directly beneath the channel, and the maximum erosion depth, which is the depth of the deepest channel reflector measured from the base of the levee. For open surface channels, we also give the actual channel floor depth measured from the seafloor. We do not present horizontal dimensions as channel or levee width, since they are only comparable, if the profiles are located perpendicular to the systems, which we cannot verify for the buried channel-levee systems. All dimensions of the channel-levee systems given in meters are calculated for a sound velocity of 1600 m/s within the upper sediment column.

4.5.1 Profile GeoB97-020/027

Profile GeoB97-020/027 is located on the Lower Fan at 8°N between 85°10.5'E and 89°29.3'E with a length of ~470 km. (Figs. 4.1 and 4.2). The distance to the shelf edge is ~1330 km. In the western part, the profile crosses the 85°E Ridge, in the eastern part the profile ends above the western flank of the Ninetyeast Ridge. East of the 85°E Ridge, the profile runs across DSDP Site 218 (Fig. 4.1). The water depth varies between 3750 m at the western end and 3525 m on an elevated part near the easternmost end of the profile (Figs. 4.3 and 4.4).

4.5.1.1 Surface channels

On the sea floor, six open channels can be identified (Figs. 4.3 and 4.4). All surface channels are characterized by erosional incisions into the underlying sediments and all surface channels except the easternmost are associated with levees. The westernmost channel reveals a channel-floor depth of 60 m and a maximum levee thickness of 40 m. The channel floor shows aggradation, and the maximum erosion depth below the levee base reaches 95 m. The next channel farther to the east at CDP 8000 is characterized by an incision of the actual channel floor into an existing older channel, building a meander loop at the crossing with the profile. The channel-floor depth is 120 m with a maximum

levee thickness of 32 m. The maximum erosion depth of this system can be recognized as 152 m. At CDP 14000, the profile crosses the next channel, which appears relatively wide, because here the channel runs nearly parallel to the profile between two loops. The depth of the channel floor is 60 m, the maximum erosion depth reaches 125 m and the levee thickness is measured to be 25 m. Near CDP 19000, the next channel-levee system is recognizable at the surface characterized by a channel-floor depth of 22 m, a levee thickness of 24 m and an erosion depth of 32 m below the levee base. In the easternmost part of the profile, directly beneath a local high at CDP 21000 on the western flank of the Ninetyeast Ridge, the sixth channel is found at the surface. This channel does not seem to reveal any attached levee structures, but shows also erosional incision and aggradation. The actual channel depth is 25 m, but a former channel depth of 70 m is identifiable.

4.5.1.2 Buried channel-levee systems

Below the surface, nearly 30 buried channel-levee systems are found in the profile down to a sub-bottom depth of 450 m. Additionally, some unleveed buried channels are found, especially east of the local high on Ninetyeast-Ridge. All channels are characterized by erosional incision, but the dimensions of the systems vary significantly: the minimum levee thickness found among the buried systems is 16 m, the maximum levee thickness reaches 48 m. The average levee thickness of all buried systems is ~27 m. The erosion depths measured from the base of the levees fluctuate between 16 and 152 m, leading to an average erosion depth of 78 m for all systems (see Table 4.1). Below 5.6 s TWT west of the 85°E Ridge and below 5.4 s TWT (~450 m blsf) between the 85°E Ridge and the Ninetyeast Ridge, no channel-levee systems are found, and the profile is characterized by partly interrupted high amplitude reflectors imaging the basin character between the 85°E Ridge and the Ninetyeast-Ridge.

4.5.1.3 Stratigraphy and average sedimentation rates

The crossing of Site 218 of DSDP Leg 22 allows correlation of horizons and calculation of average sedimentation rates along Profile Geob97-020/027 (Figs. 4.4 and 4.5). Time-depth conversion was made using sonobuoy-derived velocity information near DSDP Site 218 revealing an interval velocity of 1.6 km/s for the upper 480 m and 2.8 km/s for the sediments beneath 480 m depth (Moore et al., 1974).

Three distinct time markers can be traced along the profile: the Pleistocene-Pliocene boundary, which is found at 205 m in DSDP Site 218, the Pliocene-Miocene Boundary, which is found at 320 m, and a horizon at 697 m, dated using the nannofossil *Discoaster hamatus* to an age of 10 Ma (Curray et al., 2003; Gartner, 1974). Reflector tracing shows that the 10 Ma horizon onlaps onto a deep unconformity in the east of the profile above the flank of the Ninetyeast Ridge. With respect to the distribution of channel-levee systems we can state that the deepest respectively oldest systems are located nearly beneath or on top of the Pliocene-Miocene boundary (Fig. 4.4).

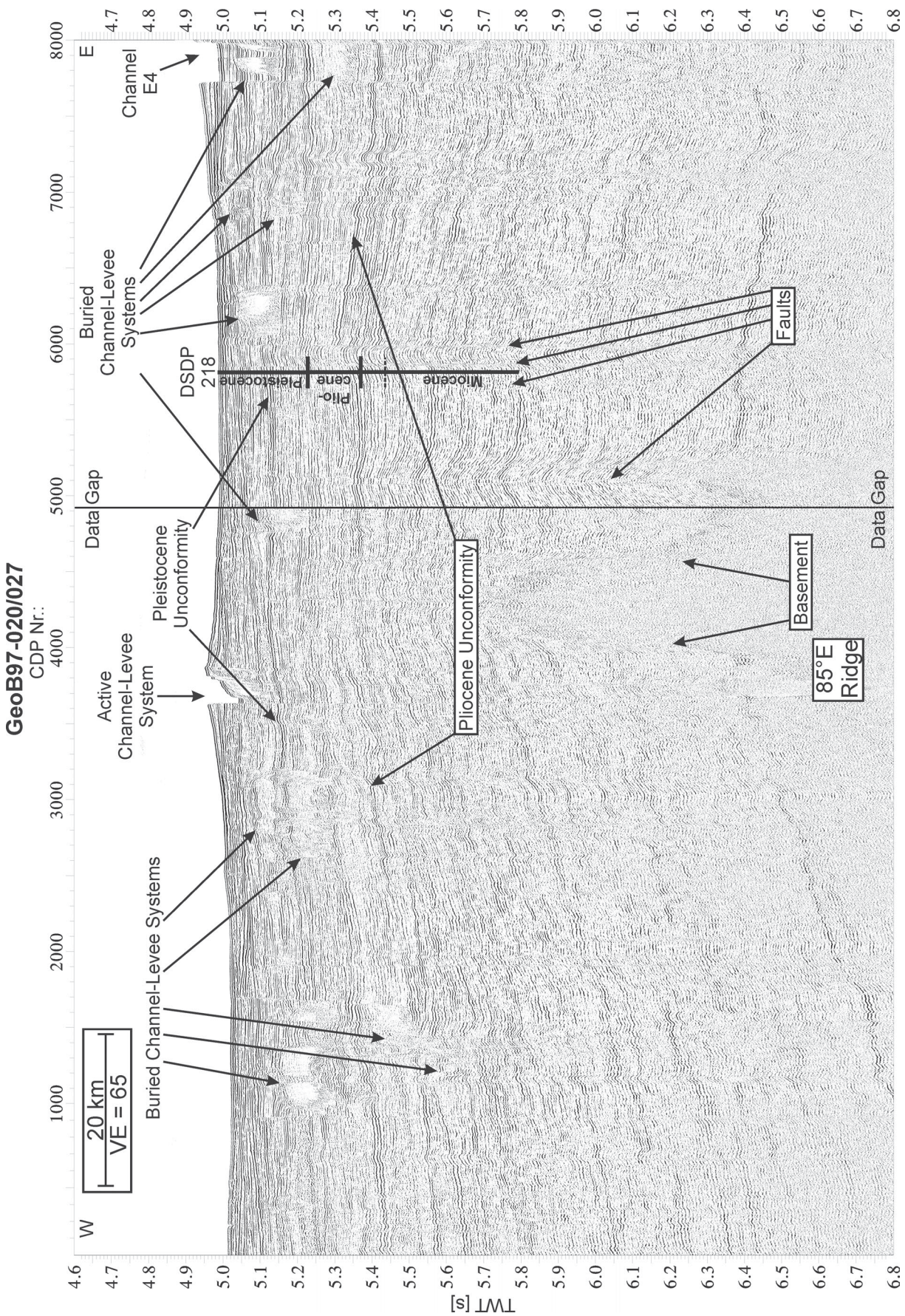

Figure 4.3 a: *Western part of GI-Gun Profile GeoB97-020/027 from the Lower Fan crossing DSDP Site 218 (see Figs. 4.1 and 4.2). Indicated channel-levee systems, unconformities and faults are described and discussed in the text. Channel naming follows the terminology of Curray et al. (2003).*

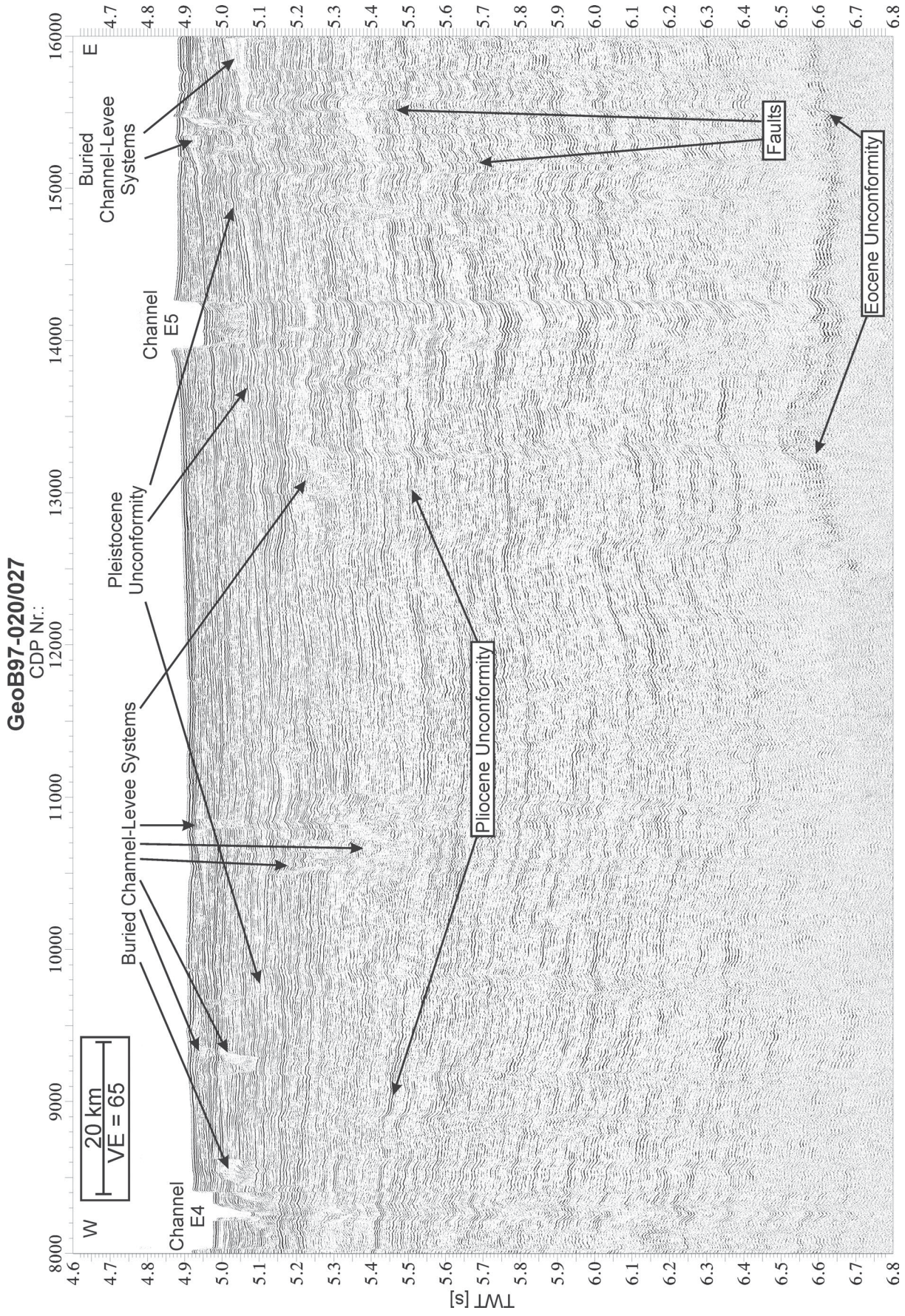

Figure 4.3 b: *Central part of Profile GeoB97-020/027.*

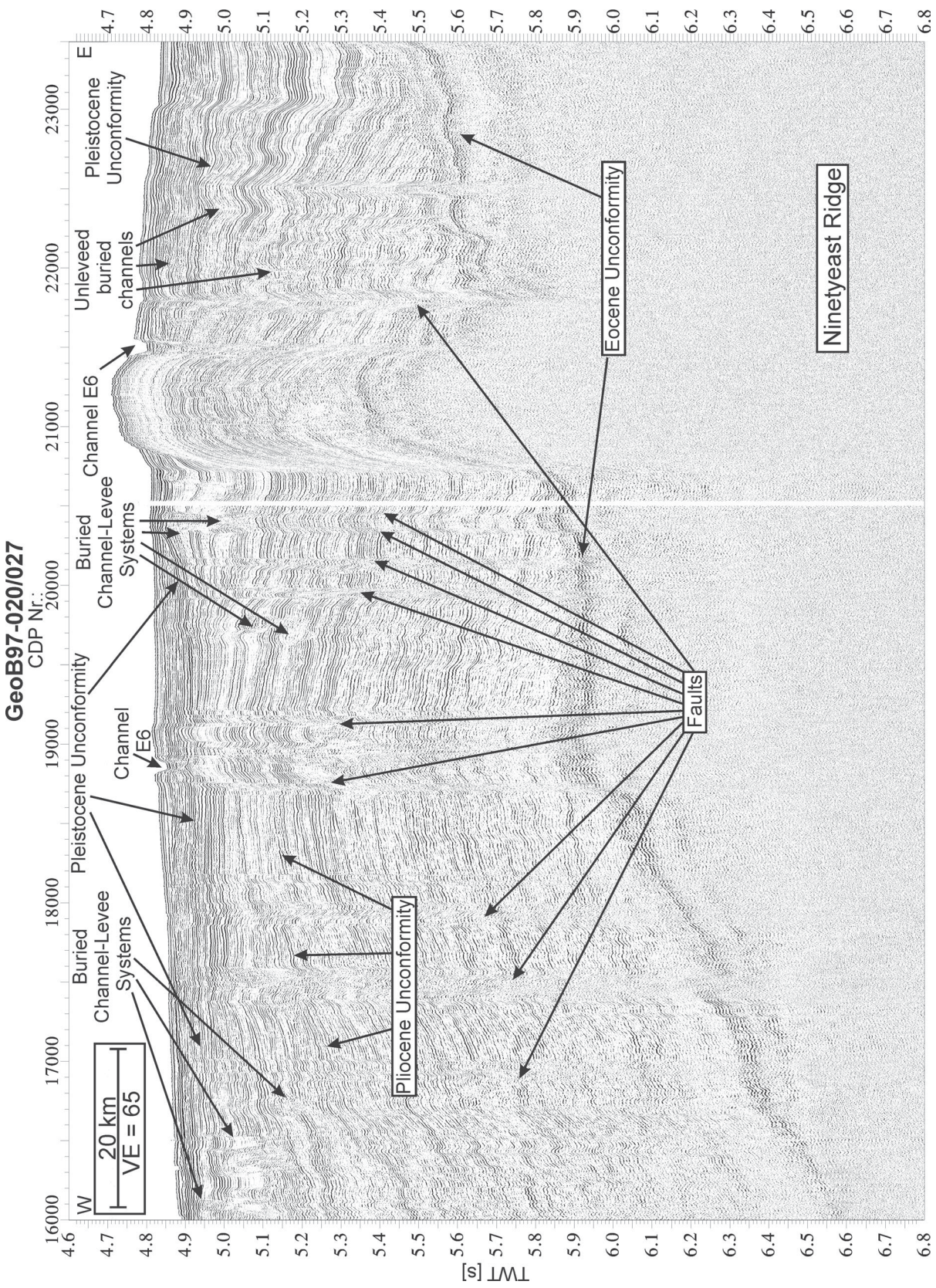

Figure 4.3 c: *Eastern part of Profile GeoB97-020/027.*

At DSDP Site 218, sedimentation rates are 11 cm/ky for the Pleistocene, 3 cm/ky for the Pliocene and 8 cm/ky for the late Miocene since 10 Ma. Studying the whole profile, we find maximum sedimentation rates at the basin center and minimum sedimentation rates above both ridges. In the center, deposition took place with a rate of 21 cm/ky in the

Pleistocene, 6.5 cm/ky in the Pliocene and 11 cm/ky in the late Miocene (Fig. 4.5). Sedimentation with smallest rates occurred above the height on the flank of the Ninetyeast Ridge in the eastern part of the profile: 4.3 cm/ky in the Pleistocene, 1.5 cm/ky in the Pliocene and 5.4 cm/ky in the late Miocene (Fig. 4.5). To demonstrate the changes of sedimentation rate along the profile, we normalize the rates to their maximum values along the profile. As a result we can state that the sedimentation rates in Pleistocene and Pliocene times decrease above the Ninetyeast Ridge to 20% of the rates found in the basin between both ridges, whereas the sedimentation rate in the late Miocene decreases above the Ninetyeast Ridge only to 50% of its maximum value. Above the 85°E Ridge, the decrease of sedimentation rate is less pronounced than above the Ninetyeast Ridge. Pleistocene sedimentation rate is here nearly 50% of its maximum, Pliocene sedimentation rate reaches 40% and Miocene sedimentation rates reaches 60% of its maximum (Fig. 4.5).

Generally, the sedimentation rates on Profile GeoB97-020/027 are highest in Pleistocene, lowest in Pliocene and medium in late Miocene. The decrease of sedimentation rates above the ridges is lowest in late Miocene and highest in Pliocene and Pleistocene. But it should be kept in mind that sedimentation rates after onset of building channel-levee systems are only rough estimates, since sedimentation varies strongly in time and space. Therefore, especially the sedimentation rates in Pleistocene can be much higher within levees, namely up to 50 orders of magnitude than the calculated averages.

4.5.1.4 Unconformities and faults

In Profile GeoB97-020/027 we identified two regional unconformities covering the complete profile. Additionally, two deep unconformities, acting as acoustically base, are found above both ridges (Figs. 4.3 and 4.4). These unconformities are characterized by strong reflection amplitudes and onlapping of basin reflectors above. The deeper of the regional unconformities is also characterized by onlaps, especially above the flanks of both ridges. This unconformity crosses the DSDP Site 218 in a depth of 265 m below the seafloor. The Pleistocene – Pliocene boundary is found here in a depth of 205 m (Curray et al., 2003; Moore et al., 1974). Assuming a sedimentation rate of 3 cm/ky (Fig. 4.5), an age of 4.8 Ma can be derived for this „Pliocene unconformity“. The shallowest unconformity, identified by onlapping reflectors as well, is located 88 m below the seafloor at DSDP Site 218. Here, at 70 m depth an age of 0.465 Ma is correlated (Curray et al., 2003). Using an average sedimentation rate of 10cm/ky for the depth between 70 m and 205 m, as suggested by Curray (2003), this upper unconformity („Pleistocene unconformity“) is found to be 0.64 Ma old. But again it should be mentioned that sedimentation in the Pleistocene is mainly characterized by building of channel-levee systems and therefore average sedimentation rates must be handeled with care.

Beside these regional unconformities, several local unconformities are visible in the seismic data, often connecting bases of channel-levee systems. However, these unconformities cannot be traced through the complete profile, because they are interrupted by

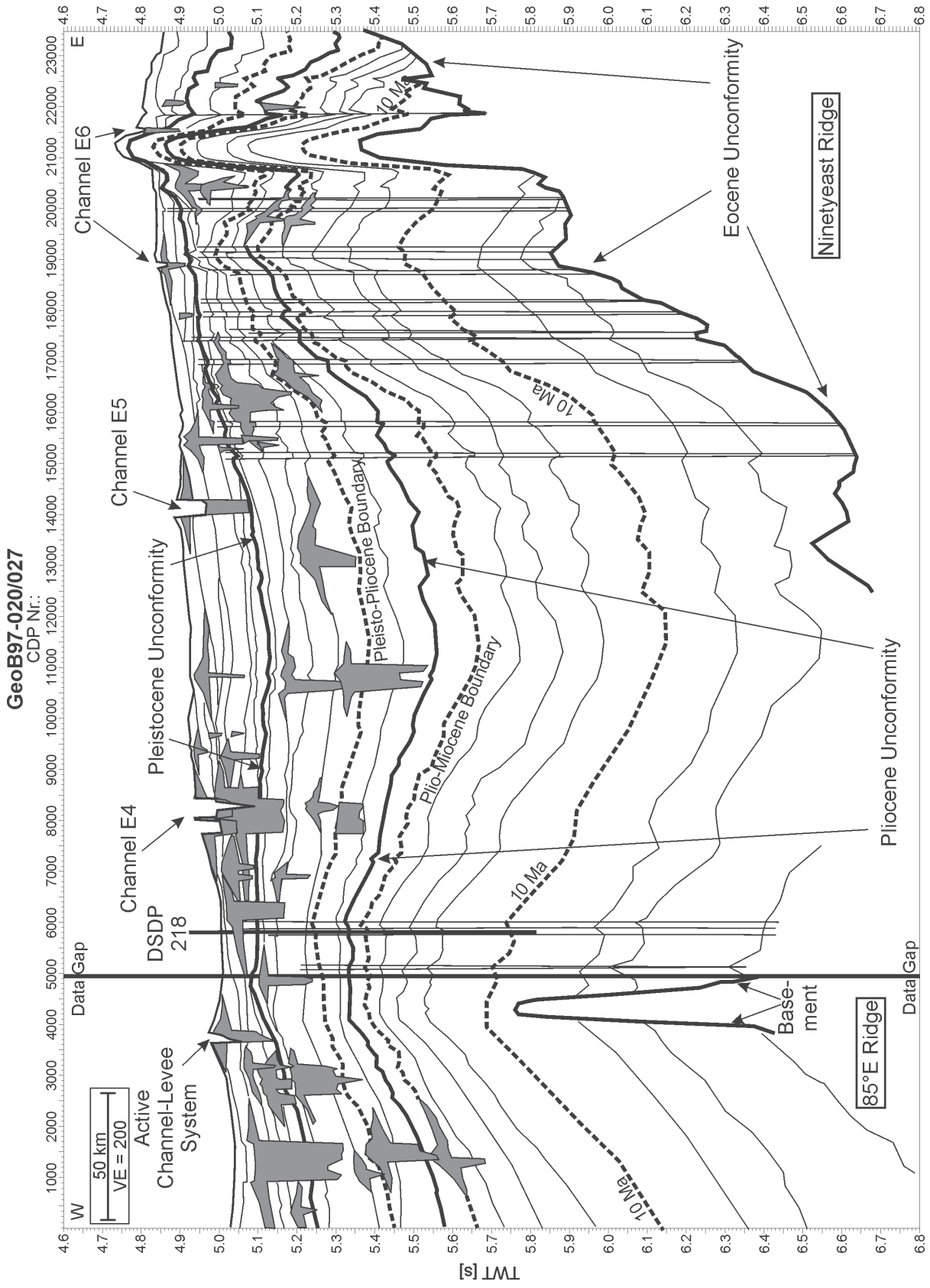

Figure 4.4: *Interpreted linedrawing of Profile GeoB97-020/027 showing channel-levee systems (gray) and regional unconformities. Age assignments are from DSDP Site 218 (Moore et al., 1974). Labeling of the channels is from Curray et al. (2003). For location, refer to Figs. 4.1 and 4.2.*

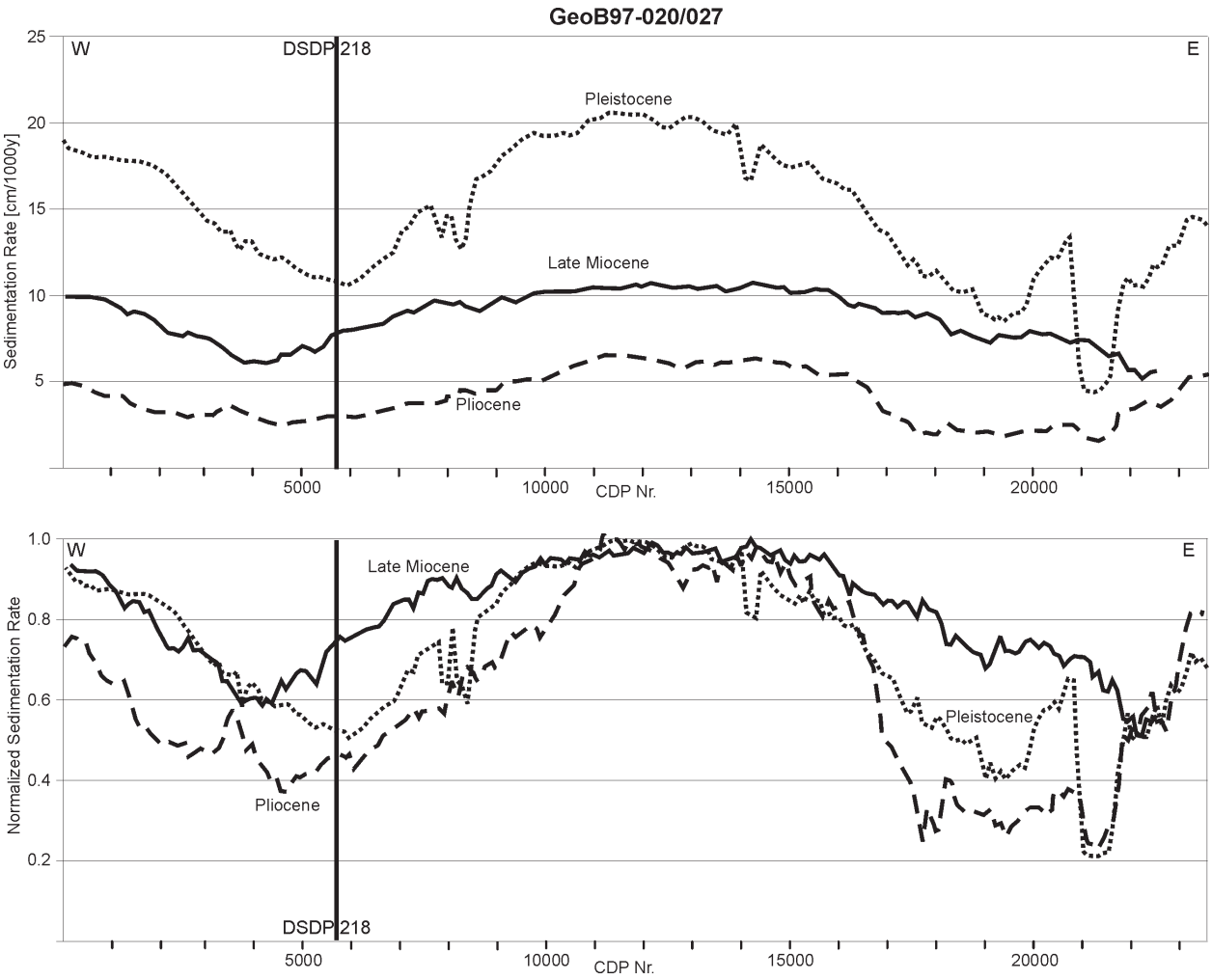

Figure 4.5: *Sedimentation rates on Profile GeoB97-020/027 in absolute values (top) and normalized on the maximum, respectively (bottom). Dotted line represents Pleistocene, dashed line Pliocene and heavy line late Miocene (<10Ma). Vertical line indicates location of DSDP Site 218.*

incising channel-levee systems or terminating on levees. Therefore these unconformities are not suitable for establishing regional stratigraphic units. Additionally, bottoms and tops of levees also appear as unconformities, but these unconformities only mark boundaries between architectural elements within submarine fans.

On the flanks of both ridges, but especially on Ninetyeast Ridge, numerous faults are visible in the seismic data. All faults can be traced down to the lower unconformity, no fault reaches the seafloor, but they are typically terminating in depths near the Pleistocene unconformity.

4.5.2 Profile GeoB97-028

Profile GeoB97-028 reaches a length of 512 km from west to east and is located on the Lower Fan between 10°43.2'N/83°59.6'E and 11°05.5'N/88°40.5'E (Figs. 4.1 and 4.2). The shelf distance is ~1000 km, and the water depth decreases from 3530 m in the west to 3270 m in the east. In the western part, the profile crosses the 85°E Ridge.

4.5.2.1 Surface channels

On Profile GeoB97-028, seven open channel-levee systems are found at the seafloor, which are all incised into underlying sediments (Figs. 4.6 and 4.7). In the westernmost

part, three small systems, settling on each other, can be identified. Their channel depths are 6 m, 12 m, and again 6 m from west to east, their levee thicknesses reach 24 m for the western and central system and 10 m for the eastern of these three systems. The maximum incision depths are measured to be 70 m, 58 m and 13 m from west to east. Farther east, two refilled channel-levee systems (at CDP 3300 and 6000) are recognizable, and the next open channel-levee system is found at CDP 8000. This system is characterized by a channel depth of 32 m, a levee thickness of 29 m and a maximum incision depth of 28 m. Farther east, the profile crosses a strongly meandering channel two times. The depth of this channel reaches 30 m by a levee thickness of 22 m and a maximum incision depth of 90 m. On top of the eastern levee of this channel, a small channel-levee system has settled with a channel depth of 10 m, a levee height of 15 m and an erosion depth of 32 m. In the easternmost part of the profile, a large channel-levee system is found, characterized by a meandering loop incising into a pre-existing channel. The depth of the channel floor reaches 89 m, the levee thickness is 24 m and the maximum incision depth is measured to 154 m.

4.5.2.2 Buried channel-levee systems

On Profile GeoB97-028, we can identify at least 60 buried channel-levee systems (Fig. 4.7). Additionally, some unleveed channels exist, especially in deeper parts of the profile. As on Profile GeoB97-020/027, all systems are characterized by deep incisions into pre-existing sediments, but they also differ strongly in vertical dimensions. The maximum levee height we identified is 49 m, the thinnest levee we found reveals a thickness of 10 m. The average value of the thickness of all levees is calculated to 24 m (Table 4.1). As maximum erosion depth, we found 153 m, whereas the minimum erosion depth is 9 m. The average erosion depth of all channels is finally determined to be 67 m. The deepest channel-levee system is found 600 m beneath the sea floor. In deeper parts, the profile is characterized by high amplitude but incoherent reflectors revealing the basin structure of the fan not only between the 85°E Ridge and the Ninetyeast Ridge, but also western of the 85°E Ridge. This lack of coherency of reflectors makes the identification of systems difficult, and we believe it to be caused by some unleveed channels.

4.5.2.3 Stratigraphy

From our linedrawing, we found three regional stratigraphic units in Profile GeoB97-028, separated by Horizons U1 and U2 (Fig. 4.7). Both unconformities are characterized by onlapping overlying reflectors. Below Unconformity U2, the reflectors follow the pre-existing topography and reveal the 85°E Ridge, the Ninetyeast Ridge and the central basin between both ridges. The deeper reflectors run nearly parallel and converge slightly above local heights. The shallower the reflectors are, the more pronounced is the convergence of the reflectors towards the flanks of the ridges, successively leveling the topography up to Reflector U2. Even if we see local unconformities beneath U2, for example above the western flank of the 85°E Ridge between 5.0 and 5.2 s TWT, above the top of the 85°E Ridge or above the western flank of the Ninetyeast Ridge, there is no evidence

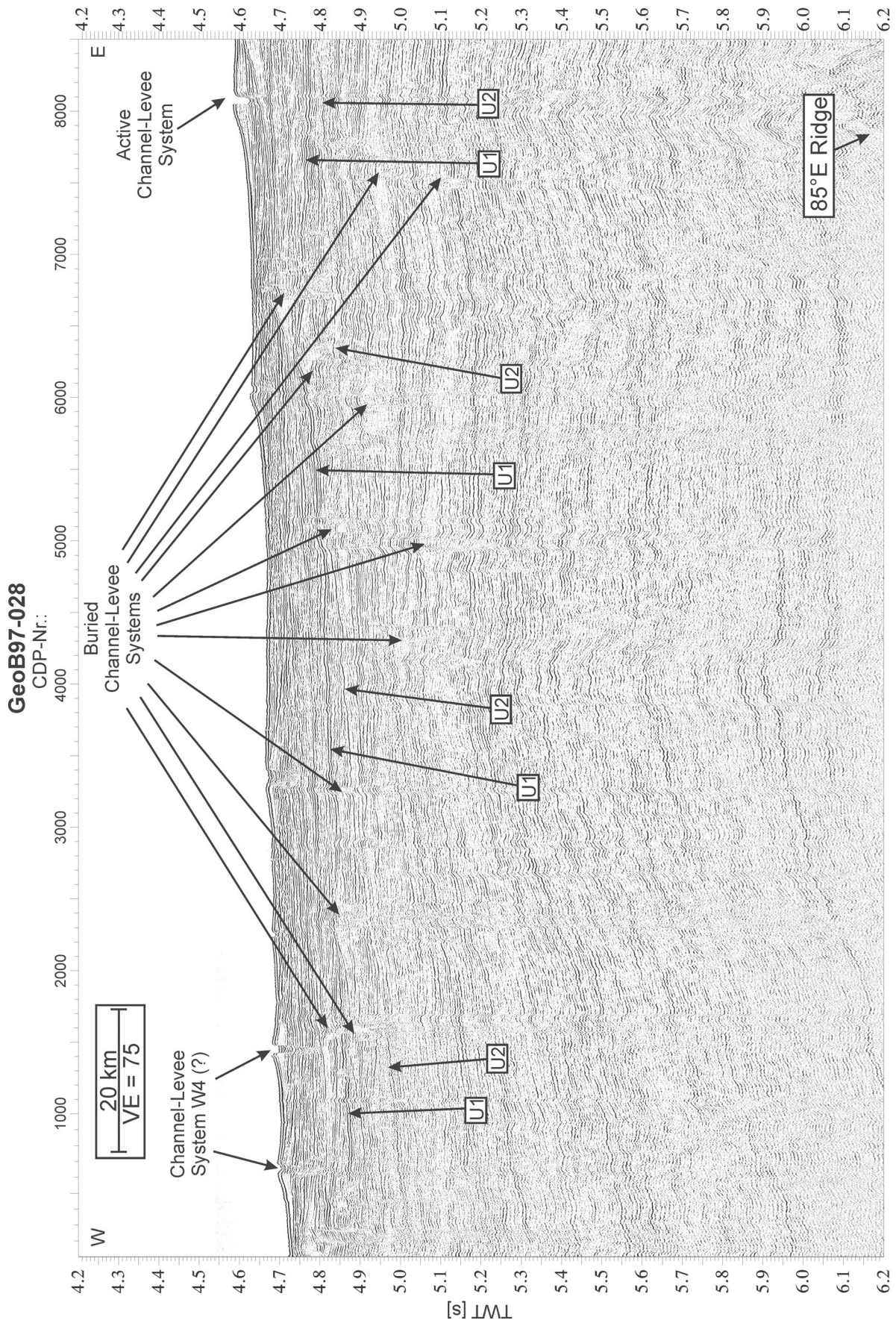

Figure 4.6 a: *GI Gun data of the western part of Profile GeoB97-028 located at 11° N (for location, see Figs. 4.1 and 4.2). Arrows pointing on channel-levee systems and unconformities discussed in the text. Notation of surface channels follows Curray et al. (2003).*

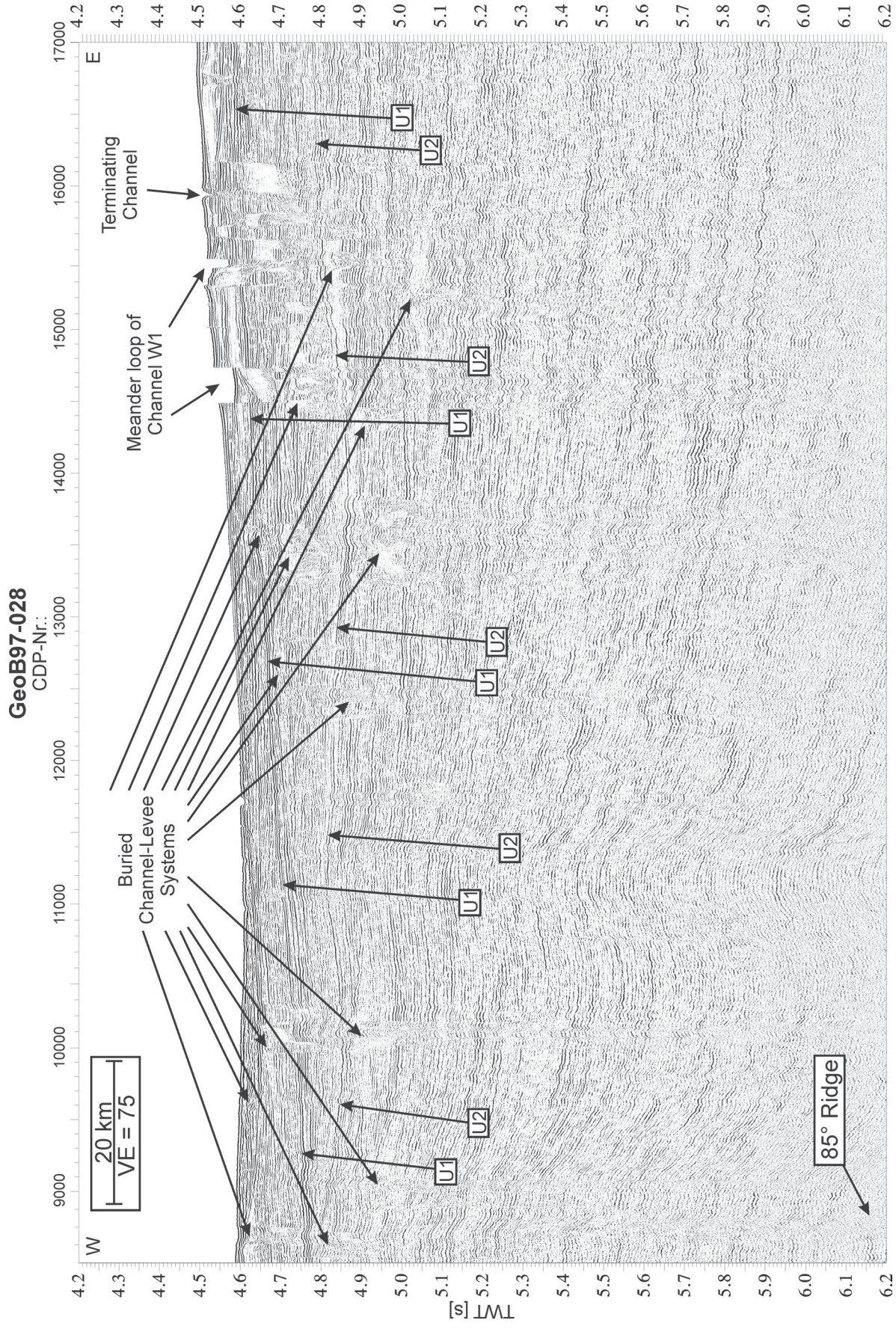

Figure 4.6 b: *GI Gun data of the central part of Profile GeoB97-028.*

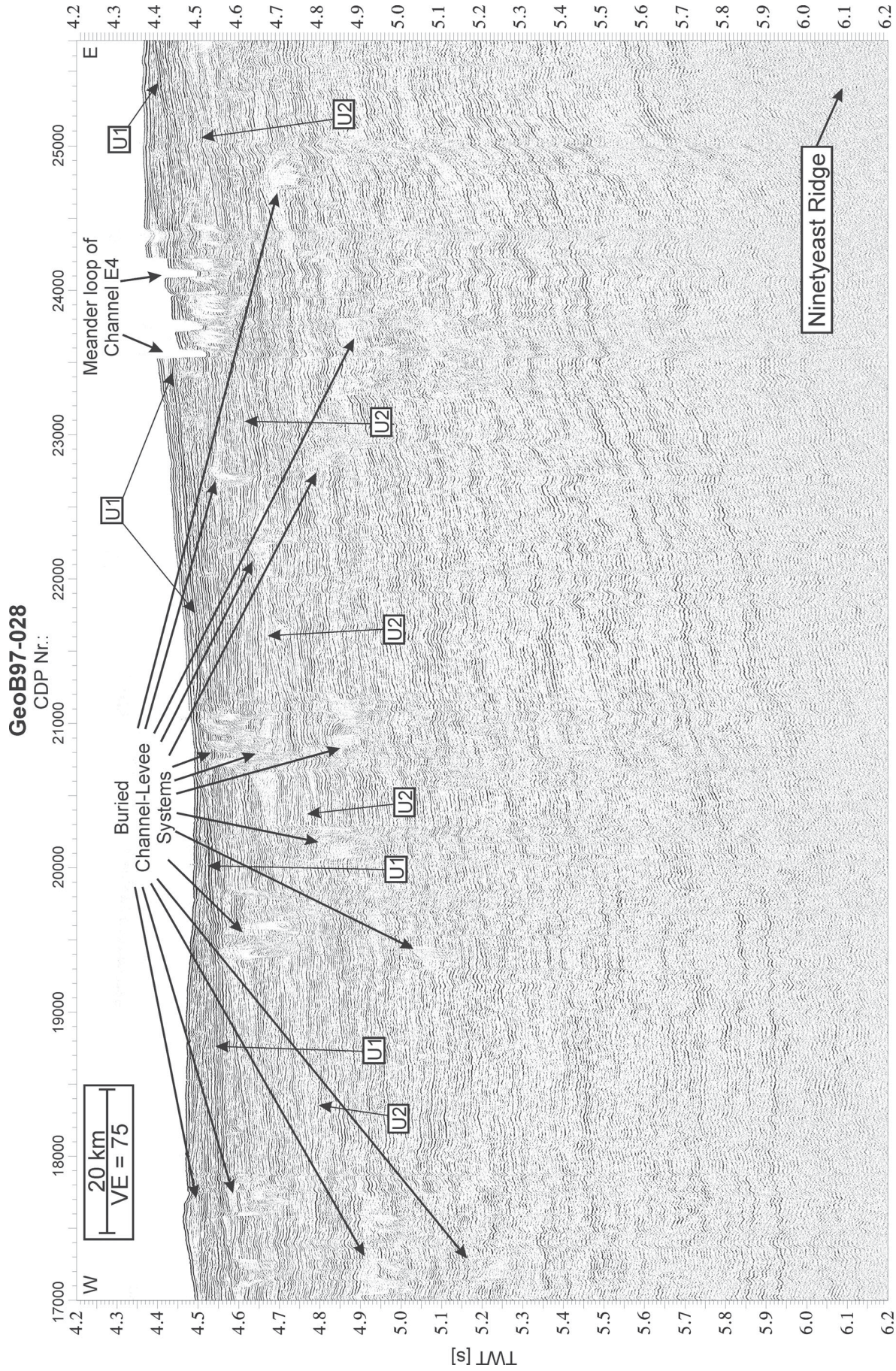

Figure 4.6 c: *GI Gun data of the eastern part of Profile GeoB97-028.*

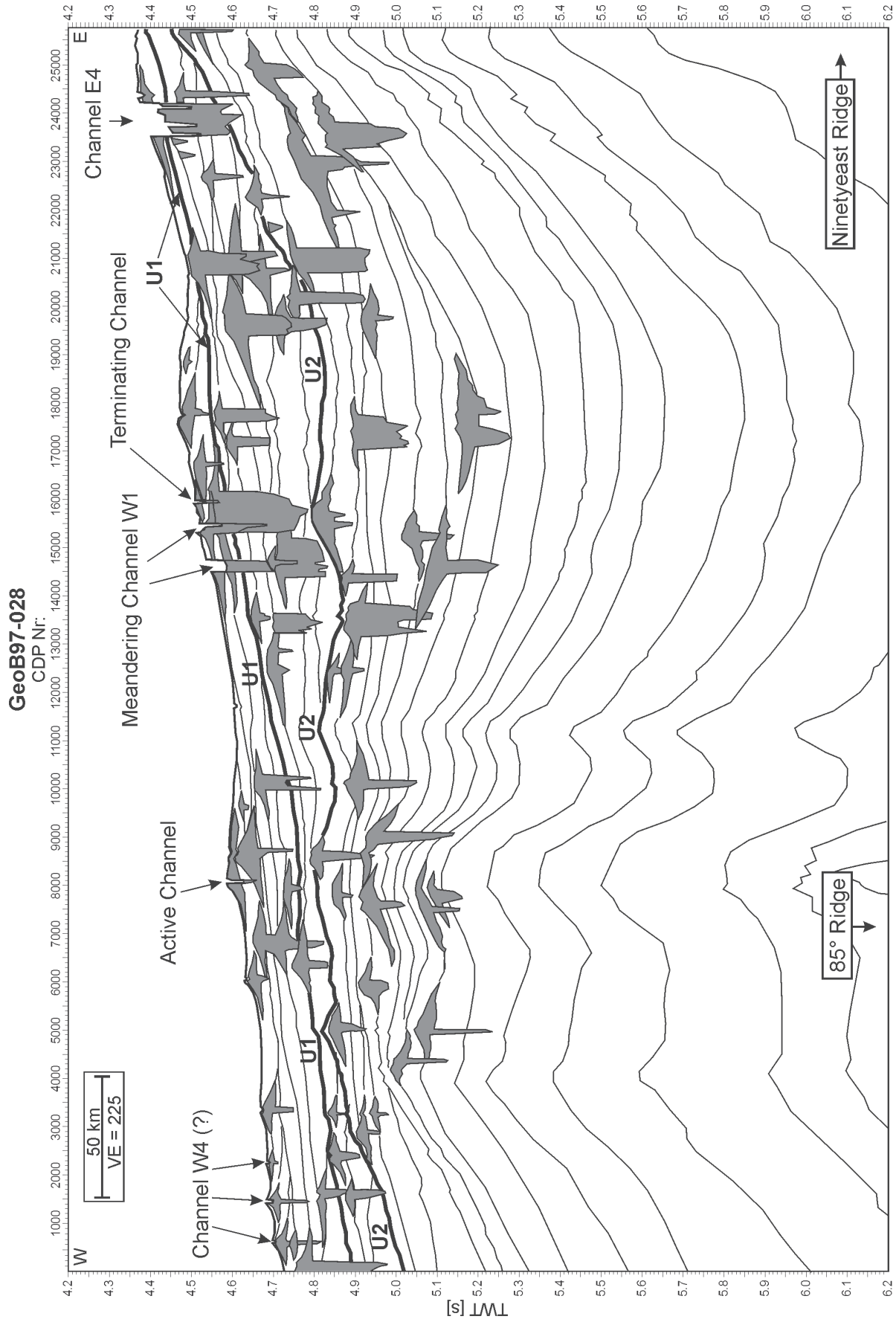

Figure 4.7: *Interpreted line drawing of Profile GeoB97-028 crossing the 85°E Ridge in the western part (Fig. 4.1). Channel-levee systems are drawn in gray, regional unconformities are highlighted as thick lines. Labeling of channels follows terminology from Curray et al. (2003).*

for a more widespread, regional unconformity beneath Unconformity U2 in our data. The stratigraphic unit between U1 and U2 shows a minimum thickness above the top of the 85°E Ridge and a maximum thickness between both ridges. Within this unit, some local unconformities are found, which are terminating on Unconformity U2. Unconformity U1 as top of this unit dips down from east to west similar as the seafloor. Since the dipping angle of U1 is higher than the dipping angle of the seafloor, the thickness of the unit above U1 increases from east to west. Most reflectors above U1 dip down also from east to west parallel to the seafloor and onlap on U1. Some local unconformities show up within the uppermost stratigraphic unit as well, i.e. in the western part of the profile below the channel-levee systems between CDP 1 and 4000.

4.5.3 Profile GeoB97-041

Profile GeoB97-041 was placed near the boundary between Lower Fan and Middle Fan at 14°N and covers 515 km between 84°35.0'E and 89°24.4'E (Figs. 4.1 and 4.2). The distance to the shelf edge is ~670 km and, as visible in Figure 4.1, the profile crosses the 85°E Ridge near its western end. The water depth decreases from 3160 m at the western end to 2860 m at the eastern end.

4.5.3.1 Surface channels

Seven large open channels were identified on Profile GeoB97-041 (Figs. 4.8 and 4.9). All of these channels are enclosed by levees, except for the westernmost channel. This westernmost channel reveals a channel floor depth of 25 m, a former deeper incision with following aggradation is not identifiable. Farther east near CDP 5500 a channel is located with a depth of 52 m, a levee thickness of 22 m and a maximum incision depth of 79 m. The next channel further east is found near CDP 9000. This channel shows a depth of 37 m, a levee thickness of 21 m and an incision depth of 41 m. Nearly 2000 CDP´s to the east, the seafloor is cut by a channel of 106 m depth, which is flanked by levees of 24 m thickness and revealing a former incision of 110 m. The next channel found at CDP 15800 is less deep and shows a depth of 33 m. Its surrounding levees reach a thickness of 18 m and, as for the westernmost channel, no evidence for a deeper incision into the actual floor is found. At CDP 18000, the deepest channel at the surface exists on Profile GeoB97-041. The depth of this channel is 113 m, the levee thickness 31 m and the incision depth is recognized as 92 m. The easternmost channel-levee system is located at CDP 24000. Here, the levees of the system are draped by sediments, but the channel remained open and shows an actual depth of 27 m. The thickness of the levees amounts to 36 m and the maximum incision depth is 92 m. Especially in the western part of the profile, several small unleveed channels are visible between the above described channels.

4.5.3.2 Buried channel-levee systems

Beside the identified channel-levee systems at the seafloor, we found a large number of buried channel-levee systems (Figs. 4.8 and 4.9). In addition, several unleveed chan-

nels could be recognized within the sediment column adding up to at least 80 buried channels on Profile GeoB97-041. Studying all the buried systems reveals a large variety of sizes (Table 4.1): as minimum levee thickness we measured 9 m, as maximum levee thickness we found 60 m. The average thickness of all levees is 27 m. The incision depths vary from 12 m to 195 m, the average is determined as 67 m. The deepest system we identified is 640 m beneath the surface, but the incoherency of the deeper reflectors aggravates their identification and therefore deeper systems might not have been recognized.

4.5.3.3 Stratigraphy

In Profile GeoB97-041, we found two characteristic horizons appearing as unconformities and separating the section into stratigraphic units (Figs. 4.8 and 4.9). In the western part of the profile, a thick unit with very low reflection amplitudes appears between CDP 1 and 3000 in a depth of 4.35 s to 4.45 s TWT. Additionally, east of CDP 14000 a thin, also rough transparent layer is identified between depths of 4.0 s and 4.3 s TWT. The tops of both transparent layers are characterized by onlapping reflectors. Both tops can be connected to the regional Unconformity U1. This unconformity runs nearly parallel to the seafloor except in the westernmost part above the 85°E Ridge, where a distinct step occurs. As in the southern profiles GeoB97-020/027 and GeoB97-028, local unconformities, connecting bases of channel-levee systems, are found within the unit between U1 and the seafloor. The bottom of the transparent layer in the west can be traced along the complete profile and is also characterized by onlaps, especially above the eastern flank of the 85°E Ridge. This unconformity (U2) shows the same step above the 85°E Ridge and diverges continuously from U1 towards the east, consequently the unit between unconformities U1 and U2 increases in thickness from west to the east. The reflectors within the unit between U1 and U2 converge to the west, most of them terminating on U2. Beneath Unconformity U2, the reflectors image the basin structure of the fan between the 85°E Ridge and the Ninetyeast Ridge and run nearly parallel in most parts of the profile except near CDP 5000 where a characteristic dome appears. Here the reflectors converge beneath U2. Between U2 and U1, the reflectors converge or terminate at this location, leading finally to a leveling of this dome at Unconformity U1. The deepest reflectors onlap in the western part of the profile onto the 85°E Ridge, which is here only covered by 500 m of sediments.

4.5.4 Profile GeoB97-059/069

Profile GeoB97-059/069 extends from Southwest to Northeast from the Middle Fan to the Upper Fan between 16°07.4'N/87°16.0'E and 17°30.0'N/90°10.0'E (Figs. 4.1 and 4.2). A course change splits the profile into a more southwest-northeast orientated western part and a more west-east orientated eastern part. The profile reaches a length of 350 km, and the distance to the shelf varies between 450 km at its southwestern end and 280

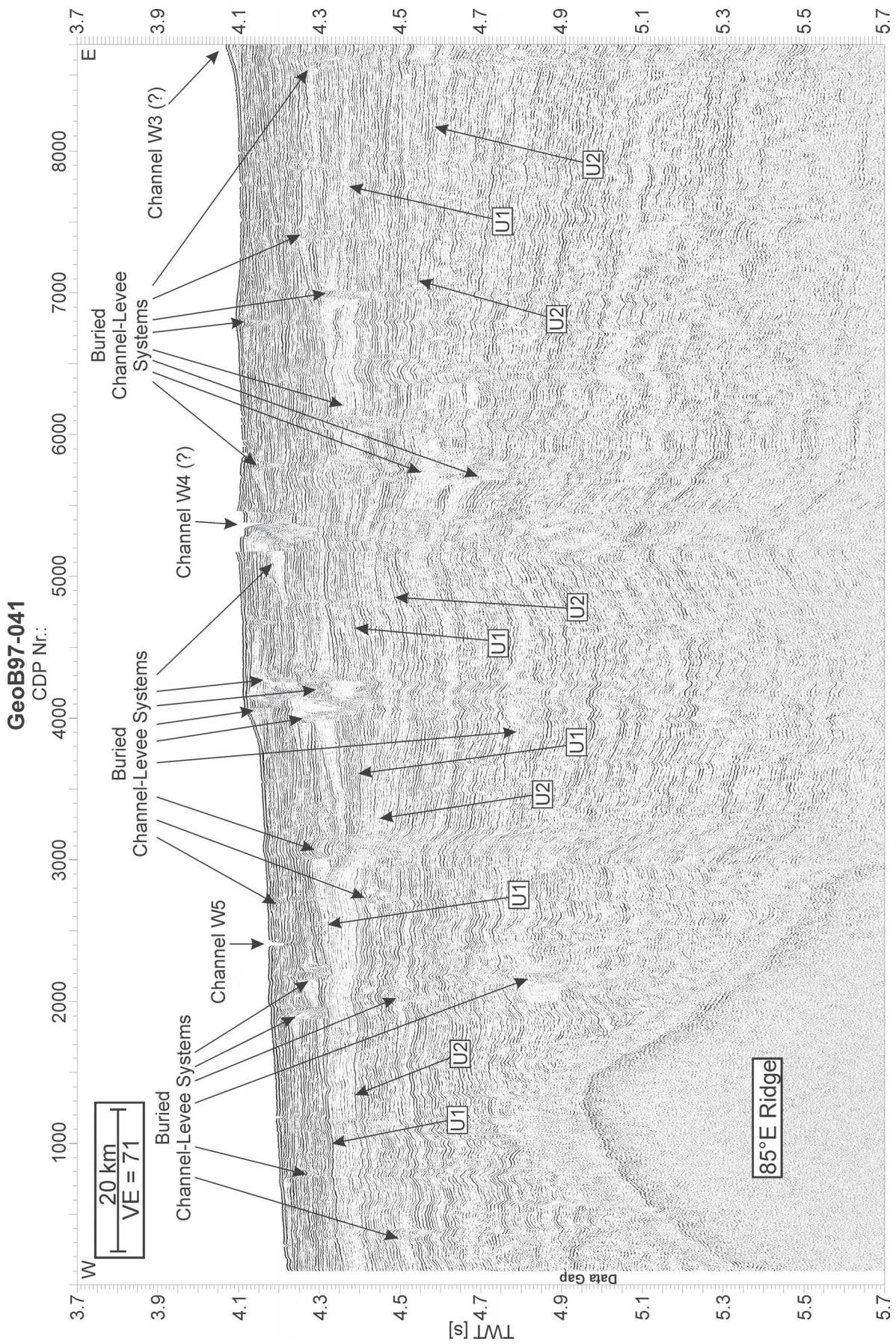

Figure 4.8 a: *GI Gun data showing the western part of Profile GeoB97-041 located at the northern edge of the Lower Fan. For location, refer to Figures 4.1 and 4.2. In the western part the data imaging a basement height of the 85°E Ridge. Regional unconformities and channel-levee systems discussed in the text are indicated. Surface channel naming follows the terminology of Curray et al. (2003).*

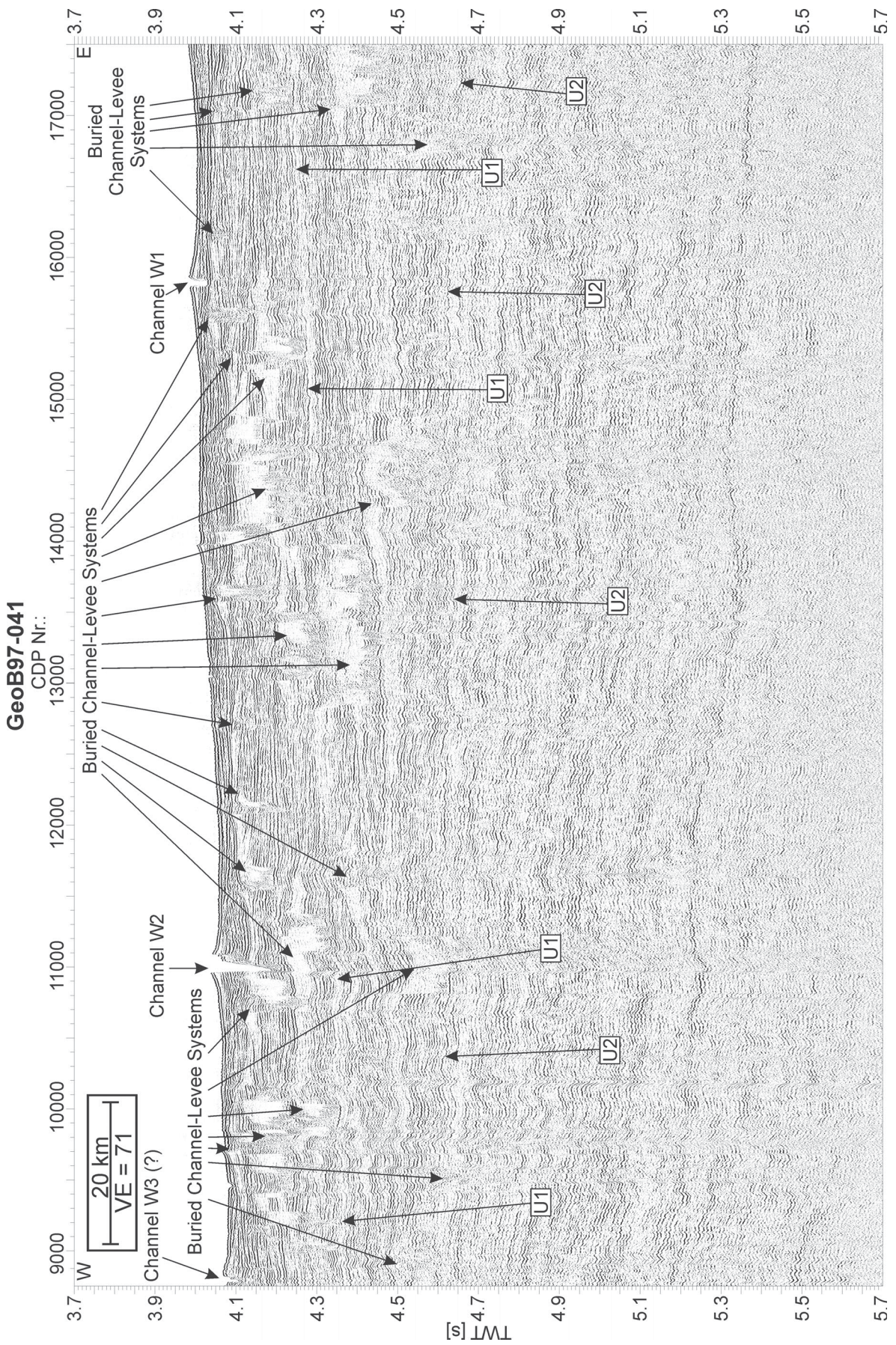

Figure 4.8 b: *GI Gun data showing the central part of Profile GeoB97-041 located at the northern edge of the Lower Fan. For location, refer to Figures 4.1 and 4.2. Regional unconformities and channel-levee systems discussed in the text are indicated. Surface channel naming follows the terminology of Curray et al. (2003).*

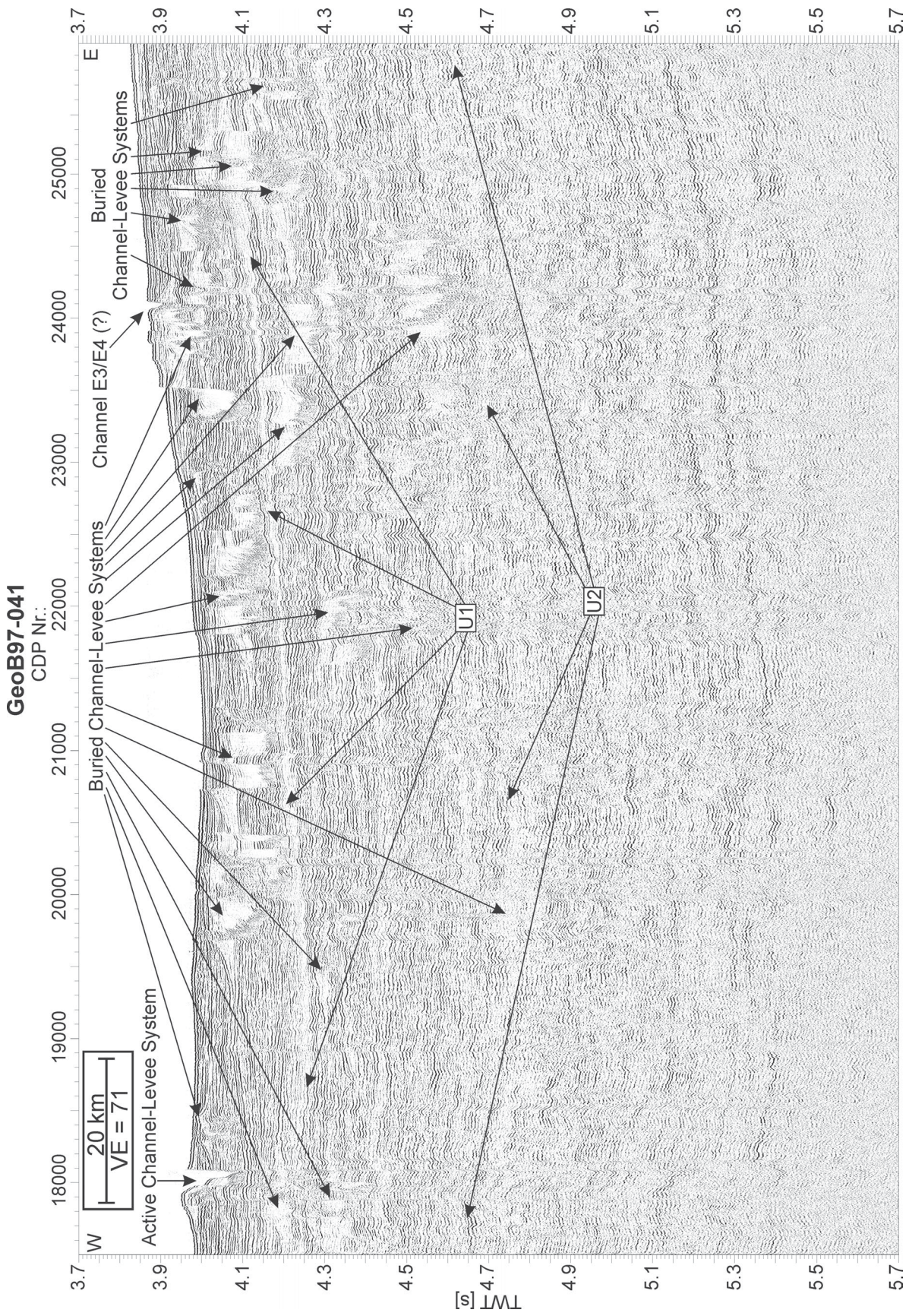

Figure 4.8 c: *GI Gun data showing the eastern part of Profile GeoB97-041 located at the northern edge of the Lower Fan. For location, refer to Figures 4.1 and 4.2. Regional unconformities and channel-levee systems discussed in the text are indicated. Surface channel naming follows the terminology of Curray et al. (2003).*

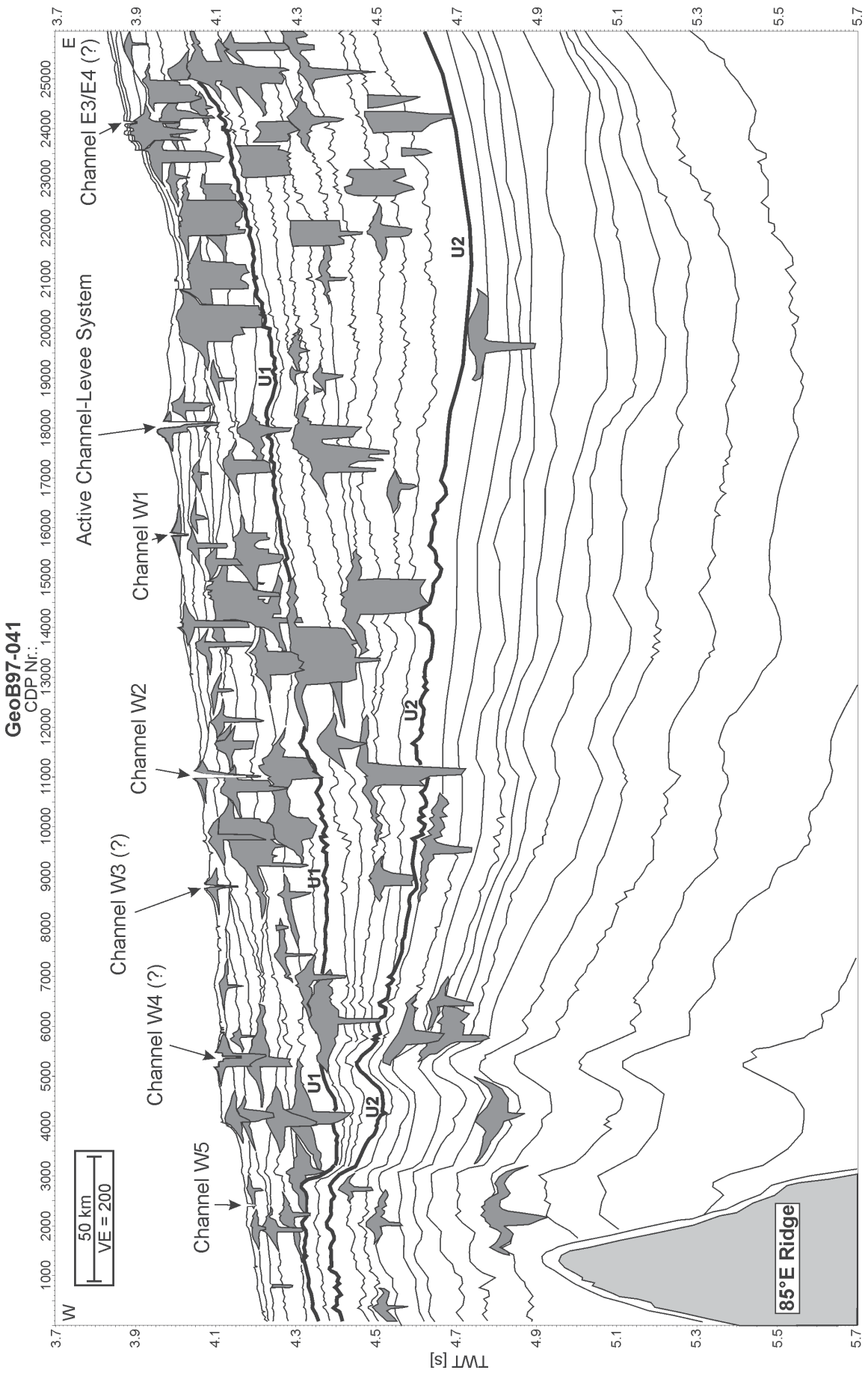

Figure 4.9: *Interpreted line drawing of Profile GeoB97-41 located at 14°N (see Figs. 4.1 and 4.2). Denotation of surface channels is adapted from Curray et al. (2003). Regional unconformities are highlighted by thick lines. Channel-levee systems are drawn in gray.*

km at the northeastern end. The water depth decreases from southwest to northeast, namely from 2720 m to 2275 m.

4.5.4.1 Surface channels

At the surface of the sediment column of Profile GeoB97-059/069 we found only two channel-levee system with open channels (Figs. 4.10 and 4.11). The westernmost of these systems is located at CDP 3600 and is characterized by a channel depth of 70 m and a maximum levee thickness of 65 m. The maximum incision depth of these systems reaches 90 m. The other open system is centered around CDP 5600 and shows a channel depth of 40 m. Its levees reveal a thickness of 38 m, the incision depth is 73 m.

Besides these two channel-levee systems, some other systems occur directly beneath the sea floor. Although these systems are completely draped, their structures remain visible in surface morphology. Since Curray et al. (2003) had shown that channels, which were rapidly refilled on the Upper Fan and the upper Middle Fan, are still open at the Lower Fan, we describe these systems as surface channel-levee systems. The westernmost of these systems is located at CDP 500. The levee thickness of this system is 53 m, the incision depth reaches 71 m. East of both open channels at CDP 8700, we found a system characterized by a levee thickness of 97 m and an incision depth of 38 m. The next channel-levee system to the east occurs at CDP 9800. The levee thickness of this system reaches 104 m, the incision depth is identified as 90 m. At CDP 11500 the next system is identified. Here we measured 67 m as levee thickness and 98 m as incision depth. The easternmost system is located at CDP 14500. A levee thickness of 115 m and an incision depth of 101 m characterize this system.

4.5.4.2 Buried channel-levee systems

As in the above-described three southern profiles, we identified numerous buried channel-levee systems on Profile GeoB97-059/069. The volumes of these systems appear larger than on the southern profiles. As a result, the fraction of the sediment column, which is built up by channel-levee systems, is larger on Profile GeoB97-059/069 than on the three other profiles located farther south. The huge lateral spreading of several levees leads to levee units extending over long distances. At some locations, it is not possible to attribute these units to distinct levees and channels, especially in the broad levee unit found in depths between 3.9 and 4.3 s TWT (Fig. 4.11). This unit, buried 800 m below the seafloor at the eastern end of the profile, is the deepest system we can identify unequivocally. The signal penetration here is not sufficient for interpretation of deeper parts, but from the visible incoherent reflections it seems likely that channel-levee systems exist also in deeper parts. In total, we identified 58 channel-levee systems with a large variability of their sizes (Table 4.1). The minimum levee thickness is 11 m, the maximum levee thickness reaches 173 m, averaging to 49 m. For the incision depth, we found a minimum of 10 m and a maximum of 155 m. The average incision depth of all systems is calculated to be 70 m.

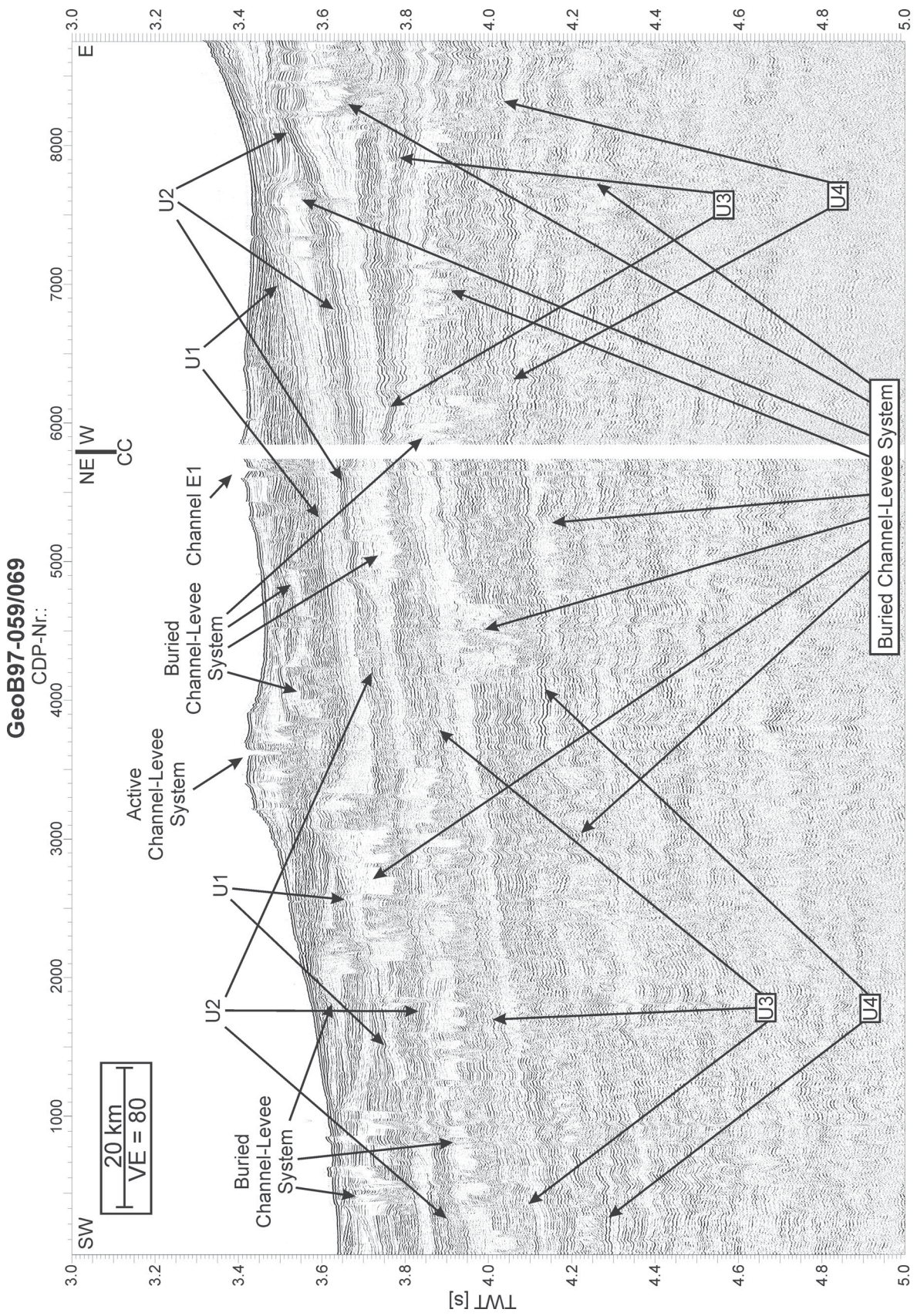

Figure 4.10 a: *GI-Gun data of the western part of Profile GeoB97-059/069 located at the Middle Fan (Figs. 4.1 and 4.2). Please note the course change near CDP Nr. 5800. Four regional unconformities separate the channel-levee systems in distinct channel-levee complexes, and levees are significantly thicker than on Lower Fan, both discussed in text. Surface channel naming follows the terminology of Curray et al. (2003).*

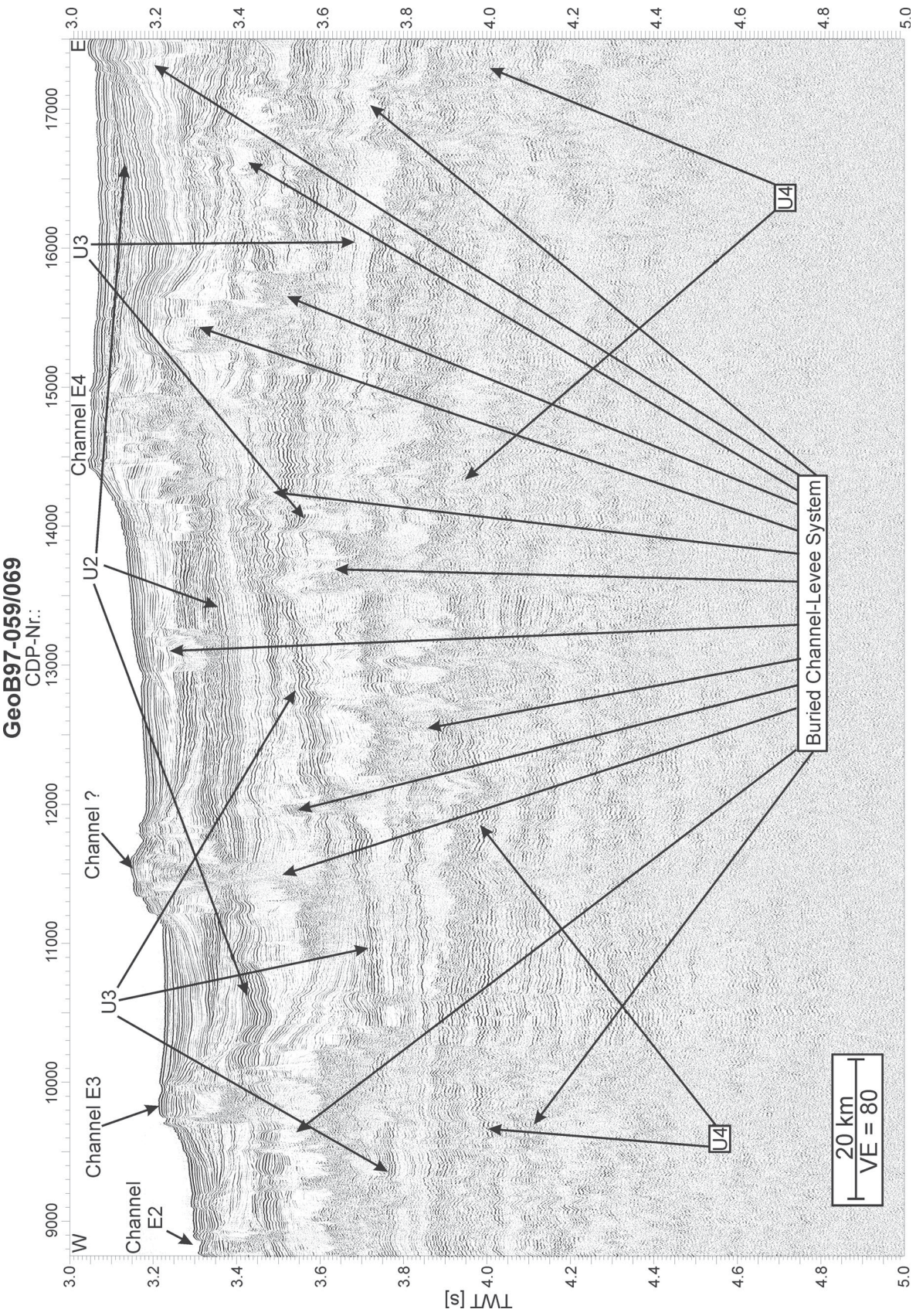

Figure 4.10 b: *GI-Gun data of the eastern part of Profile GeoB97-059/069 located at the Middle Fan (Figs. 4.1 and 4.2). Four regional unconformities separate the channel-levee systems in distinct channel-levee complexes, and levees are significantly thicker than on Lower Fan, both discussed in text. Surface channel naming follows the terminology of Curray et al. (2003).*

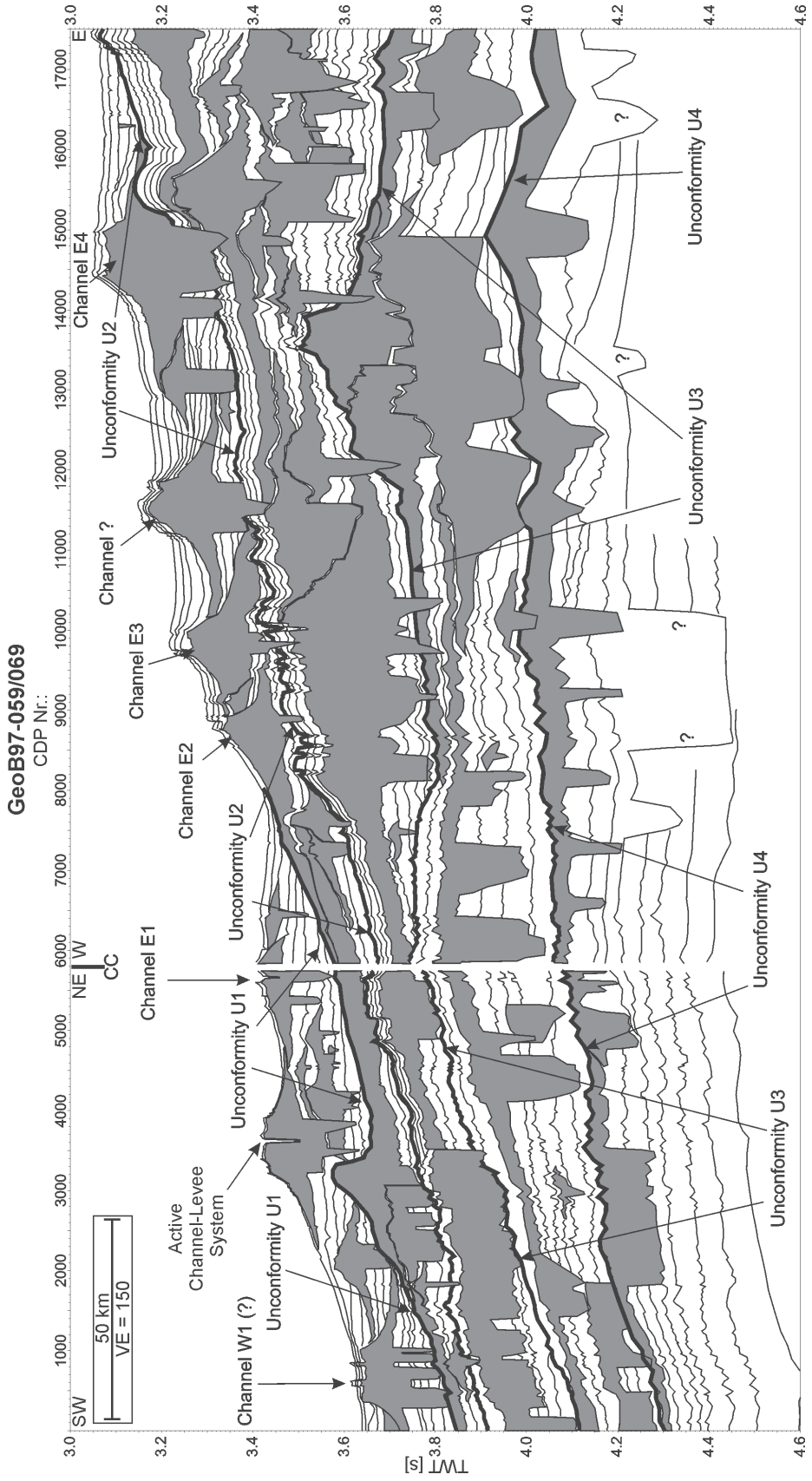

Figure 4.11: *Interpreted line drawing of Profile GeoB97-059/069 (see Figs. 4.1 and 4.2). The huge channel-levee systems are drawn in gray. The uppermost channel-levee complex covers only the western part of the profile suggesting canyon switching on the shelf. Other unconformities represent the top of extending turbidites not deposited by channelized currents. For discussion, see text. Identification of surface near channel-levee systems follows Curray et al. (2003).*

4.5.4.3 Stratigraphy

Based on our seismic data, we divide the profile into 5 stratigraphic units separated by four unconformities (Fig. 4.11). The uppermost unconformity (U1) appears only in the western part of the profile between its western end and CDP 8000, where the unconformity reaches the surface. The unconformity is represented by the top of neighboring levee systems and characterized by onlapping of all reflectors of the overlying, uppermost unit. This unit above U1 consists of nearly horizontal reflectors and intercalated channel-levee systems with horizontal bases. The second unconformity (U2) is within most of the profile the top of a package of parallel reflectors thinning slightly from east to west and terminating at CDP 3000. This package drapes several channel-levee systems. Again, the unconformity is characterized by the onlap of the overlying unit, which is mainly built of a sequence of channel-levee systems and reflectors filling the lows between the systems. The third unconformity (U3) runs nearly parallel to U2 in the western part of the profile and diverges from U2 in the eastern part. Here U3 is represented by the tops of channel-levee systems, whereas in the western part it is represented by a reflector. The deepest unconformity we found is the top of a broad levee structure with different channels at its base spreading over the whole profile.

4.5.5 Mapping of the surface channels

To compare the surface channels identified in our data with the surface channels described by Curray et al (2003) we compile both data sets in one map (Fig. 4.12).

On Profile GeoB97-0202/027 we found five surface channels which is the same number as mapped by Curray et al. (2003) in this area and our compilation shows a sufficient fit in their positions. On Profile GeoB97-028 we identified seven channels, whereas only five channels cross the profile on the map of Curray et al. (2003). The three small channels between CDP 500 and 2500 match nearly the position of Channel W4, the two channels between CDP 14000 and 16500 agree with the Channel W1 and the active channel as the easternmost channel (around CDP 24000) do with Channel E4. The channel found at CDP 8000 is mapped in a small distance west of the position of Channel W2. Naming of the channels of this profile will be discussed later.

The seven channels found in Profile GeoB97-041 are in contrast to the six channels mapped by Curray et al. (2003) at this location. The channels at CDP 2400 and 11000 correlate with Channels W5 and W2, respectively. In contrast, both channels between W5 and W2 do not match with the single Channel W3 mapped by Curray et al. (2003) between W5 and W2. Farther east, the two channels identified near CDP 16000 and 18000 correspond to Channel W1 and the active channel. But the easternmost channel on this profile is located just between Channels E3 and E4 and cannot clearly be associated with one of them.

At our northernmost profile (GeoB97-059/069), seven channels recognized at or just below the surface contrast the four channels localized by Curray et al. (2003) there. The channel at CDP 3500 matches with the active channel, the channel at CDP 9800 corre-

lates to Channel E3 and the channel at CDP 14500 to E4. Whereas the channels between the active channel and Channel E3 may correspond to Channels E1 and E2, the channels at CDP 500 and CDP 11500 match none of the channels mapped by Curray et al. (2003).

4.5.6 Downfan variations of channel-levee system parameters

In Table 4.1 we compiled all determined channel-levee parameters of the four seismic profiles described above. The number of the channel-levee systems decreases with shelf distance, explicitly from 18.7 systems/100 km profile length at an average shelf distance of 365 km to 6.6 systems/100 km profile length at a shelf distance of 1330 km. In addition, the depth of the deepest system decreases from north to south, namely from at least 800 m below surface to 450 m below surface. For the vertical dimensions of the levees we can state that the minimum levee thicknesses are on the same order in all profiles, but the maximum levee thickness found in Profile GeoB97-059/069 (173 m) is nearly three times larger than in the other three profiles. Consequently, the average of the levee thickness is highest with 49 m on this northernmost profile, whereas the thickness on the three southern profiles reaches only 50% of this value. The deepest erosion depth of 195 m occurs in Profile GeoB97-041, the maximum erosion depths of the other profiles are nearly equal with 152 m, 153 m and 155 m. The minima of this parameter vary between 10 and 16 m and reveal no generally north-south trend, too. Calculation of the average of the erosion depth gives the largest value (78m) for the southernmost Profile GeoB97-020/027, while this parameter reaches in the three northern profiles only 84% and 88% of this value. Accordingly, we can summarize that only

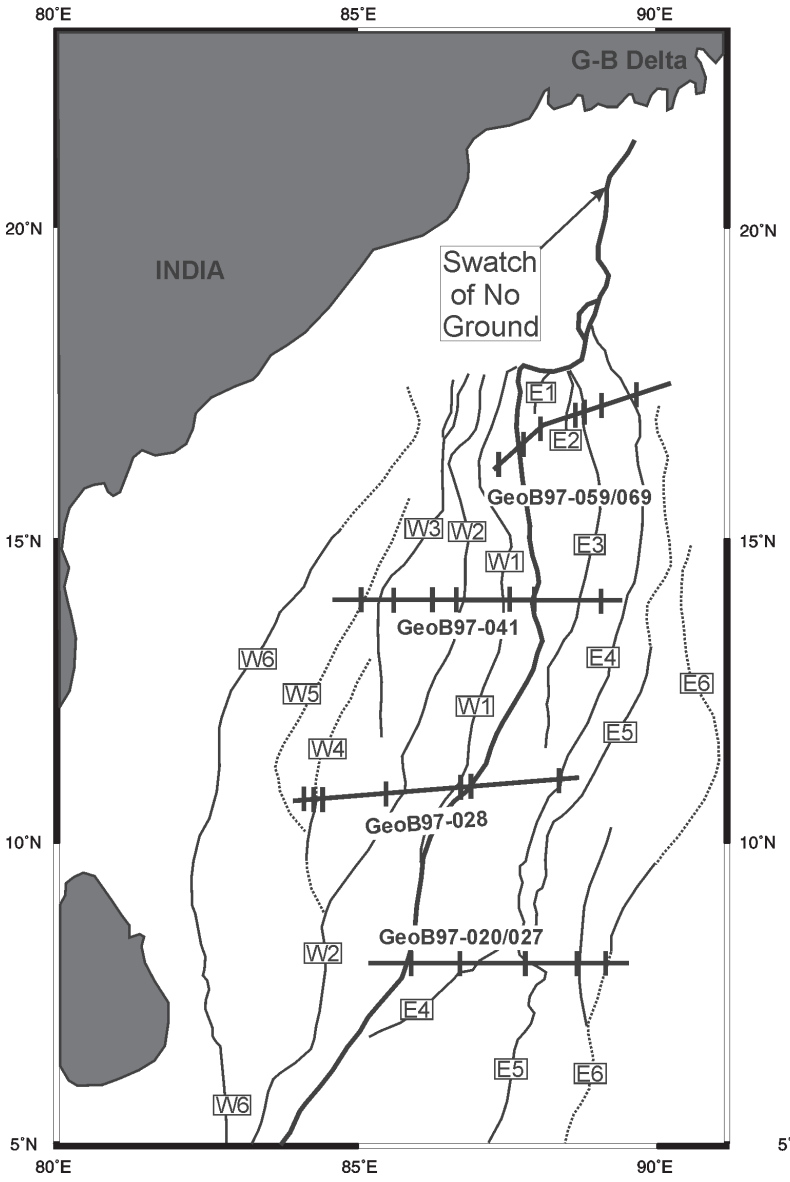

Figure 4.12: *Compilation of surface channels mapped by Curray et al. (2003) and surface channel crossing points at profiles of this study. Whereas on Profile GeoB97-020/027 all channel positions match sufficiently, discrepancies appear on other profiles as discussed in detail in Chapter 4.6.1.*

	GeoB97-020/027	GeoB97-028	GeoB97-041	GeoB97-059/069
Shelf distance [km]	1330	1000	670	365
Length [km]	470	512	515	309 *
Systems [#]	31	64	84	58
Systems/Length [#/100 km]	6.6	12.5	16.3	18.7
Depth of deepest system [m]	450	600	640	>800
Max. Levee Height [m]	48	49	60	173
Min. Levee Height [m]	16	10	9	11
Average Levee Height [m]	27	24	27	49
Max. Erosion depth [m]	152	153	195	155
Min. Erosion Depth [m]	16	9	12	10
Average Erosion Depth [m]	78	67	67	70

* projected on a west-east profile.

Table 4.1: *Parameter of channel-levee systems identified in the seismic profiles.*

the average incision depth shows a north-south increase, but the number of systems, depth of deepest system and average levee height decrease from north to south.

4.6. Discussion

4.6.1 Identification and sequence of surface channels

As mentioned above in the data description, compiling of surface channels identified in our data and surface channels mapped by Curray et al (2003) shows different degrees of congruence, and in particular in our data more surface channels can be identified. This is probably due to the uncertainty of comparing maps and due to the fact that Curray et al. (2003) mapped only distinct channels which could be correlated between their lines. Additionally, their work based mainly on analog echo sounder data collected before 1986 and navigation data from older cruises may have had not the adequate accuracy (Curray et al., 2003) as GPS navigation used during SO 125 cruise. However, we will not discuss all channel positions in details, but give emphasis to the active channel, Channel E4 and the temporal succession of channels.

The active channel can be recognized in all profiles, since it settles on top of all channel-levee systems on the seafloor (Figs. 4.4, 4.7, 4.9 and 4.11). In Profiles GeoB97-020/027, GeoB97-041 and GeoB97-059/069, the locations of the active channel correlate with the positions in the map of Curray et al. (2003) (Fig. 4.12), but in Profile GeoB97-028 a discrepancy arises (Figs. 4.7 and 4.11). In particular, tracing of the bases of the channel-levee systems reveals that the channel-levee system at CDP 8000 is placed on top of all other channel-levee systems (Fig. 4.7). At the locations of Channel W1 and the active channel (which merge just south of 10°N) after Curray et al. (2003), we found a large meandering channel crossing two times the profile and a small channel settling on its eastern levee between CDP 14500 and 16000. Both channels are traced over some profiles collected during SO 125 Cruise in this area revealing that the small channel does not meander and that its depth decreases significantly, suggesting that this small channel terminates near 11° N and is not connected to the active channel farther south (Spieß et

al., 1998). It is also improbable that the active channel terminates near 11°N, since Holocene turbidites are found on the Lower Fan near the active channel (Weber et al., 2003). Comparing the morphology to the linedrawings of Curray et al. (2003, their Fig. 29), the large meandering channel is interpreted to be indeed Channel W1. This leads us to the conclusion that at 11°N the active channel is located nearly 140 km farther west than mapped by Curray et al. (2003).

The only other surface channel, which we can trace from our northernmost profile to southernmost profile, is Channel E4. Based on the mapped locations, Channel E4 is recognized in Profiles GeoB97-059/069, GeoB97-028 and GeoB97-020/027 (Figs. 4.4, 4.9, 4.11 and 4.12). Additionally, size and shape of this channel correspond well with the linedrawing of Channel E4 published by Curray et al. (2003, their Fig. 25). In Profile GeoB97-041, the easternmost surface channel in our data is found directly in the middle between Channels E3 and E4 of Curray et al. (2003). Therefore it may be possible, that this channel corresponds to Channel E3 and that Channel E4 is located east of Profile GeoB97-041. However, comparison of location and morphology of Channel E4 in Profile GeoB97-028 with the channel just north it, which Weber et al. (2003) interpreted as abandoned since 300,000 yrs, reveals a strong similarity. Consequently, we interpret Channel E4 as abandoned since 300,000 yrs. In contrast, Curray et al. (2003) assumed a maximum age of 125,000 yrs for Channel E4. Nevertheless, this assumption bases not on dating of sediments, but (1) on the interpretation of Channel E4 as the oldest channel of the most recent Subfan D and (2) that the base of this subfan represents the last time of high sea-level (Curray et al., 2003). This discrepancy in the age of Channel E4 suggests that the dating of Subfan D or the association of Channel E4 to Subfan D may be improved by combining available data as well as collecting new data to increase the seismic and bathymetric coverage.

From our seismic data we can establish a succession for the surface channels for each side, east and partly west of the active channel, but since none of our profiles covers all channels, it is difficult to present a succession for all observed surface channel-levee systems in the region. In Profile GeoB97-020/027 (Fig. 4.4), tracing of the bases of channel-levee systems leads to the interpretation, that Channel E6 is the oldest channel followed by Channel E5 and by Channel E4. Profile GeoB97-059/069 reveals a sequence from E2 through E3 to E4, E1 seems to be the latest active channel before the presently active channel (Fig. 4.11). For the western channels, a general eastward sequence is assumed from the Profile GeoB97-041, even if it is not possible to assign each of these channels (Fig. 4.9). Unfortunately, channels E6 and E5 as well as E2 and E3 are not imaged by the same profile and therefore a direct relationship is not visible. However, in Profile GeoB97-059/069 the Unconformity U2 rises from west to east and reaches nearly the surface at the eastern end. This may suggest that the farther east located Channels E5 and E6 are associated to a deeper, older complex than the Channels E2, E3 and E4 (Fig. 4.11). On the other hand, it is not possible to relate directly the western channels to

the eastern channels, but it seems that the western channels are located in a younger complex than E2, E3 and E4 (Fig. 4.11). Moreover, the draping of the eastern channels in contrast to the undraped western channels in Profile GeoB97-041 (Fig. 4.9) and westward downdipping of Unconformity U1 in GeoB97-028 (Fig. 4.7) also support the assumption that the western channels are younger than Channels E3 and E4. Finally, Channel E1 settling directly beneath the levee of the active system is interpreted to be the youngest abandoned channel (Fig. 4.11). As a result, we propose a sequence of surface channels starting with E6 and followed by E5, E2, E3 and E4. After Channel E4, the western channels were active, probably with an eastward succession from W5 to W1, and after that, Channel E1 was the last active channel before the present active system. This is in contrast to the results of Curray et al. (2003), who found a westward sequence of channels E4 to E3 to E2 to E1 followed by an eastward sequence of W3 to W2 to W1 finally to the now active channel.

To sum up, we found different results as Curray et al. (2003) concerning the location of the active channel at 11°N, the age of channel E4 and the sequence of the surface channels. This is probably the result of different seismic systems and resolutions as well as navigation systems used, but generally there is first a lack of dating of the channel-levee systems and second a lack of long range side-scan sonar data or multibeam data covering large areas to image the surface channels over the whole fan as it was done on the Amazon Fan or the Congo Fan (Babonneau et al., 2002; Curray et al., 2003; Damuth et al., 1988; Flood et al., 1991; Pirmez and Flood, 1995).

4.6.2 Succession of channel-levee complexes on the upper Middle Fan

As described in Chapter 4.5.4, we identified four seismic units on the upper Middle Fan separated by regional unconformities (Fig. 4.11). Following the terminology used by descriptions of the Amazon Fan, we call these units consisting of several channel-levee systems „channel-levee complexes“ (Flood et al., 1991; Lopez, 2001; Pirmez and Flood, 1995). Generally, channel-levee complexes grow on submarine fans during glacial sea-level fall and lowstands, when shelf areas fell dry and rivers can directly deliver their sediment load to the fan (Flood et al., 1991; Lopez, 2001; Weimer, 1991). This has been shown for the quaternary Amazon Fan, where the channel-levee complexes were built during isotopic stages 2, 3, 4, 6 and 8 (Flood and Piper, 1997; Lopez, 2001). During interglacial sea level rises and highstands as e.g. Holocene, only hemipelagic or pelagic sediments were deposited and the fan was inactive (Flood and Piper, 1997; Lopez, 2001). Partly, the channel-levee complexes on Amazon Fan are further separated by mass-flow deposits (Flood and Piper, 1997; Lopez, 2001). However, the Bengal Fan has been revealed as active during the Holocene sea-level rise and highstand at least along the presently active channel-levee system (Weber et al., 1997; Weber et al., 2003).

In our seismic data from the upper Middle Bengal Fan, separation of the channel-levee complexes is associated with unconformities, but without evidence for mass-flow deposits (Figs. 4.10 and 4.11). Unconformity U4 represents the top of several directly

neighboring levees spreading over the whole Profile GeoB97-059/069. These levees cannot be distinguished suggesting that the different channels associated to the levees were active simultaneously or in rapid succession. Unconformity U3 is splitted in two parts: in the western part, the unconformity is interpreted to be the top of flat lying turbidites, whereas in the eastern part the unconformity corresponds to the top of levees. Unconformity 2 is the top of a package of parallel reflectors. Because this package thins out towards the west and finally terminates, we interpret this package as turbidites, which were deposited by unchannelized turbiditic currents originating from sources in the east, probably the Indo-Burman Ranges. Therefore, this unconformity may represent not necessarily an inactivity of the fan, but instead a phase of intensified generation of unchannelized turbiditic currents at the eastern edge of the Bengal Fan. The drape on top of the eastern channels E2, E3 and E4 is also restricted to the eastern part of the profile and therefore interpreted as turbidites having their source in the East as well. On Profile GeoB97-041, this drape is also found above the easternmost channel (Figs. 4.8c and 4.9). In contrast to the other unconformities, Unconformity U1 terminates within Profile GeoB97-059/069, i.e. U1 reaches the surface in the middle of the profile (Fig. 4.11). In consequence, the eastern Channels E2, E3 and E4 belong to a different channel-levee complex than the active channel and Channel E1. The westward shifting between the last two complexes may be the result of a canyon shifting as suggested by Curray et al. (Curray et al., 2003), which was also described by Flood and Piper (1997) for the Amazon Fan.

Since there is no deep drilling on the Upper Fan and upper Middle Fan, we have no possibility to date the different channel-levee complexes yet. The only age information available reveals that the active channel started at 12,800 yr BP and that Channel E4 was active before 300,000 yr BP (Weber et al., 1997; Weber et al., 2003). Channel E4 is located at the top of an eastward sequence of at least seven individual channel-levee systems. This may suggest that this sequence has developed during the interglacial highstand of isotopic stage 9 and that the turbidites basing this complex were deposited during the rapid sea-level rise at the transition from isotopic stage 9 to 10. Even this is speculative, but it demonstrates that the simple association of channel-levee complexes to glacial lowstands is not sufficient to completely explain the architecture of the Bengal Fan.

Our interpretations of channel-levee complexes on the upper Middle Fan are in contrast to the results presented by Curray et al. (2003). This contrast appears first in the association of surface channels to different channel-levee complexes as mentioned above, and second in the distribution of the channel-levee complexes (or subfans as named by Curray et al. (2003)). The differences may be again the result of the different seismic systems and resolutions used. However, dated as active before 300,000 yrs BP, Channel E4 would be a part to Subfan C of Curray et al. (2003), which is believed as active between 465,000 yr BP and 125,000 yr BP. This interpretation supports generally the assumption, that channel-levee complexes on the Bengal Fan were not only active during one glacial lowstand period. But finally only sampling and dating of sediments of the differ-

ent channel-levee complexes and their separating unconformities can provide an adequate stratigraphy as published for the Amazon Fan.

4.6.3 Downfan change of turbidity currents

As mentioned in Chapter 4.5.6, the average of the maximum levee thickness decreases significantly downfan, whereas the average of the channel incision depth increases slightly downfan (Table 4.1). Moreover, even if we cannot measure the horizontal extent of the buried levees exactly since we do not know, if the profiles crossing the channels perpendicular, it is evident that the levees on the upper Middle Fan are characterized by a significantly larger extent than on the Lower Fan (Figs. 4.4, 4.7, 4.9 and 4.11). Piston cores taken from the surface channel-levee systems show an increase of grain size along the channel from Upper Fan to Lower Fan and an increase of grain size across the channel levee system with fine grained sediment in the levees and coarse grained sediments in the channel (Weber et al., 2003). Similar results of downfan grain size distribution are found in channel levee systems on Amazon Fan during ODP Leg 155 (Hiscott et al., 1997). From Amazon Fan it is also reported that grain size within the levees decreases with increasing levee thickness (Hiscott et al., 1997). This is interpreted by building levees from mixed-load turbidity currents with coarse-grained material at the bottom and fine-grained material at the top. If the levees become thicker, only fine-grained material can be deposited by overspill. Then the coarse-grained material remains upfan completely channelized and is deposited further downfan, where levees are flatter (Hiscott et al., 1997). The same mechanism is probably responsible for the observed changes of vertical dimensions of the channel-levee systems on the Bengal Fan. Mixed-load turbidity currents loose their fine-grained fraction by overspill on the Upper Fan and upper Middle Fan and build there thick and broad levees. The increasing erosional incision depth from north to south indicates that erosional power of turbidity currents increases downfan. Increasing erosional power may suggest downfan increase of turbidity currents velocities. In contrast, the channel gradient decreases downfan, which indicates that currents slow in velocity downfan (Curray et al. 2003). However, due to the loose of the fine-grained top, the coarse-grained fraction of the turbidity currents increases, and therefore the currents become denser downfan. This may lead to downfan increasing velocities, even though channel gradients decrease from Upper Fan to Lower Fan.

4.6.4 Sedimentation rates and onset of channel-levee systems at 8°N

As described in Chapter 4.5.1, sedimentation rates were calculated for Pleistocene, Pliocene and late Miocene (<10 Ma) based on tracing of the respective boundaries from DSDP Site 218 along Profile GeoB97-020/027 (Figs. 4.4 and 4.5). The estimated sedimentation rates vary in time and space. Particularly, we found for the late Miocene an accumulation rate of 8.7 cm/ky averaged over the complete profile, with a maximum of 10.6 cm/ky in the central basin and a minimum of 5.4 cm/ky above the Ninetyeast Ridge. The Pliocene is characterized by a sedimentation rate of 4.0 cm/ky on average, a maximum sedimentation rate of 6.5 cm/ky and a minimum sedimentation rate of 1.5 cm/ky. For

the Pleistocene, we reveal an average rate of 14.7 cm/ky, which increase to a maximum of 20.6 cm/ky in the central basin and decrease to a minimum of 4.3 cm/ky above the Ninetyeast Ridge.

Comparison with results of ODP Leg 116, located more than 1000 km south of Profile GeoB97-020/027, shows similar sedimentation rates for the late Miocene. During this period, sedimentation occurred with rates between 8.5 and 11 cm/ky at the three sites of ODP Leg 116 (Cochran, 1990). In the latest Miocene at 5.8-6.7 Ma, a decrease of sedimentation rates occurred at ODP Leg 116 leading to a value lower than 7 cm/ky for the Pliocene (Cochran, 1990; Stow et al., 1990). Therefore it seems that during Pliocene times sedimentation rate is similar or slightly higher at ODP Leg 116 than in the basin between 85° E Ridge and Ninetyeast-Ridge at 8° N. For the Pleistocene, an average sedimentation rate of 25 cm/ky is found at ODP Leg 116 for the last million years (Cochran, 1990). In particular, maximum rates of 35 cm/ky occurred in the late Pleistocene, whereas in the Holocene the sedimentation rate dropped down to 1.5-2.5 cm/ky (Stow et al., 1990). However, it is difficult to compare the Pleistocene sedimentation rates of ODP Leg 116 with our results, since a hiatus of 1 my is found in the early Pleistocene at ODP Leg 116 (Cochran, 1990; Stow et al., 1990), yet it is not reported, if such a hiatus also appeared at DSDP Site 218. It might be possible, that this hiatus was not detect at DSDP Site 218 due to the used spot coring method. However, the similar or slightly higher sedimentation rates at ODP Leg 116 suggest a highly efficient sediment transport to the southern Lower Fan. Beside the values of the sedimentation rates, also their variance between basin and ridges along Profile GeoB97-020/027 differs from Miocene to Pliocene and Pleistocene. Generally, the decrease of sedimentation above the 85°E Ridge and Ninetyeast Ridge is highest during Pliocene, middle during Pleistocene and lowest during Miocene (Figure 4.5).

Two hypotheses may explain the different sedimentation pattern in time and space: first, the observed pattern is the result of tectonics in the deposition area, or second, the result of changes of sediment supply, which in turn depends from tectonics in the source area, i.e. the Himalayas.

Considering the tectonics in the Bay of Bengal, it may be possible, that during Miocene the ridge elevations were lower than in Pliocene and Pleistocene suggesting that local or regional uplift of both ridges occurred since then. In general, the area of Profile GeoB97-020/027 is influenced by intraplate deformation of Indian Ocean lithosphere (Curray and Munasinghe, 1989; Gordon et al., 1998; Krishna et al., 2001a). This deformation is mainly associated with long-wavelength (100-300 km) folding of the basement and overlying sediments or reverse basement faulting of 5-20 km wide blocks (Krishna et al., 2001a). Since in most parts of the profile we do not image the basement and since the north-south compression of the lithosphere leads to east-west stretching folds, we are not able to detect such folding in our seismic data. For the ridges it is known that their formation at 8°N occurred between 85 Ma and 82 Ma and around 73 Ma for the Ninetyeast

Ridge and 85°E Ridge, respectively (Krishna, 2003; Krishna et al., 2001b). The Ninetyeast Ridge was affected by deformation activity in Miocene leading to fracturing and excessive subsidence between 1°N and 11°S (Krishna et al., 2001b). For the southern part of the 85°E Ridge, the so-called „buried-hills“, converging has been found at 4°N for the late Pliocene deformation event. Additionally, the Afanasy-Nikitin seamounts, representing the southern termination of the 85°E Ridge, converged in late Miocene and late Pleistocene. As a result of the convergence, uplift of the Afanasy-Nikitin seamounts occurred during late Miocene (Krishna, 2003; Krishna et al., 2001a). In summary, it seems not unlikely to us that the differences in decrease of sedimentation rate above the ridges during Miocene, Pliocene and Pleistocene may caused by local or regional uplift of both ridges at 8°N during Pliocene and Pleistocene, as a result of intraplate deformation of the Indian Ocean lithosphere.

Following the second hypothesis, the different sedimentation patterns may also be produced by a change of sediment supply. At ODP 116, the decrease of sedimentation rate in late Miocene is accompanied by a change in lithology from silty gray turbidites to muddy dark turbidites (Cochran, 1990; Stow et al., 1990). Cochran (1990) suggested that low sedimentation rates in Pliocene are caused by a high sea-level at this time, trapping the Himalayan material on the Bengal Shelf and Delta, which may be supported by increasing sedimentation rates in Pliocene found in troughs in the Bengal Basin (Alam et al., 2003). In contrast, Derry and France-Lanord (1996) concluded from clay mineralogy studies at ODP Leg 116 cores that the decrease of sedimentation rate during late Miocene and Pliocene is the result of decreased physical erosion in the Himalayas. This decreased erosion rate suggests in turn a reduction of tectonic uplift of the Himalayas during late Miocene and Pliocene (Derry and France-Lanord, 1996).

A further indication of a change in sediment supply in latest Miocene may be the fact that our seismic data suggests the onset of channel-levee systems at this time on Profile GeoB97-020/027 at 8°N (Fig. 4.4). This can be interpreted either that development of channel-levee systems on the Bengal Fan started in the latest Miocene or that channel-levee systems, which prograding downfan, reached 8°N first in latest Miocene. The larger number of systems in the northern profiles may support the second assumption. On the other hand, the pattern of surface channels is characterized by tributaries, i.e. the active channel re-occupied older channels (Curray et al., 2003), suggesting that the observed decrease of buried systems from north to south imaging a similar tributary pattern. Moreover, the active channel developed mainly between 12,000 yr BP and 9,700 yr BP (Weber et al., 1997), and even if the active channel re-occupied Channel W1 at 10°N (Fig. 4.2) as mapped by Curray et al. (2003), prograding of the active channel from 17°N to 10°N must have occurred during a few thousand years. Therefore it seems probable that the onset of channel-levee systems at 8°N marks indeed the onset of channel-levee system development itself in the Bengal Fan.

The suggested absence of channel-levee systems before the latest Miocene indicates in turn either the absence of a point source, i.e. a distinct canyon, or the inability of turbidity currents to build channel-levee systems. Beside the slope angle, mainly the grain-size controls the construction of levees by turbidity currents debouching from a canyon, and on low angle slopes, small grain sizes support the self-channelization of turbidity currents (Imran et al., 1998). Therefore, the onset of channel-levee systems in the latest Miocene may have been caused by a decrease of grain size of turbidity currents as was also observed in the sedimentary record at ODP Leg 116 (Cochran, 1990; Stow et al., 1990). But it is also possible that changes in the foreland led to erosion and stable existence of a canyon in latest Miocene. It is known that at this time the erosion regime in the Ganges-Brahmaputra basin changes from physical erosion to chemical weathering, accompanied by intensification of the Asian monsoon (Derry and France-Lanord, 1996). The change to chemical weathering suggests an increase of sediment residence time in the flood-plain foreland basin (Derry and France-Lanord, 1996), which may again indicate the evolution of a large river and delta system. In contrast, Alam et al. (2003) proposed that present basin configuration with the development of the Ganges-Brahmaputra Delta was first established during the later part of Pliocene. Nevertheless, it seems likely that the onset of widespread development of channel-levee systems in latest Miocene is caused by the creation of a canyon incised into the Bengal Shelf. Generally, it is surprising that the onset of channel-levee systems is accompanied by a decrease of sedimentation rate, which is in contrast to the Indus Fan, where increased sedimentation rates are coincident with the building of large channel-levee complexes (Clift and Gaedicke, 2002).

Summing up, the onset of channel-levee systems synchronous to changes of sedimentological parameters at ODP Leg 116 may indicate a significant change in sediment supply and transport regime from the Bengal Basin into the Bengal Fan. In turn, the change in sediment supply depends from tectonics in the source area of the Ganges-Brahmaputra river system. The change in supply and transport of sediments may result in a more basin-concentrated and slope-gradient-driven sedimentation since the latest Miocene, supporting the above-mentioned hypothesis that changes in sedimentation caused the more pronounced decrease of sedimentation rates above the ridges during Pliocene and Pleistocene times compared to the Miocene.

Considering all this, we can finally state that both, tectonics or a change in sediment supply, can be responsible for the different sedimentation patterns we observe for the late Miocene, Pliocene and Pleistocene. Finally, it may also be possible that both processes influenced synchronously the sedimentation on the Bengal Fan. A synchronism of the discussed tectonic events in the Bengal Fan and the changes of sediment character caused probably by tectonic events in the Himalayas may suggest consequently that uplift of ridges in the Bay of Bengal coincides with a reduced uplift of the Himalayas.

4.6.5 Unconformities in the Lower Fan

In the Lower Bengal Fan, we identified in all three profiles two regional unconformities extending over the whole profile (Figs. 4.4, 4.7 and 4.9). Additionally, we found in the southernmost Profile GeoB97-020/027 deep unconformities above both ridges, the 85°E Ridge and the Ninetyeast Ridge, whereas in Profile Geob97-041 only above the 85°E Ridge a deep unconformity is visible (Figs. 4.4 and 4.9). From comparison with seismic lines published by Moore et al. (1974) and Curray et al. (2003), we interpret the deep unconformity above the Ninetyeast Ridge as the Paleocene-Eocene hiatus, which separates pre-collision and post-collision sediments and therefore represents the base of the Bengal Fan itself (Curray et al., 2003). In contrast, the pre-collision sediments terminate generally at 10° N above the 85°E Ridge (Krishna, 2003). Seismic lines presented by Krishna (2003, their Fig. 7) image the basement of the 85°E Ridge in a depth 0.7 s TWT near 8°N. Moreover, the basement topography of the 85°E Ridge is highly undulating due to its origin as hot-spot trace built by separate volcanoes, and these basement highs are also free of pre-collision sediments (Gopala Rao et al., 1997; Krishna, 2003). These basement elevations are related to gravity lows due to overcompacted metasediments (more denser than volcanic rocks) adjacent to the ridge and flexure of the lithosphere (Krishna, 2003). Such a distinct gravity low, found in both satellite-derived and ship borne gravimetric data, is directly crossed by Profile GeoB97-041 at 14°N above the location of the 85°E Ridge (Krishna, 2003, their Fig. 6; Subrahmanyam et al., 2001, their Fig. 2). Therefore, we interpret the deep unconformities in the western parts of Profile GeoB97-020/027 and Profile GeoB97-041 as volcanic basement of the 85°E Ridge (Figs. 4.4 and 4.9).

On Profile GeoB97-020/027, the two shallow regional unconformities we found were dated at DSDP Site 218 to have Pliocene (4.8 Ma) and Pleistocene (0.64 Ma) age (Figs. 4.3 and 4.4). Hence, these unconformities correspond well in time with the Pliocene and Pleistocene unconformities found in the central Indian Ocean (Krishna et al., 2001a). Here, the unconformities are related to folding events in the oceanic lithosphere due to intraplate deformation at the diffuse plate boundary, but they are also correlated to changes in lithology at ODP Leg 116 sites (Cochran, 1990; Krishna et al., 2001a; Stow et al., 1990). In contrast, Profile GeoB97-020/027 is located outside of the folding areas mapped by Krishna et al. (2001a): they suggested that the Pliocene unconformity developed only south of 7°N, that the Pleistocene folding is concentrated near the equator and that north of the equator the deformation occurred quasi-continuous since the Pliocene. On the other hand, Profile GeoB97-020/027 is at least located within the area of the diffuse plate boundary (Gordon et al., 1998). However, beside the unconformities, we identified several faults in the sediments, mainly above the Ninetyeast-Ridge, but also above the 85°E Ridge. All these faults terminate within the Pleistocene, suggesting tectonic events during Pleistocene times. Since most of the faults terminate near the Pleistocene unconformity, it is likely that faulting coincided with deformation events in the Pleistocene as was also found in the central Indian Ocean (Krishna et al., 2001a). And finally, as discussed in detail in

Chapter 4.6.4, there is evidence for local or regional uplift of both the 85°E Ridge and the Ninetyeast Ridge, as a consequence of intraplate deformation at Profile GeoB97-020/027. Therefore we can conclude that the Pliocene and Pleistocene unconformities we found at 8°N are equivalent to the unconformities identified in the central Indian Ocean and, as it was done there, can be also related to tectonic events as well as changes in sediment character.

By comparing our seismic data with seismic data published by Moore et al. (1974) and Curray et al. (2003) from the vicinity of DSDP Site 218, the question arises why we do not image the late Miocene unconformity, which is found in their data. This unconformity is located at a depth of 0.45 s TWT (i.e. 360 m) at DSDP Site 218 (Moore et al., 1974). However, at this depth an unconformity does not appear in our seismic data (see marker in Fig. 4.3a). This is probably the result of the difference in the seismic systems, especially of the higher resolution of the seismic system used in our study. The Miocene unconformity found around ODP Leg 116 is interpreted by Cochran (1990) to correspond to the Miocene unconformity at DSDP Site 218. In contrast, Krishna et al. (2001a) stated that the Miocene unconformity is restricted to a region south of 1°S. Consequently, they suggested that the late Miocene unconformity found at DSDP Site 218 is the lateral equivalent of the Pliocene folding event in the central Indian Ocean and marks the onset of deformation at DSDP Site 218. Nevertheless, from our data we conclude that at 8°N only a Pleistocene unconformity and a Pliocene unconformity developed. If these unconformities mark deformation events, then the first deformation event at 8°N occurred in early Pliocene, and the Pleistocene deformation event is not restricted to areas south of the equator as suggested by Krishna et al. (2001a).

As described in Chapters 4.5.2 and 4.5.3, unconformities also appear in the northern profiles on the Lower Fan, GeoB97-028 and GeoB97-041 (Figs. 4.6, 4.7, 4.8 and 4.9). Unfortunately, no drill sites exist in these areas of the Bengal Fan, and we have no North-South profiles to correlate the unconformities in Profiles GeoB97-028 and GeoB97-041 with DSDP Site 218. Therefore, no age can be given for the unconformities on the northern Lower Fan, and we are not able link the unconformities identified in all three profiles on the Lower Fan by seismic data. But assuming that the onset of the channel-levee systems occurred in latest Miocene as in Profile GeoB97-020/027, both unconformities in both profiles were established in Pliocene and Pleistocene. However, again the question arises if the unconformities are the result of tectonics or changes in sedimentation.

In Profile GeoB97-028, up-domed reflectors above and east of the 85°E Ridge at CDP 11000 are visible, which become slightly flatter from the base of the profile up to Unconformity U2 (Fig. 4.7). Beneath U2, a local unconformity is found at 5.0-5.2 s TWT depth in the western part of the profile between CDP 1 and 4000. However, this unconformity does not continue above the eastern flank of the 85°E Ridge, where the reflectors converge in this depth, but are not onlapping. If a tectonic event (uplift) occurred, one would expect to find an unconformity on both sides of the ridge. Therefore, the local

unconformity west of the ridge is probably the result of an asymmetric sedimentation on the two sides of the ridge. The slight flattening of the up-domed reflectors upwards to U2 may be the result of a leveling by turbiditic sedimentation followed by a change of sedimentation associated with Unconformity U2. This change in sedimentation may represent either a phase of non-deposition, a change of the quality of the turbidity currents resulting in a depositional style preferably filling depressions/basins or a shifting of the sediment source, i.e. the feeding canyon. On the other hand, it is also possible that the reflection pattern is caused by a continuous uplift of the 85°E Ridge, which finally ended at Unconformity U2. In the eastern part of the profile above the western flank of the Ninetyeast Ridge, the reflectors below U2 are nearly parallel layered, suggesting also a tectonic cause for this unconformity. Therefore, if a tectonic movement caused U2, it must have occurred nearly simultaneously at both ridges, the 85°E Ridge and the Ninetyeast Ridge. Finally, it may also be possible that both tectonic events and change in sedimentation caused U2 simultaneously. In contrast to Unconformity U2, Unconformity U1 is not up-domed, but dips down slightly from east to west, diverging from the seafloor. Therefore, we interpret this unconformity as the result of a westward shifting of the source canyon.

More than 300 km farther north, the reflectors and especially the unconformities in Profile GeoB97-041 show a different character (Fig. 4.9). Here a dome appears east of the 85°E Ridge at CDP 5000, which is leveled between Unconformity U2 and U1. Directly above the ridge, a distinct step is found at CDP 3000 terminating at U1. Both the step and the dome appear steeper than the dome in Profile GeoB97-028, and leveling of the dome below U2 is less pronounced than in Profile GeoB97-028. Therefore, it seems possible that both unconformities in Profile GeoB97-041 are caused by tectonics, i.e., an uplift of the 85°E Ridge. Whereas U2 may mark the end of a more continuous uplift, U1 may represent an uplift event of the 85°E Ridge. But again, the wedge shape of the unit between U1 and U2 can also be the result of an eastward shift of the canyon feeding the channel-levee systems. Moreover, it is also conceivable that both occurred simultaneously, the end of an uplift of the 85°E Ridge, and a shifting of the canyon, and produced as a result the Unconformity U2. This explanation may also be used for Unconformity U1: a westward shift of the canyon could have caused the onlapping on U1 in the eastern part of the profile. Unfortunately, the eastern end of Profile GeoB97-041 is too far away from the Ninetyeast Ridge to identify a possible influence of tectonic processes there.

Comparing of Profile GeoB97-041 with the sequences H1 to H8 identified by Gopala Rao et al. (1997) between 14.64°N and 12.98°N reveals that the top of the sequence H2 fits in depth with U2 in our data. In contrast, there is no equivalent unconformity for U1 in the data of Gopala Rao (1997). Additionally, we could not identify a sequence boundary in the depth of the base of H2, but the base of H3 may correspond to the strong reflector in center of Profile GeoB-041 at 5.3 s TWT (Figs. 4.8b and 4.9). The top of H2 is interpreted as the late Pleistocene unconformity also found at ODP Leg 116 drill sites (Gopala Rao et al., 1997). Nevertheless, assuming only slightly higher sedimentation rates at Profile

GeoB97-041 compared to GeoB97-020/027, which is supported by similar sedimentation rates trends at DSDP Site 218 and ODP Leg 116 sites, we propose a Pliocene age for U2 and a Pleistocene age for U1 at Profile GeoB97-041.

To summarize, most unconformities found in all three profiles GeoB97-020/027, GeoB97-028 and GeoB97-041 on the Lower Fan show at least evidence for tectonic events at 8°N, 11°N and 14° N, although Profiles GeoB97-028 and GeoB97-041 are not located within the previously identified area of intraplate deformation (Gordon et al., 1998; Krishna et al., 2001a). Unconformities at 8°N have Pliocene and Pleistocene ages and are interpreted to be equivalent to unconformities identified in the central Indian Ocean, which are associated with deformation events of the lithosphere there. Unconformities at 11°N and 14°N cannot be dated exactly, but a Pliocene and Pleistocene age is proposed for unconformities at 14°N, too. However, due to the lack of North-South profiles it is unclear, if unconformities found in the three profiles on the Lower Fan are connected, and, if tectonic events were responsible, whether they were local or regional. On the other hand, it cannot be excluded that changes in sediment supply or canyon switching caused unconformities or contributed to unconformities. In other words, tectonic events in the Bay of Bengal and changes of sediment supply may have occurred simultaneously. Since sediment supply is mainly controlled by erosion of the Himalayas, which essentially depends on its uplift rates, a simultaneity would indicate a link between tectonic events in the crust underlying the Bay of Bengal and in the Himalayas, or, a link between tectonic events in the source and sink areas of Bengal Fan turbidites. This interpretation is supported by Krishna et al. (2001a), who proposed also a link between deformation events in the Indian Ocean crust, uplift in the sediment source area and sediment supply. A possible mechanism for such link could be a lock of the subduction zone, which may lead to both a decreased uplift and an increased compressional stress in the Indian Plate, which finally results in deformation events.

4.7 Conclusions

From analysis and interpretation of four long high-resolution seismic profiles located on the Lower Bengal Fan (at 8°N, 11°N, 14°N) and on the Middle Bengal Fan around 17°N (Figs. 4.1 and 4.2) we conclude the following:

1) Several surface and numerous buried channel-levee systems were identified in all profiles. All systems are characterized by erosional incisions into the underlying sediments.
2) A significant downfan decrease of the average levee thickness and a slight downfan increase of the average erosion depth are observed (Table 4.1) suggesting that mix-load turbidity currents loose their fine fraction on the Upper Fan and Middle Fan building there thick levees. The resulting changes of the flows seem to cause an increasing erosional capability of the currents during their downfan travel.
3) The high resolution of our data lead to a more precise identification of architectural elements, which seems to require some reinterpretation of results of Curray et al. (2003)

concerning the sequence of surface channels as well as the location of the active channel at 11° N (Figs. 4.7 and 4.12). However, long-range surface mapping and more detailed high-resolution seismic is needed to establish a complete pattern for the surface channels.

4) On the upper Middle Fan, four channel-levee complexes separated by regional unconformities were identified (Profile GeoB97-059/069, Fig. 4.11). The unconformities are caused by switching of the feeding canyon and by phases of generation of non-channelized turbidity currents from the shelf edge. Since the youngest channel of one complex was active before the end of isotopic stage 9 and the active channel was fed by turbidity currents during Holocene sea-level rise and highstand (Weber et al., 1997; Weber et al., 2003), we interpret the Bengal Fan as active even during sea-level rises and highstands. This interpretation is supported by the absence of hemipelagic drapes and mass-flow deposits between the channel-levee complexes.
5) On Profile GeoB97-020/027 (8° N) across DSDP Site 218, we found a varying sedimentation pattern in time and space (Fig. 4.5). Generally, sedimentation rates are highest in Pleistocene, lowest in Pliocene and moderate in late Miocene. A decrease of sedimentation above the 85°E Ridge and the Ninetyeast Ridge is observed, but rates vary during Pleistocene, Pliocene and Miocene: the decrease above ridges is highest during Pliocene, moderate during Pleistocene and lowest during Miocene.
6) The onset of channel-levee systems at 8°N occurred in latest Miocene simultaneously to a change of lithology at ODP Leg 116, indicating a significant modification of sediment supply and transport (Fig. 4.4). This may be caused by (1) a change of the erosional regime in the drainage area of the Ganges-Brahmaputra Rivers due to tectonic and/or climatic changes, or (2) the first establishment of a canyon incised into the Bengal Shelf.
7) Two regional unconformities were identified on Profile GeoB97-020/027 and dated at DSDP Site 218 to have Pleistocene and Pliocene age (Fig. 4.4). These unconformities are interpreted to be equivalent to unconformities found in the central Indian Ocean, which are related to deformation events of the lithosphere as well changes in sediment character (Cochran, 1990; Krishna et al., 2001a; Stow et al., 1990). Faults terminating within Pleistocene sediments also suggest tectonic events at least in Pleistocene. In contrast to older data from the vicinity of DSDP Site 218 (Curray et al., 2003; Curray and Moore, 1971; Moore et al., 1974) and to results from the central Indian Ocean around ODP Leg 116 (Krishna et al., 2001a; Stow et al., 1990), a Miocene unconformity does not appear in our seismic data at 8°N.
8) At the Lower Fan, two regional unconformities were detected in Profiles GeoB97-028 (11°N) and GeoB97-041 (14°N) (Figs. 4.7 and 4.9). We are not able to link and date exactly these unconformities, but we believe Pliocene and Pleistocene ages for the unconformities at 14°N. Tectonics, changes in sediment supply, or shifting of the canyon supplying the turbidity currents, or a coincidence of all these factors, may have

caused the unconformities. However, it is unclear, if tectonic events are local or regional and related to similar events farther south.

9) The varying sedimentation in time and space observed at 8°N as well as unconformities identified at 8°N, 11° and 14° are interpreted as a result of tectonic events (uplift of the ridges) in the Bengal Fan or as changes in sediment supply and character, which in turn depend mainly on tectonics in the source areas of the rivers feeding the Bengal Fan. However, it is reasonable to think that tectonic events in the Bengal Fan and changes in sediments occurred simultaneously and caused together the sedimentation pattern found on Lower Bengal Fan. Such simultaneity was also observed at ODP Leg 116 for Pleistocene and Pliocene unconformities (Krishna et al., 2001a). All observations suggest a link between tectonic events in the source and sinks areas of Bengal Fan turbidites.

4.8. Acknowledgements

We thank the captains and crews as well as all seismic watch-keepers of R/V Sonne cruise 125 for their support. Lars Zühlsdorff provided the software GeoApp for geometry setting. This work was funded by DFG, Grant SP296/14, and BMBF, Grant 03G0125A.

Chapter 5: Summary and perspectives

The Bengal Fan has developed as a direct result of the plate tectonic movement of India and its collision with Asia, resulting in the orogeny of the Himalayas and the uplift of the Tibetan Plateau. Erosion of the Himalayas since Eocene times had formed the largest submarine fan on Earth today. Accordingly, the Bengal Fan is well suited to study the erosional history of the Himalayas, which is the result of a close interaction of global and regional climate and tectonic processes. Additionally, its extraordinary dimensions make the Bengal Fan an excellent target to analyze architecture and depositional processes on submarine fans in general. Especially the evolution and structure of large channel-levee systems as main architectural elements of submarine fans are of high interest due to their possible potential as hydrocarbon reservoirs.

During three cruises with the German research vessel R/V Sonne in the Bay of Bengal, high-resolution seismic data, sediment echosounder Parasound data and bathymetric swathsounder Hydrosweep data were collected to image the architecture and morphology of several study areas located on the Middle and Lower Bengal Fan. This work focuses first on a study area located around the active channel-levee system on the Middle Bengal Fan where a densely spaced grid of Parasound and Hydrosweep data was collected together with several seismic lines. From previous geophysical and geological studies it was known that this system was active during the Holocene and levees mainly grew between 12,800 and 9,700 yr BP (Hübscher et al., 1997; Weber et al., 1997). The second focus of this work is the analysis of four up to 500 km long west-east seismic profiles placed at 8°N, 11°N, 14°N on the LowerFan and around 17°N on the Middle Fan.

The collected data allow for the first time to image in very high-resolution the structure and morphology of the active channel-levee system on the Middle Bengal Fan. Additionally, the architecture of buried systems, the stacking pattern of the individual systems as well as distinct complexes of channel-levee systems so far not reported have been revealed from high-resolution seismic data. New depositional models describing the initiation and development of the active and buried systems of the Middle Bengal Fan have been developed. Furthermore, a new seismic stratigraphy based on high-resolution multichannel seismic data, which were previously not collected in the Bay of Bengal, has been established for the Middle and Lower Bengal Fan.

In the main study area around 16°30´N in 2600 m water depth, located nearly 400 km south of the shelf edge, a combined analysis of Parasound and Hydrosweep data imaging the active channel-levee system was carried out. The channel is here characterized by highly variable sinuosities, and an exceptionally low channel slope compared to other large mud-rich submarine fans. The channel-levee system can be subdivided into inner and outer zones of significantly different depositional architecture.

The inner zone shows a prominent vertical separation. Based on a single Parasound line, this separation was previously interpreted as a successively constriction of a wide channel (Hübscher et al., 1997). However, the combined analysis of Parasound and Hydro-

sweep data revealed, that this separation represents an inner zone consisting of the active channel and numerous cut-off loops. The outer zone represents the undisturbed levees, which are characterized by a complex vertical and lateral pattern of wedge-shaped and parallel-layered sedimentary units, not previously described from other channel-levee systems. Wedge shaped units of different dimensions are found at the outer bends of the active channel and of cut-off loops deposited by overspilling from mainly channelized turbidity currents at sharp bends. Parallel units are caused by huge turbidity currents significantly exceeding the cross-section of the channel and spreading their sediment load over wide areas.

Within the study area, more than 20 cut-off loops were identified over a channel length of 90 km. Therefore, channel avulsion within the active channel-levee system is a frequent process. In particular, channel avulsions seem to have occurred on average every 750 years in the southern part of the study area. This repetitious process of loop growing and levee breaching is caused by erosion through turbidity currents in highly sinuous channels. The high number of channel avulsions and cut-off loops is in contrast to most other large mud-rich submarine fans and process models of channel-levee systems. By comparing the morphological parameter with other submarine fans, the only remarkable difference seems to be the exceptionally low channel slope gradient. Since a complex interaction between channel slopes and flow parameters of turbidity currents controls the channel planform, the combination of the low slope gradient and character of turbidity currents is interpretd to cause mainly the outstanding number of cut-off loops in the active channel levee system on the Middle Bengal Fan.

Thus, the combined analysis of the hydroacoustic data revealed new insights into the morphology, structure and processes of the active channel-levee system, characterizing this system as unique in comparison to other submarine fans. However, Parasound data are limited to the upper 100 m of the sediment column, and therefore high resolution seismic data were used to investigate deeper structures and the initiation of the active channel-levee system on the Middle Bengal Fan. The analysis of GI-Gun and Watergun data reveals that all cut-off loops and active channel segments are erosional incised into the underlying sediments. The channel of the active system is characterized by a broad spectrum of different and complex behaviors. In particular, the channel floor aggraded vertically and migrated laterally simultaneously, but the ratio between vertical and lateral migration varied, not only along the channel, but also during the development of one channel loop. Nevertheless, channel loops have never aggraded above the surrounding seafloor, which may have caused a relatively long lifetime of the system, explaining also the large number of cut-off loops within the active channel-levee system.

In contrast to the active system, one buried system with similar dimensions shows no cut-off loops but aggradation above the pre-existing surrounding seafloor. The aggradation probably favored early channel abandonment and a relatively shorter lifetime, which may have prevented the development of cut-off loops. Additionally, this buried system

shows a different behavior than the active system, namely exclusive lateral migration at the beginning, followed by simultaneous lateral migration and vertical aggradation. The differences in morphology and evolution to the active system indicate that turbidity currents with different characteristics as load, density or velocity developed each system. The described architecture and evolution of both systems differ significantly from channel-levee systems on Amazon Fan (e.g. Lopez, 2001) and does not follow the process model of Peakall et al. (2000a, b), but shows similar behaviors as submarine channels in Tertiary Congo Fan (Kolla et al., 2001).

Generally, the upper ~600 m of the Middle Bengal Fan consist of different sized channel-levee systems intercalated by High Amplitude Reflection Packets (HARPS) of varying thicknesses. The HARPS are interpreted as sheet-like sand bodies deposited as a result of channel avulsions followed by unchannelized flows into intrachannel lows or deposited as terminating lobes at channel mouths. Significant downfan thinning of channel-levee systems with parallel thickening of the basal HARPS within the main study area around 16°30´N indicate that channel termination occurred on the Middle Fan. The axes of all channels appear as Chaotic High Amplitude Reflectors (CHARS) interpreted as sands deposited from mixed-load turbidity currents. Due to the aggradation and migration of channels sand bodies were formed, which likely have hydrocarbon reservoir potential.

A 350 km long SW-NE profile from the upper Middle Bengal Fan shows that the channel-levee systems can be grouped into four large complexes separated by regional unconformities. These unconformities are interpreted as the result of canyon switching or as widespread turbidites deposited by non-channelized currents. Mass-flow deposits or thick hemipelagic drapes were not identified in the Middle Bengal Fan, wich is in contrast to the Amazon Fan (e.g. Lopez, 2001). Since the youngest channel of one complex was active before the end of Isotopic Stage 9 and the presently active channel grew during Holocene times (Weber et al., 1997; Weber et al., 2003), the Bengal Fan is thought to have been active even during sea-level rises and highstands.

Analysis of all surface and buried channel-levee systems identified in seismic profiles from the Middle Fan and Lower Fan reveals that all channels are characterized by erosional incisions. On average, the incision depth increases slightly downfan whereas the average levee thickness decreases significantly. This depositional pattern suggests that mixed-load turbidity currents lost their fine fraction on the Upper Fan and Middle Fan, and gaining more erosional capability during downfan travel. For the first time, the onset of channel-levee systems could be dated at 8°N, where age information is available from DSDP Site 218. There, the onset occurred in the latest Miocene at the same time as lithological changes are found at ODP Leg 116 at the distal end of the Bengal Fan. Both indicate a significant modification of sediment supply and transport. This may be caused either by changes in the erosional regime in the Himalayas due to tectonic and/or climatic changes or by the first cut of a canyon into the shelf.

On the Lower Fan, regional unconformities not hitherto reported were found in all three profiles. The unconformities of the southernmost profile at 8°N could be dated at DSDP Site 218. These unconformities have Pliocene and Pleistocene age and correspond well in time with unconformities found in the central Indian Ocean. There, the unconformities are related to deformation events of the lithosphere and changes in sediment character (Cochran, 1990; Krishna et al., 2001a). The unconformities in the presented high-resolution seismic data are probably caused by tectonic events or sediment changes and interpreted to be the equivalents of the unconformities found in the central Indian Ocean. Additionally, faults terminating within Pleistocene sediments suggest tectonic events in Pleistocene times. Ages from DSDP Site 218 were used to calculate sedimentation rates along 8°N revealing that Pleistocene rates were highest, Pliocene rates were lowest and late Miocene rates were in between. Decrease of sedimentation rates above the 85°E-Ridge and the Ninetyeast Ridge in the Bay of Bengal varied through time, namely most pronounced during Pliocene and least pronounced during late Miocene.

In general, the unconformities and the sedimentation pattern in time and space found on the Lower Fan can be interpreted as a result of tectonic events, mainly uplift of the ridges, or as result from varying sediment supply. However, for the unconformities in Pliocene and Pleistocene it is observed at ODP Leg 116 that lithological changes occurred simultaneously to tectonic events in the Indian Ocean (Krishna et al., 2001a). Therefore, it is not unlikely that unconformities and variations in sedimentation rates are caused from a combination of tectonics in Indian Ocean Lithosphere and changes in sediment supply. Since changes in sediment supply depend on the tectonics of the Himalayas, it is reasonable that a link between tectonic events in the Himalayas and in the Indian Ocean lithosphere exists as also suggested by Krishna et al. (2001a), although this link cannot be further elucidated by this study.

In summary, this study revealed new insights into architecture and evolution of individual channel-levee systems on the Bengal Fan as well as architecture and depositional processes of the Middle Fan and Lower Fan itself and complemented previous work in this region lead by Curray and coworkers (e.g. Curray et al., 2003) as well as Indian scientists (e.g., Gopala Rao et al., 1997; Krishna et al., 2001a, b). However, several questions still remain open, since the sheer size of the Bengal Fan makes it difficult to gain a full picture of processes in the region given the limited data sets yet available. Furthermore, some results of this study differ from results recently summarized by Curray et al. (2003), namely the sequence of surface channels and their association to distinct complexes on the Middle Fan as well as locations of the surface channels including the active one. These discrepancies indicate that long-range side-scan sonar surface mapping and additional high-resolution seismic data may be required to establish the pattern of surface channels and architectural elements. High-resolution 3-D seismic data could improve the understanding of the complex evolutions and behaviors of the individual channel-levee

systems on the Bengal Fan. Finally such data would help to predict the reservoir potential of these or similar systems.

Generally, an important lack of knowledge exists with respect to the ages and lifespans of individual channel-levee systems, channel-levee complexes and unconformities identified in the high-resolution seismic data. Downfan high-resolution seismic profiles would be essential to correlate both, the channel-levee complexes identified at the upper Middle Fan and the unconformities found at the northern Lower Fan, to the DSDP Site 218, which is the northernmost drill site so far. Furthermore, such profiles would reveal if the unconformities are linked and if they represent regional or local events. Only drilling and coring can close the gaps in dating and answer the resulting questions. As an example, one interesting aspect would be the filling time of the cut-off loops and their potential as high-resolution marine recorders for environmental changes, since these units of 50 to 100 m thickness may have been deposited in times of less than 1000 years.

So far, only two surface channels were dated, but more age-determinations and samples from channel-levee systems and complexes may reveal if and how the growth of such systems was controlled by climatic and sea level changes. Finally, the general erosion history of the Himalayas and consequently the regional climate and tectonics as well as interactions between both should be recorded in sediments in the Bengal Fan in different resolutions depending on depositional milieu. Thus, two IODP proposals (552-full3 and 609-pre) were submitted and supported as part of this research project to investigate the above-mentioned objectives and to propose sites of different depths and different shelf distances (France-Lanord et al., 2001; Spieß et al., 2002). Both proposals base mainly on the seismic data presented in this work. Seismic data for Proposal 552-full3 were submitted to the IODP data bank and the proposal was ranked as 2A („Possibly viable proposal for 2004 or later“). Additionally, a research cruise using the French ship „Marione Dufresne“ to collect long gravity cores was scheduled for autumn 2003, but was actually postponed to the near future.

References

Alam, M., Alam, M., Curray, J.R., Chowdhury, M.L.R. and Gani, M.R., 2003. An overview of the sedimentary geology of the Bengal basin in relation to the regional tectonic framework and basin-fill history. Sedimentary Geology 155, 179-208.

Allison, M.A., Khan, S.R., Goodbred Jr., S.L. and Kuehl, S.A., 2003. Stratigraphic evolution of the late Holocene Ganges-Brahmaputra lower delta plain. Sedimentary Geology 155, 317-342.

Babonneau, N., Savoye, B., Cremer, M. and Klein, B., 2002. Morphology and architecture of the present canyon and channel system of the Zaire deep-sea fan. Marine and Petroleum Geology 19, 445-467.

Banakar, V.K., Galy, A., Sukumaran, N.P., Parthiban, G. and Volvaiker, A.Y., 2003. Himalayan sedimentary pulses recorded by silicate detritus within a ferromanganese crust from the Central Indian Ocean. Earth and Planetary Science Letters 205, 337-348.

Biswas, S.and Majumdar, R.K., 1997. Seismicity and tectonics of the Bay of Bengal: Evidence for intraplate deformation of the northern Indian plate. Tectonophysics 269, 323-336.

Bouma, A.H., 2000. Coarse-grained and fine-grained turbidite systems as end member models: applicability and dangers. Marine and Petroleum Geology 17, 137-143.

Bouma, A.H., 2001. Fine-grained submarine fans as possible recorders of long- and short-term climatic changes. Global and Planetary Change 28, 85-91.

Brune, J.N., Curray, J., Dorman, L. and Raitt, R., 1992. A proposed super-thick sedimentary basin, Bay of Bengal. Geophysical Researches Letters 19(6), 565-568.

Caress, D.W. and Chayes, D.N., 1996. Improved processing of Hydrosweep DS Multibeam data on the R/V Maurice Ewing. Marine Geophysical Researches 18, 631-650.

Clark, J.D., Kenyon, N.H. and Pickering, K.T., 1992. Quantitative analysis of the geometry of submarine channels: Implications for the classification of submarine fans. Geology 20, 633-636.

Clift, P. and Gaedicke, C., 2002. Accelerated mass flux to the Arabian Sea during the middle to late Miocene. Geology 30(3), 207-210.

Cochran, J.R., 1990. Himalayan uplift, sea level, and the record of Bengal Fan sedimentation at the ODP Leg 116 sites. In: Cochran, J.R. and Stow D.A. (Eds.), Proceedings of the Ocean Drilling Program, Scientific Results, Leg 116. Ocean Drilling Program, College Station, Texas, pp. 397-414.

Curray, J.R., 1994. Sediment volume and mass beneath the Bay of Bengal. Earth and Planetary Science Letters 125, 371-383.

Curray, J.R. and Moore, D.G., 1971. Growth of the Bengal deep-sea fan and denudation in the Himalayas. Geological Society of America Bulletin 82, 563-573.

Curray, J.R. and Munasinghe, T., 1989. Timing of intraplate deformation, northeastern Indian Ocean. Earth and Planetary Science Letters 94(1-2), 71-77.

Curray, J.R., Emmel, F.J. and Moore, D.G., 2003. The Bengal Fan: morphology, geometry, stratigraphy, history and processes. Marine and Petroleum Geology 19, 1191-1223.

Damuth, J.E., Flood, R.D., Kowsman, R.O., Belderson, R.H. and Gorini, M.A., 1988. Anatomy and grow pattern of Amazon Deep-Sea Fan as revealed by long-range side-scan sonar (GLORIA) and high-resolution seismic studies. American Association of Petroleum Geologists Bulletin 72(8), 885-911.

Derry, L.A. and France-Lanord, C., 1996. Neogene Himalayan weathering history and river 87Sr/86Sr: impact on the marine Sr record. Earth and Planetary Science Letters 142, 59-74.

Dietz, R.S., 1953. Possible deep-sea turbidity-current channels in the Indian Ocean. Geological Society of America Bulletin 64, 375-378.

Droz, L., Rigaut, F., Cochonat, P. and Tofani, R., 1996. Morphology and recent evolution of the Zaire turbidite system (Golf of Guinea). GSA Bulletin 108, 253-269.

Emmel, F.J. and Curray, J.R., 1985. Bengal Fan, Indian Ocean. In: Bouma, A.H., Normark, W.R. and Barnes, N.E. (Eds.), Submarine Fans and Related Turbidite Systems. Springer, New York, pp. 107-112.

Flood, R.D., Manley, P.L., Kowsmann, R.O., Appi, C.J. and Pirmez, C., 1991. Seismic facies and late quaternary growth of Amazon submarine fan. In: Weimer, P. and Link, M.H. (Eds.), Seismic facies and sedimentary processes of submarine fans and turbidite systems. Springer, New York, pp. 415-433.

Flood, R.D., Piper, D.J.W. and Klaus, A., 1995. Proceedings Ocean Drilling Program, initial reports. Ocean Drilling Program, College Station, TX.

Flood, R.D. and Piper, D.J.W., 1997. Amazon Fan sedimentation: the relationship to equatorial climate change, continental denudation, and sea-level fluctuations. In: Flood, R.D., Piper, D.J.W., Klaus, A. and Peterson, L.C. (Eds.), Proceedings of the Ocean Drilling Program, Scientific Results. Ocean Drilling Program, College Station, Texas, pp. 653-675.

France-Lanord, C. and Derry, L.A., 1994. $\delta^{13}C$ of organic carbon in the Bengal Fan: source evolution and transport of C3 and C4 plant carbon to marine sediments. Geochimica et Cosmochimica Acta 58, 4809-4814.

France-Lanord, C., Spieß, V., Molnar, P. and Curray, J.R., 2001. Neogene and late Paleogene record of Himalayan orogeny and climate: a transect across Middle Bengal Fan, IODP Proposal 552-full3.

Gartner, S., 1974. Nannofossil biostratigraphy, Leg 22, Deep Sea Drilling Project. In: von der Borch, C.C. and Sclater, J.C. (Eds.), Initial Reports of the Deep Sea Drilling Project, Leg 22. US Government Printing Office, Washington, D.C., pp. 577-599.

Goodbred Jr., S.L. and Kuehl, S.A., 2000a. Enormous Ganges-Brahmaputra sediment discharge during strengthened early Holocene monsoon. Geology 28(12), 1083-1086.

Goodbred Jr., S.L. and Kuehl, S.A., 2000b. The significance of large sediment supply, active tectonism, and eustasy on margin sequence development: Late Quaternary stratigraphy and evolution of the Ganges -Brahmaputra delta. Sedimentary Geology 133, 227-248.

Goodbred Jr., S.L., Kuehl, S.A., Steckler, M.S. and Sarker, M.H., 2003. Controls on facies distribution and stratigraphic preservation in the Ganges-Brahmaputra delta sequence. Sedimentary Geology 155, 301-316.

Gopala Rao, D., Bhattacharya, G.C., Ramana, M.V., Subrahmanyam, V., Ramprasad, T., Krishna, K.S., Chaubey, A.K., Murty, G.P.S., Srinivas, K., Desa, M., Reddy, S.I., Ashalta, B., Subrahmanyam, C., Mital, G.S., Drolia, R.K., Rai, S.N., Ghosh, S.K., Singh, R.N., Majumdar, R., 1994. Analysis of Multi-Channel Seismic Reflection and Magnetic Data Along 13° Latitude Across the Bay of Bengal. Marine Geophysical Researches 16, 225-236.

Gopala Rao, D., Krishna, K.S. and Sar, D., 1997. Crustal evolution and sedimentation history of the Bay of Bengal since the Cretaceous. Journal of Geophysical Research 102(B8), 17,747-17,768.

Gordon, R.G., DeMets, C. and Royer, J.-Y., 1998. Evidence for long-term diffuse deformation of the lithosphere of the equatorial Indian Ocean. Nature 395, 370-374.

Grant, J.A. and Schreiber, R., 1990. Modern Swathe Sounding and Sub-Bottom Profiling Technology for Research Applications: The Atlas Hydrosweep and Parasound Systems. Marine Geophysical Researches 12, 9-19.

Gutowski, M., Breitzke, M. and Spieß, V., 2002. Fast static correction methods for high-frequency multichannel marine seismic reflection data: A high-resolution seismic study of channel-levee systems on the Bengal Fan. Marine Geophysical Researches 23, 57-75.

Harrison, T.M., Copeland, P., Kidd, W.S.F. and Yin, A., 1992. Raising Tibet. Science 255, 1663-1670.

Harrison, T.M., Copeland, P., Kidd, W.S.F. and Lovera, O.M., 1995. Activation of the Nyainqentanghla shear zone: Implications for uplift of the southern Tibetan Plateau. Tectonics 14, 658-676.

Harrison, T.M., Grove, M., Lovera, O.M. and Catlos, E.J., 1998. A model for the origin of the Himalayan anatexis and inverted metamorphism. Journal of Geophysical Research 103(B11), 27,017-27,032.

Heroy, D.C., Kuehl, S.A. and Goodbred Jr., S.L., 2003. Mineralogy of the Ganges and Brahmaputra Rivers: implications for river switching and Late Quaternary climate change. Sedimentary Geology 155, 343-359.

Hesse, R., 1995. Long-distance correlation of spill-over turbidites on the western levee of the Nortwest Atlantic Mid-Ocean Channel (NAMOC), Labrador Sea. In: Pickering, K.T., Hiscott, R.N., Kenyon, N.H., Ricci Lucchi, F. and Smith, R.D.A. (Eds.), Atlas of Deep Water Environments: Architectural Style in Turbidite Systems. Chapman and Hall, Oxford, U.K., pp. 276-281.

Hiscott, R.N., Hall, F.R. and Pirmez, C., 1997. Turbidity-current overspill from the Amazon channel: Texture of the silt/sand load, paleoflow from anisotropy of magnetic susceptibility and implications for flow processes. In: Flood, R.D., Piper, D.J.W., Klaus, A. and Peterson, L.C. (Eds.), Proceedings of the Ocean Drilling Program, scientific results, Leg155. Ocean Drilling Program, College Station, TX, pp. 53-78.

Hübscher, C., Spieß, V., Breitzke, M. and Weber, M.E., 1997. The youngest channel-levee system of the Bengal-Fan: Results from digital echosounder data. Marine Geology 141, 125-145.

Hübscher, C., Breitzke, M., Michels, K., Kudrass, H.R., Spieß, V. and Wiedicke, M., 1998. Late Quaternary seismic stratigraphy of the eastern Bengal Shelf. Marine Geophysical Researches 20, 57-81.

Imran, J., Parker, G. and Katopodes, N., 1998. A numerical model of channel interception on submarine fans. Journal of Geophysical Research 103(C1), 1219-1238.

Kastens, K.A. and Shor, A.N., 1985. Depositional Process of a Meandering Channel on Mississippi Fan. The American Association of Petroleum Geologists Bulletin 69(2), 190-202.

Kenyon, N.H., Amir, A. and Cramp, A., 1995. Geometry of the younger sediment bodies of the Indus Fan. In: Pickering, K.T., Hiscott, R.N., Kenyon, N.H., Ricci Lucchi, F. and Smith, R.D.A. (Eds.), Atlas of Deep Water Environments: Architectural style in Turbidite Systems. Chapman and Hall, London, pp. 89-93.

Klaucke, I. and Hesse, R., 1996. Fluvial features in the deep-sea: new insights from the glacigenic submarine drainage system of the Nortwest Atlantic Mid-Ocean Channel in the Labrador Sea. Sedimentary Geology 106, 223-234.

Klaucke, I., Hesse, R. and Ryan, W.B.F., 1998. Morphology and structure of a distal submarine trunk: The North-west Atlantic Mid-Ocean Channel between lat 53°N and 44°30´N. GSA Bulletin 110(1), 22-34.

Kolla, V. and Schwab, A.M., 1995. Indus Fan: Multi channel seismic reflection images of channel-levee-overbank complexes. In: Pickering, K.T., Hiscott, R.N., Kenyon, N.H., Ricci Lucchi, F. and Smith, R.D.A. (Eds.), Atlas of Deep Water Environments: Architectural style in Turbidite Systems. Chapman & Hall, London, pp. 100-104.

Kolla, V., Bourges, P., Urruty, J.-M. and Safa, P., 2001. Evolution of deep-water Tertiary sinuous channels offshore Angola (west Africa) and implications for reservoir architecture. AAPG Bulletin 85(8), 1373-1405.

Kottke, B., Schwenk, T., Breitzke, M., Wiedicke, M., Kudrass, H.-R. and Spieß, V., 2003. Acoustic Facies and depositional processes in the upper submarine canyon Swatch of No Ground (Bay of Bengal). Deep Sea Research II 50(5), 979-1001.

Krishna, K.S., Bull, J.M. and Scrutton, R.A., 2001a. Evidence for multiphase folding of the central Indian Ocean lithosphere. Geology 29(8), 715-718.

Krishna, K.S., Neprochnov, Y.P., Gopala Rao, D. and Grinko, B.N., 2001b. Crustal structure and tectonics of the Ninetyeast Ridge from seismic and gravity studies. Tectonics 20(3), 416-433.

Krishna, K.S., 2003. Structure and evolution of the Afanasy Nikitin seamount, buried hills and 85°E Ridge in the northeastern Indian Ocean. Earth and Planetary Science Letters 209, 379-394.

Kudrass, H.R. and Shipboard Scientific Party, 1994. Cruise Report SO93/1-3. Bundesanstalt für Geowissenschaften und Rohstoffe, Hannover.

Kudrass, H.R. and Shipboard Scientific Party, 1998. Cruise report SO 126. Bundesanstalt für Geowissenschaften und Rohstoffe, Hannover.

Kudrass, H.R., Michels, K.H., Wiedicke, M. and Suckow, A., 1998. Cyclones and tides as feeders of a submarine canyon off Bangladesh. Geology 26(8), 715-718.

Lee, T.T. and Lawver, L.A., 1995. Cenozoic plate reconstruction of Southeast Asia. Tectonophysics 251, 85-138.

Lopez, M., 2001. Architecture and depositional pattern of the Quarternary deep-sea fan of the Amazon. Marine and Petroleum Geology 18, 479-486.

Maslin, M. and Mikkelsen, N., 1997. Amazon Fan mass-transported deposits and underlying interglacial deposits: age estimates and fan dynamics. In: Flood, R.D., Piper, D.J.W., Klaus, A., and Peterson, L.C. (Eds.), Proceedings Ocean Drilling Program, scientific results, Leg 155. Ocean Drilling Program, College Station, TX, pp. 653-678.

McHugh, C.M.G. and Ryan, W.B.F., 2000. Sedimentary features associated with channel overbank flow: examples from the Monterey Fan. Marine Geology 163, 199-215.

Michels, K.H., Kudrass, H.R., Hübscher, C., Suckow, A. and Wiedicke, M., 1998. The submarine delta of the Ganges-Brahmaputra: Cyclone-dominated sedimentation patterns. Marine Geology 149, 133-154.

Michels, K.H., Suckow, A., Breitzke, M., Kudrass, H.R. and Kottke, B., 2003. Sediment transport processes in the shelf canyon „Swatch of no Ground“ (Bay of Bengal). Deep Sea Research II 50(5), 1003-1022.

Milliman, J.D. and Meade, R.H., 1983. Worldwide delivery of river sediments to the ocean. Journal of Geology 91, 1-21.

Molnar, P., England, P. and Martinod, J., 1993. Mantle dynamics, the uplift of the Tibetan Plateau, and the Indian monsoon. Reviews of Geophysics 31, 357-396.

Moore, D.G., Curray, J.R., Raitt, R.W. and Emmel, F.J., 1974. Stratigraphic-seismic section correlations and implications to Bengal Fan history. In: von der Borch, C.C. and Sclater, J.C. (Eds.), Initial reports of the Deep Sea Drilling Project, Leg 22. US Government Printing Office, Washington, D.C., pp. 403-412.

Pan, Y. and Kidd, W.S.F., 1992. Nyainqentanglha shear zone: A late Miocene extensional detachment in the southern Tibetan Plateau. Geology 20, 775-778.

Peakall, J., McCaffrey, B. and Kneller, B., 2000a. A process model for the evolution, morphology and architecture of sinuous submarine channels. Journal of Sedimentary Research 70(3), 434-448.

Peakall, J., McCaffrey, W.D., Kneller, B.C., Stelting, C.E., McHargue and T.R., Schweller, W.J., 2000b. A process model for the evolutuion of submarine fan channels: implications for sedimentary architecture. In: Bouma, A.H. and Stone, C.G. (Eds.), Fine-grained turbidite systems. AAPG Memoir 72/SEPM Special Publication 68, pp. 73-88.

Piper, D.J.W. and Normark, W.R., 1983. Turbidite depositional patterns and flow characteristics, Navy submarine fan. Sedimentology 30, 681-694.

Piper, D.J.W. and Deptuck, M., 1997. Fine-grained turbidites of the Amazon Fan: Facies characterisation and interpretation. In: Flood, R.D., Piper, D.J.W., Klaus, A. and Peterson, L.C. (Eds.), Proceedings of the Ocean Drilling Program, Scientific Results, Leg 155. Ocean Drilling Program, College Station, TX, pp. 79-108.

Pirmez, C. and Flood, R.D., 1995. Morphology and structure of Amazon channel. In: Flood, R.D., Piper, D.J.W., Klaus, A. et al. (Eds.), Proceedings of the Ocean Drilling Program, Initial Report. Ocean Drilling Program, College Station, TX, pp. 23-45.

Popescu, I., Lericolais, G., Panin, N., Wong, H.K. and Droz, L., 2001. Late Quaternary channel avulsions on the Danube deep-sea fan, Black Sea. Marine Geology 179, 25-37.

Richards, M., Bowman, M. and Reading, H., 1998. Submarine-fan systems I: characterization and stratigraphic prediction. Marine and Petroleum Geology 15, 689-717.

Richards, M. and Bowman, M., 1998. Submarine fans and related depositional systems II: variability in reservoir architecture and wireline log character. Marine and Petroleum Geology 15, 821-839.

Schwenk, T., Spieß, V., Hübscher, C. and Breitzke, M., 2003. Frequent channel avulsions within the active channel-levee system of the middle Bengal Fan - an exeptional channel-levee development derived from Parasound and Hydrosweep data. Deep Sea Research II 50(5), 1023-1045.

Smith, W.H.F. and Sandwell, D.T., 1997. Global sea floor topography from satellite altimetry and ship depth soundings. Science 277(5334), 1956-1962.

Spieß, V., 1993. Digitale Sedimentechographie - Neue Wege zu einer hochauflösenden Akustostratigraphie. Berichte Fachbereich Geowissenschaften, Universität Bremen, 35, Bremen, 1-199 pp.

Spieß, V., Hübscher, C., Breitzke, M., Böke, W., Krell, A., von Larcher, T., Matschkowski, T., Schwenk, T., Wessels, A., Zühlsdorff, L., Zühlsdorff, S., 1998. Report and preliminary results of R/V Sonne cruise 125, Cochin - Chittagong, 17.10. - 17.11.97. Berichte Fachbereich Geowissenschaften, Universität Bremen, 123, Bremen, 128 pp.

Spieß, V., France-Lanord, C., Molnar, P., Curray, J.R., Kudrass, H.R., Kuehl, S., Goodbred, S. and Revil, A., 2002. The Himalaya-Bengal System: Studying links between Land and Ocean, Climate and Tectonics, „Source“ and „Sink“ by a multiplatform approach for drilling in the Bay of Bengal, IODP Proposal 609-pre.

Stelting, C.E. et al., 1985. Migratory characteristics of a mid-fan menader belt, Mississippi Fan. In: Bouma, A.H., Normark, W.R. and Barnes, N.E. (Eds.), Submarine fans and related turbidite sequences. Springer Verlag, New York, pp. 283-290.

Stockwell, J.W., 1997. Free software in education: A case study of CWP/SU: Seismic Uni*x. Leading Edge 16, 1045-1049.

Stow, D.A.V., Amano, K., Balson, P.S., Brass, G.W., Corrigan, J., Raman, C.V., Tiercelin, J.-J., Townsend, M., Wijayananda, N.P., 1990. Sediment facies and processes on the distal Bengal Fan, Leg 116. In: Cochran, J.R. and Stow, D.A. (Eds.), Proceedings of the Ocean Drilling Program, Scientific Results, Leg 116. Ocean Drilling Program, College Station, Texas, pp. 377-396.

Stow, D.A.V. and Mayall, M., 2000. Deep-water sedimentary systems: New models for the 21st century. Marine and Petroleum Geology 17, 125-135.

Subrahmanyam, C., Thakur, N.K., Gangadhara Rao, T., Khanna, R., Ramana and M.V., Subrahmanyam, V., 1999. Tectonics of the Bay of Bengal: new insights from satellite-gravity and ship-born geophysical data. Earth and Planetary Science Letters 171, 237-251.

Subrahmanyam, V., Krishna, K.S., Radhakrishna Murthy, I.V., Sarma, K.V.L.N.S., Desa, M., Raman, M.V., Kamesh Raju, K.A., 2001. Gravity anomalies and crustal structure of the Bay of Bengal. Earth and Planetary Science Letters 192, 447-456.

Twichell, D.C., Kenyon, N.H., Parson, L. and McGregor, B.A., 1991. Depositional Patterns of the Mississippi Fan Surface: Evidence from GLORIA II and High-Resolution Seismic Profiles. In: Weimer, P. and Link, M.H. (Eds.), Seismic facies and sedimentary processes of submarine fans and turbidite systems. Springer Verlag, New York, pp. 349-363.

von der Borch, C.C., Sclater, J.C. et al., 1974. Initial reports of the Deep Sea Drilling Project, Leg 22. US Government Printing Office, Washington, DC, 890 pp.

Weber, M.E., Wiedicke, M.H., Kudrass, H.R., Hübscher, C. and Erlenkeuser, H., 1997. Active growth of the Bengal Fan during sea-level rise and highstand. Geology 25(4), 315-318.

Weber, M.E., Wiedicke-Hombach, M., Kudrass, H.R. and Erlenkeuser, H., 2003. Bengal Fan sediment transport activity and response to climate forcing inferred from sediment physical properties. Sedimentary Geology 155, 361-381.

Weimer, P., 1991. Seismic facies, characteristics, and variations in channel evolution, Mississippi Fan (Plio-Pleistocene), Gulf of Mexico. In: Weimer, P. and Link, M.H. (Eds.), Seismic facies and sedimentary processes of submarine fans and turbidite systems. Springer, New York, pp. 323-347.

Wessel, P. and Smith, W.H.F., 1998. New, improved version of Generic Mapping Tools released. EOS Transactions, American Geophysical Union, 79(47), 579.

Wiedicke, M., Kudrass, H.R. and Hübscher, C., 1999. Oolithic beach barriers of the last glacial sea-level lowstand at the outer Bengal shelf. Marine Geology 157, 7-18.

Zühlsdorff, L., 1999. High resolution multi-frequency seismic surveys at the eastern Juan de Fuca Ridge flank and the Cascadia Margin - Evidence fro thermally and tectonically driven fluid upflow in marine sediments. Berichte Fachbereich Geowissenschaften, Universität Bremen, 147, Bremen, 118 pp.

Acknowledgments

I would like to thank Prof. Dr. V. Spieß for giving my the opportunity to work on this dissertation, giving my constant advice as well as support and being open for fruitful discussions. I would also like to thank Prof. Dr. Ralph Schneider for writing the secondary expertise and for his patience.

Next, I thank all my colleagues from MTU/FB 5 at the University of Bremen for working in productive and relaxed atmosphere. Hanno von Lom provided tools for enhanced processing of Hydrosweep data and solved uncountable computer problems. Lars Zühlsdorff provided the geometry software GeoApp and answered all questions about seismic processing. Sebastian Krastel gave also assistance for seismic processing and many helpful comments for the second manuscript. Thanks to the students Annedore Seifert and Nicole Albrecht for additional support during processing of the huge amount of seismic data. Monika Breitzke did some pre-processing of the data. Finally, Angelika Rinkel provided important administrative support.

The first manuscript was significantly improved by constructive reviews of R. Hesse and U. v. Rad. Discussions with Joe Curray, Christian France-Lanord, Christian Hübscher, Michel Lopez and Jeff Peakall expanded my understanding of channel-levee systems and the Bengal Fan.

Many thanks also to Carolyn Scheurle and Claudia Wienberg for editorial assistance.

This work was greatly supported by all colleagues who operated as seismic watchkeeper during SO 125 Cruise and as Parasound/Hydrosweep watchkeeper during the cruises SO 93, SO 125, and SO 126 in 24-hour schedules. Collecting of the high quality data had not been possible without the excellent work of captains and crews during these expeditions.

Collecting and processing of the data were funded by the BMBF (Grant 03G0125A), DFG (Grant SP296/14) and the Graduiertenkolleg „Stoff-Flüsse in marine Geosystemen“.

All maps in this work were created using the public domain software Generic Mapping Tools (GMT) (Wessel and Smith, 1998). Hydrosweep data processing was carried out with the public domain software MultiBeam (Caress and Chayes, 1996). Seismic processing was made with the Seismic Un*x (SU) software package (Stockwell, 1997). Interpretation was provided by the software Kingdome Suite, given as a donation of Seismic-Micro Technology, Inc.

Last but not least I would like to thank my family supporting me all the years and all my friends keeping me in contact with the real life outside the „ivory tower“.